

## PDF hosted at the Radboud Repository of the Radboud University Nijmegen

The following full text is a publisher's version.

For additional information about this publication click this link.

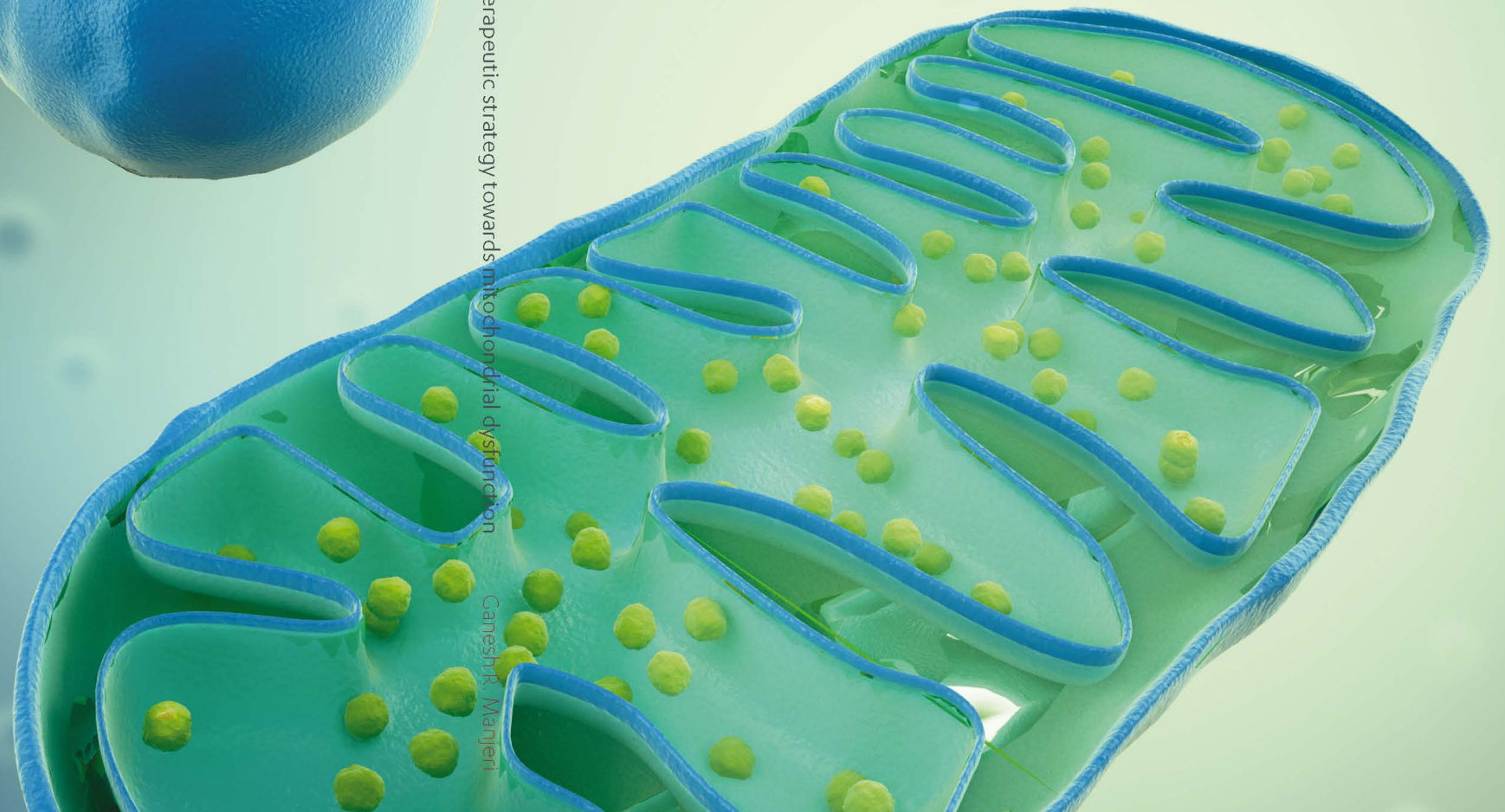
<http://hdl.handle.net/2066/165619>

Please be advised that this information was generated on 2017-12-05 and may be subject to change.



# CHARACTERIZATION OF THE *Ndufs4*<sup>-/-</sup> MODEL to evaluate a novel therapeutic strategy towards mitochondrial dysfunction

Ganesh R. Manjeri



CHARACTERIZATION OF THE *Ndufs4*<sup>-/-</sup> MODEL to evaluate a novel therapeutic strategy towards mitochondrial dysfunction

Ganesh R. Manjeri

**Characterization of the *Ndufs4*<sup>-/-</sup> model  
to evaluate a novel therapeutic strategy  
towards mitochondrial dysfunction**

Ganesh R. Manjeri

*To Appa, Mummy and Karthik*

# **Characterization of the $Ndufs4^{-/-}$ model to evaluate a novel therapeutic strategy towards mitochondrial dysfunction**

## **Proefschrift**

ter verkrijging van de graad van doctor  
aan de Radboud Universiteit Nijmegen  
op gezag van de rector magnificus Prof. dr. P.P.G. Hodiamont,  
volgens besluit van het college van decanen  
in het openbaar te verdedigen op maandag 20 februari 2017  
om 12:30 uur precies

door

**Ganesh Ramesh Manjeri**

geboren op 14 January 1984

te Mysore, India

**Promotor(en)**

Prof. dr. J.A.M. Smeitink

Prof. dr. R. Brock

**Copromotor(en)**

Dr. P.H. Willems

Dr. W.J.H. Koopman

**Manuscriptcommissie**

Prof. dr. B. Wieringa

Prof. dr. A. Heerschap

Prof. dr. ir. J. Keijer (Wageningen Universiteit)

# **Characterization of the $Ndufs4^{-/-}$ model to evaluate a novel therapeutic strategy towards mitochondrial dysfunction**

**Doctoral thesis**

to obtain the degree of doctor  
from Radboud University Nijmegen  
on the authority of the Rector Magnificus Prof. dr. P.P.G. Hodiament,  
according to the decision of the Council of Deans  
to be defended in public on Monday 20 February 2017  
at 12:30 hours

by

**Ganesh Ramesh Manjeri**

born on 14 January 1984

in Mysore, India

**Supervisor(s)**

Prof. dr. J.A.M. Smeitink

Prof. dr. R. Brock

**Co-supervisor(s)**

Dr. P.H. Willems

Dr. W.J.H. Koopman

**Doctoral Thesis Committee**

Prof. dr. B. Wieringa

Prof. dr. A. Heerschap

Prof. dr. ir. J. Keijer (Wageningen University)



The research presented in this thesis was performed at the Department of Biochemistry, Radboud University Medical Center, financially supported by 'Prinses Beatrix Fonds' (No: OP-05-04) and Netherlands Organization for Scientific Research (NWO) Centers for Systems Biology Research Initiative (CSBR09/013V). Printing of this thesis was financially supported by Department of Biochemistry

**ISBN 978-94-6182-759-3**

Cover design, layout and printing: Off Page, The Netherlands

© 2017 Ganesh Ramesh Manjeri

All rights reserved. No parts of this publication may be reported or transmitted, in any form or by any means, without permission of the author.



## Table of Contents

<b>Chapter 1</b>	Complex I deficiency: Causes, consequences and treatment options with focus towards the NDUFS4 subunit	11
<b>Chapter 2</b>	Biochemical characterization of the oxidative phosphorylation system in tissues of high energy demand in a mouse model of isolated complex I deficiency	45
<b>Chapter 3</b>	Skeletal muscle mitochondria of the NDUFS4 <sup>-/-</sup> mice display normal pyruvate oxidation and ATP production	69
<b>Chapter 4</b>	Isoflurane anesthetic hypersensitivity and progressive respiratory depression in a mouse model with isolated mitochondrial Complex I deficiency	97
<b>Chapter 5</b>	Increased mitochondrial ATP production capacity in brain of healthy mice and a mouse model of isolated complex I deficiency after isoflurane anesthesia	115
<b>Chapter 6</b>	How to deal with oxygen radicals stemming from mitochondrial fatty acid oxidation	131
<b>Chapter 7</b>	Evaluation of the therapeutic potential of the antioxidant Trolox in a mouse model with an isolated mitochondrial CI deficiency	153
<b>Chapter 8</b>	General summary and Future perspectives	179
<b>Chapter 9</b>	Samenvatting	195
	List of Publications	203
	Curriculum Vitae	205
	Acknowledgements	207



# CHAPTER

## **Complex I deficiency: Causes, consequences and treatment options with focus towards the NDUFS4 subunit**

Partially published in

Roestenberg, P., **Manjeri, G.R.**, Valsecchi, F., Smeitink, J.A., Willems, P.H., and Koopman, W.J. (2012). Pharmacological targeting of mitochondrial complex I deficiency: the cellular level and beyond.

**Mitochondrion** 12, 57-65.

Valsecchi, F., Koopman, W.J., **Manjeri, G.R.**, Rodenburg, R.J., Smeitink, J.A., and Willems, P.H. (2010). Complex I disorders: causes, mechanisms, and development of treatment strategies at the cellular level. **Developmental disabilities research reviews** 16, 175-182.

1



## Introduction

### Mitochondrial Complex I (CI)

Complex I (CI), or NADH: ubiquinone oxidoreductase, is the first multisubunit enzyme complex of the mitochondrial oxidative phosphorylation (OXPHOS) system. In most cells, the OXPHOS system is responsible for the vast majority of cellular ATP production, with ATP being the primary source of energy to power the cell's activities. CI liberates electrons from NADH and passes them via a series of protein-coupled redox centres to the electron acceptor ubiquinone (Hirst and Roessler 2016, Wirth, Brandt et al. 2016). In well-coupled mitochondria, the electron flux through the respiratory chain (RC) part of the OXPHOS system leads to the building of an electrochemical proton gradient across the mitochondrial inner membrane (MIM), the proton motive force (PMF), which is used by the fifth complex of the system, complex V or F<sub>1</sub>F<sub>0</sub>-ATP synthase, to generate ATP. The complex is composed of 44 subunits, 14 of which are the so-called core subunits (Fiedorczuk, Letts et al. 2016, Lenaz, Tioli et al. 2016, Sanchez-Caballero, Guerrero-Castillo et al. 2016, Wirth, Brandt et al. 2016). Seven of these core subunits are encoded by the mitochondrial (mt) DNA (ND1, ND2, ND3, ND4, ND4L, ND5, ND6 and ND7) and 7 by the nuclear (n)DNA (NDUFV1, NDUFV2, NDUFS1, NDUFS2, NDUFS3, NDUFS7, and NDUFS8). The function of the remaining 30 subunits, the accessory subunits, which all are encoded by the nDNA, is still incompletely understood but it is believed that they play a crucial role in CI assembly, biogenesis stabilization, and/or functional regulation (Valsecchi, Koopman et al. 2010, Balsa, Marco et al. 2012, Roestenberg, Manjeri et al. 2012).

### Genetics of inherited isolated CI deficiency

Inherited isolated CI deficiency can result from mutations in either mtDNA- or nDNA-encoded CI structural subunits or nDNA-encoded CI assembly factors (Smeitink, Sengers et al. 2001, Smeitink, van den Heuvel et al. 2001, Koopman, Willems et al. 2012). The first mtDNA mutation associated with human disease was described in 1988 (Wallace, Zheng et al. 1988). Individual mitochondria contain multiple mtDNA copies and mutations are generally inherited via the mother (maternal inheritance). Mutations can be present in a variable amount of mtDNA copies, a phenomenon referred to as heteroplasmy. The degree of heteroplasmy is an important contributor to the severity of the disease. To date, genetic defects causing inherited isolated CI deficiency have been reported for all 7 mtDNA-encoded CI subunits. Mutations in nDNA-encoded CI subunits are frequently inherited in an autosomal recessive fashion, meaning that both parents have to be heterozygous carriers. For successful

prenatal diagnosis, it is necessary that causative nuclear gene mutations are known. In this respect, disease-causing mutations have been demonstrated in genes encoding the following CI subunits: *NDUFV1* (Schuelke, Smeitink et al. 1999), *NDUFV2* (Benit, Beugnot et al. 2003), *NDUFS1* (Benit, Chretien et al. 2001, Martin, Blazquez et al. 2005, Iuso, Scacco et al. 2006, Hoefs, Skjeldal et al. 2010), *NDUFS2* (Loeffen, Elpeleg et al. 2001), *NDUFS3* (Benit, Slama et al. 2004), *NDUFS4* (van den Heuvel, Ruitenbeek et al. 1998), *NDUFS6* (Kirby, Salemi et al. 2004), *NDUFS7* (Triepels, van den Heuvel et al. 1999), *NDUFS8* (Loeffen, Smeitink et al. 1998), *NDUFA1* (Fernandez-Vizarra, Bugiani et al. 2007), *NDUFA2* (Hoefs, Dieteren et al. 2008), *NDUFA9* (van den Bosch, Gerards et al. 2012), *NDUFA10* (Hoefs, van Spronsen et al. 2011), *NDUFA11* (Berger, Hershkovitz et al. 2008), *NDUFA12* (Ostergaard, Rodenburg et al. 2011), *NDUFA13* (Angebault, Charif et al. 2015), *NDUFB3* (Alston, Howard et al. 2016) and *NDUFB9* (Haack, Madignier et al. 2012). In addition inherited isolated CI deficiency can be caused by mutations in nDNA-encoded proteins involved in CI assembly and/or stabilization. Mutations have been found in *NDUFAF1* (Dunning, McKenzie et al. 2007), *NDUFAF2* (Hoefs, Dieteren et al. 2008), *NDUFAF3* (Saada, Vogel et al. 2009), *NDUFAF4* (Saada, Edvardson et al. 2008), *C8orf38* (Pagliarini, Calvo et al. 2008), *C20orf7* (Sugiana, Pagliarini et al. 2008), *ACAD9* (Garone, Donati et al. 2013), *FOXRED1* (Zurita Rendon, Antonicka et al. 2016) and *NUBPL* (Kevelam, Rodenburg et al. 2013).

### **The *NDUFS4* gene and its product**

NADH dehydrogenase [ubiquinone] iron-sulphur protein 4 or *NDUFS4* is an accessory subunit of CI encoded by the nDNA. Its gene encodes an 18kDa protein also referred to as the AQDQ subunit and is localized on chromosome 5q11.1 (Emahazion, Beskow et al. 1998, van den Heuvel, Ruitenbeek et al. 1998, Scacco, Petruzzella et al. 2003). The subunit is located at a strategic position within CI at the junction between the peripheral mass protruding into the matrix and the membrane moiety of CI (Petruzzella, Vergari et al. 2001). The *NDUFS4* gene consists of 5 exons interspersed by large introns spanning in total over 122 kb. The gene encodes 175 amino acids and displays a high degree of conservation in all known mammalian sequences (Papa 2002, Budde, van den Heuvel et al. 2003, De Rasmø, Panelli et al. 2008). The human precursor *NDUFS4* protein contains two phosphorylation consensus sites, one at position 36-38 (RTS) in the 42 amino acids long leader sequence and the other one at position 171-173 (RVS) in the 133 amino acids long mature protein (Budde, van den Heuvel et al. 2002). Phosphorylation of the Serine 173 in the RVS site by cAMP-dependent protein kinase, or protein kinase A (PKA), increases its affinity for cytosolic Hsp70 (De Rasmø, Panelli et al. 2008). This, in turn, facilitates its import and subsequent cleavage to the mature



form and incorporation in CI. Thus, PKA-mediated phosphorylation of the *NDUFS4* subunit leads to an increase in CI activity (Schwoch, Trinczek et al. 1990, Papa, Rasmussen et al. 2012, Valsecchi, Ramos-Espiritu et al. 2013).

### **Pathogenic *NDUFS4* mutations**

The *NDUFS4* gene is regarded as a mutational hotspot in human CI deficiency (Petruzzella and Papa 2002, Scacco, Petruzzella et al. 2003, Panelli, Petruzzella et al. 2008). To date, nine disease causing *NDUFS4* mutations have been reported (Pagniez-Mammeri, Loublier et al. 2012). These include a 5-bp duplication, resulting in a frameshift at codon K158 (**K158fs**) extending the mature protein by 14 amino acids and destroying the PKA phosphorylation consensus site (RVS) at position 171-173 (van den Heuvel, Ruitenbeek et al. 1998), three nonsense mutations, resulting in a marked decrease (**W96X** and **R106X**) (Budde, van den Heuvel et al. 2000, Benit, Steffann et al. 2003, Ugalde, Janssen et al. 2004) or even the complete absence (**W15X**) (Petruzzella, Panelli et al. 2005) of fully assembled CI, a splice acceptor site mutation of intron 1 (c.99-1G>A), resulting in complete skipping of exon 2 and accumulation of a truncated protein of 39 amino acids (**S34fs**) (Benit, Steffann et al. 2003), a deletion resulting in a frameshift (**K154fs**) (Anderson, Chung et al. 2008), a point mutation (**D119H**) (Leshinsky-Silver, Lebre et al. 2009), a **c.351-2A>G** mutation, predicted to alter *NDUFS4* splicing resulting in mRNA instability (Calvo, Tucker et al. 2010) and a **c.393dupA** frameshift mutation (Lamont, Beaulieu et al. 2016).

### **Patient characteristics**

Neurodevelopmental disorders with major implications on survival rates are observed in patients suffering from mutations in nuclear genes encoding structural subunits of CI (Shoubridge 2001, Distelmaier, Koopman et al. 2009). Children with *NDUFS4* mutations present with Leigh or Leigh-like syndrome, which is characterized by symmetrical bilateral necrotic lesions and capillary proliferation in different regions of the central nervous system. Clinical signs and symptoms include muscular hypotonia, dystonia, developmental delay, abnormal eye movements, seizures, respiratory irregularities, lactic acidemia and neonatal cardiomyopathy (Loeffen, Smeitink et al. 2000). Recently, Assouline et al summarized general phenotypes observed in patients with *NDUFS4* mutations, which included apart from the abovementioned signs and symptoms, pyramidal syndrome, psychomotor retardation / regression, depressed tendon reflexes and hepatomegaly. Intra-uterine growth retardation, in some patients accompanied by premature birth and vomiting, was also occasionally observed. Muscle impairment with atrophy,

rhabdomyolysis or abnormal electromyography (EMG), liver impairment, peripheral neuropathy, anaemia, hyperkinesia's/dystonia/athetoid movements and deafness/sensorineural hearing loss were not described in these patients. Death, in patients with a shorter life expectancy, was always caused due to cardio-respiratory failure (Assouline, Jambou et al. 2012).

### **Cell biological consequences of pathogenic *NDUFS4* mutations**

*C1 expression and intrinsic catalytic activity* – Blue native polyacrylamide gel electrophoresis (BN-PAGE) of mitochondrial-enriched fractions from primary skin fibroblasts of patients with a pathogenic mutation in the *NDUFS4* gene invariably showed a single ~830-kDa subcomplex that lacked in gel activity (Scacco, Petruzzella et al. 2003, Ugalde, Janssen et al. 2004, Petruzzella, Panelli et al. 2005, Verkaart, Koopman et al. 2007a). Intriguingly, the same fractions displayed a marked rotenone-sensitive NADH: ubiquinone oxidoreductase, or CI, activity in a spectrophotometric assay using freeze-thawing rather than mild detergent solubilisation (Budde, van den Heuvel et al. 2003, Scacco, Petruzzella et al. 2003, Ugalde, Janssen et al. 2004). These data suggest that the ~830-kDa subcomplex lacks the dehydrogenase moiety. Analysis of the amount of immunoreactive ~830-kDa subcomplex in patient fibroblasts with a mutation in the *NDUFS4* gene showed a significant decrease as compared to the amount of ~1-MDa holocomplex in healthy control fibroblasts. Regression analysis of data from 13 CI deficient patients including 4 patients with a pathogenic *NDUFS4* mutation revealed a positive linear correlation between the spectrophotometrically measured CI activity and the amount of holocomplex or its ~830-kDa subcomplex (Valsecchi, Koopman et al. 2010). This linear relationship was interpreted to suggest that CI deficiency is primarily a CI expression problem rather than a CI intrinsic catalytic problem. Furthermore, it was concluded that the role of the *NDUFS4* subunit is to reinforce the physical coupling between the ~830-kDa subcomplex and the dehydrogenase moiety. The latter conclusion is in agreement with the general idea that the *NDUFS4* subunit plays an important role in maintaining CI stability (Kruse, Watt et al. 2008). In the case of the W96X and R106X mutation, a parallel decrease in complex III (CIII) activity was observed, suggesting a functional interaction between CI and CIII (Ugalde, Janssen et al. 2004). More recently, evidence was provided that in the absence of the *NDUFS4* subunit CI activity is preserved in a supercomplex that also includes CIII (Calvaruso, Willems et al. 2012). This finding may explain the presence of a significant amount of CI activity, referred to as residual CI activity, in skin fibroblasts and muscle biopsies of patients with a pathogenic *NDUFS4* mutation.

*Mitochondrial membrane potential, cellular ROS production and intracellular Ca<sup>2+</sup> homeostasis* – Primary skin fibroblasts of patients with a pathogenic mutation in the *NDUFS4* gene invariably showed increased oxidation rates of H<sub>2</sub>Et and CM-H<sub>2</sub>DCFDA (Verkaart, Koopman et al. 2007a). When the rate of ROS production grossly exceeds the capacity of the cell's antioxidant systems their level will increase to such a degree that cellular molecules will be damaged leading to cellular dysfunction and, eventually, cell death. However, patient skin fibroblasts maintained in standard culture medium failed to show any increase in lipid peroxidation (Verkaart, Koopman et al. 2007b). In sharp contrast, healthy control fibroblasts treated with rotenone displayed a significant increase in lipid peroxidation which was completely prevented by the mitochondrial-targeted antioxidant MitoQ. Patient fibroblasts neither showed a change in cytosolic and/or mitochondrial thiol redox state (Koopman, Verkaart et al. 2005, Verkaart, Koopman et al. 2007b). Taken together, these data demonstrate that CI deficient fibroblasts maintained in standard culture medium are adequately adapted to the increased rate of ROS production. In addition to an increase in ROS production rate, fibroblasts of patients with a pathogenic mutation in the *NDUFS4* gene invariably showed a less negative mitochondrial membrane potential ( $\Delta\psi$ ) (Distelmaier, Visch et al. 2009). Regression analysis of data from 10 CI deficient patients including 3 patients with a pathogenic mutation in the *NDUFS4* gene revealed a negative linear correlation between the mitochondrial membrane potential and the rate of CM-DCF formation. A similar negative linear correlation was observed between the mitochondrial membrane potential and the Ca<sup>2+</sup> content of the endoplasmic reticulum (ER). ER Ca<sup>2+</sup>, through its stimulus-induced release from the ER into the ER-mitochondrial contact sites and its consequent uptake by the mitochondria, is responsible for the stimulus-induced increase in mitochondrial ATP production (Willems, Valsecchi et al. 2008, Valsecchi, Esseling et al. 2009). Indeed, CI deficient patient fibroblasts showed a significant decrease in stimulus-induced mitochondrial Ca<sup>2+</sup> mobilization and ATP production (Visch, Rutter et al. 2004, Visch, Koopman et al. 2006). Treatment of patient fibroblasts with the water-soluble vitamin E analog, Trolox (6-hydroxy-2,5,7,8-tetramethylchroman-2-carboxylic acid), lowered the rate of CM-DCF formation, normalized  $\Delta\psi$  and increased the ER Ca<sup>2+</sup> content. Subsequent stimulation showed an enhanced increase in cytosolic Ca<sup>2+</sup> concentration and a normalized increase in mitochondrial Ca<sup>2+</sup> concentration, NADH level and ATP production (Distelmaier, Visch et al. 2009). These findings exemplify the feasibility that certain aspects of the cell's physiology may be altered in complex I deficiency as a consequence of the increased rate of reactive oxygen species (ROS) production. Consequences of nDNA-encoded mutations in CI are schematically represented in (Figure 1).

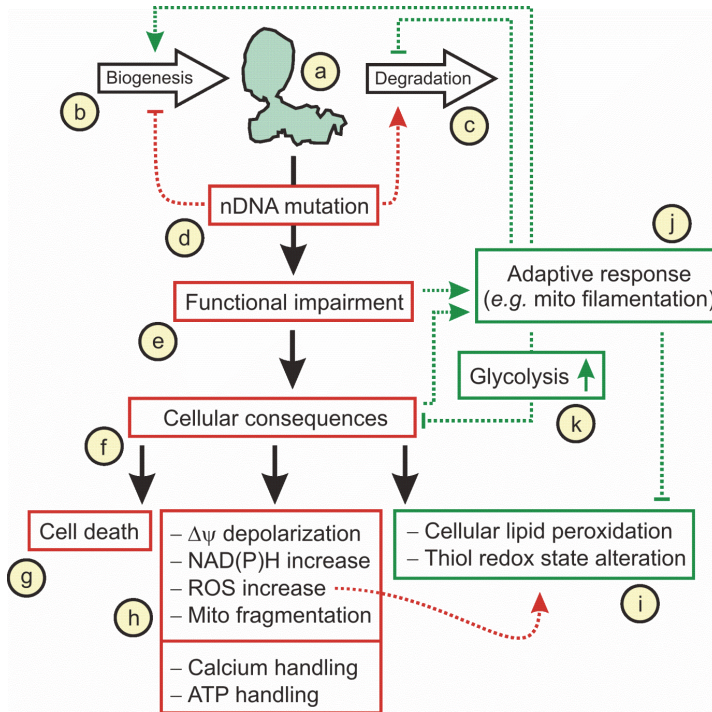


**Figure 1. Consequences of nDNA-encoded mutations in CI.** The total amount of fully assembled and active CI within the cell (a) is determined by the balance between CI biogenesis (b) and degradation (c). Mutations in nDNA-encoded CI subunits (d) lead to functional impairment of CI (e) and induce changes in cellular physiology (f, h). If these changes are not properly counterbalanced by adaptive responses (j), including alterations in mitochondrial morphology and glycolysis upregulation (k), cell death can occur (g). This is likely reflected by the fact that fibroblasts from patients with isolated CI deficiency display increased ROS levels but no increased cellular lipid peroxidation or changes in thiol redox state (i). This figure is based upon experimental data obtained in fibroblasts of patients with nDNA-encoded isolated CI deficiency. Primary and possible adaptive pathways are indicated in red and green, respectively. **Abbreviations:** Dy, mitochondrial membrane potential; NADH, reduced nicotinamide adenine dinucleotide; NADPH, reduced nicotinamide adenine dinucleotide phosphate; nDNA, nuclear DNA; ROS, reactive oxygen species.

### Mouse models for *Ndufs4* deficiency

*The Whole-body (WB) Ndufs4<sup>-/-</sup> mouse* – The WB *Ndufs4<sup>-/-</sup>* mouse was generated by deletion of exon 2, resulting in a frame shift and undetectable levels of the *Ndufs4* protein (Kruse, Watt et al. 2008). During the first ~30 days of life, i.e. until ~P30, behaviour of *Ndufs4<sup>-/-</sup>* mice was similar to that of their wild type and heterozygous littermates (Fig. 2). However, already at ~P12, *Ndufs4<sup>-/-</sup>* mice were smaller and lighter

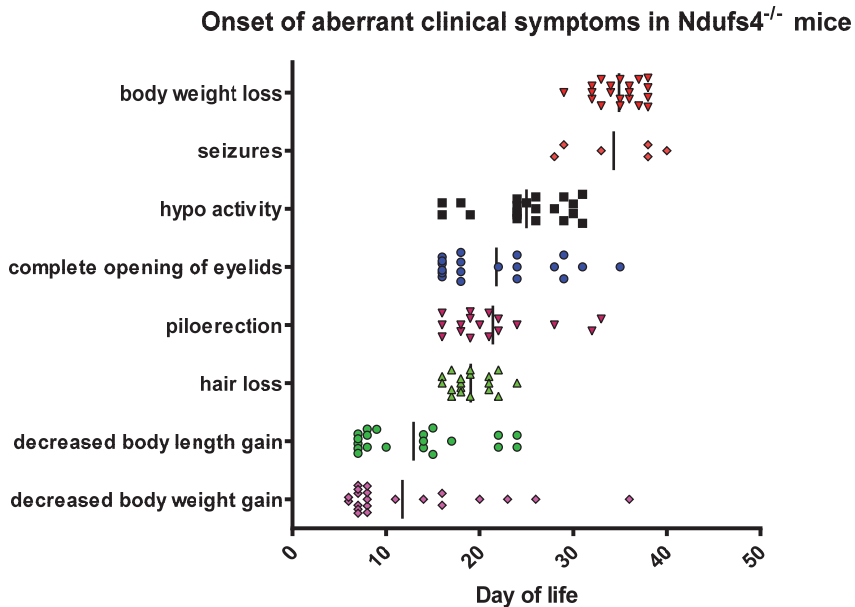


**Figure 2. Onset of aberrant clinical symptoms in *Ndufs4*<sup>-/-</sup> mice.** *Ndufs4*<sup>-/-</sup> mice (n=23) were phenotypically characterized by comparing them to their WT litter mates (n=23). The “X-axis” is denoted by day of life, when the symptom was first observed in the *Ndufs4*<sup>-/-</sup> mice as compared to its WT counterpart. The “Y-axis” represents the phenotype / symptom observed in the *Ndufs4*<sup>-/-</sup> mouse.

than their wild type littermates. At day 20 of life, most *Ndufs4*<sup>-/-</sup> animals lost their body hair, which grew back during the next hair-growth cycle. Between P35 and P50, *Ndufs4*<sup>-/-</sup> animals stopped gaining weight and started to display weight loss. This was accompanied by worsening ataxia, stopped grooming and, finally, death from a fatal encephalomyopathy. Further phenotypic features of the *Ndufs4*<sup>-/-</sup> mice include a decreased body temperature (2°C), cataracts, blindness, hearing loss, loss of motor skills and lethargy (Kruse, Watt et al. 2008). *Ndufs4*<sup>-/-</sup> animals displayed significantly higher serum lactate levels than wild type mice. On the other hand, *in vivo* <sup>31</sup>P-NMR spectroscopy analysis of ATP turnover reactions in hindlimb muscle revealed the lack of any difference in resting ATP demand and maximal rate of mitochondrial ATP production between *Ndufs4*<sup>-/-</sup> and wild type mice. A similar observation was reached for the resting O<sub>2</sub> consumption rate determined by *in vivo* optical spectroscopy of haemoglobin and myoglobin saturation levels. Mitochondrial ultrastructure appeared normal although large subsarcolemmal clusters of mitochondria were present in the *soleus* but not in the extensor *digitorum longus* muscle fibers of *Ndufs4*<sup>-/-</sup> mice.

Furthermore, a marked decrease in CI activity was observed in *Ndufs4*<sup>-/-</sup> mice while cytochrome c oxidase (COX) activity was similar to wild type. Progressive neuronal deterioration and gliosis were observed in specific brain areas of the *Ndufs4*<sup>-/-</sup> mice. These observations corresponded to behavioural changes during disease advance, with early involvement of the olfactory bulb, cerebellum, and vestibular nuclei (Quintana, Kruse et al. 2010). Neurons, particularly in those brain regions, showed aberrant mitochondrial morphology. Electron microscopy analysis revealed that mitochondria were swollen and/or displayed a compact cristae structure. Activation of caspase 8, but not caspase 9, in the affected brain regions of *Ndufs4*<sup>-/-</sup> mice was suggested to reflect initiation of the extrinsic apoptotic pathway. The limited caspase 3 activation and the predominance of ultrastructural features of necrotic cell death suggest a switch from apoptosis to necrosis in affected neurons. From these data it was suggested that dysfunctional CI in specific brain regions results in progressive glial activation that, in turn, promotes neuronal death and ultimately mortality of the mouse. CI activity in submitochondrial particles from liver of *Ndufs4*<sup>-/-</sup> mice was undetectable using spectrophotometric assays. However, CI-driven O<sub>2</sub> consumption in intact liver cells was about half that of wild type. Native gel electrophoresis revealed reduced levels of intact CI. In our laboratory BN-PAGE has been performed on different tissues of the *Ndufs4*<sup>-/-</sup> mouse. Instead of fully assembled CI an inactive 830-kDa subcomplex was observed (Calvaruso, Willems et al. 2012, Valsecchi, Grefte et al. 2013). A similarly sized 830-kDa CI subcomplex has been reported in patients with *NDUFS4* mutations (Ugalde, Janssen et al. 2004, Ogilvie, Kennaway et al. 2005, Vogel, Dieteren et al. 2007, Papa, Petruzzella et al. 2009, Valsecchi, Koopman et al. 2010). Taken together, these findings suggest that when the *Ndufs4* subunit is absent, CI fails to assemble properly or is instable.

*The whole body Ndufs4<sup>fkyl/fky</sup> mouse* – Leong et al (Leong, Komen et al. 2012) inserted a transposable element into the *Ndufs4* gene causing aberrant transcript splicing and absence of the *Ndufs4* protein in all tissues of the homozygous *Ndufs4<sup>fkyl/fky</sup>* mouse. The physical and behavioral symptoms displayed by the *Ndufs4<sup>fkyl/fky</sup>* mouse included temporary fur loss, growth retardation, unsteady gait and abnormal body posture when suspended from the tail. Similar phenotypic changes were observed in the *Ndufs4*<sup>-/-</sup> mouse (Kruse, Watt et al. 2008). *Ndufs4* protein was not detected in any of the tissues analysed namely, brain, heart, muscle, liver and kidney. CI enzymatic activity was significantly reduced in all tissues tested. ATP synthesis capacity, which was determined in the presence of glutamate and malate, was significantly reduced in brain and heart of the *Ndufs4<sup>fkyl/fky</sup>* mutant. Analysis of CI in the *Ndufs4<sup>fkyl/fky</sup>*

mutant by BN-PAGE revealed a faster migrating crippled subcomplex. This crippled subcomplex lacked subunits of the N-module that contains the NADH binding site. This subcomplex contained two assembly factors which were not present in fully assembled CI. Further, metabolomic analysis in blood by tandem mass spectrometry established increased hydroxyacylcarnitine, glycine, phenylalanine and homocitrulline. The increased level of hydroxyacylcarnitine was interpreted to suggest that CI dysfunction causes an imbalance of NADH and NAD<sup>+</sup> resulting in inhibited mitochondrial fatty acid  $\beta$ -oxidation.

*The Nes Ndufs4<sup>-/-</sup> and PC Ndufs4<sup>-/-</sup> mouse* – Two different brain-specific *Ndufs4<sup>-/-</sup>* mouse models have been generated (Quintana, Kruse et al. 2010). Mice that brain-specifically lack *Ndufs4* were generated by crossing *Ndufs4<sup>lox/lox</sup>* mice with mice expressing Cre recombinase from the *Nestin* locus. The phenotype of the resulting “*Nes Ndufs4<sup>-/-</sup>*” mouse generally resembled that of the WB *Ndufs4<sup>-/-</sup>* mouse including retarded growth, loss of motor ability, breathing abnormalities, and a maximum life span of approximately 7 weeks. Because both the WB and *Nes Ndufs4<sup>-/-</sup>* mouse showed cell death of Purkinje cells in the lobules of the cerebellum, also a Purkinje cell specific *Ndufs4<sup>-/-</sup>* mouse was generated. This PC *Ndufs4<sup>-/-</sup>* mouse displayed only mild behavioural and neuropathological abnormalities. Combined with the results obtained in the WB *Ndufs4<sup>-/-</sup>* and *Nes Ndufs4<sup>-/-</sup>* mouse models, this suggests that death of Purkinje cells in *Nes Ndufs4<sup>-/-</sup>* animals is likely a secondary effect possibly due to dysregulation of the cerebellar circuitry or hypersensitivity to hypoxia (Quintana, Kruse et al. 2010).

*The Conditional WB Ndufs4<sup>-/-</sup> mouse* – Conditional knockout of the *Ndufs4* gene was achieved by crossing *Ndufs4<sup>lox/lox</sup>* mice with mice bearing an inducible Cre recombinase gene. The latter gene can be induced in most cells by tamoxifen (Quintana, Kruse et al. 2010). Tamoxifen treatment at day ~P60 induced a large decrease in abundance of the *Ndufs4* protein in most brain regions. Effects in other tissues have not been reported. Seven months after tamoxifen treatment the mice displayed a phenotype that resembled that of early stage WB *Ndufs4<sup>-/-</sup>* mice. This rather mild phenotype, also in comparison to *Nes Ndufs4<sup>-/-</sup>* mice, might be explained by incomplete or absent recombination in some brain regions, despite intensive tamoxifen treatment. Alternatively, complete absence of *Ndufs4* during animal development might have more severe consequences than its (partial) absence at a later stage of development.

*The Ndufs4-PM mouse* – This mouse model was generated by introducing a point mutation in the *Ndufs4* gene, resulting in loss of the last 10-15 amino acids of the last exon of the protein (Ingraham, Burwell et al. 2009). Interestingly, heterozygous

mice showed expression and even integration of mutant *Ndufs4* protein in holo-CI. In heart mitochondria, the amount of wild type *Ndufs4* protein present in holo-CI was 2.5-fold higher than that of the mutant subunit. The presence of the mutant subunit resulted in a significant decrease in CI activity and CI-linked  $O_2$  consumption and increased lactate levels. The clinical phenotype of the heterozygous *Ndufs4*-PM mouse was not reported. In sharp contrast to the other four mouse models, homozygote *Ndufs4*-PM mice were not viable and their presence in the early embryonic state (<E9) could not be demonstrated. This suggests that in homozygous animals the presence of a mutated *Ndufs4* protein leads to a much more severe phenotype than its complete absence.

*The (Conditional) Heart-specific Ndufs4<sup>-/-</sup> mouse* – Sterky *et al* (Sterky, Hoffman *et al.* 2012) generated a heart specific *Ndufs4<sup>-/-</sup>* mouse by disrupting the *Ndufs4* gene in heart tissue. Although they observed a dramatic reduction of CI activity, oxidation of CI-linked substrates was only mildly reduced in intact heart mitochondria. As previously reported by Calvaruso *et al* (Calvaruso, Willems *et al.* 2012), they demonstrated the formation of supercomplexes with CI activity. Chouchani *et al* (Chouchani, Methner *et al.* 2014) showed that heart-specific *Ndufs4<sup>-/-</sup>* mice developed a severe hypertrophic cardiomyopathy which occurred in the absence of increased levels of mitochondrial hydrogen peroxide, accumulation of oxidative damage makers and induction of apoptosis or tissue fibrosis. This suggests that CI dysfunction alone might be sufficient to drive the hypertrophic cardio-myopathy independently of elevated levels of mitochondrial hydrogen peroxide and increased oxidative damage. Karamanlidis *et al* (Karamanlidis, Lee *et al.* 2013), created a conditional heart specific *Ndufs4<sup>-/-</sup>* mouse and observed a 60% decrease in CI-linked respiration. However, the conditional heart specific *Ndufs4<sup>-/-</sup>* mouse maintained a normal cardiac function *in vivo* and a high energy phosphate content in the isolated perfused heart. They developed accelerated heart failure with pressure overload. The increased NADH/NAD<sup>+</sup> ratio, due to inhibition of CI, caused inhibition of Sirt3 resulting in protein acetylation and sensitization of the mitochondrial permeability transition pore (mPTP). NAD<sup>+</sup> precursor supplementation partially normalized the NADH/NAD<sup>+</sup> ratio, protein acetylation and mPTP sensitivity. The authors concluded that NAD<sup>+</sup> precursor supplementation could be a potential therapeutic approach for mitochondrial dysfunction.

*The Conditional Hematopoietic-, Liver- and TLR2/4-specific Ndufs4<sup>-/-</sup> mouse models* – Jin *et al* (Jin, Wei *et al.* 2014) used the WB *Ndufs4<sup>-/-</sup>* mouse to investigate the effect



of CI deficiency on innate immunity and bone remodelling and observed systemic inflammation and osteoporosis. They then created a conditional hematopoietic system-specific *Ndufs4*<sup>-/-</sup> mouse and observed an intrinsic change in lineage from osteoclast to macrophage. Next, they created a conditional liver-specific *Ndufs4*<sup>-/-</sup> mouse and observed an increase in fatty acid and lactate concentration in the circulation, causing a further activation of the *Ndufs4*<sup>-/-</sup> macrophages by the induction of ROS and a decrease in osteoclast lineage commitment in *Ndufs4*<sup>-/-</sup> progenitors. Finally, they showed that inflammation and osteoporosis could be abated in a conditional Toll like receptor 2/4 (TLR2/4)-specific *Ndufs4*<sup>-/-</sup> mouse. It was concluded that healthy mitochondria suppress macrophage activation and inflammation while promoting osteoclast differentiation and bone resorption via cell-autonomous and systemic regulation.

### Pharmacological intervention in complex I deficiency

*In vivo* treatment of CI deficiency is tremendously challenging because a possible beneficial drug effect also depends on the way of administration, concentration, (bio) distribution, turnover and clearance. In addition, (long term) drug effectiveness and toxicity have to be considered. The possibilities of pharmacological intervention in the case of mitochondrial disorders have been extensively reviewed (Finsterer and Segall 2010, Hersh 2010, Jin, Randazzo et al. 2010, Moncada 2010, Valsecchi, Koopman et al. 2010, Wallace, Fan et al. 2010, Wenz, Williams et al. 2010, Koopman, Beyrath et al. 2016). In our research, we have successfully applied an antioxidant (Trolox) and a benzothiazepine (CGP37157) to mitigate several cellular consequences of CI deficiency. Below, we briefly present several strategies that might prove useful for mitigation of the clinical consequences of CI deficiency.

*The non-mitochondria-targeted antioxidants vitamin E, vitamin C and N-acetyl cysteine amide (AD4)* – Because of its lipophilic nature, **vitamin E** or  $\alpha$ -tocopherol can effectively detoxify lipid peroxy radicals (Niki 1991). Chronic oral administration of vitamin E significantly reduced the increase in mitochondrial oxidative damage, the decrease in mitochondrial manganese-dependent superoxide dismutase (MnSOD or SOD2) and the decrease in mitochondrial state 3 respiration in brain of aging mice (Navarro, Gomez et al. 2005). These effects were paralleled by an increased lifespan and preservation of neurological performance and exploratory activity. Importantly, the levels of  $\alpha$ -tocopherol in mouse brain increased from 11.5 to 26.2 nmol/g brain, showing that it was able to cross the blood brain barrier. In humans there is still controversy on the use of vitamin E supplementation (Navarro and Boveris 2010). For

instance, a meta-analysis claimed that vitamin E supplementation increases human mortality (Bjelakovic, Nikolova et al. 2007). However, these results are challenged by clinical evidence that vitamin E supplements are safe at high dosages (Hathcock, Azzi et al. 2005) and by the reported effects of vitamins E and C in the reduction of the prevalence/incidence of Alzheimer disease in an elderly population (Zandi, Anthony et al. 2004). **Vitamin C**, or ascorbate, is well known for its antioxidant capacity. Because of its aqueous nature, vitamin C cannot detoxify lipid peroxyl radicals (Niki 1991). However, it is very effective in regenerating active vitamin E from its radicals formed during the detoxification of lipid peroxyl radicals. Human skin fibroblasts have the ability to import vitamin C via a  $\text{Na}^+$ -dependent carrier (Welch, Bergsten et al. 1993). In human skin fibroblasts from patients with respiratory chain deficiencies, vitamin C was able to reduce superoxide production while increasing respiratory chain function (Sharma and Mongan 2001). In aging human fibroblasts *in vitro*, ascorbate prevented the age-dependent decline in respiratory chain activities (Ghneim and Al-Sheikh 2010). **N-acetyl cysteine amide** or AD4 is a blood-brain-barrier penetrating antioxidant that can decrease oxidative stress both *in vitro* and *in vivo*. *Ndufs4*<sup>-/-</sup> mice were injected intraperitoneally with AD4 (150mg/kg/day) from postnatal day 21 to 28. This short period of administration was sufficient to delay the onset of the neurodegenerative phenotype and improve the motor defects observed in *Ndufs4*<sup>-/-</sup> mice, stressing a role for elevated ROS in the development of the disease phenotype (Liu, Zhang et al. 2015).

*The mitochondria-targeted antioxidants mitoquinone (MitoQ), SkQ and Szeto-Schiller (SS)-31 peptide* – Currently, there are several strategies that allow oxidants to be targeted to mitochondria in living cells (Finsterer and Segall 2010, Hersh 2010, Jin, Randazzo et al. 2010, Moncada 2010, Valsecchi, Koopman et al. 2010, Wallace, Fan et al. 2010, Wenz, Williams et al. 2010). Here, we will discuss the triphenylphosphonium (TPP) compounds and Szeto-Schiller (SS) peptides in more detail. One group of compounds which specifically accumulate in mitochondria consists of antioxidants that are covalently linked to the triphenylphosphonium (TPP) cation. These molecules are engineered in such a way that they pass phospholipid bilayers without requiring a specific uptake mechanism. Because of their positive charge, they preferentially accumulate (500-1000 fold) within mitochondria in a  $\Delta\psi$ -dependent manner (Murphy and Smith 2007). A potential drawback of these compounds might be their dependence on  $\Delta\psi$ , which, as we have reported (Distelmaier, Visch et al. 2009), is less negative in human CI deficiency. As a consequence, their concentration might not reach the sufficiently high values in cells of CI deficient patients. A well-

studied member of the TPP family is [10-(4,5-dimethoxy-2-methyl-3,6-dioxo-1,4-cyclohexadien-1-yl)decyl]triphenylphosphonium, referred to as **mitoquinone** or MitoQ. Given its relatively large hydrophobicity, MitoQ is preferentially adsorbed to the matrix-facing leaflet of the MIM, with its TPP moiety at the membrane surface at the level of the fatty acid carbonyls and its alkyl chain and ubiquinol moiety inserted into the hydrophobic core of the lipid bilayer (Murphy and Smith 2007). In healthy fibroblasts treated with rotenone (100 nM, 72 h), MitoQ prevented rotenone-induced mitochondrial elongation and lipid peroxidation but did not block rotenone-induced H<sub>2</sub>O<sub>2</sub> oxidation regarded as a measure of mitochondrial superoxide production (Koopman, Verkaart et al. 2005). This is compatible with MitoQ being localized inside the MIM and thereby preventing oxidation of mitochondrial lipids. Our results show that MitoQ can accumulate to sufficiently high levels in complex I deficient patient fibroblasts. Use of MitoQ in mouse models as well as patients *in vivo*, revealed that its use is safe *in vivo*, even during long term use. Administration in the drinking water of mice resulted in measurable levels of MitoQ in all tissues, including brain, although the concentrations differed between organs (Rodriguez-Cuenca, Cocheme et al. 2010). This illustrates that MitoQ is able to cross the blood-brain barrier which is an important hurdle in therapies for CI deficiency. Furthermore, MitoQ was excreted in the urine and bile as unchanged MitoQ or with sulfation or glucuronidation of the quinol ring with no indication of other metabolites (Li, Zhang et al. 2007, Ross, Prime et al. 2008). In addition to MitoQ also other antioxidant variants like MitoVitE, MitoTEMPO and MitoPBN have been developed (Murphy and Smith 2007). The detailed *in vivo* characteristics of these compounds and their effects in CI deficiency require further investigation. Skulachev *et al* developed [10-(6'-plastoquinonyl)decyl]triphenylphosphonium, referred to as **SkQ** (Skulachev, Anisimov et al. 2009). SkQ consists of a plastoquinone moiety linked to TPP. When compared to MitoQ, SkQ displayed a higher permeability in a variety of *in vitro*, *ex vivo* and *in vivo* models (Antonenko, Avetisyan et al. 2008). Moreover, SkQ was shown to possess a strong antioxidant activity at relatively low (nM) concentrations, whereas at relatively high ( $\mu$ M) concentrations SkQ was shown to act as a pro-oxidant. Applied *in vivo*, SkQ displayed beneficial effects during hydrogen peroxide- and ischemia-induced heart arrhythmia, heart infarction, kidney ischemia and stroke (Bakeeva, Barskov et al. 2008). Currently, no data of SkQ in relation to CI deficiency are available. However, it would be interesting to determine whether SkQ is able to influence the downstream effects of CI deficiency. Another group of mitochondria-targeted antioxidants are the so called **Szeto-Schiller (SS) peptides**. This is a novel class of small cell permeable peptide antioxidants that target to mitochondria in a  $\Delta\psi$ -

independent manner. The structural motif of these peptides centres on alternating aromatic residues and basic amino acids (Szeto 2006). SS-peptides are small and relatively easy to synthesize, readily soluble in water, and resistant to peptidase degradation. Besides, they display a high blood-brain barrier permeability and a relatively long elimination half-life in sheep and rats, which allows their testing in neurological disease models (Szeto 2006). In cell experiments, SS-31 accumulated 5000-fold in the mitochondrial fraction. SS-31 was localized close to the site(s) of mitochondrial ROS production and protected against mitochondrial oxidative damage and further ROS production (Zhao, Zhao et al. 2004). SS-31 prevented  $\Delta\psi$  depolarization, reduced cellular ROS and inhibited apoptosis in neurons treated with the pro-oxidant tert-butyl-hydroperoxide (Zhao, Luo et al. 2005). The effects of SS-peptides in CI deficiency models are currently unknown.

*The benzothiazepine CGP37157* – CGP37157, a benzothiazepine, is an inhibitor of mitochondrial  $\text{Na}^+/\text{Ca}^{2+}$  exchange (Cox and Matlib 1993). CGP37157 normalized aberrant mitochondrial  $\text{Ca}^{2+}$  handling during hormone stimulation of cybrid cells carrying the  $\text{tRNA}^{\text{lys}}$  mutation associated with MERRF (Myoclonic Epilepsy with Ragged Red Fibres) syndrome (Brini, Pinton et al. 1999). To directly interfere with aberrant mitochondrial  $\text{Ca}^{2+}$  signalling, we investigated the effect of CGP37157 in fibroblasts from patients with isolated CI deficiency (Visch, Rutter et al. 2004). Short-term pre-treatment with CGP37157 (1  $\mu\text{M}$ , 2 min) fully normalized the amplitude of the hormone-induced mitochondrial  $\text{Ca}^{2+}$  signal, without altering this parameter in healthy fibroblasts. Also the hormone-induced increase in mitochondrial and cytosolic ATP concentration, which were significantly lowered in these patient fibroblasts, were fully normalized by CGP37157 treatment. The effect of CGP37157 was independent of the presence of extracellular  $\text{Ca}^{2+}$ , excluding a stimulatory effect on  $\text{Ca}^{2+}$  entry across the plasma membrane. These findings suggest that the mitochondrial  $\text{Na}^+/\text{Ca}^{2+}$  exchanger is a potential target for drugs aiming to restore or improve  $\text{Ca}^{2+}$ -stimulated mitochondrial ATP synthesis.

*Riboflavin* – Riboflavin, or vitamin B2, is a precursor of flavin mononucleotide (FMN) and flavin adenine dinucleotide (FAD), which function as cofactors in CI and CII, respectively. *In vitro*, riboflavin treatment of CI-deficient patient fibroblasts virtually normalized the rate of ATP production (Bar-Meir, Elpeleg et al. 2001). *In vivo*, riboflavin supplementation, with or without co-administration of carnitine, was reported to be effective in a number of patients with CI deficiency. Primary effects included improvement of muscle tone, exercise capacity/tolerance and serum lactate levels, although the results of the treatment substantially differed between different

studies [reviewed by (Marriage, Clandinin et al. 2003)]. A mechanism was proposed in which riboflavin inhibits the proteolytic breakdown of CI, leading to an increase in CI enzymatic activity (Vergani, Barile et al. 1999, Gold and Cohen 2001, Marriage, Clandinin et al. 2003). Dosages of riboflavin used in treatment of OXPHOS patients ranged between 9-300 mg/day without observation of adverse effects (Marriage, Clandinin et al. 2003). Although the results obtained with riboflavin vary, they clearly demonstrate that in some patients with CI deficiency, riboflavin alone or in combination with other supplements is beneficial (Marriage, Clandinin et al. 2003, Panetta, Smith et al. 2004).

*The modulators of PGC-1 $\alpha$  activity fibrates and resveratrol* – Peroxisome proliferator-activated receptor (PPAR) co-activator 1 $\alpha$  (PGC-1 $\alpha$ ), is a transcriptional factor regulator that stimulates transcription of genes involved in cellular energy metabolism (Scarpulla 2008, Wenz 2009). PGC-1 $\alpha$  influences mitochondrial biogenesis and function by modulating the transcription of the mtDNA transcription factor A (Tfam) gene (Wu, Puigserver et al. 1999). Several ways to therapeutically modulate PGC-1 $\alpha$  have been reported. The pan (*i.e.* a, d and g) PPAR agonist **bezafibrate** has been demonstrated to increase the activity of CI and other ETC enzymes (complex III and complex IV) in healthy and OXPHOS-deficient cells through PGC-1 $\alpha$  upregulation (Bastin, Aubey et al. 2008). In COX10 KO mice displaying progressive myopathy, bezafibrate stimulated OXPHOS gene expression in skeletal muscle and induced a global increase in oxidative metabolism (Wenz, Diaz et al. 2008). **Resveratrol** is a polyphenolic phytoalexin that is abundantly present in grapes, peanuts and red wine. It stimulates sirtuin activity and thereby transcription of nDNA-encoded genes involved in energy metabolism (Shin, Cho et al. 2009, Ungvari, Labinskyy et al. 2009). Dietary delivery of resveratrol increased mitochondrial abundance and aerobic capacity in cultured endothelial cells and mice (Baur, Pearson et al. 2006, Lagouge, Argmann et al. 2006, Robb, Winkelmolen et al. 2008, Csiszar, Labinskyy et al. 2009). Resveratrol also affects the cellular antioxidant system. Both oral and subcutaneously injected resveratrol altered the activities of the key antioxidant enzymes glutathione peroxidase (GPx), catalase (CAT) and (mitochondrial) manganese superoxide dismutase (MnSOD) and increased the mitochondrial content in heart, brain and liver (Robb, Winkelmolen et al. 2008). A double blind healthy volunteer study showed that frequent administration of resveratrol is well-tolerated, but results in low plasma concentrations even at a 4-hr oral administration regime (Almeida, Vaz-da-Silva et al. 2009). As far as we know, no data are currently available on side effects of continuous resveratrol administration. PGC-1 $\alpha$  levels in skeletal muscle can also be stimulated

by endurance exercise via a mechanism involving repetitive changes in cytosolic free  $\text{Ca}^{2+}$  concentration and AMP-activated protein kinase (AMPK) activation (Wu, Kanatous et al. 2002, Ojuka 2004, Benton, Wright et al. 2008). It was suggested that, in healthy subjects, endurance exercise increases skeletal muscle oxidative capacity by improving the metabolic flux through CI (Daussin, Zoll et al. 2008). Endurance exercise improved the physiological and biochemical features in muscles of patients with mtDNA mutations (Taivassalo and Haller 2004, Taivassalo and Haller 2005).

*Rapamycin* – Rapamycin is a specific inhibitor of the mechanistic target of rapamycin (mTOR) signalling pathway. Johnson and co-workers investigated the use of rapamycin as a potential therapeutic strategy in the WB *Ndufs4*<sup>-/-</sup> mice and observed a delay in onset of neurological symptoms, reduction in neuroinflammation, prevention of brain lesions and increase in median and maximum survival age (Kruse, Watt et al. 2008, Johnson, Yanos et al. 2013). The median survival age in males and females was reported to be (114 and 111 days) respectively. Although, they could not delineate the exact mechanism of rescue, they observed that rapamycin induced a metabolic shift from glycolysis to amino acid catabolism thus alleviating the buildup of glycolytic intermediates.

*Nicotinamide Riboside* – Nicotinamide Riboside (NR) is used as a precursor for nicotinamide adenine dinucleotide or  $\text{NAD}^+$ . Karamanlidis et al treated the conditional heart specific *Ndufs4*<sup>-/-</sup> mouse with NR and observed partial normalization of the  $\text{NAD}^+/\text{NADH}$  ratio, the protein acetylation level and the sensitivity of the mitochondrial permeability transition pore (mPTP) (Karamanlidis, Lee et al. 2013).

*The poly (adenine diphosphate-ribose) polymerase (PARP)-1 inhibitor PJ34* – PARP proteins are involved in DNA repair and programmed cell death. Felici et al treated *Ndufs4*<sup>-/-</sup> mice with the PARP inhibitor N-(6-oxo-5,6-dihydrophenanthridin-2-yl)-(N,Ndimethylamino) acetamide hydrochloride (PJ34) from postnatal day 30 to 50 and observed increased exploratory behaviour and motor skills (Felici, Cavone et al. 2014). PJ34 treatment reduced astrogliosis in the olfactory bulb and motor cortex but did not reduce neuronal loss. Finally, PJ34 did not delay death. Recently, it was speculated that NR and PJ34 improve mitochondrial function by increasing the intracellular levels of  $\text{NAD}^+$  (Cerutti, Pirinen et al. 2014).

*Stabilization of CI* – Observations in patient and mouse cells indicate that CI is stabilized by its physical interaction with CIII (Acin-Perez, Bayona-Bafaluy et al. 2004, Fernandez-Vizarra, Bugiani et al. 2007). Even when the stability of CI is seriously compromised as is the case in the absence of the NDUFS4 subunit, partially assembled

CI can associate with CIII into supercomplexes resulting in rotenone-sensitive CI activity (Ogilvie, Kennaway et al. 2005, Lazarou, McKenzie et al. 2007, Calvaruso, Willems et al. 2012, Sterky, Hoffman et al. 2012). Another important determinant of the structural and functional integrity of CI is the MIM lipid cardiolipin (Schlame, Rua et al. 2000, Sharpley, Shannon et al. 2006, Houtkooper and Vaz 2008). Cardiolipin is very sensitive to peroxidation by mitochondrial ROS and cardiolipin peroxidation was demonstrated to decrease CI activity in bovine heart and rat heart/liver mitochondria (Petrosillo, Matera et al. 2009). This means that prevention of mitochondrial ROS production and/or ensuing cardiolipin peroxidation might be a good strategy to increase CI stability in patient cells as well as *in vivo*. This idea is in agreement with the above-discussed observation that MitoQ prevents superoxide-mediated lipid peroxidation and consequent changes in mitochondrial morphology in rotenone-treated healthy skin fibroblasts (Verkaart, Koopman et al. 2007b).

### **Nutritional intervention: the ketogenic diet**

Nutritional approaches like a ketogenic diet may be very useful. Ketogenic diets have a high fat content, are adequate in protein and low in carbohydrates. During the regime of a ketogenic diet, ketone bodies are used as a substitute for glucose to generate energy for the brain. Intriguingly, ketone bodies appear to be a more efficient source of energy per unit of oxygen than glucose (Veech, Chance et al. 2001). Evidence has been provided that a ketogenic diet induces a coordinated upregulation of mitochondrial genes involved in energy metabolism and might stimulate mitochondrial biogenesis as well (Yudkoff, Daikhin et al. 2001).

### **Environmental strategy: Hypoxia**

Recently, Jain and co-workers used hypoxia as an alternative strategy to target mitochondrial dysfunction in WB *Ndufs4*<sup>-/-</sup> mice (Jain, Zazzeron et al. 2016). They observed that *Ndufs4*<sup>-/-</sup> mice exposed to chronic hypoxia (11% Oxygen) displayed a marked improvement in survival. In sharp contrast, *Ndufs4*<sup>-/-</sup> mice exposed to chronic hyperoxia (55% Oxygen) died within 2-11 days of exposure. Hypoxia improved body weight gain, maintenance of core body temperature and neurologic behavior. Moreover, hypoxia dramatically reduced the development of lesions accompanied with microglial proliferation in the olfactory bulb, cerebellum and brainstem. Hypoxia furthermore reduced  $\alpha$ -hydroxybutyrate, which is a circulating plasma marker for Leigh disease (Thompson Legault, Strittmatter et al. 2015), and plasma lactate. Hypoxia did not improve the dramatically reduced activity of CI in brain mitochondria. The authors speculated that chronic hypoxia leads to hypoxia inducible factor

(HIF)-dependent transcriptional regulation, which is known to activate important biochemical pathways including redox-neutral ATP production and a decreased flux through pyruvate dehydrogenase thus preventing mitochondrial ROS generation. In addition, the lower availability of oxygen under hypoxia lowers the availability of oxygen as a substrate in the generation of ROS.



## Aims and Scope of this thesis

As already discussed above, treatment of patient fibroblasts with the water-soluble vitamin E analog, Trolox, lowered the rate of CM-DCF formation, normalized  $\Delta\psi$  and normalized the ER  $\text{Ca}^{2+}$  content, the latter thought to underly the observed normalization of the stimulus-induced increase in mitochondrial ATP production (Distelmaier, Visch et al. 2009). Also discussed above is our finding that Trolox increased the expression of fully assembled CI in fibroblasts from a panel of 13 CI deficient patients including 4 patients with a pathogenic *NDUFS4* mutation (Valsecchi, Koopman et al. 2010). The latter observation lead to the fundamentally important conclusion that CI deficiency is primarily a CI expression problem rather than a CI intrinsic catalytic problem and that therefore therapeutic strategies aimed at stabilizing CI and thus at increasing the expression of CI are a promising avenue.

The main aim of this thesis was to understand the pathophysiological consequences of isolated mitochondrial CI deficiency by using the *Ndufs4*<sup>-/-</sup> mouse. To this end, I compared the phenotypic manifestations in 23 *Ndufs4*<sup>-/-</sup> mice to their wild type littermates starting from postnatal day 0 to their predefined humane endpoint as defined by the Ethical Committee of Animal Welfare (Figure 2). In **Chapter 2**, I determined the biochemical consequences of isolated CI deficiency on mitochondrial ATP generating capacity and activity of individual OXPHOS complexes in tissues of high energy demand, namely skeletal muscle, heart and brain. In **Chapter 3**, I use the skeletal muscle data of chapter 2 in a systems biology approach to explore the consequences of isolated CI deficiency on skeletal muscle bioenergetics. In **Chapter 4**, through a longitudinal investigation, I discuss the consequences of isoflurane anaesthesia in *Ndufs4*<sup>-/-</sup> mice. In **Chapter 5**, I study the effect of isoflurane anaesthesia of *Ndufs4*<sup>-/-</sup> mice on the mitochondrial ATP production capacity and activity of individual OXPHOS complexes in brain. I show that, contrary to previous hypotheses, increased sensitivity to isoflurane anaesthesia in CI deficient mice is not due to reduction in brain mitochondrial ATP production capacity. In **Chapter 6**, I discuss the special position of neurons, whose deterioration, because they are highly susceptible to oxidative damage, might underlie most of the clinical signs and symptoms observed in *Ndufs4*<sup>-/-</sup> mice. In **Chapter 7**, I present the results of my *in vivo* study with *Ndufs4*<sup>-/-</sup> mice regarding the therapeutic potential of Trolox. In **Chapter 8**, I present the general conclusions of my thesis and discuss future directions of the field of research of which it forms part.

## References

- Acin-Perez, R., M. P. Bayona-Bafaluy, P. Fernandez-Silva, R. Moreno-Loshuertos, A. Perez-Martos, C. Bruno, C. T. Moraes and J. A. Enriquez (2004). "Respiratory complex III is required to maintain complex I in mammalian mitochondria." *Mol Cell* **13**(6): 805-815.
- Almeida, L., M. Vaz-da-Silva, A. Falcao, E. Soares, R. Costa, A. I. Loureiro, C. Fernandes-Lopes, J. F. Rocha, T. Nunes, L. Wright and P. Soares-da-Silva (2009). "Pharmacokinetic and safety profile of trans-resveratrol in a rising multiple-dose study in healthy volunteers." *Mol Nutr Food Res* **53 Suppl 1**: S7-15.
- Alston, C. L., C. Howard, M. Olahova, S. A. Hardy, L. He, P. G. Murray, S. O'Sullivan, G. Doherty, J. P. Shield, I. P. Hargreaves, A. A. Monavari, I. Knerr, P. McCarthy, A. A. Morris, D. R. Thorburn, H. Prokisch, P. E. Clayton, R. McFarland, J. Hughes, E. Crushell and R. W. Taylor (2016). "A recurrent mitochondrial p.Trp22Arg NDUFB3 variant causes a distinctive facial appearance, short stature and a mild biochemical and clinical phenotype." *J Med Genet* **53**(9): 634-641.
- Anderson, S. L., W. K. Chung, J. Frezzo, J. C. Papp, J. Ekstein, S. DiMauro and B. Y. Rubin (2008). "A novel mutation in NDUFS4 causes Leigh syndrome in an Ashkenazi Jewish family." *J Inher Metab Dis* **31 Suppl 2**: S461-467.
- Angebault, C., M. Charif, N. Guegen, C. Piro-Megy, B. Mousson de Camaret, V. Procaccio, P. O. Guichet, M. Hebrard, G. Manes, N. Leboucq, F. Rivier, C. P. Hamel, G. Lenaers and A. Roubertie (2015). "Mutation in NDUFA13/GRIM19 leads to early onset hypotonia, dyskinesia and sensorial deficiencies, and mitochondrial complex I instability." *Hum Mol Genet* **24**(14): 3948-3955.
- Antonenko, Y. N., A. V. Avetisyan, L. E. Bakeeva, B. V. Chernyak, V. A. Chertkov, L. V. Domnina, O. Y. Ivanova, D. S. Izyumov, L. S. Khailova, S. S. Klishin, G. A. Korshunova, K. G. Lyamzaev, M. S. Muntyan, O. K. Nepryakhina, A. A. Pashkovskaya, O. Y. Pletjushkina, A. V. Pustovidko, V. A. Roginsky, T. I. Rokitskaya, E. K. Ruuge, V. B. Saprunova, Severina, II, R. A. Simonyan, I. V. Skulachev, M. V. Skulachev, N. V. Sumbatyan, I. V. Sviryaeva, V. N. Tashlitsky, J. M. Vassiliev, M. Y. Vyssokikh, L. S. Yaguzhinsky, A. A. Zamyatnin, Jr. and V. P. Skulachev (2008). "Mitochondria-targeted plastoquinone derivatives as tools to interrupt execution of the aging program. 1. Cationic plastoquinone derivatives: synthesis and in vitro studies." *Biochemistry (Mosc)* **73**(12): 1273-1287.
- Assouline, Z., M. Jambou, M. Rio, C. Bole-Feysot, P. de Lonlay, C. Barnerias, I. Desguerre, C. Bonnemains, C. Guillermet, J. Steffann, A. Munnich, J. P. Bonnefont, A. Rotig and A. S. Lebre (2012). "A constant and similar assembly defect of mitochondrial respiratory chain complex I allows rapid identification of NDUFS4 mutations in patients with Leigh syndrome." *Biochim Biophys Acta* **1822**(6): 1062-1069.
- Bakeeva, L. E., I. V. Barskov, M. V. Egorov, N. K. Isaev, V. I. Kapelko, A. V. Kazachenko, V. I. Kirpatovsky, S. V. Kozlovsky, V. L. Lakomkin, S. B. Levina, O. I. Pisarenko, E. Y. Plotnikov, V. B. Saprunova, L. I. Serebryakova, M. V. Skulachev, E. V. Stelmashook, I. M. Studneva, O. V. Tskitishvili, A. K. Vasilyeva, I. V. Victorov, D. B. Zorov and V. P. Skulachev (2008). "Mitochondria-targeted plastoquinone derivatives as tools to interrupt execution of the aging program. 2. Treatment of some ROS- and age-related diseases (heart arrhythmia, heart infarctions, kidney ischemia, and stroke)." *Biochemistry (Mosc)* **73**(12): 1288-1299.
- Balsa, E., R. Marco, E. Perales-Clemente, R. Szklarczyk, E. Calvo, M. O. Landazuri and J. A. Enriquez (2012). "NDUFA4 is a subunit of complex IV of the mammalian electron transport chain." *Cell Metab* **16**(3): 378-386.
- Bar-Meir, M., O. N. Elpeleg and A. Saada (2001). "Effect of various agents on adenosine triphosphate synthesis in mitochondrial complex I deficiency." *J Pediatr* **139**(6): 868-870.

- Bastin, J., F. Aubey, A. Rotig, A. Munnich and F. Djouadi (2008). "Activation of peroxisome proliferator-activated receptor pathway stimulates the mitochondrial respiratory chain and can correct deficiencies in patients' cells lacking its components." *J Clin Endocrinol Metab* **93**(4): 1433-1441.
- Baur, J. A., K. J. Pearson, N. L. Price, H. A. Jamieson, C. Lerin, A. Kalra, V. V. Prabhu, J. S. Allard, G. Lopez-Lluch, K. Lewis, P. J. Pistell, S. Poosala, K. G. Becker, O. Boss, D. Gwinn, M. Wang, S. Ramaswamy, K. W. Fishbein, R. G. Spencer, E. G. Lakatta, D. Le Couteur, R. J. Shaw, P. Navas, P. Puigserver, D. K. Ingram, R. de Cabo and D. A. Sinclair (2006). "Resveratrol improves health and survival of mice on a high-calorie diet." *Nature* **444**(7117): 337-342.
- Benit, P., R. Beugnot, D. Chretien, I. Giurgea, P. De Lonlay-Debeney, J. P. Issartel, M. Corral-Debrinski, S. Kerscher, P. Rustin, A. Rotig and A. Munnich (2003). "Mutant NDUFV2 subunit of mitochondrial complex I causes early onset hypertrophic cardiomyopathy and encephalopathy." *Hum Mutat* **21**(6): 582-586.
- Benit, P., D. Chretien, N. Kadhom, P. de Lonlay-Debeney, V. Cormier-Daire, A. Cabral, S. Peudenier, P. Rustin, A. Munnich and A. Rotig (2001). "Large-scale deletion and point mutations of the nuclear NDUFV1 and NDUFS1 genes in mitochondrial complex I deficiency." *Am J Hum Genet* **68**(6): 1344-1352.
- Benit, P., A. Slama, F. Cartault, I. Giurgea, D. Chretien, S. Lebon, C. Marsac, A. Munnich, A. Rotig and P. Rustin (2004). "Mutant NDUFS3 subunit of mitochondrial complex I causes Leigh syndrome." *J Med Genet* **41**(1): 14-17.
- Benit, P., J. Steffann, S. Lebon, D. Chretien, N. Kadhom, P. de Lonlay, A. Goldenberg, Y. Dumez, M. Dommergues, P. Rustin, A. Munnich and A. Rotig (2003). "Genotyping microsatellite DNA markers at putative disease loci in inbred/multiplex families with respiratory chain complex I deficiency allows rapid identification of a novel nonsense mutation (IVS1nt -1) in the NDUFS4 gene in Leigh syndrome." *Hum Genet* **112**(5-6): 563-566.
- Benton, C. R., D. C. Wright and A. Bonen (2008). "PGC-1alpha-mediated regulation of gene expression and metabolism: implications for nutrition and exercise prescriptions." *Appl Physiol Nutr Metab* **33**(5): 843-862.
- Berger, I., E. Hershkovitz, A. Shaag, S. Edvardson, A. Saada and O. Elpeleg (2008). "Mitochondrial complex I deficiency caused by a deleterious NDUFA11 mutation." *Ann Neurol* **63**(3): 405-408.
- Bjelakovic, G., D. Nikolova, L. L. Gluud, R. G. Simonetti and C. Gluud (2007). "Mortality in randomized trials of antioxidant supplements for primary and secondary prevention: systematic review and meta-analysis." *JAMA* **297**(8): 842-857.
- Brini, M., P. Pinton, M. P. King, M. Davidson, E. A. Schon and R. Rizzuto (1999). "A calcium signaling defect in the pathogenesis of a mitochondrial DNA inherited oxidative phosphorylation deficiency." *Nat Med* **5**(8): 951-954.
- Budde, S. M., L. P. van den Heuvel, A. J. Janssen, R. J. Smeets, C. A. Buskens, L. DeMeirleir, R. Van Coster, M. Baethmann, T. Voit, J. M. Trijbels and J. A. Smeitink (2000). "Combined enzymatic complex I and III deficiency associated with mutations in the nuclear encoded NDUFS4 gene." *Biochem Biophys Res Commun* **275**(1): 63-68.
- Budde, S. M., L. P. van den Heuvel, R. J. Smeets, D. Skladal, J. A. Mayr, C. Boelen, V. Petruzzella, S. Papa and J. A. Smeitink (2003). "Clinical heterogeneity in patients with mutations in the NDUFS4 gene of mitochondrial complex I." *J Inherit Metab Dis* **26**(8): 813-815.
- Budde, S. M., L. P. van den Heuvel and J. A. Smeitink (2002). "The human complex I NDUFS4 subunit: from gene structure to function and pathology." *Mitochondrion* **2**(1-2): 109-115.

- Calvaruso, M. A., P. Willems, M. van den Brand, F. Valsecchi, S. Kruse, R. Palmiter, J. Smeitink and L. Nijtmans (2012). "Mitochondrial complex III stabilizes complex I in the absence of NDUFS4 to provide partial activity." *Hum Mol Genet* **21**(1): 115-120.
- Calvo, S. E., E. J. Tucker, A. G. Compton, D. M. Kirby, G. Crawford, N. P. Burt, M. Rivas, C. Guiducci, D. L. Bruno, O. A. Goldberger, M. C. Redman, E. Wiltshire, C. J. Wilson, D. Altschuler, S. B. Gabriel, M. J. Daly, D. R. Thorburn and V. K. Mootha (2010). "High-throughput, pooled sequencing identifies mutations in NUBPL and FOXRED1 in human complex I deficiency." *Nat Genet* **42**(10): 851-858.
- Cerutti, R., E. Pirinen, C. Lamperti, S. Marchet, A. A. Sauve, W. Li, V. Leoni, E. A. Schon, F. Dantzer, J. Auwerx, C. Viscomi and M. Zeviani (2014). "NAD(+)-dependent activation of Sirt1 corrects the phenotype in a mouse model of mitochondrial disease." *Cell Metab* **19**(6): 1042-1049.
- Chouchani, E. T., C. Methner, G. Buonincontri, C. H. Hu, A. Logan, S. J. Sawiak, M. P. Murphy and T. Krieg (2014). "Complex I deficiency due to selective loss of Ndufs4 in the mouse heart results in severe hypertrophic cardiomyopathy." *PLoS One* **9**(4): e94157.
- Cox, D. A. and M. A. Matlib (1993). "A role for the mitochondrial Na(+)-Ca<sup>2+</sup> exchanger in the regulation of oxidative phosphorylation in isolated heart mitochondria." *J Biol Chem* **268**(2): 938-947.
- Csiszar, A., N. Labinskyy, J. T. Pinto, P. Ballabh, H. Zhang, G. Losonczy, K. Pearson, R. de Cabo, P. Pacher, C. Zhang and Z. Ungvari (2009). "Resveratrol induces mitochondrial biogenesis in endothelial cells." *Am J Physiol Heart Circ Physiol* **297**(1): H13-20.
- Daussin, F. N., J. Zoll, E. Ponsot, S. P. Dufour, S. Doutreleau, E. Lonsdorfer, R. Ventura-Clapier, B. Mettauer, F. Piquard, B. Geny and R. Richard (2008). "Training at high exercise intensity promotes qualitative adaptations of mitochondrial function in human skeletal muscle." *J Appl Physiol* (1985) **104**(5): 1436-1441.
- De Rasmio, D., D. Panelli, A. M. Sardanelli and S. Papa (2008). "cAMP-dependent protein kinase regulates the mitochondrial import of the nuclear encoded NDUFS4 subunit of complex I." *Cell Signal* **20**(5): 989-997.
- Distelmaier, F., W. J. Koopman, L. P. van den Heuvel, R. J. Rodenburg, E. Mayatepek, P. H. Willems and J. A. Smeitink (2009). "Mitochondrial complex I deficiency: from organelle dysfunction to clinical disease." *Brain* **132**(Pt 4): 833-842.
- Distelmaier, F., H. J. Visch, J. A. Smeitink, E. Mayatepek, W. J. Koopman and P. H. Willems (2009). "The antioxidant Trolox restores mitochondrial membrane potential and Ca<sup>2+</sup>-stimulated ATP production in human complex I deficiency." *J Mol Med (Berl)* **87**(5): 515-522.
- Dunning, C. J., M. McKenzie, C. Sugiana, M. Lazarou, J. Silke, A. Connelly, J. M. Fletcher, D. M. Kirby, D. R. Thorburn and M. T. Ryan (2007). "Human CIA30 is involved in the early assembly of mitochondrial complex I and mutations in its gene cause disease." *EMBO J* **26**(13): 3227-3237.
- Emahazion, T., A. Beskow, U. Gyllensten and A. J. Brookes (1998). "Intron based radiation hybrid mapping of 15 complex I genes of the human electron transport chain." *Cytogenet Cell Genet* **82**(1-2): 115-119.
- Felici, R., L. Cavone, A. Lapucci, D. Guasti, D. Bani and A. Chiarugi (2014). "PARP inhibition delays progression of mitochondrial encephalopathy in mice." *Neurotherapeutics* **11**(3): 651-664.
- Fernandez-Vizarra, E., M. Bugiani, P. Goffrini, F. Carrara, L. Farina, E. Procopio, A. Donati, G. Uziel, I. Ferrero and M. Zeviani (2007). "Impaired complex III assembly associated with BCS1L gene mutations in isolated mitochondrial encephalopathy." *Hum Mol Genet* **16**(10): 1241-1252.

- Fiedorczuk, K., J. A. Letts, G. Degliesposti, K. Kaszuba, M. Skehel and L. A. Sazanov (2016). "Atomic structure of the entire mammalian mitochondrial complex I." *Nature*.
- Finsterer, J. and L. Segall (2010). "Drugs interfering with mitochondrial disorders." *Drug Chem Toxicol* **33**(2): 138-151.
- Garone, C., M. A. Donati, M. Sacchini, B. Garcia-Diaz, C. Bruno, S. Calvo, V. K. Mootha and S. Dimauro (2013). "Mitochondrial encephalomyopathy due to a novel mutation in ACAD9." *JAMA Neurol* **70**(9): 1177-1179.
- Ghneim, H. K. and Y. A. Al-Sheikh (2010). "The effect of aging and increasing ascorbate concentrations on respiratory chain activity in cultured human fibroblasts." *Cell Biochem Funct* **28**(4): 283-292.
- Gold, D. R. and B. H. Cohen (2001). "Treatment of mitochondrial cytopathies." *Semin Neurol* **21**(3): 309-325.
- Haack, T. B., F. Madignier, M. Herzer, E. Lamantea, K. Danhauser, F. Invernizzi, J. Koch, M. Freitag, R. Drost, I. Hillier, B. Haberberger, J. A. Mayr, U. Ahting, V. Tiranti, A. Rotig, A. Iuso, R. Horvath, M. Tesarova, I. Baric, G. Uziel, B. Rolinski, W. Sperl, T. Meitinger, M. Zeviani, P. Freisinger and H. Prokisch (2012). "Mutation screening of 75 candidate genes in 152 complex I deficiency cases identifies pathogenic variants in 16 genes including NDUFB9." *J Med Genet* **49**(2): 83-89.
- Hathcock, J. N., A. Azzi, J. Blumberg, T. Bray, A. Dickinson, B. Frei, I. Jialal, C. S. Johnston, F. J. Kelly, K. Kraemer, L. Packer, S. Parthasarathy, H. Sies and M. G. Traber (2005). "Vitamins E and C are safe across a broad range of intakes." *Am J Clin Nutr* **81**(4): 736-745.
- Hersh, S. P. (2010). "Mitochondria: an emerging target for therapeutics." *Clin Pharmacol Ther* **87**(6): 630-632.
- Hirst, J. and M. M. Roessler (2016). "Energy conversion, redox catalysis and generation of reactive oxygen species by respiratory complex I." *Biochim Biophys Acta* **1857**(7): 872-883.
- Hoefs, S. J., C. E. Dieteren, F. Distelmaier, R. J. Janssen, A. Epplen, H. G. Swarts, M. Forkink, R. J. Rodenburg, L. G. Nijtmans, P. H. Willems, J. A. Smeitink and L. P. van den Heuvel (2008). "NDUFA2 complex I mutation leads to Leigh disease." *Am J Hum Genet* **82**(6): 1306-1315.
- Hoefs, S. J., O. H. Skjeldal, R. J. Rodenburg, B. Nedregaard, E. P. van Kaauwen, U. Spiekerkotter, J. C. von Kleist-Retzow, J. A. Smeitink, L. G. Nijtmans and L. P. van den Heuvel (2010). "Novel mutations in the NDUFS1 gene cause low residual activities in human complex I deficiencies." *Mol Genet Metab* **100**(3): 251-256.
- Hoefs, S. J., F. J. van Spronsen, E. W. Lenssen, L. G. Nijtmans, R. J. Rodenburg, J. A. Smeitink and L. P. van den Heuvel (2011). "NDUFA10 mutations cause complex I deficiency in a patient with Leigh disease." *Eur J Hum Genet* **19**(3): 270-274.
- Houtkooper, R. H. and F. M. Vaz (2008). "Cardiolipin, the heart of mitochondrial metabolism." *Cell Mol Life Sci* **65**(16): 2493-2506.
- Ingraham, C. A., L. S. Burwell, J. Skalska, P. S. Brookes, R. L. Howell, S. S. Sheu and C. A. Pinkert (2009). "NDUFS4: creation of a mouse model mimicking a Complex I disorder." *Mitochondrion* **9**(3): 204-210.
- Iuso, A., S. Scacco, C. Piccoli, F. Bellomo, V. Petruzzella, R. Trentadue, M. Minuto, M. Ripoli, N. Capitanio, M. Zeviani and S. Papa (2006). "Dysfunctions of cellular oxidative metabolism in patients with mutations in the NDUFS1 and NDUFS4 genes of complex I." *J Biol Chem* **281**(15): 10374-10380.
- Jain, I. H., L. Zazzeron, R. Goli, K. Alexa, S. Schatzman-Bone, H. Dhillon, O. Goldberger, J. Peng, O. Shalem, N. E. Sanjana, F. Zhang, W. Goessling, W. M. Zapol and V. K. Mootha (2016). "Hypoxia as a therapy for mitochondrial disease." *Science* **352**(6281): 54-61.

- Jin, H., J. Randazzo, P. Zhang and P. F. Kador (2010). "Multifunctional antioxidants for the treatment of age-related diseases." *J Med Chem* **53**(3): 1117-1127.
- Jin, Z., W. Wei, M. Yang, Y. Du and Y. Wan (2014). "Mitochondrial complex I activity suppresses inflammation and enhances bone resorption by shifting macrophage-osteoclast polarization." *Cell Metab* **20**(3): 483-498.
- Johnson, S. C., M. E. Yanos, E. B. Kayser, A. Quintana, M. Sangesland, A. Castanza, L. Uhde, J. Hui, V. Z. Wall, A. Gagnidze, K. Oh, B. M. Wasko, F. J. Ramos, R. D. Palmiter, P. S. Rabinovitch, P. G. Morgan, M. M. Sedensky and M. Kaeberlein (2013). "mTOR inhibition alleviates mitochondrial disease in a mouse model of Leigh syndrome." *Science* **342**(6165): 1524-1528.
- Karamanlidis, G., C. F. Lee, L. Garcia-Menendez, S. C. Kolwicz, Jr., W. Suthammarak, G. Gong, M. M. Sedensky, P. G. Morgan, W. Wang and R. Tian (2013). "Mitochondrial complex I deficiency increases protein acetylation and accelerates heart failure." *Cell Metab* **18**(2): 239-250.
- Kevelam, S. H., R. J. Rodenburg, N. I. Wolf, P. Ferreira, R. J. Luning, L. G. Nijtmans, A. Mitchell, H. A. Arroyo, D. Rating, A. Vanderver, C. G. van Berkel, T. E. Abbink, P. Heutink and M. S. van der Knaap (2013). "NUBPL mutations in patients with complex I deficiency and a distinct MRI pattern." *Neurology* **80**(17): 1577-1583.
- Kirby, D. M., R. Salemi, C. Sugiana, A. Ohtake, L. Parry, K. M. Bell, E. P. Kirk, A. Boneh, R. W. Taylor, H. H. Dahl, M. T. Ryan and D. R. Thorburn (2004). "NDUFS6 mutations are a novel cause of lethal neonatal mitochondrial complex I deficiency." *J Clin Invest* **114**(6): 837-845.
- Koopman, W. J., J. Beyrath, C. W. Fung, S. Koene, R. J. Rodenburg, P. H. Willems and J. A. Smeitink (2016). "Mitochondrial disorders in children: toward development of small-molecule treatment strategies." *EMBO Mol Med* **8**(4): 311-327.
- Koopman, W. J., S. Verkaart, H. J. Visch, F. H. van der Westhuizen, M. P. Murphy, L. W. van den Heuvel, J. A. Smeitink and P. H. Willems (2005). "Inhibition of complex I of the electron transport chain causes O<sub>2</sub><sup>-</sup>-mediated mitochondrial outgrowth." *Am J Physiol Cell Physiol* **288**(6): C1440-1450.
- Koopman, W. J., P. H. Willems and J. A. Smeitink (2012). "Monogenic mitochondrial disorders." *N Engl J Med* **366**(12): 1132-1141.
- Kruse, S. E., W. C. Watt, D. J. Marcinek, R. P. Kapur, K. A. Schenkman and R. D. Palmiter (2008). "Mice with mitochondrial complex I deficiency develop a fatal encephalomyopathy." *Cell Metab* **7**(4): 312-320.
- Lagouge, M., C. Argmann, Z. Gerhart-Hines, H. Meziane, C. Lerin, F. Daussin, N. Messadeq, J. Milne, P. Lambert, P. Elliott, B. Geny, M. Laakso, P. Puigserver and J. Auwerx (2006). "Resveratrol improves mitochondrial function and protects against metabolic disease by activating SIRT1 and PGC-1alpha." *Cell* **127**(6): 1109-1122.
- Lamont, R. E., C. L. Beaulieu, F. P. Bernier, R. Sparkes, A. M. Innes, C. Jackel-Cram, C. Ober, J. S. Parboosingh and E. G. Lemire (2016). "A novel NDUFS4 frameshift mutation causes Leigh disease in the Hutterite population." *Am J Med Genet A*.
- Lazarou, M., M. McKenzie, A. Ohtake, D. R. Thorburn and M. T. Ryan (2007). "Analysis of the assembly profiles for mitochondrial- and nuclear-DNA-encoded subunits into complex I." *Mol Cell Biol* **27**(12): 4228-4237.
- Lenaz, G., G. Tioli, A. I. Falasca and M. L. Genova (2016). "Complex I function in mitochondrial supercomplexes." *Biochim Biophys Acta* **1857**(7): 991-1000.
- Leong, D. W., J. C. Komen, C. A. Hewitt, E. Arnaud, M. McKenzie, B. Phipson, M. Bahlo, A. Laskowski, S. A. Kinkel, G. M. Davey, W. R. Heath, A. K. Voss, R. P. Zahedi, J. J. Pitt, R. Chrast, A. Sickmann, M. T. Ryan, G. K. Smyth, D. R. Thorburn and H. S. Scott (2012). "Proteomic and

metabolomic analyses of mitochondrial complex I-deficient mouse model generated by spontaneous B2 short interspersed nuclear element (SINE) insertion into NADH dehydrogenase (ubiquinone) Fe-S protein 4 (Ndufs4) gene." *J Biol Chem* **287**(24):20652-20663.

- Leshinsky-Silver, E., A. S. Lebre, L. Minai, A. Saada, J. Steffann, S. Cohen, A. Rotig, A. Munnich, D. Lev and T. Lerman-Sagie (2009). "NDUFS4 mutations cause Leigh syndrome with predominant brainstem involvement." *Mol Genet Metab* **97**(3): 185-189.
- Li, Y., H. Zhang, J. P. Fawcett and I. G. Tucker (2007). "Quantitation and metabolism of mitoquinone, a mitochondria-targeted antioxidant, in rat by liquid chromatography/tandem mass spectrometry." *Rapid Commun Mass Spectrom* **21**(13): 1958-1964.
- Liu, L., K. Zhang, H. Sandoval, S. Yamamoto, M. Jaiswal, E. Sanz, Z. Li, J. Hui, B. H. Graham, A. Quintana and H. J. Bellen (2015). "Glial lipid droplets and ROS induced by mitochondrial defects promote neurodegeneration." *Cell* **160**(1-2): 177-190.
- Loeffen, J., O. Elpeleg, J. Smeitink, R. Smeets, S. Stockler-Ipsiroglu, H. Mandel, R. Sengers, F. Trijbels and L. van den Heuvel (2001). "Mutations in the complex I NDUFS2 gene of patients with cardiomyopathy and encephalomyopathy." *Ann Neurol* **49**(2): 195-201.
- Loeffen, J., J. Smeitink, R. Triepels, R. Smeets, M. Schuelke, R. Sengers, F. Trijbels, B. Hamel, R. Mullaart and L. van den Heuvel (1998). "The first nuclear-encoded complex I mutation in a patient with Leigh syndrome." *Am J Hum Genet* **63**(6): 1598-1608.
- Loeffen, J. L., J. A. Smeitink, J. M. Trijbels, A. J. Janssen, R. H. Triepels, R. C. Sengers and L. P. van den Heuvel (2000). "Isolated complex I deficiency in children: clinical, biochemical and genetic aspects." *Hum Mutat* **15**(2): 123-134.
- Marriage, B., M. T. Clandinin and D. M. Glerum (2003). "Nutritional cofactor treatment in mitochondrial disorders." *J Am Diet Assoc* **103**(8): 1029-1038.
- Martín, M. A., A. Blazquez, L. G. Gutierrez-Solana, D. Fernandez-Moreira, P. Briones, A. L. Andreu, R. Garesse, Y. Campos and J. Arenas (2005). "Leigh syndrome associated with mitochondrial complex I deficiency due to a novel mutation in the NDUFS1 gene." *Arch Neurol* **62**(4): 659-661.
- Moncada, S. (2010). "Mitochondria as pharmacological targets." *Br J Pharmacol* **160**(2): 217-219.
- Murphy, M. P. and R. A. Smith (2007). "Targeting antioxidants to mitochondria by conjugation to lipophilic cations." *Annu Rev Pharmacol Toxicol* **47**: 629-656.
- Navarro, A. and A. Boveris (2010). "Brain mitochondrial dysfunction in aging, neurodegeneration, and Parkinson's disease." *Front Aging Neurosci* **2**.
- Navarro, A., C. Gomez, M. J. Sanchez-Pino, H. Gonzalez, M. J. Bandez, A. D. Boveris and A. Boveris (2005). "Vitamin E at high doses improves survival, neurological performance, and brain mitochondrial function in aging male mice." *Am J Physiol Regul Integr Comp Physiol* **289**(5): R1392-1399.
- Niki, E. (1991). "Action of ascorbic acid as a scavenger of active and stable oxygen radicals." *Am J Clin Nutr* **54**(6 Suppl): 1119S-1124S.
- Ogilvie, I., N. G. Kennaway and E. A. Shoubridge (2005). "A molecular chaperone for mitochondrial complex I assembly is mutated in a progressive encephalopathy." *J Clin Invest* **115**(10): 2784-2792.
- Ojuka, E. O. (2004). "Role of calcium and AMP kinase in the regulation of mitochondrial biogenesis and GLUT4 levels in muscle." *Proc Nutr Soc* **63**(2): 275-278.
- Ostergaard, E., R. J. Rodenburg, M. van den Brand, L. L. Thomsen, M. Duno, M. Batbayli, F. Wibrand and L. Nijtmans (2011). "Respiratory chain complex I deficiency due to NDUFA12 mutations as a new cause of Leigh syndrome." *J Med Genet* **48**(11): 737-740.

- Pagliarini, D. J., S. E. Calvo, B. Chang, S. A. Sheth, S. B. Vafai, S. E. Ong, G. A. Walford, C. Sugiana, A. Boneh, W. K. Chen, D. E. Hill, M. Vidal, J. G. Evans, D. R. Thorburn, S. A. Carr and V. K. Mootha (2008). "A mitochondrial protein compendium elucidates complex I disease biology." *Cell* **134**(1): 112-123.
- Pagniez-Mammeri, H., S. Loublier, A. Legrand, P. Benit, P. Rustin and A. Slama (2012). "Mitochondrial complex I deficiency of nuclear origin I. Structural genes." *Mol Genet Metab* **105**(2): 163-172.
- Panelli, D., V. Petruzzella, R. Vitale, D. De Rasmio, A. Munnich, A. Rotig and S. Papa (2008). "The regulation of PTC containing transcripts of the human NDUFS4 gene of complex I of respiratory chain and the impact of pathological mutations." *Biochimie* **90**(10): 1452-1460.
- Panetta, J., L. J. Smith and A. Boneh (2004). "Effect of high-dose vitamins, coenzyme Q and high-fat diet in paediatric patients with mitochondrial diseases." *J Inher Metab Dis* **27**(4): 487-498.
- Papa, S. (2002). "The NDUFS4 nuclear gene of complex I of mitochondria and the cAMP cascade." *Biochim Biophys Acta* **1555**(1-3): 147-153.
- Papa, S., V. Petruzzella, S. Scacco, A. M. Sardanelli, A. Iuso, D. Panelli, R. Vitale, R. Trentadue, D. De Rasmio, N. Capitanio, C. Piccoli, F. Papa, M. Scivetti, E. Bertini, T. Rizza and G. De Michele (2009). "Pathogenetic mechanisms in hereditary dysfunctions of complex I of the respiratory chain in neurological diseases." *Biochim Biophys Acta* **1787**(5): 502-517.
- Papa, S., D. D. Rasmio, Z. Technikova-Dobrova, D. Panelli, A. Signorile, S. Scacco, V. Petruzzella, F. Papa, G. Palmisano, A. Gnoni, L. Micelli and A. M. Sardanelli (2012). "Respiratory chain complex I, a main regulatory target of the cAMP/PKA pathway is defective in different human diseases." *FEBS Lett* **586**(5): 568-577.
- Petrosillo, G., M. Matera, N. Moro, F. M. Ruggiero and G. Paradies (2009). "Mitochondrial complex I dysfunction in rat heart with aging: critical role of reactive oxygen species and cardiolipin." *Free Radic Biol Med* **46**(1): 88-94.
- Petruzzella, V., D. Panelli, A. Torracio, A. Stella and S. Papa (2005). "Mutations in the NDUFS4 gene of mitochondrial complex I alter stability of the splice variants." *FEBS Lett* **579**(17): 3770-3776.
- Petruzzella, V. and S. Papa (2002). "Mutations in human nuclear genes encoding for subunits of mitochondrial respiratory complex I: the NDUFS4 gene." *Gene* **286**(1): 149-154.
- Petruzzella, V., R. Vergari, I. Puziferri, D. Boffoli, E. Lamantea, M. Zeviani and S. Papa (2001). "A nonsense mutation in the NDUFS4 gene encoding the 18 kDa (AQDQ) subunit of complex I abolishes assembly and activity of the complex in a patient with Leigh-like syndrome." *Hum Mol Genet* **10**(5): 529-535.
- Quintana, A., S. E. Kruse, R. P. Kapur, E. Sanz and R. D. Palmiter (2010). "Complex I deficiency due to loss of Ndufs4 in the brain results in progressive encephalopathy resembling Leigh syndrome." *Proc Natl Acad Sci U S A* **107**(24): 10996-11001.
- Robb, E. L., L. Winkelmoen, N. Visanji, J. Brotchie and J. A. Stuart (2008). "Dietary resveratrol administration increases MnSOD expression and activity in mouse brain." *Biochem Biophys Res Commun* **372**(1): 254-259.
- Rodriguez-Cuenca, S., H. M. Cocheme, A. Logan, I. Abakumova, T. A. Prime, C. Rose, A. Vidal-Puig, A. C. Smith, D. C. Rubinsztein, I. M. Fearnley, B. A. Jones, S. Pope, S. J. Heales, B. Y. Lam, S. G. Neogi, I. McFarlane, A. M. James, R. A. Smith and M. P. Murphy (2010). "Consequences of long-term oral administration of the mitochondria-targeted antioxidant MitoQ to wild-type mice." *Free Radic Biol Med* **48**(1): 161-172.



- Roestenberg, P., G. R. Manjeri, F. Valsecchi, J. A. Smeitink, P. H. Willems and W. J. Koopman (2012). "Pharmacological targeting of mitochondrial complex I deficiency: the cellular level and beyond." *Mitochondrion* **12**(1): 57-65.
- Ross, M. F., T. A. Prime, I. Abakumova, A. M. James, C. M. Porteous, R. A. Smith and M. P. Murphy (2008). "Rapid and extensive uptake and activation of hydrophobic triphenylphosphonium cations within cells." *Biochem J* **411**(3): 633-645.
- Saada, A., S. Edvardson, M. Rapoport, A. Shaag, K. Amry, C. Miller, H. Lorberboum-Galski and O. Elpeleg (2008). "C6ORF66 is an assembly factor of mitochondrial complex I." *Am J Hum Genet* **82**(1): 32-38.
- Saada, A., R. O. Vogel, S. J. Hoefs, M. A. van den Brand, H. J. Wessels, P. H. Willems, H. Venselaar, A. Shaag, F. Barghuti, O. Reish, M. Shohat, M. A. Huynen, J. A. Smeitink, L. P. van den Heuvel and L. G. Nijtmans (2009). "Mutations in NDUFAF3 (C3ORF60), encoding an NDUFAF4 (C6ORF66)-interacting complex I assembly protein, cause fatal neonatal mitochondrial disease." *Am J Hum Genet* **84**(6): 718-727.
- Sanchez-Caballero, L., S. Guerrero-Castillo and L. Nijtmans (2016). "Unraveling the complexity of mitochondrial complex I assembly: A dynamic process." *Biochim Biophys Acta* **1857**(7): 980-990.
- Scacco, S., V. Petruzzella, S. Budde, R. Vergari, R. Tamborra, D. Panelli, L. P. van den Heuvel, J. A. Smeitink and S. Papa (2003). "Pathological mutations of the human NDUFS4 gene of the 18-kDa (AQDQ) subunit of complex I affect the expression of the protein and the assembly and function of the complex." *J Biol Chem* **278**(45): 44161-44167.
- Scarpulla, R. C. (2008). "Transcriptional paradigms in mammalian mitochondrial biogenesis and function." *Physiol Rev* **88**(2): 611-638.
- Schlame, M., D. Rua and M. L. Greenberg (2000). "The biosynthesis and functional role of cardiolipin." *Prog Lipid Res* **39**(3): 257-288.
- Schuelke, M., J. Smeitink, E. Mariman, J. Loeffen, B. Plecko, F. Trijbels, S. Stockler-Ipsiroglu and L. van den Heuvel (1999). "Mutant NDUFV1 subunit of mitochondrial complex I causes leukodystrophy and myoclonic epilepsy." *Nat Genet* **21**(3): 260-261.
- Schwach, G., B. Trinczek and C. Bode (1990). "Localization of catalytic and regulatory subunits of cyclic AMP-dependent protein kinases in mitochondria from various rat tissues." *Biochem J* **270**(1): 181-188.
- Sharma, P. and P. D. Mongan (2001). "Ascorbate reduces superoxide production and improves mitochondrial respiratory chain function in human fibroblasts with electron transport chain deficiencies." *Mitochondrion* **1**(2): 191-198.
- Sharpley, M. S., R. J. Shannon, F. Draghi and J. Hirst (2006). "Interactions between phospholipids and NADH:ubiquinone oxidoreductase (complex I) from bovine mitochondria." *Biochemistry* **45**(1): 241-248.
- Shin, S. M., I. J. Cho and S. G. Kim (2009). "Resveratrol protects mitochondria against oxidative stress through AMP-activated protein kinase-mediated glycogen synthase kinase-3beta inhibition downstream of poly(ADP-ribose)polymerase-LKB1 pathway." *Mol Pharmacol* **76**(4): 884-895.
- Shoubridge, E. A. (2001). "Nuclear genetic defects of oxidative phosphorylation." *Hum Mol Genet* **10**(20): 2277-2284.
- Skulachev, V. P., V. N. Anisimov, Y. N. Antonenko, L. E. Bakeeva, B. V. Chernyak, V. P. Elichev, O. F. Filenko, N. I. Kalinina, V. I. Kapelko, N. G. Kolosova, B. P. Kopnin, G. A. Korshunova, M. R. Lichinitser, L. A. Obukhova, E. G. Pasyukova, O. I. Pisarenko, V. A. Roginsky, E. K. Ruuge, Senin, II, Severina, II, M. V. Skulachev, I. M. Spivak, V. N. Tashlitsky, V. A. Tkachuk, M. Y.

- Vysokikh, L. S. Yaguzhinsky and D. B. Zorov (2009). "An attempt to prevent senescence: a mitochondrial approach." *Biochim Biophys Acta* **1787**(5): 437-461.
- Smeitink, J., R. Sengers, F. Trijbels and L. van den Heuvel (2001). "Human NADH:ubiquinone oxidoreductase." *J Bioenerg Biomembr* **33**(3): 259-266.
  - Smeitink, J., L. van den Heuvel and S. DiMauro (2001). "The genetics and pathology of oxidative phosphorylation." *Nat Rev Genet* **2**(5): 342-352.
  - Sterky, F. H., A. F. Hoffman, D. Milenkovic, B. Bao, A. Paganelli, D. Edgar, R. Wibom, C. R. Lupica, L. Olson and N. G. Larsson (2012). "Altered dopamine metabolism and increased vulnerability to MPTP in mice with partial deficiency of mitochondrial complex I in dopamine neurons." *Hum Mol Genet* **21**(5): 1078-1089.
  - Sugiana, C., D. J. Pagliarini, M. McKenzie, D. M. Kirby, R. Salemi, K. K. Abu-Amero, H. H. Dahl, W. M. Hutchison, K. A. Vascotto, S. M. Smith, R. F. Newbold, J. Christodoulou, S. Calvo, V. K. Mootha, M. T. Ryan and D. R. Thorburn (2008). "Mutation of C20orf7 disrupts complex I assembly and causes lethal neonatal mitochondrial disease." *Am J Hum Genet* **83**(4): 468-478.
  - Szeto, H. H. (2006). "Mitochondria-targeted peptide antioxidants: novel neuroprotective agents." *AAPS J* **8**(3): E521-531.
  - Taivassalo, T. and R. G. Haller (2004). "Implications of exercise training in mtDNA defects--use it or lose it?" *Biochim Biophys Acta* **1659**(2-3): 221-231.
  - Taivassalo, T. and R. G. Haller (2005). "Exercise and training in mitochondrial myopathies." *Med Sci Sports Exerc* **37**(12): 2094-2101.
  - Thompson Legault, J., L. Strittmatter, J. Tardif, R. Sharma, V. Tremblay-Vaillancourt, C. Aubut, G. Boucher, C. B. Clish, D. Cyr, C. Daneault, P. J. Waters, L. Consortium, L. Vachon, C. Morin, C. Laprise, J. D. Rioux, V. K. Mootha and C. Des Rosiers (2015). "A Metabolic Signature of Mitochondrial Dysfunction Revealed through a Monogenic Form of Leigh Syndrome." *Cell Rep* **13**(5): 981-989.
  - Triepels, R. H., L. P. van den Heuvel, J. L. Loeffen, C. A. Buskens, R. J. Smeets, M. E. Rubio Gozalbo, S. M. Budde, E. C. Mariman, F. A. Wijburg, P. G. Barth, J. M. Trijbels and J. A. Smeitink (1999). "Leigh syndrome associated with a mutation in the NDUFS7 (PSST) nuclear encoded subunit of complex I." *Ann Neurol* **45**(6): 787-790.
  - Ugalde, C., R. J. Janssen, L. P. van den Heuvel, J. A. Smeitink and L. G. Nijtmans (2004). "Differences in assembly or stability of complex I and other mitochondrial OXPHOS complexes in inherited complex I deficiency." *Hum Mol Genet* **13**(6): 659-667.
  - Ungvari, Z., N. Labinskyy, P. Mukhopadhyay, J. T. Pinto, Z. Bagi, P. Ballabh, C. Zhang, P. Pacher and A. Csizsar (2009). "Resveratrol attenuates mitochondrial oxidative stress in coronary arterial endothelial cells." *Am J Physiol Heart Circ Physiol* **297**(5): H1876-1881.
  - Valsecchi, F., J. J. Esseling, W. J. Koopman and P. H. Willems (2009). "Calcium and ATP handling in human NADH:ubiquinone oxidoreductase deficiency." *Biochim Biophys Acta* **1792**(12): 1130-1137.
  - Valsecchi, F., S. Grefte, P. Roestenberg, J. Joosten-Wagenaars, J. A. Smeitink, P. H. Willems and W. J. Koopman (2013). "Primary fibroblasts of NDUFS4(-/-) mice display increased ROS levels and aberrant mitochondrial morphology." *Mitochondrion* **13**(5): 436-443.
  - Valsecchi, F., W. J. Koopman, G. R. Manjeri, R. J. Rodenburg, J. A. Smeitink and P. H. Willems (2010). "Complex I disorders: causes, mechanisms, and development of treatment strategies at the cellular level." *Dev Disabil Res Rev* **16**(2): 175-182.
  - Valsecchi, F., L. S. Ramos-Espiritu, J. Buck, L. R. Levin and G. Manfredi (2013). "cAMP and mitochondria." *Physiology (Bethesda)* **28**(3): 199-209.

- van den Bosch, B. J., M. Gerards, W. Sluiter, A. P. Stegmann, E. L. Jongen, D. M. Hellebrekers, R. Oegema, E. H. Lambrichts, H. Prokisch, K. Danhauser, K. Schoonderwoerd, I. F. de Coo and H. J. Smeets (2012). "Defective NDUFA9 as a novel cause of neonatally fatal complex I disease." *J Med Genet* **49**(1): 10-15.
- van den Heuvel, L., W. Ruitenbeek, R. Smeets, Z. Gelman-Kohan, O. Elpeleg, J. Loeffen, F. Trijbels, E. Mariman, D. de Bruijn and J. Smeitink (1998). "Demonstration of a new pathogenic mutation in human complex I deficiency: a 5-bp duplication in the nuclear gene encoding the 18-kD (AQDQ) subunit." *Am J Hum Genet* **62**(2): 262-268.
- Veech, R. L., B. Chance, Y. Kashiwaya, H. A. Lardy and G. F. Cahill, Jr. (2001). "Ketone bodies, potential therapeutic uses." *IUBMB Life* **51**(4): 241-247.
- Vergani, L., M. Barile, C. Angelini, A. B. Burlina, L. Nijtmans, M. P. Freda, C. Brizio, E. Zerbetto and F. Dabbeni-Sala (1999). "Riboflavin therapy. Biochemical heterogeneity in two adult lipid storage myopathies." *Brain* **122 ( Pt 12)**: 2401-2411.
- Verkaart, S., W. J. Koopman, J. Cheek, S. E. van Emst-de Vries, L. W. van den Heuvel, J. A. Smeitink and P. H. Willems (2007)**b**. "Mitochondrial and cytosolic thiol redox state are not detectably altered in isolated human NADH:ubiquinone oxidoreductase deficiency." *Biochim Biophys Acta* **1772**(9): 1041-1051.
- Verkaart, S., W. J. Koopman, S. E. van Emst-de Vries, L. G. Nijtmans, L. W. van den Heuvel, J. A. Smeitink and P. H. Willems (2007)**a**. "Superoxide production is inversely related to complex I activity in inherited complex I deficiency." *Biochim Biophys Acta* **1772**(3): 373-381.
- Visch, H. J., W. J. Koopman, A. Leusink, S. E. van Emst-de Vries, L. W. van den Heuvel, P. H. Willems and J. A. Smeitink (2006). "Decreased agonist-stimulated mitochondrial ATP production caused by a pathological reduction in endoplasmic reticulum calcium content in human complex I deficiency." *Biochim Biophys Acta* **1762**(1): 115-123.
- Visch, H. J., G. A. Rutter, W. J. Koopman, J. B. Koenderink, S. Verkaart, T. de Groot, A. Varadi, K. J. Mitchell, L. P. van den Heuvel, J. A. Smeitink and P. H. Willems (2004). "Inhibition of mitochondrial Na<sup>+</sup>-Ca<sup>2+</sup> exchange restores agonist-induced ATP production and Ca<sup>2+</sup> handling in human complex I deficiency." *J Biol Chem* **279**(39): 40328-40336.
- Vogel, R. O., C. E. Dieteren, L. P. van den Heuvel, P. H. Willems, J. A. Smeitink, W. J. Koopman and L. G. Nijtmans (2007). "Identification of mitochondrial complex I assembly intermediates by tracing tagged NDUFS3 demonstrates the entry point of mitochondrial subunits." *J Biol Chem* **282**(10): 7582-7590.
- Wallace, D. C., W. Fan and V. Procaccio (2010). "Mitochondrial energetics and therapeutics." *Annu Rev Pathol* **5**: 297-348.
- Wallace, D. C., X. X. Zheng, M. T. Lott, J. M. Shoffner, J. A. Hodge, R. I. Kelley, C. M. Epstein and L. C. Hopkins (1988). "Familial mitochondrial encephalomyopathy (MERRF): genetic, pathophysiological, and biochemical characterization of a mitochondrial DNA disease." *Cell* **55**(4): 601-610.
- Welch, R. W., P. Bergsten, J. D. Butler and M. Levine (1993). "Ascorbic acid accumulation and transport in human fibroblasts." *Biochem J* **294 ( Pt 2)**: 505-510.
- Wenz, T. (2009). "PGC-1alpha activation as a therapeutic approach in mitochondrial disease." *IUBMB Life* **61**(11): 1051-1062.
- Wenz, T., F. Diaz, B. M. Spiegelman and C. T. Moraes (2008). "Activation of the PPAR/PGC-1alpha pathway prevents a bioenergetic deficit and effectively improves a mitochondrial myopathy phenotype." *Cell Metab* **8**(3): 249-256.
- Wenz, T., S. L. Williams, S. R. Bacman and C. T. Moraes (2010). "Emerging therapeutic approaches to mitochondrial diseases." *Dev Disabil Res Rev* **16**(2): 219-229.

- Willems, P. H., F. Valsecchi, F. Distelmaier, S. Verkaart, H. J. Visch, J. A. Smeitink and W. J. Koopman (2008). "Mitochondrial Ca<sup>2+</sup> homeostasis in human NADH:ubiquinone oxidoreductase deficiency." *Cell Calcium* **44**(1): 123-133.
- Wirth, C., U. Brandt, C. Hunte and V. Zickermann (2016). "Structure and function of mitochondrial complex I." *Biochim Biophys Acta* **1857**(7): 902-914.
- Wu, H., S. B. Kanatous, F. A. Thurmond, T. Gallardo, E. Isotani, R. Bassel-Duby and R. S. Williams (2002). "Regulation of mitochondrial biogenesis in skeletal muscle by CaMK." *Science* **296**(5566): 349-352.
- Wu, Z., P. Puigserver, U. Andersson, C. Zhang, G. Adelmant, V. Mootha, A. Troy, S. Cinti, B. Lowell, R. C. Scarpulla and B. M. Spiegelman (1999). "Mechanisms controlling mitochondrial biogenesis and respiration through the thermogenic coactivator PGC-1." *Cell* **98**(1): 115-124.
- Yudkoff, M., Y. Daikhin, I. Nissim, A. Lazarow and I. Nissim (2001). "Brain amino acid metabolism and ketosis." *J Neurosci Res* **66**(2): 272-281.
- Zandi, P. P., J. C. Anthony, A. S. Khachaturian, S. V. Stone, D. Gustafson, J. T. Tschanz, M. C. Norton, K. A. Welsh-Bohmer, J. C. Breitner and G. Cache County Study (2004). "Reduced risk of Alzheimer disease in users of antioxidant vitamin supplements: the Cache County Study." *Arch Neurol* **61**(1): 82-88.
- Zhao, K., G. Luo, S. Giannelli and H. H. Szeto (2005). "Mitochondria-targeted peptide prevents mitochondrial depolarization and apoptosis induced by tert-butyl hydroperoxide in neuronal cell lines." *Biochem Pharmacol* **70**(12): 1796-1806.
- Zhao, K., G. M. Zhao, D. Wu, Y. Soong, A. V. Birk, P. W. Schiller and H. H. Szeto (2004). "Cell-permeable peptide antioxidants targeted to inner mitochondrial membrane inhibit mitochondrial swelling, oxidative cell death, and reperfusion injury." *J Biol Chem* **279**(33): 34682-34690.
- Zurita Rendon, O., H. Antonicka, R. Horvath and E. A. Shoubridge (2016). "A Mutation in the Flavin Adenine Dinucleotide-Dependent Oxidoreductase FOXRED1 Results in Cell-Type-Specific Assembly Defects in Oxidative Phosphorylation Complexes I and II." *Mol Cell Biol* **36**(16): 2132-2140.





# CHAPTER

## **Biochemical characterization of the oxidative phosphorylation system in tissues of high energy demand in a mouse model of isolated complex I deficiency**

**Manjeri G.R.**, Blanchet L., Janssen A.J., Fransen J.A.,  
Van der Zee, C.E., Rodenburg R.J., Smeitink J.A.,  
Koopman, W.J.H., Willems P.H.

# 2

## Abstract

We reported before that the maximal rate of mitochondrial ATP production expressed per mg of protein or mitochondrial ATP production capacity is not altered in a mitochondrial-enriched fraction from skeletal muscle, whereas it is decreased in a mitochondrial-enriched fraction from whole brain of mice lacking the NDUFS4 subunit of complex I (CI) of the respiratory chain (RC). Here, we show that this rate is also not altered in a mitochondrial-enriched fraction from heart. To investigate the mechanism underlying the ability of skeletal muscle and heart, but not brain, to maintain their mitochondrial ATP production capacity, we determined the maximal rate of pyruvate oxidation and the maximal activities of the RC complexes II, III and IV and the mitochondrial matrix marker citrate synthase (CS) in a mitochondrial-enriched fraction. When expressed per mg of protein, the maximal rate of pyruvate oxidation showed a tendency to increase in skeletal muscle and heart, but not in brain, the maximal activity of CII was increased in skeletal muscle with a tendency to increase in heart, that of CIII showed a tendency to increase in skeletal muscle and heart and that of CIV was increased in both skeletal muscle and heart. For none of the RC complexes the maximal activity was changed in brain. Finally, maximal CS activity per mg protein was increased in skeletal muscle and heart but not in brain. Together, these data suggest that the mitochondrial ATP production capacity is maintained in skeletal muscle and heart of CI-deficient mice through an increase in abundance of components of the mitochondrial ATP generating system and that this process does not occur in the brain of these mice.



## Introduction

The oxidative phosphorylation (OXPHOS) system is organized into five multisubunit protein complexes (I, II, III, IV and V) and two electron carriers (cytochrome c and coenzyme Q). Together with cytochrome c and coenzyme Q, the complexes I, II, III and IV form the electron transport chain (ETC). The ETC oxidizes NADH and FADH<sub>2</sub> to generate an electrochemical proton gradient across the mitochondrial inner membrane, the potential energy of which is used by complex V to convert ADP to ATP (Hatefi 1985).

Except for CII, whose subunits are encoded entirely by the nuclear DNA (nDNA), all other OXPHOS complexes are built of subunits that are encoded either by the nDNA or the mitochondrial DNA (mtDNA). Genetic defects resulting in OXPHOS dysfunction are now recognized as causal to a clinically heterogeneous group of diseases, generally referred to as mitochondrial disorders (Zeviani and Di Donato 2004, Taylor and Turnbull 2005). Defects in the mtDNA may affect protein synthesis genes (22 transfer RNA genes and 2 ribosomal RNA genes) and protein encoding genes (13 OXPHOS subunit genes). Nuclear DNA mutations may affect genes encoding the remainder of the OXPHOS subunits, OXPHOS assembly factors, factors involved in mtDNA maintenance, replication and transcription and mitochondrial RNA translation and genes encoding biosynthetic enzymes for lipids or cofactors (Smeitink, Zeviani et al. 2006).

Isolated CI deficiency is the most commonly encountered single enzyme deficiency in patients with a mitochondrial disorder. CI is built of 44 subunits, 7 encoded by the mtDNA and 37 by the nDNA and pathogenic mutations have been identified in all 7 mtDNA genes and 19 of the nDNA genes (Koopman, Beyrath et al. 2016). In addition to these structural building blocks of CI, there are numerous proteins required for the assembly of the enzyme. Pathogenic mutations have also been identified in genes encoding these assembly factors (Mimaki, Wang et al. 2012, Nouws, Nijtmans et al. 2012, Pagniez-Mammeri, Rak et al. 2012).

CI deficiency is routinely established by determining its activity in a 600g supernatant, referred to as mitochondrial-enriched fraction, of a muscle tissue homogenate or a homogenate of cultured primary skin fibroblasts using a spectrophotometric assay (Janssen, Trijbels et al. 2007, Rodenburg 2011). The assay uses NADH as a substrate which requires mitochondrial lysis by sonication, detergent treatment or freeze-thawing. It is generally observed that the activity of CI, albeit lower than the lowest healthy control value, differs greatly among patients with isolated CI-deficiency (Distelmaier, Koopman et al. 2009). Information on the

amount of fully assembled CI present in a mitochondrial-enriched fraction can be obtained through Blue Native gel-electrophoresis (BN-PAGE) followed by Western blotting. Linear regression analysis revealed a positive linear correlation between the activity and amount of CI, both expressed as percentage of the same lowest control, in mitochondrial-enriched fractions from cultured skin fibroblasts of 13 patients with isolated CI deficiency (Valsecchi, Koopman et al. 2010). The slope of the regression line did not significantly differ from the line of identity, suggesting that the decrease in CI activity is primarily due to a reduced amount of fully assembled CI and not, or to a much lesser extent, to a decrease in intrinsic activity of the fully assembled complex. Intriguingly, this analysis included 4 patients with a mutation in the *Ndufs4* gene showing an obvious, albeit significantly reduced, residual CI activity in the spectrophotometric assay but no fully assembled CI on the BN-PAGE Western blot. Instead, a ~830 kDa subcomplex was observed that failed to show in-gel activity. However, the residual CI activity in the spectrophotometric assay showed a good correlation with the amount of this subcomplex on the Western blot, suggesting that this subcomplex is part of the NADH oxidizing and ubiquinone reducing enzyme in the spectrophotometric assay. Based on these results it was suggested that the primary role of the NDUF54 subunit is a regulatory one by controlling the stability and, thus, the cellular expression of the fully assembled complex. Here, it is important to note that BN-PAGE cannot replace the spectrophotometric assay as evidenced by the observation that it failed to identify a specific mutation in the *Ndufs2* gene, which caused a marked reduction in CI activity in the spectrophotometric assay but showed a normal amount of fully assembled CI on the BN-PAGE Western blot and a normal in-gel activity (Ngu, Nijtmans et al. 2012).

The ATP production capacity is routinely measured in a freshly prepared 600g supernatant of muscle tissue or cultured fibroblasts containing intact mitochondria (Janssen, Trijbels et al. 2006). The maximal rate of CI-dependent ATP production is measured in the presence of excess pyruvate, malate, ADP,  $PO_4^{3-}$  and creatine. It is generally observed that the ATP production rate is decreased in patients with isolated CI deficiency. Finally, cellular oxygen consumption is another paradigm through which CI deficiency can be analyzed. Moran and co-workers observed that CI-driven cellular oxygen consumption was diminished in patients with genetic defects in *NDUFV1* and *NDUFA1* (Moran, Rivera et al. 2010).

The first mouse model with an isolated CI deficiency was a ubiquitous *Ndufs4* deletion created by Kruse et al (Kruse, Watt et al. 2008). The authors reported that these *Ndufs4*<sup>-/-</sup> mice, which lack the NDUF54 subunit, displayed a progressive lethal

phenotype characterized by encephalomyopathy and early death around week 7. Their maximal body weight was attained around day 30 after which it declined again. From day 35 onwards, they became lethargic and hypothermic. Moreover, they displayed a progressive loss of gross motor skills as was deduced from an ataxic gait and the inability to perform on a Rotarod. Around day 40, a first increase in serum lactate occurred. Quintana *et al*, created a mouse with conditional deletion of *Ndufs4* in neurons and glial cells (Quintana, Kruse *et al.* 2010). This brain-specific *Ndufs4*<sup>-/-</sup> mouse was demonstrated to display the same progressive phenotype as the ubiquitous *Ndufs4*<sup>-/-</sup> mouse. Mice engineered to specifically lack NDUF54 in dopaminergic neurons did not show any sign of neurodegeneration, loss of striatal innervation or Parkinson's related symptoms (Sterky, Hoffman *et al.* 2012). However, decreased dopamine release and increased levels of dopamine metabolites pointed to a significant effect on dopamine homeostasis. Moreover, dopaminergic neurons of these mice appeared more sensitive to methyl-4-phenyl-1,2,3,6-tetrahydropyridine (MPTP) toxicity, suggesting that a decrease in CI activity may contribute to drug-induced Parkinson's disease. Finally, Sterky *et al* and Karamanlidis *et al* independently generated a conditional heart-specific *Ndufs4*<sup>-/-</sup> mouse and demonstrated that the absence of NDUF54 had no effect on lifespan (Sterky, Hoffman *et al.* 2012, Karamanlidis, Lee *et al.* 2013).

Kruse *et al* did not observe any detectable rotenone sensitive CI activity in submitochondrial particles obtained after sonication, freeze-thawing or Triton X-100 lysis of a mitochondrial-enriched fraction from liver of the ubiquitous *Ndufs4*<sup>-/-</sup> mouse (Kruse, Watt *et al.* 2008). Analysis of a mitochondrial-enriched fraction from several tissues of this *Ndufs4*<sup>-/-</sup> mouse after mitochondrial lysis by freeze-thawing showed CI activities normalized to that of CIV ranging from 9% (lung) to 44% (heart) of control (Calvaruso, Willems *et al.* 2012). The near absence of CI activity in skeletal muscle and brain of these mice was confirmed by Alam *et al* ((Alam, Manjeri *et al.* 2015); Chapter 3 of this thesis) and Manjeri *et al* ((Manjeri, Rodenburg *et al.* 2016); Chapter 5 of this thesis). Intriguingly, the latter two studies revealed that the maximal rate of CI-dependent ATP production expressed per mg of protein or overall tissue CI-dependent ATP production capacity, measured in an intact mitochondrial-enriched fraction in the presence of excess pyruvate, malate, ADP, PO<sub>4</sub><sup>3-</sup> and creatine, was not altered in skeletal muscle (Alam, Manjeri *et al.* 2015), whereas it was decreased in brain (Manjeri, Rodenburg *et al.* 2016). These results indicate that the absence of the NDUF54 subunit does prohibit CI-dependent ATP production and that the reduction in overall tissue CI-dependent ATP production capacity as observed in

brain is overcome in skeletal muscle. In the present study, we add additional data on the heart of this ubiquitous *Ndufs4*<sup>-/-</sup> mouse in order to elucidate the mechanism underlying the differences in CI-dependent ATP production capacity between the three tissues.

## Materials and Methods

All experiments were approved by the Regional Animal Ethics Committee (Nijmegen, The Netherlands) and performed under the guidelines of the Dutch Council for Animal Care. All efforts were made to reduce animal suffering and number of animals used in this study.

**Animals.** This study is a comparative study using skeletal muscle, heart and brain obtained from 5 WT (*Ndufs4*<sup>+/+</sup>) and 5 KO (*Ndufs4*<sup>-/-</sup>) mice with the understanding that the experimental data on skeletal muscle and brain of these mice have been published elsewhere (Alam, Manjeri et al. 2015); (Manjeri, Rodenburg et al. 2016). The genotype of the mice was confirmed by polymerase chain reaction and both male and female mice were included. Mice were group-housed at the central animal facility (CDL) of the Radboud University at 22°C on a day and night rhythm of 12 hours. The animals had *ad libitum* access to food and water and were fed on a standard animal diet (Ssniff GmbH, Soest, 76. Germany. V1534-300 R/M-H).

**Tissue harvesting for biochemical analyses.** Animals were sacrificed at PN (postnatal) 31-34 days by cervical dislocation. Skeletal muscle from the hind limbs and heart tissue were harvested and immediately put in ice-cold SETH buffer (0.25 mol/L sucrose, 2mmol/L EDTA, 10 mmol/L Tris, 5x10<sup>4</sup> U heparin/L, pH 7.4). Whole brains were transferred to ice-cold SEF buffer (0.25 mol/L sucrose, 2mmol/L EDTA, 10 mmol/L Potassium phosphate, pH 7.4), minced with a Sorvall TC2 tissue chopper and homogenized with a glass/Teflon Potter Elvehjem homogenizer within 1 h of harvest. The homogenates were centrifuged at 600g and a portion of the supernatant was used for measurement of the maximal rates of pyruvate oxidation and ATP production. The remainder of the 600g supernatant was frozen in 10 µl aliquots in liquid nitrogen and kept at -80° C for maximal enzymatic activity measurements. The protein concentration was measured according to Rodenburg (Rodenburg 2011).

**Pyruvate oxidation and ATP production measurements.** To determine the maximal pyruvate oxidation rate, the freshly prepared 600g supernatant was incubated with radiolabeled substrate ([1-14C] pyruvate). After 20 min, the reaction was stopped

and the amount of liberated radioactive  $\text{CO}_2$  ( $^{14}\text{CO}_2$ ) was quantified (Janssen, Trijbels et al. 2006). The assay medium (pH 7.4) contained  $\text{K}^+$ - phosphate buffer (30 mM; source of Pi), KCl (75 mM), Tris (8 mM), K-EDTA (1.6 mM), P<sub>1</sub>,P<sub>5</sub>-Di (adenosine-5') pentaphosphate (Ap<sub>5</sub>A; 0.2 mM),  $\text{MgCl}_2$  (0.5 mM), ADP (2 mM), creatine (20 mM), malate (1 mM) and [1- $^{14}\text{C}$ ] pyruvate (1 mM). Ap<sub>5</sub>A is a potent adenylate kinase (AK) inhibitor required to prevent interference of the AK reaction with the levels of produced ATP, as well as with the excess of ADP required for this assay. For measurement of the maximal rate of ATP production, the same assay medium was used but with pyruvate instead of [1- $^{14}\text{C}$ ] pyruvate. After 20 min, the reaction was stopped by addition of 0.1 M  $\text{HClO}_4$ . The reaction mixture was centrifuged at 14000g for 2 min at 2 °C. To the supernatant, 1.2 vol (V/V) of 0.333 M  $\text{KHCO}_3$  was added, and this mixture was diluted 2-fold. The amount of ATP and phosphocreatine formed during the reaction were measured in the supernatant using a Konelab 20XT auto-analyzer (Thermo Scientific). Mitochondrial ATP production rate was corrected using a parallel assay in which residual glycolysis was blocked by arsenite (2 mM) (Janssen, Trijbels et al. 2006).

**Respiratory chain enzyme assays.** The liquid nitrogen frozen portion of the 600g supernatant was thawed and used for measurement of the (MCA) of the complexes I (CI), II (CII), III (CIII) and IV (CIV) and citrate synthase (CS), as described by Rodenburg (Rodenburg 2011).

**Electron microscopy analyses.** Brains from 3 KO animals and 3 WT mice were harvested at PN 31-34 days after perfusion fixation in 2% (w/v) glutaraldehyde in phosphate buffer (PB) (pH 7.4). Brains were rinsed several times in PB and post fixed for 1h in 1% osmium tetroxide and 1% potassium ferrocyanide in 0.1M cacodylate buffer. Brains were dehydrated in an ascending series of aqueous ethanol solutions and subsequently transferred via a mixture of ethanol and Epon to pure Epon 812 embedding medium. Ultrathin gray sections (60-80 nm) were cut, contrasted with aqueous 3% uranyl acetate, rinsed and counter-stained with lead citrate, air dried and examined in a JEOL JEM1010 electron microscope (JEOL, Welwyn Garden City, UK) operating at 60 kV.

**Statistical Analysis.** Statistical analysis was performed using Prism 5 (GraphPad Software Inc., La Jolla, Ca). Results were expressed as mean  $\pm$  SD and comparisons between groups were performed using the nonparametric Mann-Whitney test. Statistical significance was set at ( $p < 0.05$ ).

## Results

### Linear relationship between the maximal rates of pyruvate oxidation and ATP production in skeletal muscle, heart and brain from WT and KO mice.

The maximal rates of pyruvate oxidation and ATP production were determined in the presence of excess pyruvate, malate, ADP,  $\text{PO}_4^{3-}$  and creatine in a 600g supernatant of a homogenate of skeletal muscle, heart and brain from wild type (WT) and NDUFS4 knockout (KO) mice and expressed per mg of protein. Linear regression analysis revealed a highly significant relationship between the maximal rates of pyruvate oxidation and ATP production (**Figure 1**;  $R=0.89$ ,  $p<0.0001$ ). This result indicates that the conversion of pyruvate into ATP occurs equally efficiently in mitochondria of skeletal muscle, heart and brain and that this process is not compromised by the absence of the NDUFS4 subunit of complex I (**Figure 1**).

### Citrate synthase activity is higher in skeletal muscle and heart but unaltered in brain of KO mice.

The maximal activity of citrate synthase (CS) is widely used as an indicator of mitochondrial mass (Trounce, Kim et al. 1996, Kirby, Thorburn et al. 2007). CS activity was determined in a 600g supernatant of a homogenate of skeletal muscle, heart and brain from WT and KO mice after freeze-thawing and expressed per mg of protein. Both in WT (open bars) and KO (closed bars) mice,

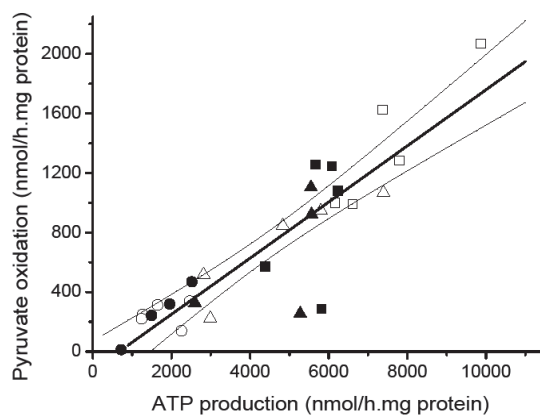


**Figure 1. Regression analysis of the relationship between the maximal rates of pyruvate oxidation and ATP production.** The maximal rates of pyruvate oxidation and ATP production were determined in the presence of excess pyruvate, malate, ADP,  $\text{PO}_4^{3-}$  and creatine in a 600g supernatant of a homogenate of skeletal muscle (circles;  $n=5$  and  $4$  for WT and KO, respectively), heart (triangles;  $n=5$  and  $4$  for WT and KO, respectively) and brain (squares;  $n=5$  for both WT and KO) from WT (open symbols) and KO (closed symbols) mice and expressed per mg of protein. Thin lines represent the upper and lower 95% confidence limit.

CS activity was highest in heart and lowest in muscle (**Figure 2**). Compared to WT mice, KO mice displayed significantly higher levels of CS in muscle (72%;  $p=0.017$ ) and heart (49%;  $p=0.002$ ). In sharp contrast, CS levels did not differ between WT and KO brain.

**Maximal rate of ATP production is unaltered in skeletal muscle and heart but lower in brain of KO mice.** The maximal rate of ATP production can be expressed per unit of CS or per mg of protein. When expressed per unit of CS, ATP production was 51% ( $p=0.04$ ), 32% ( $p=0.088$ ) and 25% ( $p=0.019$ ) lower in skeletal muscle, heart and brain, respectively, from KO mice as compared to WT mice (**Figure 3**). This result indicates that the absence of the NDUFS4 subunit decreases the ATP production capacity of the individual mitochondria and that this effect is most pronounced in skeletal muscle. However, when expressed per mg of protein, ATP production was not altered in KO skeletal muscle and KO heart, but 26% ( $p=0.028$ ) lower in KO brain. This result suggests that in KO mice, the decrease in ATP production capacity of the individual mitochondria is compensated for by an increase in mitochondrial mass in skeletal muscle and heart, but not in brain.

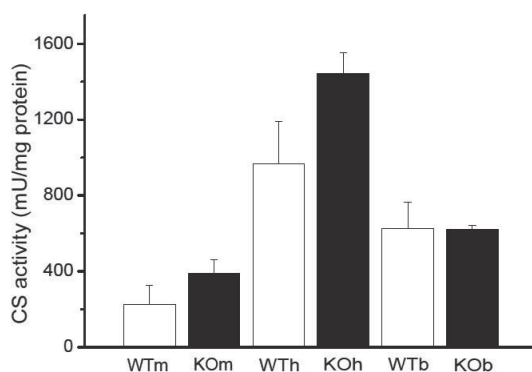


**Figure 2. Citrate synthase activity.** The maximal activity of citrate synthase (CS) was determined in a 600g supernatant of a homogenate of skeletal muscle ( $n=5$  for both WT and KO mice), heart ( $n=5$  for both WT and KO mice) and brain ( $n=5$  for both WT and KO mice) from WT (open bars) and KO (closed bars) mice after freeze-thawing and expressed per mg of protein. CS activity in WT heart was significantly higher than in WT muscle ( $p<0.001$ ) and in WT brain ( $p=0.020$ ) and significantly higher in WT brain than in WT muscle ( $p<0.001$ ). Similarly, CS activity in KO heart was significantly higher than in KO muscle ( $p<0.001$ ) and in KO brain ( $p<0.001$ ) and significantly higher in KO brain than in KO muscle ( $p<0.001$ ). WTm=WT muscle, WTh=WT heart, WTb=WT brain. Statistics for comparison between WT and KO are given in the text.

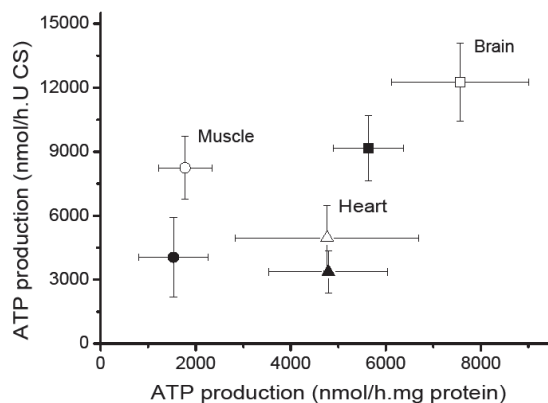


**Figure 3. Maximal rate of mitochondrial ATP production.** The maximal rate of mitochondrial ATP production was determined in a 600g supernatant of a homogenate of skeletal muscle (circles; n=5 for both WT and KO mice), heart (triangles; n=5 for both WT and KO mice) and brain (squares; n=5 for both WT and KO mice) from WT (open symbols) and KO (closed symbols) mice as described in the caption to figure 1. The values obtained were expressed as nmol per U of CS (Y-axis) or mg of protein (X-axis). When expressed per U of CS, the rate of ATP production was significantly higher in WT brain than in WT muscle ( $p=0.005$ ) and WT heart ( $P<0.001$ ), significantly higher in WT muscle than in WT heart ( $p=0.009$ ) and significantly higher in KO brain than in KO muscle ( $p=0.001$ ) and in KO heart ( $p<0.001$ ). Similarly, when expressed per mg of protein, the ATP production rate was significantly higher in WT brain than in WT muscle ( $p<0.001$ ) and WT heart ( $p=0.032$ ), significantly higher in WT heart than in WT muscle ( $P=0.011$ ), significantly higher in KO brain than in KO muscle ( $p<0.001$ ) and significantly higher in KO heart than in KO muscle ( $p=0.001$ ). Statistics for comparison between WT and KO are given in the text.

**Maximal activity of the respiratory chain complexes II, III and IV is higher in skeletal muscle and heart but unaltered in brain of KO mice.**

The maximal activity of the respiratory chain (RC) complexes was determined in the presence of complex-specific substrates in a 600g supernatant of a homogenate of skeletal muscle, heart and brain from WT and KO mice after freeze-thawing and expressed per unit of CS or mg of protein. Compared to WT mice, KO mice displayed a dramatically lower CI activity in all three tissues (**Figure 4**). However, when expressed per mg of protein, a residual activity of 28% was observed in KO heart. When expressed per unit of CS, no significant differences in CII, CIII and SCC activity were observed between WT and corresponding KO tissues (**Figures 5a-c**). On the other hand, when expressed per mg of protein, CII activity was 56% ( $p=0.033$ ) higher in KO muscle as compared to WT muscle (**Figure 5a**), while the maximal activity of CIII tended to be higher in KO skeletal muscle (45%;  $p=0.069$ ) and KO heart (11%;  $p=0.071$ ) (**Figure 5b**). Measurement of the combined



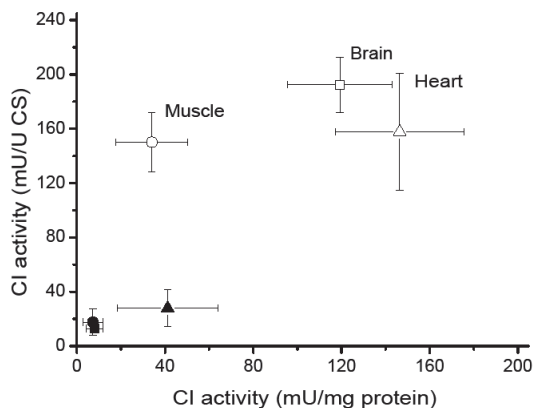


**Figure 4. Maximal CI activity.** The maximal activity of CI was determined in a 600g supernatant of a homogenate of skeletal muscle (circles; n=5 for both WT and KO mice), heart (triangles; n=5 for both WT and KO mice) and brain (squares; n=5 for both WT and KO mice) from WT (open symbols) and KO (closed symbols) mice after freeze-thawing. The values obtained were expressed as mU per U of CS (Y-axis) or mg of protein (X-axis). When expressed per U of CS, CI activity was significantly higher in WT brain than in WT muscle ( $p=0.013$ ) and significantly higher in KO heart than in KO brain ( $p=0.045$ ). Similarly, when expressed per mg of protein, CI activity was significantly higher in WT heart than in WT muscle ( $p<0.001$ ), significantly higher in WT brain than in WT muscle ( $p<0.001$ ) and significantly higher in KO heart than in KO muscle ( $p=0.012$ ) and in KO brain ( $p=0.012$ ).

activity of the complexes II and III, referred to as succinate: cyt c oxidoreductase (SCC) activity, corroborated the picture that emerged from the measurement of their individual activities (**Figure 5c**). Expression per mg of protein revealed 64% and 50% higher values in KO skeletal muscle ( $p=0.042$ ) and KO heart ( $p=0.001$ ), respectively. The KO brain did not show any alteration in CII, CIII and SCC activity.

The picture was completed by measurement of the maximal activity of CIV. When expressed per CS, no significant difference in CIV activity was observed between WT and corresponding KO tissues (**Figure 6**). However, when expressed per mg of protein, CIV activity was 70% and 51% higher in KO skeletal muscle ( $p=0.024$ ) and KO heart ( $p=0.005$ ), respectively, whereas this activity was unaltered in KO brain.

#### **Aberrant mitochondrial cristae structures in the cerebellum of *Ndufs4* KO mice.**

Quintana *et al.*, 2010, reported the cerebellum to be one of the most affected brain regions in the conditional brain specific *Ndufs4*<sup>-/-</sup> mice. In the present study, the mitochondria from cerebellar cells were analyzed on an ultrastructural level. **Figure 7A** depicts two WT cerebellar Purkinje cells characterized by a large nucleus and a clear

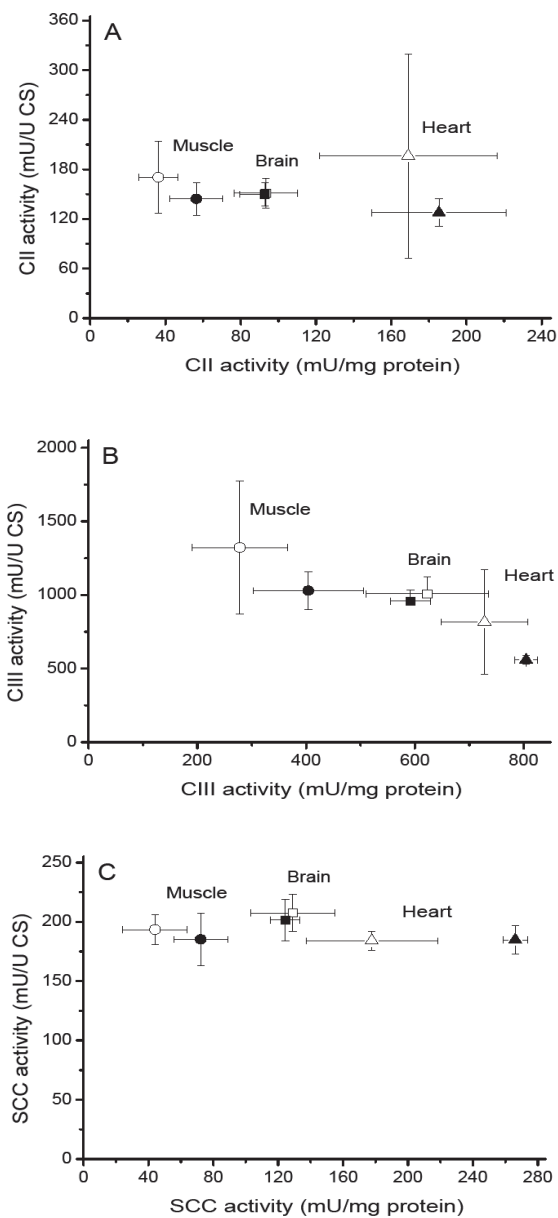


**Figure 5. Maximal CII, CIII and succinate: cyt c oxidoreductase (SCC) activity.** The maximal CII, CIII and SCC activity was determined in a 600g supernatant of a homogenate of skeletal muscle (circles; n=5 for both WT and KO mice), heart (triangles; n=5 for both WT and KO mice) and brain (squares; n=5 for both WT and KO mice) from WT (open symbols) and KO (closed symbols) mice after freeze-thawing. The values obtained were expressed as mU per U of CS (Y-axis) or mg of protein (X-axis). **a.** When expressed per mg of protein, CII activity ►

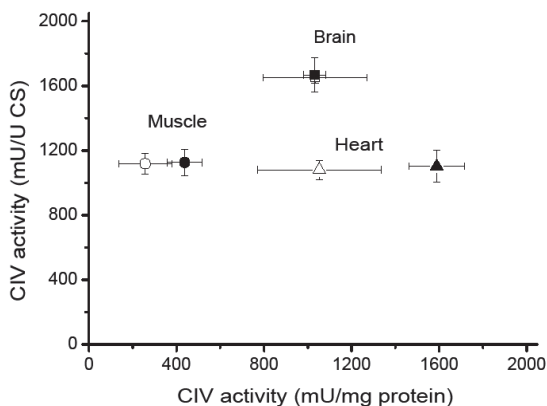


**Figure 6. Maximal CIV activity.** The maximal activity of CIV was determined in a 600g supernatant of a homogenate of skeletal muscle (circles; n=5 for both WT and KO mice), heart (triangles; n=5 for both WT and KO mice) and brain (squares; n=5 for both WT and KO mice) from WT (open symbols) and KO (closed symbols) mice after freeze-thawing. The values obtained were expressed as mU per U of CS (Y-axis) or mg of protein (X-axis). When expressed per U of CS, maximal CIV activity was significantly higher in WT brain than in WT muscle ( $p < 0.001$ ) and in WT heart ( $P < 0.001$ ) and significantly higher in KO brain than in KO muscle ( $p < 0.001$ ) and in KO heart ( $p < 0.001$ ). When expressed per mg of protein, maximal CIV activity was significantly higher in WT brain than in WT muscle ( $p < 0.001$ ), significantly higher in WT heart than in WT muscle ( $p < 0.001$ ), significantly higher in KO heart than in KO muscle ( $p < 0.001$ ) and in KO brain ( $p < 0.001$ ) and significantly higher in KO brain than in KO muscle ( $p < 0.001$ ). Statistics for comparison between WT and KO are given in the text.

- was significantly higher in WT heart than in WT muscle ( $p < 0.001$ ) and in WT brain ( $p = 0.010$ ), significantly higher in WT brain than in WT muscle ( $p < 0.001$ ), significantly higher in KO heart than in KO muscle ( $p < 0.001$ ) and in KO brain ( $p < 0.001$ ) and significantly higher in KO brain than in KO muscle ( $p = 0.003$ ). Statistics for comparison between WT and KO are given in the text.
- b.** When expressed per U of CS, CIII activity was significantly higher in KO muscle ( $p < 0.001$ ) and KO brain ( $p < 0.001$ ) than in KO heart. When expressed per mg of protein, CIII activity was significantly higher in WT heart than in WT muscle ( $p < 0.001$ ), significantly higher in WT brain than in WT muscle ( $p < 0.001$ ), significantly higher in KO heart than in KO muscle ( $p < 0.001$ ) and in KO brain ( $p < 0.001$ ) and significantly higher in KO brain than in KO muscle ( $p = 0.005$ ). Statistics for comparison between WT and KO are given in the text.
- c.** When expressed per U of CS, SCC activity was significantly higher in WT brain than in WT heart ( $p = 0.017$ ). When expressed per mg of protein, SCC activity was significantly higher in WT heart than in WT muscle ( $p < 0.001$ ) and WT brain ( $P = 0.054$ ), significantly higher in WT brain than in WT muscle ( $p < 0.001$ ), significantly higher in KO heart than in KO muscle ( $p < 0.001$ ) and KO brain ( $p < 0.001$ ) and significantly higher in KO brain than in KO muscle ( $p < 0.001$ ). Statistics for comparison between WT and KO are given in the text.

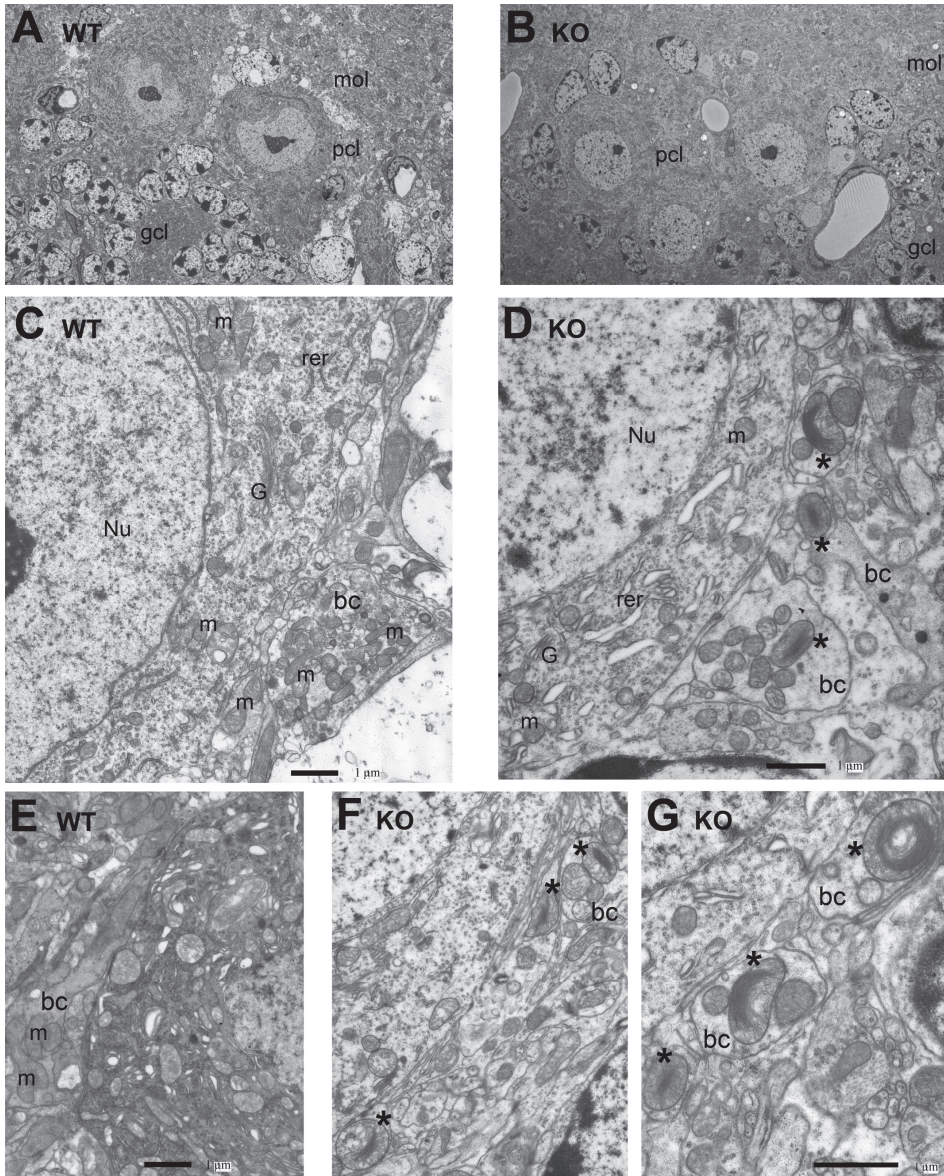


**Figure 7. Abnormal mitochondria with condensed cristae in basket cell extensions surrounding the Purkinje cells in the brain of KO mice.** Electron micrographs displaying the cerebellum Purkinje cell layer (pcl), the granular cell layer (gcl), and the cerebellum molecular layer (mol) in (A) WT and (B) KO mouse brain. Some of the small nuclei in the vicinity of the Purkinje cells are basket cells (seen at higher magnification in C-G). Magnification (in A, B) is 1000x. (C) WT cerebellum with on the left the large nucleus (Nu) of a Purkinje cell, to the right the cytoplasm containing normal healthy organelles like rough endoplasmic reticulum (rer), Golgi apparatus (G), and normal healthy mitochondria (m). In the right bottom area a ►

nucleolus. Also present are several nuclei of adjacent granule cells. Comparison of **figures 7A** and **7B** shows that the buildup of the cerebellar cortex layers is similar between WT and KO. Clearly visible are the granular cell layer, the molecular layer and the Purkinje cells surrounded by axo-somatic collaterals of inhibitory GABAergic basket cells. However, electron micrographs at higher magnification reveal the presence of abnormal mitochondria with condensed cristae in the basket cell extensions (**Figures 7 D, F and G**).

## Discussion

The present study describes a comparative analysis on the CI-dependent ATP production capacity per mitochondrial mass (after normalization to the maximal activity of CS) and per tissue mass (after normalization to the amount of protein) for three tissues of high energy demand, namely brain, heart and skeletal muscle, of a mouse model of ubiquitous CI deficiency and shows that the capacity per mitochondrial mass is significantly decreased in all three tissues, whereas the capacity per tissue mass is unaltered in heart and skeletal muscle but decreased in brain. The mouse model is engineered to globally lack the NDUFS4 subunit of the first complex of the mitochondrial ATP generating system. Ubiquitous *Ndufs4*<sup>-/-</sup> mice remain healthy until ~35 days after which they show a progressive clinical phenotype leading to early death at ~7 weeks. Tissues were removed at 31-34 days, homogenized and centrifuged at 600g to obtain a fraction enriched in intact mitochondria. CI-dependent ATP production was measured in the presence of pyruvate, malate, ADP, PO<sub>4</sub><sup>3-</sup> and creatine and expressed both per U of CS and per mg of protein. The data presented suggest that up to day 35, mitochondrial biogenesis can compensate for the decrease in CI-dependent ATP production capacity per mitochondrial mass in heart and skeletal muscle, but not in brain. Using intact heart mitochondria from a heart-specific *Ndufs4*<sup>-/-</sup> mouse, Sterky *et al* observed a tendency to decrease of the ATP production rate normalized to CS and measured

- ▶ basket cell (bc) extension is seen, containing normal mitochondria (m). (D) KO cerebellum depicting normal Purkinje cell features with healthy organelles, and to the far right 3 basket cell (bc) extensions containing abnormal mitochondria with condensed cristae (indicated with an asterisk). (E) Details of basket cell (bc) mitochondria (m) show normal cristae in WT mice, while (F) depicts mitochondria with abnormal cristae (indicated with an asterisk) in the KO mice. Magnification (in E, F) is 8000x. (G) A higher magnification in the KO mouse at 15000x is clearly demonstrating the mitochondria with condensed cristae (indicated with an asterisk) in the basket cell (bc). Bars in (C), (D), (E), and (G) are 1µm.

in the presence of either pyruvate and malate or glutamate and malate (Sterky, Hoffman et al. 2012). In addition, they observed a tendency to increase of the activity of CS. Based on these data they tentatively concluded that the *Ndufs4*<sup>-/-</sup>-deficient heart underwent a compensatory increase in mitochondrial mass in order to ensure a normal overall tissue ATP production capacity. This idea, which is substantiated in the present study, provides a logical explanation for the observation that the rate of phosphocreatine recovery was not different between ubiquitous *Ndufs4*<sup>-/-</sup> mice and their wildtype counterparts in the ischemic hind limb reperfusion paradigm (Kruse, Watt et al. 2008). Moreover, our results demonstrate the functionality of the increase in mitochondrial clusters in the subsarcolemma of the soleus muscle reported by these authors.

Increased mitochondrial biogenesis involves the activation of peroxisome-proliferator-activated receptor  $\gamma$  co-activator-1 $\alpha$  (PGC-1 $\alpha$ ); (Jornayvaz and Shulman 2010). The activity of PGC-1 $\alpha$  is controlled by several factors including the cellular energy sensor AMP-activated protein kinase (AMPK). Upon activation, PGC-1 $\alpha$  activates several transcription factors including nuclear respiratory factor 1 (NRF-1) and nuclear respiratory factor 2 (NRF-2), which activate mitochondrial transcription factor A (Tfam). Expression of PGC-1 $\alpha$  has been shown to be decreased under conditions of chronic stress (Farhoud, Nijtmans et al. 2012). On the other hand, degradation of PGC-1 $\alpha$  by the ubiquitin-proteasome system was found to be slowed down in cultured primary skin fibroblasts from CI-deficient patients (Farhoud, Nijtmans et al. 2012). Studies with cultured primary skin fibroblasts from CI-deficient patients have shown the increased oxidation of probes sensitive to reactive oxygen species (ROS); (Koopman, Nijtmans et al. 2010). If unbalanced by the antioxidant systems of the cell, this increase in ROS production results in the condition of chronic oxidative stress. It is tempting to speculate that the effect of chronic oxidative stress predominates in brain keeping PGC-1 $\alpha$  low thus preventing increased mitochondrial biogenesis, whereas in skeletal muscle and heart the effect of degradation inhibition predominates resulting in increased levels of PGC-1 $\alpha$  and thus increased mitochondrial biogenesis. Evidence favoring a beneficial effect of activation of the AMPK/PGC-1 $\alpha$  pathway comes from studies with primary skin fibroblasts of CI-deficient patients cultured in the presence of galactose showing that the AMPK activator 5-Aminoimidazole-4-carboxamide ribotide (AICAR) decreased the production of ROS and increased mitochondrial biogenesis, cell growth and cellular ATP content (Golubitzky, Dan et al. 2011).

In addition to measuring the ATP production capacity, we measured the maximal rate of pyruvate oxidation in the tissue fractions enriched in intact mitochondria.

The assay medium was exactly the same for both measurements and regression analysis revealed a linear correlation for all three tissues and regardless whether they were from the *Ndufs4*<sup>-/-</sup> mice or their wildtype counterparts. From the slope it can be calculated that ~5-6 mol of ATP is produced per mol of pyruvate. The major conclusion that can be drawn from this result is that in none of the three tissues the absence of the NDUFS4 subunit alters the efficiency with which the uptake and oxidation of pyruvate is coupled to the production and release of ATP.

As already reported by many other researchers, the absence of the NDUFS4 subunit did not lead to the absence of CI-dependent pyruvate oxidation and ATP production in an intact mitochondrial-enriched fraction. BN-PAGE analysis revealed the presence of a CI subcomplex of ~830 kDa rather than the fully assembled complex of 1 MDa (Valsecchi, Monge et al. 2012). This subcomplex failed to show in-gel activity, indicating that it lacks the functional NADH dehydrogenase module. However, in a recent study we provided evidence that CIII may functionally stabilize the ~830 kDa subcomplex and the NADH dehydrogenase module in the absence of NDUFS4 (Calvaruso, Willems et al. 2012). Apparently, this stabilization is disturbed during the freeze-thawing procedure required to measure the activity of the complex.

The above idea that mitochondrial biogenesis compensates for the decrease in CI-dependent ATP production capacity per mitochondrial mass in heart and skeletal muscle of *Ndufs4*<sup>-/-</sup> mice implicates that apart from the maximal activity of CS also the maximal activity of the individual RC complexes is increased in these tissues and that this is not the case in brain. Analysis of the maximal activity of the individual RC complexes was performed in a freeze-thawed aliquot of the mitochondrial-enriched fraction used for measurement of the ATP production capacity. The overall picture that emerges from these measurements is that of an increase in maximal activity of CII, CIII and CIV per tissue mass in KO skeletal muscle and heart. In sharp contrast, the activity per tissue mass remained unaltered in KO brain. These data indicate that normalization of the ATP production capacity to either one of the above three RC complex activities yields the wrong picture. For instance, Leong et al normalized the CI-dependent ATP production measured in the presence of glutamate and malate to the CII-dependent ATP production and concluded a significant decrease in heart and brain of NDUFS4-deficient *Ndufs4*<sup>flky/flky</sup> mice (Leong, Komen et al. 2012). Extrapolation of our result of an increase in CII activity in skeletal muscle but not brain most probably leads to the same conclusion as obtained in the present study that the ATP production capacity per tissue mass is not altered in skeletal muscle but decreased in brain.

When expressed per mitochondrial mass, the maximal activity of CII and CIII tended to be lower in skeletal muscle and heart but this was not reflected by the maximal SCC activity, measuring the combined activity of these two complexes, which showed no change. Thus, when expressed per mitochondrial mass neither of the three tissues showed a change in maximal activity of CII, CIII and CIV. Kruse *et al* reported a significant increase in maximal activity of CII, but not CIII and CIV, when normalized to CS in submitochondrial particles from liver of the ubiquitous *Ndufs4*<sup>-/-</sup> mouse (Kruse, Watt *et al.* 2008). This result suggests that in liver, CII is selectively upregulated to a larger extent than CS and, therefore, mitochondrial mass. This emphasizes our above remark that the ATP production capacity should not be expressed per activity of one of the RC complexes. In contrast to our findings, Karamanlidis *et al* reported no change in CII, CIV and CS activity in submitochondrial particles isolated from a heart-specific *Ndufs4*<sup>-/-</sup> mouse (Karamanlidis, Lee *et al.* 2013). Although details on normalization are lacking it is likely that activities were normalized to mg of protein. On the other hand, Sterky *et al* showed a significant reduction in CII activity normalized to CS in a detergent-permeabilized mitochondrial preparation from heart tissue of a heart-specific *Ndufs4*<sup>-/-</sup> mouse (Sterky, Hoffman *et al.* 2012). Although we also observe a tendency to decrease of this activity in heart, our SCC measurement shows that the combined activity of CII and CIII is not altered. In agreement with our findings no differences in maximal activity were observed for CII, CIII and CIV normalized to CS in brain of the NDUF54-deficient *Ndufs4*<sup>fkyl/fky</sup> mouse (Leong, Komen *et al.* 2012). Taken together, the results of the present study substantiate the idea that the absence of the NDUF54 does not significantly affect the maximal activity per mitochondrial mass of CII, CIII and CIV in brain, heart and skeletal muscle.

In contrast to the above conclusion that mitochondrial biogenesis can compensate for the decrease in ATP production capacity per mitochondrial mass, CI-driven oxygen consumption appeared to be halved in intact liver cells of the ubiquitous *Ndufs4*<sup>-/-</sup> mouse (Kruse, Watt *et al.* 2008). The same results were obtained with brain tissue of the brain-specific *Ndufs4*<sup>-/-</sup> mouse (Quintana, Kruse *et al.* 2010). In the present study we did not include liver but the above result obtained with brain tissue from the brain-specific *Ndufs4*<sup>-/-</sup> mouse is in agreement with our observation that this tissue lacks compensatory mitochondrial biogenesis. Also in contrast to the above conclusion that mitochondrial biogenesis can compensate for the decrease in ATP production capacity per mitochondrial mass, permeabilized cardiac myofibers from the heart-specific *Ndufs4*<sup>-/-</sup> mouse showed a reduction in CI-driven mitochondrial



respiration (Karamanlidis, Lee et al. 2013). However, in the same study no increase in CS and therefore mitochondrial biogenesis was observed (see above). It remains to be established whether these discrepancies are due to the fact that unstressed heart-specific *Ndufs4*<sup>-/-</sup> mice, unlike ubiquitous *Ndufs4*<sup>-/-</sup> mice, show no clinical phenotype.

It has been suggested that the pathophysiological consequences of isolated CI deficiency are neurological (Kruse, Watt et al. 2008, Quintana, Kruse et al. 2010, Leong, Komen et al. 2012, Quintana, Zanella et al. 2012). It is tempting to speculate that this has to do with the present observation that brain tissue is unable to perform a compensatory increase in ATP production capacity. However, our analysis involves the whole brain. Quintana *et al* reported the cerebellum to be one of the most affected brain regions in the conditional brain-specific *Ndufs4*<sup>-/-</sup> mouse (Quintana, Kruse *et al.* 2010). To gain more insight we studied the mitochondrial ultrastructure in cerebellar cells. As already reported by Quintana *et al* analysis of the electron micrographs demonstrated the presence of abnormal mitochondria with condensed cristae in the axo-somatic collaterals of the inhibitory GABAergic basket cells surrounding the Purkinje cells.

As discussed above ROS production is increased in cultured primary skin fibroblasts of CI-deficient patients (Koopman, Nijtmans et al. 2010). If unbalanced by the antioxidant systems of the cell, this increase in ROS production may result in an increase in lipid peroxidation as demonstrated by the addition of rotenone in the absence and presence of the mitochondria-targeted antioxidant mitoquinone (Koopman, Verkaart et al. 2005). It has been speculated that lipid peroxidation products such as malondialdehyde and 4-hydroxynonenal (HNE) may induce damage to vulnerable brain cells (Kayser, Sedensky et al. 2016). However, the latter authors showed that covalent modification of mitochondrial proteins by HNE was not increased in olfactory bulb, brainstem and cerebellum, brain regions showing increased degeneration in *Ndufs4*<sup>-/-</sup> mice. Similarly, Chouchani *et al* did not find any sign of oxidative damage in heart tissue of a heart-specific *Ndufs4*<sup>-/-</sup> mouse during development of severe hypertrophic cardiomyopathy (Chouchani, Methner et al. 2014). The induction of dopamine neuron death by rotenone has implicated CI in Parkinson's disease (Choi, Palmiter et al. 2011). However, these authors provided evidence that the increase in NADH-mediated dopamine production and ROS formation induced by CI inhibition alone is not sufficient to induce dopamine neuron death and that the latter requires the additional increase in microtubule depolymerization as obtained with rotenone but not with piericidin A (Choi, Palmiter et al. 2011). Leong *et al* observed increased levels of hydroxyacylcarnitine species

and inferred that CI dysfunction increases the NADH/NAD<sup>+</sup> ratio thus inhibiting mitochondrial fatty acid oxidation (Leong, Komen et al. 2012). The heart-specific *Ndufs4*<sup>-/-</sup> mouse generated by Karamanlidis *et al* also displayed an increased NADH/NAD<sup>+</sup> ratio, which was associated with inhibition of Sirtuin-3 resulting in increased protein acetylation and sensitization of the mitochondrial permeability transition pore (Karamanlidis, Lee et al. 2013). NAD<sup>+</sup> precursor supplementation partially normalized the NADH/NAD<sup>+</sup> ratio, protein acetylation and mPTP sensitivity.

In conclusion, the present study demonstrates that skeletal muscle and heart respond to a decrease in CI-dependent ATP production capacity per mitochondrial mass with an increase in mitochondrial biogenesis resulting in maintenance of the overall tissue CI-dependent ATP production capacity. The absence of such an adaptive response in brain may explain the increased degeneration observed in olfactory bulb, brainstem and cerebellum of *Ndufs4*<sup>-/-</sup> mice. Given the fact that ubiquitous and brain-specific *Ndufs4*<sup>-/-</sup> mice display the same clinical phenotype, this means that these brain regions are the primary target for therapeutic intervention (Koopman, Beyrath et al. 2016).

## References

- Alam, M. T., G. R. Manjeri, R. J. Rodenburg, J. A. Smeitink, R. A. Notebaart, M. Huynen, P. H. Willems and W. J. Koopman (2015). "Skeletal muscle mitochondria of NDUF54<sup>-/-</sup> mice display normal maximal pyruvate oxidation and ATP production." *Biochim Biophys Acta* **1847**(6-7): 526-533.
- Calvaruso, M. A., P. Willems, M. van den Brand, F. Valsecchi, S. Kruse, R. Palmiter, J. Smeitink and L. Nijtmans (2012). "Mitochondrial complex III stabilizes complex I in the absence of NDUF54 to provide partial activity." *Hum Mol Genet* **21**(1): 115-120.
- Choi, W. S., R. D. Palmiter and Z. Xia (2011). "Loss of mitochondrial complex I activity potentiates dopamine neuron death induced by microtubule dysfunction in a Parkinson's disease model." *J Cell Biol* **192**(5): 873-882.
- Chouchani, E. T., C. Methner, G. Buonincontri, C. H. Hu, A. Logan, S. J. Sawiak, M. P. Murphy and T. Krieg (2014). "Complex I deficiency due to selective loss of Ndufs4 in the mouse heart results in severe hypertrophic cardiomyopathy." *PLoS One* **9**(4): e94157.
- Distelmaier, F., W. J. Koopman, L. P. van den Heuvel, R. J. Rodenburg, E. Mayatepek, P. H. Willems and J. A. Smeitink (2009). "Mitochondrial complex I deficiency: from organelle dysfunction to clinical disease." *Brain* **132**(Pt 4): 833-842.
- Farhoud, M. H., L. G. Nijtmans, R. J. Wanders, H. J. Wessels, E. Lasonder, A. J. Janssen, R. R. Rodenburg, L. P. van den Heuvel and J. A. Smeitink (2012). "Impaired ubiquitin-proteasome-mediated PGC-1alpha protein turnover and induced mitochondrial biogenesis secondary to complex-I deficiency." *Proteomics* **12**(9): 1349-1362.
- Golubitzky, A., P. Dan, S. Weissman, G. Link, J. D. Wikstrom and A. Saada (2011). "Screening for active small molecules in mitochondrial complex I deficient patient's fibroblasts, reveals AICAR as the most beneficial compound." *PLoS One* **6**(10): e26883.
- Hatefi, Y. (1985). "The mitochondrial electron transport and oxidative phosphorylation system." *Annu Rev Biochem* **54**: 1015-1069.
- Janssen, A. J., F. J. Trijbels, R. C. Sengers, J. A. Smeitink, L. P. van den Heuvel, L. T. Wintjes, B. J. Stoltenborg-Hogenkamp and R. J. Rodenburg (2007). "Spectrophotometric assay for complex I of the respiratory chain in tissue samples and cultured fibroblasts." *Clin Chem* **53**(4): 729-734.
- Janssen, A. J., F. J. Trijbels, R. C. Sengers, L. T. Wintjes, W. Ruitenbeek, J. A. Smeitink, E. Morava, B. G. van Engelen, L. P. van den Heuvel and R. J. Rodenburg (2006). "Measurement of the energy-generating capacity of human muscle mitochondria: diagnostic procedure and application to human pathology." *Clin Chem* **52**(5): 860-871.
- Jornayvaz, F. R. and G. I. Shulman (2010). "Regulation of mitochondrial biogenesis." *Essays Biochem* **47**: 69-84.
- Karamanlidis, G., C. F. Lee, L. Garcia-Menendez, S. C. Kolwicz, Jr., W. Suthammarak, G. Gong, M. M. Sedensky, P. G. Morgan, W. Wang and R. Tian (2013). "Mitochondrial complex I deficiency increases protein acetylation and accelerates heart failure." *Cell Metab* **18**(2): 239-250.
- Kayser, E. B., M. M. Sedensky and P. G. Morgan (2016). "Region-Specific Defects of Respiratory Capacities in the Ndufs4(KO) Mouse Brain." *PLoS One* **11**(1): e0148219.
- Kirby, D. M., D. R. Thorburn, D. M. Turnbull and R. W. Taylor (2007). "Biochemical assays of respiratory chain complex activity." *Methods Cell Biol* **80**: 93-119.
- Koopman, W. J., J. Beyrath, C. W. Fung, S. Koene, R. J. Rodenburg, P. H. Willems and J. A. Smeitink (2016). "Mitochondrial disorders in children: toward development of small-molecule treatment strategies." *EMBO Mol Med* **8**(4): 311-327.

- Koopman, W. J., L. G. Nijtmans, C. E. Dieteren, P. Roestenberg, F. Valsecchi, J. A. Smeitink and P. H. Willems (2010). "Mammalian mitochondrial complex I: biogenesis, regulation, and reactive oxygen species generation." *Antioxid Redox Signal* **12**(12): 1431-1470.
- Koopman, W. J., S. Verkaart, H. J. Visch, F. H. van der Westhuizen, M. P. Murphy, L. W. van den Heuvel, J. A. Smeitink and P. H. Willems (2005). "Inhibition of complex I of the electron transport chain causes O<sub>2</sub><sup>-</sup>-mediated mitochondrial outgrowth." *Am J Physiol Cell Physiol* **288**(6): C1440-1450.
- Kruse, S. E., W. C. Watt, D. J. Marcinek, R. P. Kapur, K. A. Schenkman and R. D. Palmiter (2008). "Mice with mitochondrial complex I deficiency develop a fatal encephalomyopathy." *Cell Metab* **7**(4): 312-320.
- Leong, D. W., J. C. Komen, C. A. Hewitt, E. Arnaud, M. McKenzie, B. Phipson, M. Bahlo, A. Laskowski, S. A. Kinkel, G. M. Davey, W. R. Heath, A. K. Voss, R. P. Zahedi, J. J. Pitt, R. Chrast, A. Sickmann, M. T. Ryan, G. K. Smyth, D. R. Thorburn and H. S. Scott (2012). "Proteomic and metabolomic analyses of mitochondrial complex I-deficient mouse model generated by spontaneous B2 short interspersed nuclear element (SINE) insertion into NADH dehydrogenase (ubiquinone) Fe-S protein 4 (Ndufs4) gene." *J Biol Chem* **287**(24): 20652-20663.
- Manjeri, G. R., R. J. Rodenburg, L. Blanchet, S. Roelofs, L. G. Nijtmans, J. A. Smeitink, J. J. Driessen, W. J. Koopman and P. H. Willems (2016). "Increased mitochondrial ATP production capacity in brain of healthy mice and a mouse model of isolated complex I deficiency after isoflurane anesthesia." *J Inher Metab Dis* **39**(1): 59-65.
- Mimaki, M., X. Wang, M. McKenzie, D. R. Thorburn and M. T. Ryan (2012). "Understanding mitochondrial complex I assembly in health and disease." *Biochim Biophys Acta* **1817**(6): 851-862.
- Moran, M., H. Rivera, M. Sanchez-Arago, A. Blazquez, B. Merinero, C. Ugalde, J. Arenas, J. M. Cuezva and M. A. Martin (2010). "Mitochondrial bioenergetics and dynamics interplay in complex I-deficient fibroblasts." *Biochim Biophys Acta* **1802**(5): 443-453.
- Ngu, L. H., L. G. Nijtmans, F. Distelmaier, H. Venselaar, S. E. van Emst-de Vries, M. A. van den Brand, B. J. Stoltenborg, L. T. Wintjes, P. H. Willems, L. P. van den Heuvel, J. A. Smeitink and R. J. Rodenburg (2012). "A catalytic defect in mitochondrial respiratory chain complex I due to a mutation in NDUF52 in a patient with Leigh syndrome." *Biochim Biophys Acta* **1822**(2): 168-175.
- Nouws, J., L. G. Nijtmans, J. A. Smeitink and R. O. Vogel (2012). "Assembly factors as a new class of disease genes for mitochondrial complex I deficiency: cause, pathology and treatment options." *Brain* **135**(Pt 1): 12-22.
- Pagniez-Mammeri, H., M. Rak, A. Legrand, P. Benit, P. Rustin and A. Slama (2012). "Mitochondrial complex I deficiency of nuclear origin II. Non-structural genes." *Mol Genet Metab* **105**(2): 173-179.
- Quintana, A., S. E. Kruse, R. P. Kapur, E. Sanz and R. D. Palmiter (2010). "Complex I deficiency due to loss of Ndufs4 in the brain results in progressive encephalopathy resembling Leigh syndrome." *Proc Natl Acad Sci U S A* **107**(24): 10996-11001.
- Quintana, A., S. Zanella, H. Koch, S. E. Kruse, D. Lee, J. M. Ramirez and R. D. Palmiter (2012). "Fatal breathing dysfunction in a mouse model of Leigh syndrome." *J Clin Invest* **122**(7): 2359-2368.
- Rodenburg, R. J. (2011). "Biochemical diagnosis of mitochondrial disorders." *J Inher Metab Dis* **34**(2): 283-292.
- Smeitink, J. A., M. Zeviani, D. M. Turnbull and H. T. Jacobs (2006). "Mitochondrial medicine: a metabolic perspective on the pathology of oxidative phosphorylation disorders." *Cell Metab* **3**(1): 9-13.

- Sterky, F. H., A. F. Hoffman, D. Milenkovic, B. Bao, A. Paganelli, D. Edgar, R. Wibom, C. R. Lupica, L. Olson and N. G. Larsson (2012). "Altered dopamine metabolism and increased vulnerability to MPTP in mice with partial deficiency of mitochondrial complex I in dopamine neurons." *Hum Mol Genet* **21**(5): 1078-1089.
- Taylor, R. W. and D. M. Turnbull (2005). "Mitochondrial DNA mutations in human disease." *Nat Rev Genet* **6**(5): 389-402.
- Trounce, I. A., Y. L. Kim, A. S. Jun and D. C. Wallace (1996). "Assessment of mitochondrial oxidative phosphorylation in patient muscle biopsies, lymphoblasts, and transmitochondrial cell lines." *Methods Enzymol* **264**: 484-509.
- Valsecchi, F., W. J. Koopman, G. R. Manjeri, R. J. Rodenburg, J. A. Smeitink and P. H. Willems (2010). "Complex I disorders: causes, mechanisms, and development of treatment strategies at the cellular level." *Dev Disabil Res Rev* **16**(2): 175-182.
- Valsecchi, F., C. Monge, M. Forkink, A. J. de Groof, G. Benard, R. Rossignol, H. G. Swarts, S. E. van Emst-de Vries, R. J. Rodenburg, M. A. Calvaruso, L. G. Nijtmans, B. Heeman, P. Roestenberg, B. Wieringa, J. A. Smeitink, W. J. Koopman and P. H. Willems (2012). "Metabolic consequences of NDUFS4 gene deletion in immortalized mouse embryonic fibroblasts." *Biochim Biophys Acta* **1817**(10): 1925-1936.
- Zeviani, M. and S. Di Donato (2004). "Mitochondrial disorders." *Brain* **127**(Pt 10): 2153-2172.



# CHAPTER

## **Skeletal muscle mitochondria of the $NDUFS4^{-/-}$ mice display normal pyruvate oxidation and ATP production**

Published in:

Alam, M. T., **G. R. Manjeri**, R. J. Rodenburg, J. A. Smeitink,  
R. A. Notebaart, M. Huynen, P. H. Willems and W. J. Koopman (2015).

“Skeletal muscle mitochondria of  $NDUFS4^{-/-}$  mice display normal  
maximal pyruvate oxidation and ATP production.” **Biochim Biophys**

**Acta 1847(6-7): 526-533. (Shared 1<sup>st</sup> author)**

# 3

## Abstract

Mitochondrial ATP production is mediated by the oxidative phosphorylation (OXPHOS) system, which consists of four multi-subunit complexes (CI-CIV) and the F<sub>o</sub>F<sub>1</sub>-ATP synthase (CV). Mitochondrial disorders including Leigh Syndrome often involve CI dysfunction, the pathophysiological consequences of which still remain incompletely understood. Here we combined experimental and computational strategies to gain mechanistic insight into the energy metabolism of isolated skeletal muscle mitochondria from 5 weeks old wild-type (WT) and CI-deficient *NDUFS4*<sup>-/-</sup> (KO) mice. Enzyme activity measurements in KO mitochondria revealed a reduction of 79% in maximal CI activity ( $V_{max}$ ), which was paralleled by 45-72% increase in  $V_{max}$  of CII, CIII, CIV and citrate synthase. Mathematical modeling of mitochondrial metabolism predicted that these  $V_{max}$  changes do not affect the maximal rates of pyruvate (PYR) oxidation and ATP production in KO mitochondria. This prediction was empirically confirmed by flux measurements. *In silico* analysis further predicted that CI deficiency altered the concentration of intermediate metabolites, modestly increased mitochondrial NADH/NAD<sup>+</sup> ratio and stimulated the lower half of the TCA cycle, including CII. Several of the predicted changes were previously observed in experimental models of CI-deficiency. Interestingly, model predictions further suggested that CI deficiency only has major metabolic consequences when its activity decreases below 90% of normal levels, compatible with a biochemical threshold effect. Taken together, our results suggest that mouse skeletal muscle mitochondria possess a substantial CI overcapacity, which minimizes the effects of CI dysfunction on mitochondrial metabolism in this otherwise early fatal mouse model.



## Introduction

Mitochondria are among the prime producers of cellular ATP and consist of a matrix compartment surrounded by an inner (MIM) and outer membrane (MOM), with in between an inter-membrane space (IMS) (Kroemer 1999, Newmeyer and Ferguson-Miller 2003, Duchen 2004, Balaban, Nemoto et al. 2005, McBride, Neuspiel et al. 2006, Detmer and Chan 2007, Dieteren, Gielen et al. 2011). Mitochondrial ATP production is fueled by pyruvate (PYR), two molecules of which are generated from glucose (GLU) by glycolysis in the cytosol. PYR can be reversibly converted by lactate dehydrogenase (LDH) into lactate or imported into the mitochondrial matrix by a dedicated pyruvate carrier (Herzig, Raemy et al. 2012). Within the mitochondrion PYR is converted into acetyl coenzyme A (acetyl-CoA) that enters the tricarboxylic acid (TCA) cycle to yield two molecules of CO<sub>2</sub>, one molecule of ATP, four molecules of NADH and one molecule of FADH<sub>2</sub>. NADH and FADH<sub>2</sub> serve as substrates for the oxidative phosphorylation (OXPHOS) system to generate ATP (Duchen 2004). The OXPHOS system consists of four multi-subunit complexes (CI-CIV) that form the electron transport chain (ETC) and the ATP-generating F<sub>0</sub>F<sub>1</sub>-ATPase (CV). Within the ETC electrons donated by NADH (at CI) and FADH<sub>2</sub> (at CII) are transported to CIII and CIV by coenzyme Q<sub>10</sub> (CoQ<sub>10</sub>) and cytochrome-c (cyt-c), respectively. At CIV, electrons are donated to molecular oxygen (O<sub>2</sub>) to form water. The energy released during electron transport is utilized at CI, CIII and CIV to transport H<sup>+</sup> out of the mitochondrial matrix across the MIM. This process generates an inward-directed proton-motive force (PMF) consisting of an electrical ( $\Delta\Psi$ ) and chemical component ( $\Delta\text{pH}$ ). At CV the energy associated with H<sup>+</sup> re-entry into the mitochondria matrix is used to generate ATP from ADP and inorganic phosphate (P<sub>i</sub>).

In addition to ATP generation, mitochondria also play a key role in various other cellular processes, including reactive oxygen species (ROS) generation, calcium signaling and apoptosis induction. Therefore it is not surprising that dysfunction of the OXPHOS system, which sustains most mitochondrial functions, is associated with a broad range of human disorders (Kim, Vlkolinsky et al. 2001, Orth and Schapira 2002, DiMauro and Schon 2003, Coskun, Beal et al. 2004, Finsterer 2006, Schapira 2006, Koopman, Willems et al. 2012). Among OXPHOS disorders, deficiency of CI (OMIM 252010) is the most common (Kirby, Crawford et al. 1999, Loeffen, Smeitink et al. 2000, Smeitink, Sengers et al. 2001, Smeitink, van den Heuvel et al. 2001, Benit, Steffann et al. 2003, Carroll, Fearnley et al. 2006, Kruse, Watt et al. 2008, Distelmaier, Koopman et al. 2009, Fassone and Rahman 2012). Human CI deficiency is associated with a wide range of clinical presentations including muscle weakness, heart disease,

liver failure, respiratory failure and congenital lactic acidosis, often leading to death in early childhood (Smeitink, van den Heuvel et al. 2001, Kruse, Watt et al. 2008, Distelmaier, Koopman et al. 2009, Fassone and Rahman 2012, Koopman, Willems et al. 2012, Koopman, Distelmaier et al. 2013). CI is the largest protein complex of the *oxidative phosphorylation* system and consists of 44 different proteinaceous subunits that are encoded by either the mitochondrial (mtDNA) or nuclear DNA (Koopman, Nijtmans et al. 2010, Balsa, Marco et al. 2012, Nouws, Nijtmans et al. 2012). Regarding the cellular consequences of nDNA-encoded CI mutations, several studies with primary patient fibroblast have been carried out revealing aberrations in maximal ETC enzyme activities ( $V_{\max}$ ) and mitochondrial morphology, increased levels of cellular reactive oxygen species (ROS) and disturbed calcium and ATP homeostasis (Visch, Rutter et al. 2004, Koopman, Visch et al. 2005, Koopman, Verkaart et al. 2007, Koopman, Verkaart et al. 2008, Willems, Valsecchi et al. 2008, Willems, Smeitink et al. 2009, Koopman, Nijtmans et al. 2010).

Recently a whole-body KO mouse model of human CI deficiency became available in which one of the CI accessory subunit genes (*NDUFS4*) is deleted (Kruse, Watt et al. 2008). The *NDUFS4* gene encodes an 18-kDa protein (NDUFS4 or NADH dehydrogenase (ubiquinone) Fe-S protein 4). When *NDUFS4* is absent, proper CI assembly is hampered and its  $V_{\max}$  is reduced (van den Heuvel, Ruitenbeek et al. 1998, Smeitink, Sengers et al. 2001, Smeitink, van den Heuvel et al. 2001, Carroll, Fearnley et al. 2006, Kruse, Watt et al. 2008, Fassone and Rahman 2012, Valsecchi, Monge et al. 2012). Importantly, several symptoms of human CI deficiency are also observed in *NDUFS4*<sup>-/-</sup> animals such as developmental delays, failure to thrive, lethargy, ophthalmoplegia and progressive encephalomyopathy leading to early lethality. However, the consequences of *NDUFS4* gene deletion on mitochondrial energy metabolism, its underlying reaction rates and reactant concentrations have not been investigated yet. Here we addressed this question by combining experimental and computational strategies to evaluate: (i) if *NDUFS4* knockout affected the  $V_{\max}$  of key ETC enzymes and citrate synthase (CS), and (ii) whether *NDUFS4* knockout impacted on the maximal rates of PYR oxidation and ATP production in isolated skeletal muscle mitochondria. To this end we first adapted a previously validated dynamic model of mitochondrial metabolism (Wu, Yang et al. 2007) to our experimental conditions. Next, we used this model to predict the consequences of *NDUFS4* knockout on the steady-state values of metabolic fluxes, metabolite concentrations and physiological variables including  $\Delta y$ . This analysis predicted that a reduction of ~80% in the  $V_{\max}$  of CI did not affect the maximal rates of mitochondrial PYR oxidation and ATP production in isolated *NDUFS4*<sup>-/-</sup> skeletal

muscle mitochondria. This prediction was confirmed by experimental flux analysis and suggests that these mitochondria possess a substantial CI overcapacity that limits the impact of CI deficiency on mitochondrial metabolism.

## Materials and Methods

**Animals** – *NDUFS4*<sup>-/-</sup> knockout (KO) and wild-type (WT) mice (mixed 129/Sv: C57BL6 background) were generated by crossing heterozygote (*NDUFS4*<sup>+/-</sup>) mice. The genotype was confirmed by polymerase chain reaction (PCR) testing. Mice had *ad libitum* access to food and water and were fed on a standard animal diet (Ssniff GmbH, Soest, Germany: V1534-300 R/M-H). Animals were group housed at 22°C and maintained on a day and night rhythm of 12 hours. The animal studies were approved by the Regional Animal Ethics Committee (Nijmegen, The Netherlands) and performed under the guidelines of the Dutch Council for Animal Care. Both male and female animals were used in this study yielding similar results.

### Measurement of maximal pyruvate oxidation, ATP production and enzymatic activities in mitoplasts

– Skeletal muscle tissue from the entire hind limb was harvested from 5 wks old WT and KO animals, homogenized and centrifuged at 600g. Importantly, maximal PYR oxidation rates, ATP production rates and enzymatic activities ( $V_{max}$ ) were performed using the same 600g supernatant using standardized protocols (Janssen, Trijbels et al. 2006, Rodenburg 2011). To quantify pyruvate oxidation, mitochondrial preparations were incubated with radiolabelled substrate ([1-14C] pyruvate). After 20 min the reaction was stopped and the amount of liberated radioactive CO<sub>2</sub> (<sup>14</sup>CO<sub>2</sub>) was quantified [40]. The assay medium (pH 7.4) contained K<sup>+</sup>-phosphate buffer (30 mM; source of P<sub>i</sub>), KCl (75 mM), Tris (8 mM), K-EDTA (1.6 mM), P<sub>1</sub>P<sub>5</sub>-Di (adenosine-5') pentaphosphate (Ap5A; 0.2 mM), MgCl<sub>2</sub> (0.5 mM), ADP (2 mM), creatine (20 mM), malate (1 mM) and [1-14C] pyruvate (1 mM). AP5A is a potent adenylate kinase (AK) inhibitor required to prevent interference of the AK reaction with the levels of produced ATP, as well as with the excess of ADP required for this assay. For ATP production measurements, the same assay medium was used but with pyruvate instead of [1-14C] pyruvate. After 20 min, the reaction was stopped by addition of 0.1 M HClO<sub>4</sub>. The reaction mixture was centrifuged at 14000g for 2 min at 2 °C. To the supernatant, 1.2 vol (V/V) of 0.333 M KHCO<sub>3</sub> was added, and this mixture was diluted 2-fold. The amount of ATP and phosphocreatine formed during the reaction were measured in the supernatant using a Konelab 20XT auto-analyzer (Thermo Scientific). Mitochondrial ATP production rate was corrected using a parallel assay

in which residual glycolysis was blocked by arsenite (2 mM) (Janssen, Trijbels et al. 2006). The maximal activities of complex I (CI), complex II (CII), complex III (CIII), complex IV (CIV) and citrate synthase (CS) were measured in freeze-thawed 600g supernatants, as described in (Rodenburg 2011).

**Mathematical modeling and statistical analysis** – Dynamic modeling and statistical analysis were performed using custom scripts written in Matlab 6.1 (Mathworks, Natick, Massachusetts, U.S.A.). The latter are available upon request. Unless stated otherwise, experimental data is presented as mean±SEM (standard error of the mean) and statistical significance between datasets is assessed using an independent 2-population Student's t-test.

## Results & Discussion

**Overall experimental and computational strategy** – In this study we used mitochondria from skeletal muscle of wildtype (WT) mice and *NDUFS4*<sup>-/-</sup> (KO) mice for experimental analysis. Mitochondria were placed in an assay medium and were considered as a classical input-output (I/O) system (cartoon in Fig. 1), which converts pyruvate (PYR; input) into ATP (output) via the integrated action of transporters, the TCA cycle and the OXPHOS system (Fig. 2). To perform computational analysis of this system we adapted a mathematical model of the mitochondrial bioenergetic system that was previously validated by Beard and co-workers (Wu, Yang et al. 2007). This model consists of a collection of ordinary differential equations (ODEs) and parameters, which allows integrated simulation of the above I/O system and prediction of the underlying fluxes, metabolite concentrations and physicochemical parameters. Our overall strategy (Fig. 1) aimed to first adapt the published model to the conditions under which PYR oxidation and ATP production are measured in our experimental assay medium (explained in more detail below). This yielded a mathematical model for isolated WT mitochondria (“WT model”). Next, the WT model was adjusted by including the measured maximum activities ( $V_{\max}$ ) of CI, CII, CIII, CIV and citrate synthase (CS) in mitochondria from WT and KO mice. This was achieved by multiplying the  $V_{\max}$  values in the WT model by a “pre-factor” (KO/WT) corresponding to the experimental change observed in these values for KO mitochondria. In this way a pre-factor >1 represented an increase in  $V_{\max}$  for the KO vs. the WT condition, whereas a pre-factor <1 represented a decrease in  $V_{\max}$  for the KO vs. the WT condition. We also generated two alternative KO models (KO model B and C) to simulate the consequences of increased CS activity with respect to TCA cycle enzyme activity and mitochondrial volume (see below for details). The

KO models were used to predict the maximal PYR oxidation and ATP production rates (expressed as KO/WT ratios), which were compared with experimentally determined values for model validation, as well as other relevant reaction fluxes, metabolite concentrations and physiological parameters.

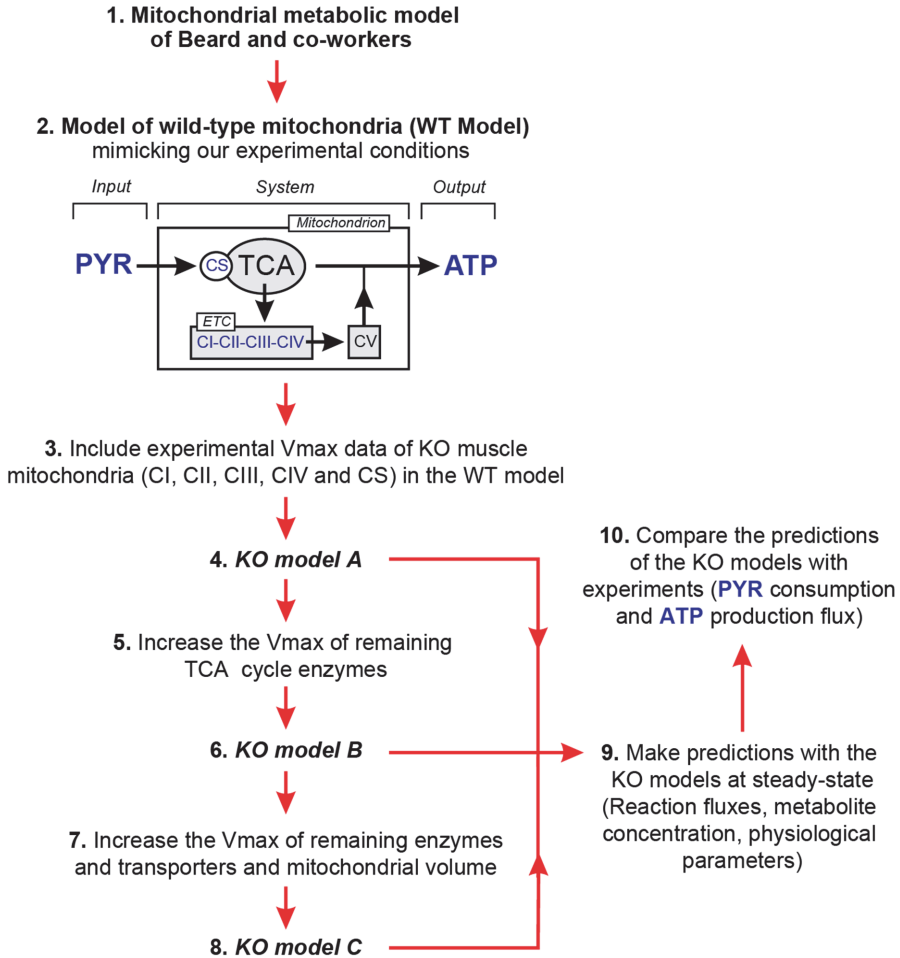
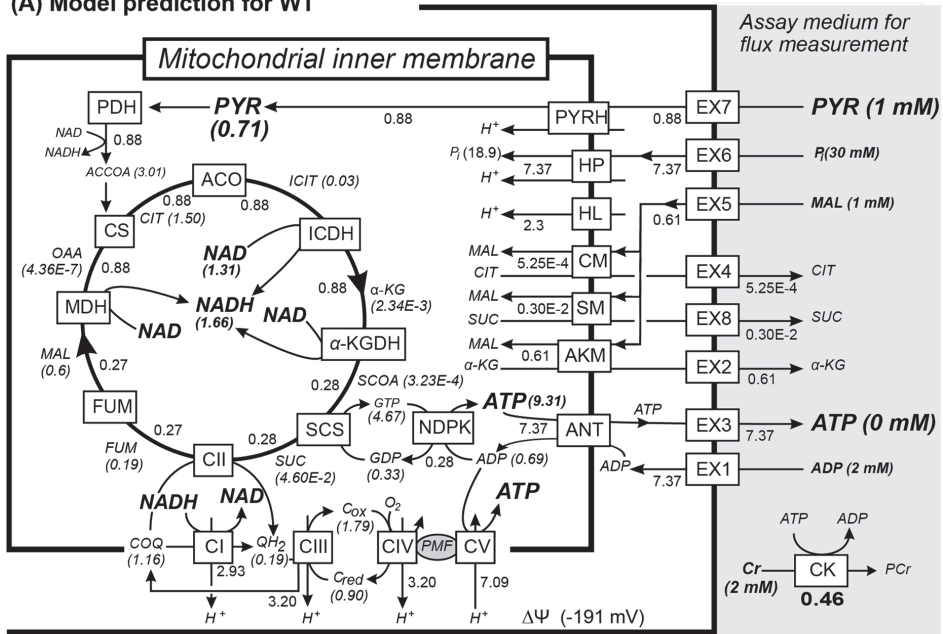


**Figure 1. Overall experimental and computational strategy.** A mathematical model of mitochondrial metabolism developed by Beard and coworkers [39] was adapted to match our experimental conditions. This yielded a model for isolated mitochondria from skeletal muscle of wild-type mice (WT model). By including experimental data, the WT model was adapted to create various KO models (A, B and C) for simulating mitochondrial metabolism in isolated muscle mitochondria from *NDUFS4*<sup>-/-</sup> (KO) mice with isolated complex I deficiency. Predicted PYR oxidation and ATP consumption rates were compared with experimental flux measurements for model validation and predictive analysis (see main text for details).

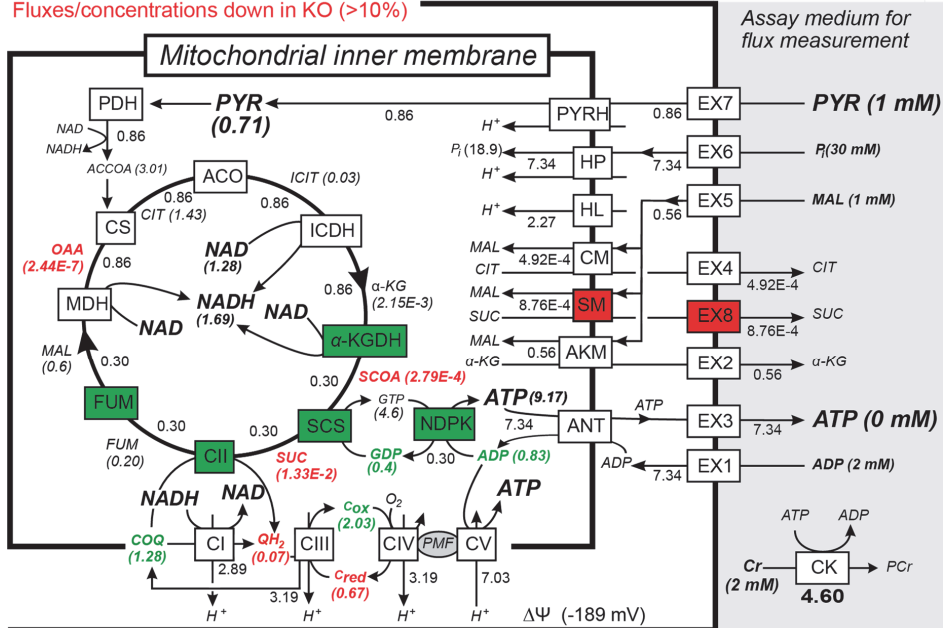
## (A) Model prediction for WT



## (B) Model prediction for KO

Fluxes/concentrations up in KO (&gt;10%)

Fluxes/concentrations down in KO (&gt;10%)



**WT model** – The model of Beard et al (Wu, Yang et al. 2007) consists of three compartments (mitochondrial matrix, inter-membrane space and buffer space) and incorporates 43 flux expressions including TCA cycle fluxes, OXPHOS fluxes, substrate and cation fluxes, passive permeation fluxes and buffer reaction fluxes (Fig. 2). This model also contains various TCA control pathways including regulation of pyruvate dehydrogenase (PDH),  $\alpha$ -ketoglutarate dehydrogenase ( $\alpha$ -KGDH), aconitase (ACO) and fumarase (FUM; for a full list see Table 2 in (Wu, Yang et al. 2007)). All reactions in the model are thermodynamically balanced, and its parameters are validated using experimental data (LaNoue, Nicklas et al. 1970, Kohn, Achs et al. 1979, Kohn, Achs et al. 1979, Kohn and Garfinkel 1983, Bose, French et al. 2003, Wu, Yang et al. 2007). To generate the WT model we first removed metabolites, reactions and constant state variables from the Beard model that were not relevant under our experimental conditions (see Supplement for full details). These include two ATP-consuming reactions in the buffer space (*i.e.* hexokinase and adenylate kinase), one reaction for passive AMP permeation, one adenylate kinase reaction in the inter-membrane

- ◀ **Figure 2. Predicted metabolic consequences of mitochondrial complex I deficiency in isolated mouse skeletal muscle mitochondria.** (A) Isolated mitochondria were placed in an assay medium (grey) for experimental analysis. This was modeled using the depicted metabolic network containing exchange fluxes, TCA cycle and the mitochondrial oxidative phosphorylation (OXPHOS) system. Numerals represent the predicted steady-state values of fluxes (in  $\text{mmol s}^{-1}$  (l mito volume)<sup>-1</sup> or  $\text{mmol s}^{-1}$  (l cyto volume)<sup>-1</sup>) and metabolite concentrations (in mM) for the WT situation. (B) Similar to panel A, but now for mitochondria from *NDUFS4*<sup>-/-</sup> (KO) animals. Colors indicate whether a flux or concentration is increased (green), decreased (red) or not affected (white) in the KO model. **Abbreviations:** ACCOA, Acetyl-CoA; ACO, Aconitase; ADP, Adenosine diphosphate; AKM,  $\alpha$ -ketoglutarate ( $\alpha$ -KG) / malate (MAL) antiporter; ANT, Adenine nucleotide translocase; ATP, Adenosine triphosphate; CI, Complex I; CII, Complex II or Succinate dehydrogenase; CIII, Complex III; CIT, Citrate; CIV, Complex IV; CK, Creatine kinase; CM, Citrate (CIT) / malate (MAL) antiporter; COQ, Oxidized ubiquinol; Cox, Oxidized cytochrome-c; Cred, Reduced cytochrome-c; CS, Citrate synthase; CV, Complex V or FoF1-ATPase; EX1, ADP exchange with assay medium; EX2,  $\alpha$ -KG exchange with assay medium; EX3, ATP exchange with assay medium; EX4, CIT exchange with assay medium; EX5, MAL exchange with assay medium; EX6, Pi exchange with assay medium; EX7, PYR exchange with assay medium; EX8, SUC exchange with assay medium; FUM, Fumarase; FUM, Fumarate; GDP, Guanosine diphosphate; GTP, Guanosine triphosphate; H<sup>+</sup>, Hydrogen; HL, H<sup>+</sup>-leak; HP, H<sup>+</sup>-Pi cotransporter; ICDH, Isocitrate dehydrogenase; ICIT, Isocitrate; MAL, Malate; MDH, Malate dehydrogenase; NAD<sup>+</sup>, Nicotinamide adenine dinucleotide; NADH, Reduced NAD<sup>+</sup>; NDPK, Nucleoside diphosphokinase; OAA, Oxaloacetate; PDH, Pyruvate dehydrogenase; Pi, Inorganic phosphate; PYR, Pyruvate; PYRH, PYR-H<sup>+</sup> cotransporter; QH<sub>2</sub>, Reduced ubiquinol; SCOA, Succinyl-CoA; SCS, Succinyl-CoA synthetase; SM, Succinate (SUC) / malate (MAL) antiporter; SUC, Succinate;  $\alpha$ -KG,  $\alpha$ -ketoglutarate;  $\alpha$ -KGDH,  $\alpha$ -ketoglutarate dehydrogenase;  $\Delta\psi$ , mitochondrial membrane potential

space, two substrate transport reactions (isocitrate and fumarate transport). Next, various metabolite concentrations were adapted to match the conditions of our experimental assay (e.g. [PYR]=1 mM, [P<sub>i</sub>]=30 mM, [malate] ([MAL])= 1 mM, [ATP]= 0 mM, [ADP]= 2 mM; a full list is provided in Supplementary Table S2). The final WT model consisted of 46 state variables (including  $\Delta y$ ) and 37 flux expressions. Analysis of this model at steady-state (i.e. compatible with the experimental conditions of the PYR and ATP flux assays) yielded predictions of various fluxes, reactant concentrations and derived variables for the WT situation (Fig. 2A).

**Experimental analysis of ETC complex and citrate synthase in isolated skeletal muscle mitochondria from KO mice** – The  $V_{\max}$  of CI was reduced by 79% in KO vs. WT mitochondria (Table 1; “Experimental data,  $V_{\max}$  values”). This reduction in CI activity was paralleled by a 45-72% increase in  $V_{\max}$  of the other ETC enzymes and of the TCA-cycle enzyme citrate synthase (CS)

**KO models** – To create KO model A, the  $V_{\max}$  values for CI, CII, CIII, CIV and CS in the WT model were multiplied by the fractional change in this parameter in KO vs. WT (Table 1: “Parameters in the model”). The predictions of KO model A at steady-state are summarized in Figure 2B. Interestingly, although CI activity was reduced by 79% in KO muscle mitochondria the model predicted no change in the maximal PYR oxidation (input of the system) or ATP production (Table 1; “Predicted by the model, Flux values”). The latter was confirmed by experimental analysis (Table 1; “Experimental data, Flux values”). The lack of effect of *NDUFS4*<sup>-/-</sup> knockout on PYR and ATP fluxes might relate to the fact that mitochondria were isolated from 5 wks old KO mice. At this age the pathophysiological phenotype of the *NDUFS4* gene deletion are still relatively mild (Kruse, Watt et al. 2008).

Maximal CS activity was 1.72 higher in KO than in WT mitochondria. This might reflect a general increase in TCA-cycle enzyme level/activity and/or an increase in mitochondrial volume [e.g.(Mazat, Rossignol et al. 2001)]. To explore the potential effect of such changes on PYR and ATP fluxes in KO mitochondria we generated two additional KO models (KO model B and C). KO model B was derived from KO model A by increasing the activity of all TCA cycle enzymes by a “CS factor” of 1.72. KO model C was derived from KO model A by increasing the  $V_{\max}$  of all other enzymes/transporters in the model and mitochondrial volume by the CS-factor of 1.72. KO model B correctly predicted the lack of change in PYR and ATP fluxes, whereas KO model C predicted that these fluxes should be 59-69% higher in KO than in WT mitochondria (Table 1). This suggests that the increase in CS maximal activity might



reflect a general increase in the level of TCA enzymes but cannot be considered a measure of mitochondrial volume.

**Metabolic changes in skeletal muscle mitochondria from KO mice** – Comparing the predictions of the WT model (Fig. 2A) and those of KO model A (Fig. 2B) highlighted changes in the TCA cycle and metabolite transport system. Interestingly, the TCA cycle was divided into an “upper” and “lower” segment defined by its reaction fluxes (Fig. 2B; lower segment colored green). To the best of our knowledge such a bifurcation of the TCA cycle was not reported previously in CI deficiency. The upper segment consists of reactions of Citrate synthase (CS), Aconitase (ACO), Isocitrate dehydrogenase (ICDH) and Malate dehydrogenase (MDH). The lower segment consists of  $\alpha$ -ketoglutarate dehydrogenase ( $\alpha$ -KGDH), Succinyl-CoA synthetase (SCS), Succinate dehydrogenase (CII) and Fumarase (FUM). In the upper TCA segment, WT steady-state reaction fluxes were more than 3-fold higher than those within the lower segment (Fig. 2A). In the WT case, the flux through ICDH flux (0.89 mM/s) gets divided at the end of the upper half segment of the TCA cycle: 69% of the flux (0.61 mM/s) goes out of the mitochondrial matrix to the IMS via the  $\alpha$ -ketoglutarate ( $\alpha$ -KG) / malate (MAL) antiporter (AKM) mechanism. The latter reaction is also the most active among the three antiporter mechanisms that bring MAL into the mitochondrial matrix to participate in initial part of the upper segment of the TCA cycle. Utilizing this flux, the upper TCA segment, along with Pyruvate dehydrogenase (PDH) generates 3 NADH molecules to fuel CI (Fig. 2A). The remaining part (31%) of the ICDH flux goes to  $\alpha$ -KGDH (0.27 mM/s) to enter the lower half of the TCA cycle to fuel CII and also produce 1 ATP and 1 NADH molecule. The two remaining antiport mechanisms for MAL entry into the TCA cycle are the Citrate (CIT) / malate (MAL) antiporter (CM) and the Succinate (SUC) / malate (MAL) antiporter (SM). Together, CM and SM only contribute 0.5% to the total MAL entry to the matrix (Fig. 2A). Figure 2A further shows that in WT mitochondria the upper and lower TCA segments mainly provide substrates to CI and CII, respectively. Obviously, the combined action of CI and CII then provides electrons to the other ETC complexes to sustain the PMF and fuel ATP generation by CV. Of note, a substantial part of the entering PYR does not contribute to ATP production. Every PYR produces 4 NADH after entering the TCA cycle. ATP produced per NADH oxidized, which is same as ATP produced per  $O_2$  consumed, can be calculated simply by dividing the CV flux by the CIV flux. For the WT mice  $CV/CIV = 7.09/3.20 = 2.22$ . According to this calculation we should have obtained  $363 * 4 * 2.22 = 3223$  nmol/h/mg protein ATP, which is 45% higher than the observed ATP flux (Table 1). In the KO mice, the expected ATP production rate is  $391 *$

$4 * (7.03/3.19) = 3447$  nmol/h/mg protein, which is 65% higher than the experimental value. The lower rate of observed vs. predicted ATP production may be due to the absence in the model of other PYR-consuming mechanisms, for instance conversion into lactate (LAC). In addition to the above, analysis of the KO model suggested various changes in other reaction fluxes and metabolite concentrations (Fig. 2B). In the CI-deficient state the lower segment of the TCA cycle carried 10-11% more flux than the WT model. Also the ICDH flux distribution to the lower segment and to the antiport mechanism was altered in the KO model. Of the ICDH flux, 35% is diverted towards the lower segment (31% in WT) and 65% towards the AKM system (69% in WT) to transport MAL into the matrix. Reducing CI activity by 80% only marginally affected its flux. It was also predicted that the flux through the upper part of the TCA cycle was only slightly reduced in KO mitochondria. This reduction is compensated by an increase (11%) in flux through the lower part of the TCA cycle, explaining the absence of effect on the total mitochondrial ATP production rate. The KO model further predicted a change in the steady-state matrix concentration of intermediate metabolites (Fig. 2B). Our predictions are compatible with the results of Mazat *et al* [48], where a reduction in ETC complex activity only slightly affected the fluxes of these complexes but major changes occurred in the concentration of metabolites associated with the affected complexes. With respect to CI, the KO model predicts a reduction in its upstream metabolite (reduced ubiquinol; "QH<sub>2</sub>" or ubiquinol: decreased by 65%) and an increase in its downstream metabolite (oxidized ubiquinol; "COQ" or ubiquinone: increased by 11%). Compatible with the measured increase in  $V_{max}$  of CII and CIII in KO mitochondria, the KO model predicts a decrease in the concentration of intermediate metabolites downstream of these complexes (*i.e.* succinate and reduced cytochrome-c were down by 71% and 26%, respectively). Similarly, the increased  $V_{max}$  of CIII in the KO model was associated with an increase in its upstream metabolites oxidized ubiquinol ("COQ"; by 11%) and oxidized cytochrome-c ("C<sub>ox</sub>"; by 13%). Mitochondrial NADH/NAD<sup>+</sup> ratio and  $\Delta y$  were predicted to be (slightly) increased and depolarized, respectively. The latter predictions are compatible with results obtained in patient fibroblasts with inherited CI deficiency and cells treated with the CI inhibitor rotenone (Distelmaier, Koopman *et al.* 2009, Koopman, Nijtmans *et al.* 2010).

**Predicting the consequences of CI deficiency** – Patients with isolated CI deficiency display a variably reduced CI activity ( $V_{max}$ ) in muscle homogenates and primary fibroblasts (Valsecchi, Monge *et al.* 2012). During the last years, the consequences of isolated CI deficiency in primary patient fibroblasts have been extensively studied

at the cellular level (Visch, Rutter et al. 2004, Koopman, Visch et al. 2005, Koopman, Verkaar et al. 2007, Koopman, Verkaar et al. 2008, Koopman, Nijtmans et al. 2010). Native gel electrophoresis revealed variable amounts of holo-CI in patient cells, where in general three patterns were observed (i) the amount of active holo-CI was reduced (NDUFS2, NDUFS7, NDUFS8) (ii) the amount of active holo-CI was reduced and a ~830-kDa CI was present (NDUFV1, NDUFS1) (iii) or only a ~830-kDa CI was present (NDUFS4) (Valsecchi, Koopman et al. 2010, Blanchet, Buydens et al. 2011). Analysis of total cell homogenates by Western blotting revealed that the level of the 39-kDa CI subunit was twofold reduced in patient cohorts as compared to the controls, however cellular expression levels of other OXPHOS complex subunits was not altered significantly (Koopman, Verkaar et al. 2007). To gain further insight into the metabolic consequences of CI activity reduction at steady-state we performed various simulation runs with the WT model using different  $V_{\max}$  values for CI (*i.e.* lowering it from 100% to 1% of its normal maximal activity). A complete overview of the numerical data generated by these simulations (*i.e.* steady-state reaction fluxes, metabolite concentrations and physiological parameters) is provided in Supplementary Tables S4 and S5. Of note, the WT model was not compatible with a CI activity of 0%, which resulted in all fluxes being zero. The relationship between residual CI activity and key variables in the model are summarized in Figure 3. Most of the fluxes of the OXPHOS complexes (Fig. 3A), TCA cycle (Fig. 3B) and trans-MIM exchangers (Fig. 3C) were not altered by moderate CI activity reduction. As discussed above, the CII flux increased with decreasing CI activity (Fig. 3A), compatible with the predicted activation of the lower half of the TCA cycle (Fig. 3B).

In general, reaction fluxes became substantially affected when CI activity was reduced by more than 90%. Compatible with our experimental observations and KO model predictions (Table 1), PYR oxidation and ATP production only were substantially reduced when CI activity was lowered by more than 90% (Fig. 3D). The concentration of ATP, ADP, GTP, GDP,  $P_i$  (Fig. 3E), TCA intermediates (Fig. 3F), matrix ions (Fig. 4G) and metabolites involved in redox homeostasis (Fig. 4H) were generally not affected by moderate CI activity reduction. Again, these parameters changed when CI activity was reduced by more than 90%. This suggests that steady-state energy homeostasis under non substrate-limited conditions is not affected when a certain (critical) amount of residual CI activity remains. In other words, CI activity can be inhibited to a certain threshold value (in our case near to 90% inhibition) before its consequences become apparent. Similar observations were made in various rotenone-treated rat tissues, where mitochondrial  $O_2$  consumption substantially dropped only when CI was inhibited by more than 80% (Rossignol, Malgat et al. 1999, Mazat, Rossignol et

al. 2001). Overcapacity of OXPHOS complexes is not specific for CI (Davey and Clark 1996, Mazat, Rossignol et al. 2001). For instance, a reduction in CIV activity by almost 50% had virtually no effect on CIV flux and O<sub>2</sub> consumption in patient cells (Kuznetsov, Clark et al. 1996, Mazat, Rossignol et al. 2001).

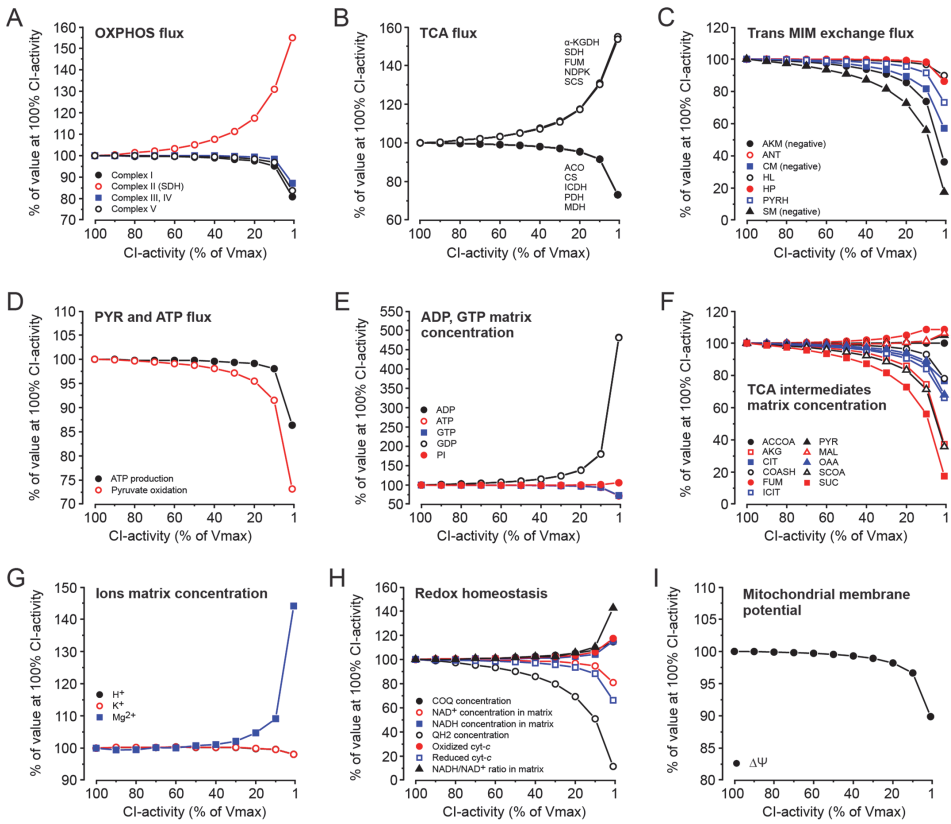


**Figure 3. Predicted consequences of CI deficiency in isolated mouse skeletal muscle mitochondria.** The  $V_{max}$  of CI (x-axis) was gradually reduced from 100% to 1% of that in the WT model and the effect on various steady-state metabolic fluxes, concentrations and other variables was predicted. To facilitate visual inspection, values on the y-axis were expressed as % of their value at 100% CI activity. (A) Effect of increasing CI deficiency on the flux through the OXPHOS system (CI, CII, CIII=CIV, and CV). (B) Similar to panel A, but now for TCA fluxes. (C) Similar to panel A, but now for exchange fluxes across the mitochondrial inner membrane (MIM). (D) Similar to panel A, but now for pyruvate (PYR) and ATP fluxes. (E) Similar to panel A, but now for ADP and GTP concentration in the mitochondrial matrix. (F) Similar to panel A, but now for TCA cycle intermediates. (G) Similar to panel A, but now for the free concentration of H<sup>+</sup>, K<sup>+</sup> and Mg<sup>2+</sup> in the mitochondrial matrix. (H) Similar to panel A, but now for redox-related parameters. (I) Similar to panel A, but now for mitochondrial membrane potential  $\Delta\psi$  (See main text for details).

Metabolic control analysis (MCA) of the WT model revealed that the control coefficient for CI equaled 0.013, which was lower than a previously reported value (Davey and Clark 1996). Our model also predicted control coefficients for CII, CIII, CIV and CV (see Supplementary Fig. S1) that were lower than previously reported values (Rossignol, Malgat et al. 1999). In general, lower control coefficients are associated with a higher threshold value (Rossignol, Letellier et al. 2000, Mazat, Rossignol et al. 2001). In this sense, the high CI threshold value predicted by our model might be considered too high. This might be due the fact that although the original model was parametrized using experimental data (Wu, Yang et al. 2007), it was not a skeletal muscle-specific model. Compatible with previous results in genetic and inhibitor-induced fibroblast models of CI deficiency (Distelmaier, Koopman et al. 2009, Koopman, Nijtmans et al. 2010, Balsa, Marco et al. 2012), the WT model predicted that a reduction in CI activity was associated with redox alterations (e.g. an increase in NADH/NAD<sup>+</sup> ratio; Fig. 3H) and partial Dy depolarization (Fig. 3I).

## Summary and conclusion

This study combines experimental and *in silico* strategies to gain insight into the consequences of isolated mitochondrial CI deficiency in isolated skeletal muscle mitochondria from *NDUFS4*<sup>-/-</sup> mice. We demonstrate that *NDUFS4*<sup>-/-</sup> gene deletion reduces maximal CI activity and is paralleled by increased activity of CII, CIII, CIV and CS. Surprisingly, *NDUFS4* knockout did not affect the maximal rate of PYR oxidation and ATP production. Mathematical modeling suggests that this phenomenon might be due to increased activity of the lower half of the TCA cycle, including CII. It further appears that mouse skeletal muscle mitochondria possess a substantial CI overcapacity, which further minimizes the effects of partial CI deficiency on mitochondrial metabolism. This means that CI activity can be inhibited to a certain threshold value (in our case near to 90% inhibition) before its consequences become apparent. We conclude that the metabolic consequences of CI dysfunction in KO mitochondria are minimized by CII-mediated fueling of the OXPHOS system and CI overcapacity. This still leaves open the possibility that mitochondrial ATP generation becomes limited when energy substrates are scarce and/or cellular energy demands increase during cell activation.

## Acknowledgements

This work was supported by the CSBR (Centre for Systems Biology Research) initiative from the Netherlands Organisation for Scientific Research (NWO; No: CSBR09/013V). We are grateful to Dr. D.A. Beard (Department of Molecular and Integrative Physiology, University of Michigan, Ann Arbor, Michigan, USA) for supplying us with the original model.

## References

- Balaban, R. S., S. Nemoto and T. Finkel (2005). "Mitochondria, oxidants, and aging." *Cell* **120**(4): 483-495.
- Balsa, E., R. Marco, E. Perales-Clemente, R. Szklarczyk, E. Calvo, M. O. Landazuri and J. A. Enriquez (2012). "NDUFA4 is a subunit of complex IV of the mammalian electron transport chain." *Cell Metab* **16**(3): 378-386.
- Benit, P., J. Steffann, S. Lebon, D. Chretien, N. Kadhom, P. deLonlay, A. Goldenberg, Y. Dumez, M. Dommergues, P. Rustin, A. Munnich and A. Rotig (2003). "Genotyping microsatellite DNA markers at putative disease loci in inbred/multiplex families with respiratory chain complex I deficiency allows rapid identification of a novel nonsense mutation (IVS1nt -1) in the NDUFS4 gene in Leigh syndrome." *Hum Genet* **112**(5-6): 563-566.
- Blanchet, L., M. C. Buydens, J. A. Smeitink, P. H. Willems and W. J. Koopman (2011). "Isolated mitochondrial complex I deficiency: explorative data analysis of patient cell parameters." *Curr Pharm Des* **17**(36): 4023-4033.
- Bose, S., S. French, F. J. Evans, F. Joubert and R. S. Balaban (2003). "Metabolic network control of oxidative phosphorylation: multiple roles of inorganic phosphate." *J Biol Chem* **278**(40): 39155-39165.
- Carroll, J., I. M. Fearnley, J. M. Skehel, R. J. Shannon, J. Hirst and J. E. Walker (2006). "Bovine complex I is a complex of 45 different subunits." *J Biol Chem* **281**(43): 32724-32727.
- Coskun, P. E., M. F. Beal and D. C. Wallace (2004). "Alzheimer's brains harbor somatic mtDNA control-region mutations that suppress mitochondrial transcription and replication." *Proc Natl Acad Sci U S A* **101**(29): 10726-10731.
- Davey, G. P. and J. B. Clark (1996). "Threshold effects and control of oxidative phosphorylation in nonsynaptic rat brain mitochondria." *J Neurochem* **66**(4): 1617-1624.
- Detmer, S. A. and D. C. Chan (2007). "Functions and dysfunctions of mitochondrial dynamics." *Nat Rev Mol Cell Biol* **8**(11): 870-879.
- Dieteren, C. E., S. C. Gielen, L. G. Nijtmans, J. A. Smeitink, H. G. Swarts, R. Brock, P. H. Willems and W. J. Koopman (2011). "Solute diffusion is hindered in the mitochondrial matrix." *Proc Natl Acad Sci U S A* **108**(21): 8657-8662.
- DiMauro, S. and E. A. Schon (2003). "Mitochondrial respiratory-chain diseases." *N Engl J Med* **348**(26): 2656-2668.
- Distelmaier, F., W. J. Koopman, L. P. van den Heuvel, R. J. Rodenburg, E. Mayatepek, P. H. Willems and J. A. Smeitink (2009). "Mitochondrial complex I deficiency: from organelle dysfunction to clinical disease." *Brain* **132**(Pt 4): 833-842.
- Duchon, M. R. (2004). "Mitochondria in health and disease: perspectives on a new mitochondrial biology." *Mol Aspects Med* **25**(4): 365-451.
- Fassone, E. and S. Rahman (2012). "Complex I deficiency: clinical features, biochemistry and molecular genetics." *J Med Genet* **49**(9): 578-590.
- Finsterer, J. (2006). "Central nervous system manifestations of mitochondrial disorders." *Acta Neurol Scand* **114**(4): 217-238.
- Herzig, S., E. Raemy, S. Montessuit, J. L. Veuthey, N. Zamboni, B. Westermann, E. R. Kunji and J. C. Martinou (2012). "Identification and functional expression of the mitochondrial pyruvate carrier." *Science* **337**(6090): 93-96.
- Janssen, A. J., F. J. Trijbels, R. C. Sengers, L. T. Wintjes, W. Ruitenbeek, J. A. Smeitink, E. Morava, B. G. van Engelen, L. P. van den Heuvel and R. J. Rodenburg (2006). "Measurement

- of the energy-generating capacity of human muscle mitochondria: diagnostic procedure and application to human pathology." *Clin Chem* **52**(5): 860-871.
- Kim, S. H., R. Vlkolinsky, N. Cairns, M. Fountoulakis and G. Lubec (2001). "The reduction of NADH ubiquinone oxidoreductase 24- and 75-kDa subunits in brains of patients with Down syndrome and Alzheimer's disease." *Life Sci* **68**(24): 2741-2750.
  - Kirby, D. M., M. Crawford, M. A. Cleary, H. H. Dahl, X. Dennett and D. R. Thorburn (1999). "Respiratory chain complex I deficiency: an underdiagnosed energy generation disorder." *Neurology* **52**(6): 1255-1264.
  - Kohn, M. C., M. J. Achs and D. Garfinkel (1979). "Computer simulation of metabolism in pyruvate-perfused rat heart. II. Krebs cycle." *Am J Physiol* **237**(3): R159-166.
  - Kohn, M. C., M. J. Achs and D. Garfinkel (1979). "Computer simulation of metabolism in pyruvate-perfused rat heart. III. Pyruvate dehydrogenase." *Am J Physiol* **237**(3): R167-173.
  - Kohn, M. C. and D. Garfinkel (1983). "Computer simulation of metabolism in palmitate-perfused rat heart. II. Behavior of complete model." *Ann Biomed Eng* **11**(6): 511-531.
  - Koopman, W. J., F. Distelmaier, J. A. Smeitink and P. H. Willems (2013). "OXPHOS mutations and neurodegeneration." *EMBO J* **32**(1): 9-29.
  - Koopman, W. J., L. G. Nijtmans, C. E. Dieteren, P. Roestenberg, F. Valsecchi, J. A. Smeitink and P. H. Willems (2010). "Mammalian mitochondrial complex I: biogenesis, regulation, and reactive oxygen species generation." *Antioxid Redox Signal* **12**(12): 1431-1470.
  - Koopman, W. J., S. Verkaart, S. E. van Emst-de Vries, S. Grefte, J. A. Smeitink, L. G. Nijtmans and P. H. Willems (2008). "Mitigation of NADH: ubiquinone oxidoreductase deficiency by chronic Trolox treatment." *Biochim Biophys Acta* **1777**(7-8): 853-859.
  - Koopman, W. J., S. Verkaart, H. J. Visch, S. van Emst-de Vries, L. G. Nijtmans, J. A. Smeitink and P. H. Willems (2007). "Human NADH:ubiquinone oxidoreductase deficiency: radical changes in mitochondrial morphology?" *Am J Physiol Cell Physiol* **293**(1): C22-29.
  - Koopman, W. J., H. J. Visch, S. Verkaart, L. W. van den Heuvel, J. A. Smeitink and P. H. Willems (2005). "Mitochondrial network complexity and pathological decrease in complex I activity are tightly correlated in isolated human complex I deficiency." *Am J Physiol Cell Physiol* **289**(4): C881-890.
  - Koopman, W. J., P. H. Willems and J. A. Smeitink (2012). "Monogenic mitochondrial disorders." *N Engl J Med* **366**(12): 1132-1141.
  - Kroemer, G. (1999). "Mitochondrial control of apoptosis: an overview." *Biochem Soc Symp* **66**: 1-15.
  - Kruse, S. E., W. C. Watt, D. J. Marcinek, R. P. Kapur, K. A. Schenkman and R. D. Palmiter (2008). "Mice with mitochondrial complex I deficiency develop a fatal encephalomyopathy." *Cell Metab* **7**(4): 312-320.
  - Kuznetsov, A. V., J. F. Clark, K. Winkler and W. S. Kunz (1996). "Increase of flux control of cytochrome c oxidase in copper-deficient mottled brindled mice." *J Biol Chem* **271**(1): 283-288.
  - LaNoue, K., W. J. Nicklas and J. R. Williamson (1970). "Control of citric acid cycle activity in rat heart mitochondria." *J Biol Chem* **245**(1): 102-111.
  - Loeffen, J. L., J. A. Smeitink, J. M. Trijbels, A. J. Janssen, R. H. Triepels, R. C. Sengers and L. P. van den Heuvel (2000). "Isolated complex I deficiency in children: clinical, biochemical and genetic aspects." *Hum Mutat* **15**(2): 123-134.
  - Mazat, J. P., R. Rossignol, M. Malgat, C. Rocher, B. Faustin and T. Letellier (2001). "What do mitochondrial diseases teach us about normal mitochondrial functions...that we already knew: threshold expression of mitochondrial defects." *Biochim Biophys Acta* **1504**(1): 20-30.

- McBride, H. M., M. Neuspiel and S. Wasiak (2006). "Mitochondria: more than just a powerhouse." *Curr Biol* **16**(14): R551-560.
- Newmeyer, D. D. and S. Ferguson-Miller (2003). "Mitochondria: releasing power for life and unleashing the machineries of death." *Cell* **112**(4): 481-490.
- Nouws, J., L. G. Nijtmans, J. A. Smeitink and R. O. Vogel (2012). "Assembly factors as a new class of disease genes for mitochondrial complex I deficiency: cause, pathology and treatment options." *Brain* **135**(Pt 1): 12-22.
- Orth, M. and A. H. Schapira (2002). "Mitochondrial involvement in Parkinson's disease." *Neurochem Int* **40**(6): 533-541.
- Rodenburg, R. J. (2011). "Biochemical diagnosis of mitochondrial disorders." *J Inher Metab Dis* **34**(2): 283-292.
- Rossignol, R., T. Letellier, M. Malgat, C. Rocher and J. P. Mazat (2000). "Tissue variation in the control of oxidative phosphorylation: implication for mitochondrial diseases." *Biochem J* **347 Pt 1**: 45-53.
- Rossignol, R., M. Malgat, J. P. Mazat and T. Letellier (1999). "Threshold effect and tissue specificity. Implication for mitochondrial cytopathies." *J Biol Chem* **274**(47): 33426-33432.
- Schapira, A. H. (2006). "Mitochondrial disease." *Lancet* **368**(9529): 70-82.
- Smeitink, J., R. Sengers, F. Trijbels and L. van den Heuvel (2001). "Human NADH:ubiquinone oxidoreductase." *J Bioenerg Biomembr* **33**(3): 259-266.
- Smeitink, J., L. van den Heuvel and S. DiMauro (2001). "The genetics and pathology of oxidative phosphorylation." *Nat Rev Genet* **2**(5): 342-352.
- Valsecchi, F., W. J. Koopman, G. R. Manjeri, R. J. Rodenburg, J. A. Smeitink and P. H. Willems (2010). "Complex I disorders: causes, mechanisms, and development of treatment strategies at the cellular level." *Dev Disabil Res Rev* **16**(2): 175-182.
- Valsecchi, F., C. Monge, M. Forkink, A. J. de Groof, G. Benard, R. Rossignol, H. G. Swarts, S. E. van Emst-de Vries, R. J. Rodenburg, M. A. Calvaruso, L. G. Nijtmans, B. Heeman, P. Roestenberg, B. Wieringa, J. A. Smeitink, W. J. Koopman and P. H. Willems (2012). "Metabolic consequences of NDUFS4 gene deletion in immortalized mouse embryonic fibroblasts." *Biochim Biophys Acta* **1817**(10): 1925-1936.
- van den Heuvel, L., W. Ruitenbeek, R. Smeets, Z. Gelman-Kohan, O. Elpeleg, J. Loeffen, F. Trijbels, E. Mariman, D. de Bruijn and J. Smeitink (1998). "Demonstration of a new pathogenic mutation in human complex I deficiency: a 5-bp duplication in the nuclear gene encoding the 18-kD (AQDQ) subunit." *Am J Hum Genet* **62**(2): 262-268.
- Visch, H. J., G. A. Rutter, W. J. Koopman, J. B. Koenderink, S. Verkaart, T. de Groot, A. Varadi, K. J. Mitchell, L. P. van den Heuvel, J. A. Smeitink and P. H. Willems (2004). "Inhibition of mitochondrial Na<sup>+</sup>-Ca<sup>2+</sup> exchange restores agonist-induced ATP production and Ca<sup>2+</sup> handling in human complex I deficiency." *J Biol Chem* **279**(39): 40328-40336.
- Willems, P. H., J. A. Smeitink and W. J. Koopman (2009). "Mitochondrial dynamics in human NADH:ubiquinone oxidoreductase deficiency." *Int J Biochem Cell Biol* **41**(10): 1773-1782.
- Willems, P. H., F. Valsecchi, F. Distelmaier, S. Verkaart, H. J. Visch, J. A. Smeitink and W. J. Koopman (2008). "Mitochondrial Ca<sup>2+</sup> homeostasis in human NADH:ubiquinone oxidoreductase deficiency." *Cell Calcium* **44**(1): 123-133.
- Wu, F., F. Yang, K. C. Vinnakota and D. A. Beard (2007). "Computer modeling of mitochondrial tricarboxylic acid cycle, oxidative phosphorylation, metabolite transport, and electrophysiology." *J Biol Chem* **282**(34): 24525-24537.



## 1. SUPPLEMENTARY MATERIALS AND METHODS

### **Modelling the effects of *NDUFS4* knockout and increasing levels of CI deficiency -**

To predict the consequences of *NDUFS4* knockout or increasing levels of CI deficiency we used a model of the mitochondrial bioenergetic system developed previously. Full details regarding the rate laws, ODE, estimated parameters, initial conditions and experimental validation are provided in the original paper [1]. We adapted this model to match the conditions under which our experimental data was obtained as described in the next section.

### **Removing metabolites and reactions from the original model of Wu *et al.*, 2007 [1]**

- The original Wu model consists of three compartments and 43 flux expressions that mathematically describe the TCA cycle, OXPHOS system, substrate/ion homeostasis, passive permeation fluxes and buffer reaction fluxes. We first deleted reactions from the model that were not relevant in our experimental setup. These consisted of two ATP-consuming reactions in the buffer space (*i.e.* hexokinase 'J\_HK' and adenylate kinase 'J\_AKe'), one reaction for passive AMP permeation ('J\_AMP'), one adenylate kinase reaction in the inter-membrane space ('J\_AKi'), and two substrate transport reactions (isocitrate 'J\_ICITt' and fumarate transport 'J\_FUMt'). This was achieved by either completely removing the reactions from the model or by setting their  $V_{\max}$  value to zero. Similarly, several state variables were constant or absent in our experimental system and were either removed from the model or assumed constant (**Table S1**).

**Table S1. Metabolites removed from the original model of Wu *et al.*, 2007 [1].**

<b>Mitochondrial matrix</b>	
AMP	Not relevant as the ODE for AMP <sub>x</sub> in the model is zero
Oxygen (O <sub>2</sub> )	Constant
Total CO <sub>2</sub> (CO <sub>2,tot</sub> )	Constant
<b>Mitochondrial intermembrane space</b>	
Isocitrate (ICIT)	Not relevant in the model
Fumarate (FUM)	Not relevant in the model as V <sub>max</sub> of FUMt is zero
AMP	Reaction for passive AMP permeation and AK were removed
Hydrogen (H <sup>+</sup> )	Constant
Magnesium (Mg <sup>2+</sup> )	Constant
Potassium (K <sup>+</sup> )	Constant
<b>Cytoplasm/buffer space</b>	
Hydrogen (H <sup>+</sup> )	Constant
Magnesium (Mg <sup>2+</sup> )	Constant
Potassium (K <sup>+</sup> )	Constant
Glucose (GLC)	Not relevant as HK is not present in the model
Glucose 6 phosphate (G6P)	Not relevant as HK is not present in the model
Isocitrate (ICIT)	Not used in the model
Fumarate (FUM)	Not relevant in the model as V <sub>max</sub> of FUMt is zero
AMP	Reaction for passive AMP permeation and AK were removed
Phosphocreatine (PCr)	Creatine was used instead of Phosphocreatine

**1.1.2. Model adaptation for the wild type and *NDUFS4* knockout condition** – To mimic our experimental assay conditions, we first changed the initial concentration of all relevant metabolites in the model (**Table S2**). For all other metabolites their initial concentration was left unchanged ([1]). The resulting model was used to simulate the wildtype (WT) condition ('WT model'). In case of the *NDUFS4* knockout (KO) situation, we adapted the WT model in 3 different ways to yield 3 different KO models (KO model A, B and C).

**1.1.3. KO model A** – In KO model A, the experimentally obtained V<sub>max</sub> values for CI, CII, CIII, CIV and CS were changed in the WT model according to the experimental values in **Table 1**. For this purpose, the original V<sub>max</sub> of CI in the WT model (*i.e.* that published in [1]) was multiplied by a factor of 0.21. Similarly, the V<sub>max</sub> value of CII, CIII, CIV and CS was multiplied by 1.56, 1.45, 1.70, and 1.72 respectively (see **Table S3** for numerical values). The V<sub>max</sub> values of all other enzymes were identical to their original values published in [1].

**KO model B and KO model C** – To investigate whether an increase in the level of mitochondrial TCA cycle enzymes or mitochondrial mass (as suggested by the 1.72-fold higher  $V_{\max}$  of CS) might play a role in the KO situation we also modified KO model A to generate KO model B, in which the  $V_{\max}$  of all TCA cycle enzymes was increased by the ‘CS-factor’ of 1.72. Finally, to study potential effects of mitochondrial volume on model predictions KO model A was adapted to yield KO model C. In the latter model the mitochondrial volume and  $V_{\max}$  of all other remaining enzymes was increased by the ‘CS-factor’ of 1.72.

**Table S2. Adjusted initial metabolite concentrations in the model**

Metabolite	Initial concentration (M) (In WT and KO model)
ADP	2.00E-03
Phosphate (P <sub>i</sub> )	3.00E-02
Creatine (Cr)	2.00E-02
Pyruvate (PYR)	1.00E-03
Malate (MAL)	1.00E-03
Aspartate (ASP)	0
Citrate (CIT)	0
α-ketoglutarate (AKG)	0
Succinate (SUC)	0
Glutamate (GLU)	0

**Performing model simulations** – After setting the initial concentration and model parameters according to the experimental conditions, we solved the ODE model using the *ode15s* function of MATLAB. Simulations were run until the steady-state condition was reached. This required running the simulations for 1200 seconds. To simulate various degrees of CI deficiency and its metabolic consequences under steady-state conditions we performed simulation runs with the WT model using different  $V_{\max}$  values for CI (i.e. by stepwise reducing the maximal CI activity from 100% to 1% of this value in the WT model).

**Analysis of the control coefficient for CI-CV in the WT model** – Control coefficients of all mitochondrial complexes (CI-CV) were calculated according to Mazat et al 2001 [2]. **Figure S1A-E** represent threshold curve of mitochondrial complexes CI-CV respectively, where flux through each enzyme (y-axis) is plotted against the % inhibition

of the enzyme (y-axis). The control coefficient is given by the initial slope of the obtained “threshold curve”. **Figure S1F** depicts the effect of CI-CV activity reduction (x-axis) on the flux through CIV, representing mitochondrial oxygen consumption. The latter becomes affected when CI-CIV activity is reduced by more than 80%.

**Table S3. Adjusted parameters (reaction rate coefficient) in the various models**

Reactions	WT [1]	KO Model A	KO Model B	KO Model C
<b>Complex I (CI)</b>	32364.8187	<b>6796.612</b>	<b>6796.612</b>	<b>6796.612</b>
<b>Complex II (CII or SDH; also in TCA)</b>	0.08578868	<b>0.13383</b>	<b>0.13383</b>	<b>0.13383</b>
<b>Complex III (CIII)</b>	0.79081375	<b>1.14668</b>	<b>1.14668</b>	<b>1.14668</b>
<b>Complex IV (CIV)</b>	0.00010761	<b>0.000183</b>	<b>0.000183</b>	<b>0.000183</b>
Complex V (CV; $F_1F_0$ -ATPase)	8120.39325	8120.3932	8120.39325	<b>13967.07639</b>
Aconitase (ACO)	0.02766541	0.0276654	<b>0.047584505</b>	<b>0.047584505</b>
$\alpha$ -ketoglutarate dehydrogenase ( $\alpha$ -KGDH)	0.08763	0.08763	<b>0.1507236</b>	<b>0.1507236</b>
<b>Citrate synthase (CS)</b>	9.82530751	<b>16.89953</b>	<b>16.89953</b>	<b>16.89953</b>
Fumarase (FUM)	0.00707728	0.0070773	<b>0.012172922</b>	<b>0.012172922</b>
Glutamate oxaloacetate transaminase (GOT)	4.55139184	4.5513918	<b>7.828393965</b>	<b>7.828393965</b>
Isocitrate dehydrogenase (ICDH)	0.49204755	0.4920476	<b>0.846321786</b>	<b>0.846321786</b>
Pyruvate dehydrogenase (PDH)	0.20509364	0.2050936	<b>0.352761061</b>	<b>0.352761061</b>
Malate dehydrogenase (MDH)	0.07706001	0.07706	<b>0.132543217</b>	<b>0.132543217</b>
Nucleoside diphosphokinase (NDPK)	0.02554352	0.0255435	0.02554352	<b>0.043934854</b>
Succinyl-CoA synthetase (SCS)	0.44852045	0.4485205	<b>0.771455174</b>	<b>0.771455174</b>
$\alpha$ -ketoglutarate ( $\alpha$ -KG) / malate (MAL) antiporter (AKM)	0.28209145	0.2820915	0.28209145	<b>0.485197294</b>
Adenine nucleotide translocase (ANT)	0.00752212	0.0075221	0.00752212	<b>0.012938046</b>
Citrate (CIT) / malate (MAL) antiporter (CM)	80.4321103	80.43211	80.4321103	<b>138.3432297</b>
Glutamate (GLU)- $H^+$ cotransporter (GLUH)	272511422	272511422	272511422	<b>468719645.8</b>
Malate (MAL) / $P_i$ anti-transporter (MALP)	16.0624419	16.062442	16.0624419	<b>27.62740007</b>
Aspartate (ASP) / Glutamate (GLU) antiporter (AG)	5.87E-05	5.87E-05	5.87E-05	<b>0.000100964</b>
$H^+$ -leak (HL)	4758023.13	4758023.1	4758023.13	<b>8183799.784</b>
$H^+$ - $P_i$ cotransporter (HP)	33355685	33355685	33355685	<b>57371778.2</b>
PYR- $H^+$ cotransporter (PYRH)	299677927	299677927	299677927	<b>515446034.4</b>
Succinate (SUC) / malate (MAL) antiporter (SM)	96.9956183	96.995618	96.9956183	<b>166.8324635</b>
Creatine kinase (CK)	1.00E+07	1.00E+07	1.00E+07	1.00E+07
$P_i$ exchange with assay medium (EX6)	327	327	327	<b>562.44</b>
Permeability coefficients for TCA intermediates	85	85	85	<b>146.2</b>

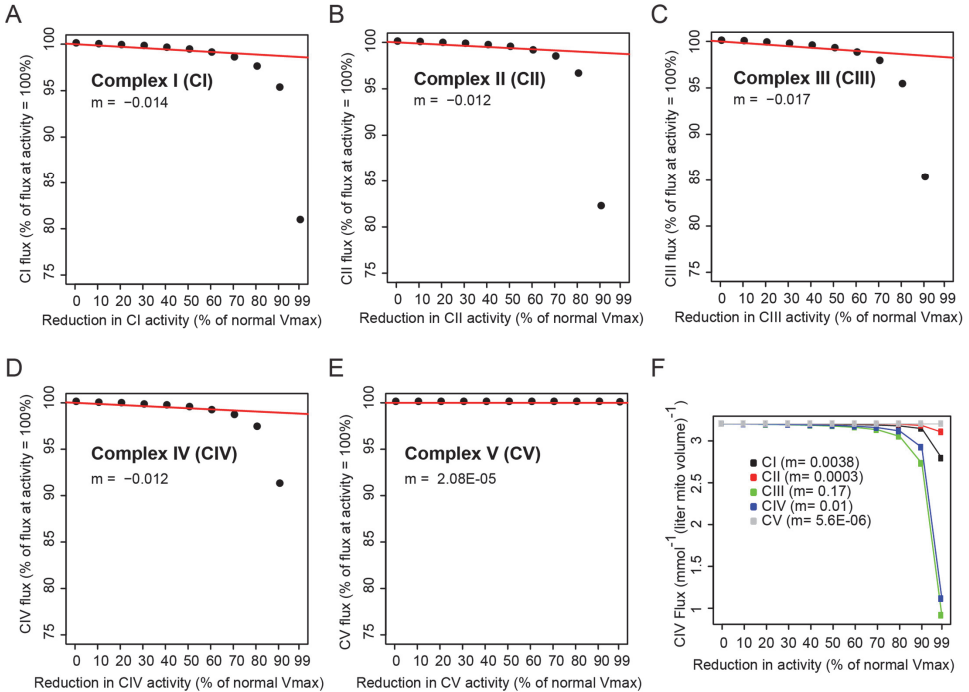


**Figure S1. Control coefficients of CI-CV.** Using the WT model, the activity of CI-CV (x-axis) was gradually lowered from 100% to 1%. The corresponding flux value was plotted on the y-axis. The initial slope ( $m$ ) of each curve (red lines) was used as a measure of the control coefficient. **(A)** Analysis of complex I (CI). **(B)** Analysis of complex II (CII). **(C)** Analysis of complex III (CIII). **(D)** Analysis of complex IV (CIV). **(E)** Analysis of complex V (CV). **(F)** Effect of lowering the activity of CI-CV on the flux through CIV (*i.e.* oxygen consumption).

## SUPPLEMENTARY REFERENCES

- F. Wu, F. Yang, K.C. Vinnakota, D.A. Beard, Computer modeling of mitochondrial tricarboxylic acid cycle, oxidative phosphorylation, metabolite transport, and electrophysiology, *J. Biol. Chem.* 282 (2007) 24525–24537. doi:10.1074/jbc.M701024200.
- J.P. Mazat, R. Rossignol, M. Malgat, C. Rocher, B. Faustin, T. Letellier, What do mitochondrial diseases teach us about normal mitochondrial functions...that we already knew: threshold expression of mitochondrial defects, *Biochim. Biophys. Acta.* 1504 (2001) 20–30.

## SUPPLEMENTARY RESULTS

**Table S4. Predicted effect of progressive CI deficiency on steady-state reaction fluxes.**

Name	100% CI	90% CI	80% CI
<b>OXPHOS system enzymes (mmol s<sup>-1</sup> (l mito volume)<sup>-1</sup>)</b>			
1: Complex I (CI)	2.932	2.930	2.927
2: Complex II (CII or SDH; also in TCA)	0.272	0.274	0.276
3: Complex III (CIII)	3.204	3.203	3.202
4: Complex IV (CIV)	3.204	3.203	3.202
5: Complex V (CV; FoF1-ATPase)	7.095	7.092	7.088
<b>TCA cycle enzymes (mmol s<sup>-1</sup> (l mito volume)<sup>-1</sup>)</b>			
6: Aconitase (ACO)	0.885	0.884	0.882
7: $\alpha$ -ketoglutarate dehydrogenase ( $\alpha$ -KGDH)	0.275	0.277	0.279
8: Complex II (CII or SDH; also in OXPHOS)	0.272	0.274	0.276
9: Citrate synthase (CS)	0.886	0.885	0.883
10: Fumarase (FUM)	0.272	0.274	0.276
11: Isocitrate dehydrogenase (ICDH)	0.885	0.884	0.882
12: Pyruvate dehydrogenase (PDH)	0.886	0.885	0.883
13: Malate dehydrogenase (MDH)	0.886	0.885	0.883
14: Nucleoside diphosphokinase (NDPK)	0.275	0.277	0.279
15: Succinyl-CoA synthetase (SCS)	0.275	0.277	0.279
<b>Trans MIM metabolite/ion exchangers (mmol s<sup>-1</sup> (l mito volume)<sup>-1</sup>)</b>			
16: $\alpha$ -ketoglutarate ( $\alpha$ -KG) / malate (MAL) antiporter (AKM)	-0.610	-0.607	-0.604
17: Adenine nucleotide translocase (ANT)	7.370	7.369	7.366
18: Citrate (CIT) / malate (MAL) antiporter (CM)	-5.2E-04	-5.2E-04	-5.2E-04
19: H <sup>+</sup> -leak (HL)	2.294	2.293	2.292
20: H <sup>+</sup> -P <sub>i</sub> cotransporter (HP)	7.370	7.369	7.366
21: PYR-H <sup>+</sup> cotransporter (PYRH)	0.886	0.885	0.883
22: Succinate (SUC) / malate (MAL) antiporter (SM)	-0.003	-0.003	-0.003
<b>Other (mol s<sup>-1</sup> (l mito volume)<sup>-1</sup>), CK (mmol s<sup>-1</sup> (l cyto volume)<sup>-1</sup>)</b>			
23: ADP exchange with assay medium (EX1)	7.370	7.369	7.366
24: $\alpha$ -KG exchange with assay medium (EX2)	-0.610	-0.607	-0.604
25: ATP exchange with assay medium (EX3)	7.370	7.369	7.366
26: CIT exchange with assay medium (EX4)	-5.2E-04	-5.2E-04	-5.2E-04
27: Creatine kinase (CK)	-0.462	-0.462	-0.461
28: MAL exchange with assay medium (EX5)	0.614	0.611	0.607
29: P <sub>i</sub> exchange with assay medium (EX6)	7.370	7.369	7.366
30: PYR exchange with assay medium (EX7)	0.886	0.885	0.883
31: SUC exchange with assay medium (EX8)	-0.003	-0.003	-0.003

	70% CI	60% CI	50% CI	40% CI	30% CI	20% CI	10% CI	1% CI
	2.923	2.918	2.912	2.902	2.887	2.859	2.792	2.370
	0.278	0.281	0.286	0.292	0.302	0.320	0.356	0.422
	3.201	3.200	3.198	3.195	3.190	3.179	3.148	2.792
	3.201	3.200	3.198	3.195	3.190	3.179	3.148	2.792
	7.083	7.075	7.066	7.051	7.028	6.984	6.869	5.938
	0.880	0.878	0.874	0.869	0.860	0.845	0.811	0.649
	0.281	0.284	0.289	0.295	0.305	0.322	0.357	0.422
	0.278	0.281	0.286	0.292	0.302	0.320	0.356	0.422
	0.881	0.878	0.875	0.869	0.861	0.846	0.812	0.650
	0.278	0.281	0.286	0.292	0.302	0.320	0.356	0.422
	0.880	0.878	0.874	0.869	0.860	0.845	0.811	0.649
	0.881	0.878	0.875	0.869	0.861	0.846	0.812	0.650
	0.881	0.878	0.875	0.869	0.861	0.846	0.812	0.650
	0.281	0.284	0.289	0.295	0.305	0.322	0.357	0.422
	0.281	0.284	0.289	0.295	0.305	0.322	0.357	0.422
	-0.599	-0.593	-0.585	-0.574	-0.555	-0.524	-0.454	-0.227
	7.364	7.360	7.354	7.346	7.333	7.306	7.227	6.360
	-5.2E-04	-5.1E-04	-5.1E-04	-5.0E-04	-4.9E-04	-4.7E-04	-4.3E-04	-3.0E-04
	2.290	2.287	2.283	2.278	2.269	2.253	2.217	2.062
	7.364	7.360	7.354	7.346	7.333	7.306	7.227	6.360
	0.881	0.878	0.875	0.869	0.861	0.846	0.812	0.650
	-0.003	-0.003	-0.003	-0.003	-0.002	-0.002	-0.002	-0.001
	7.364	7.360	7.354	7.346	7.333	7.306	7.227	6.360
	-0.599	-0.593	-0.585	-0.574	-0.555	-0.524	-0.454	-0.227
	7.364	7.360	7.354	7.346	7.333	7.306	7.227	6.360
	-5.2E-04	-5.1E-04	-5.1E-04	-5.0E-04	-4.9E-04	-4.7E-04	-4.3E-04	-3.0E-04
	-0.461	-0.461	-0.461	-0.460	-0.459	-0.458	-0.453	-0.398
	0.603	0.597	0.588	0.577	0.558	0.526	0.456	0.228
	7.364	7.360	7.354	7.346	7.333	7.306	7.227	6.360
	0.881	0.878	0.875	0.869	0.861	0.846	0.812	0.650
	-0.003	-0.003	-0.003	-0.003	-0.002	-0.002	-0.002	-0.001

**Table S5. Predicted effect of progressive CI deficiency on steady-state metabolite concentration and physiological parameters**

Variables	100% CI	90% CI	80% CI	70% CI
<b>Concentration in mitochondrial matrix (M)</b>				
1: ACCOA (Acetyl-CoA)	3.010	3.010	3.010	3.010
2: ADP (Adenosine diphosphate)	0.685	0.694	0.707	0.719
3: $\alpha$ -KG ( $\alpha$ -ketoglutarate)	0.002	0.002	0.002	0.002
4: ATP (Adenosine triphosphate)	9.315	9.306	9.293	9.281
5: CIT (Citrate)	1.502	1.496	1.487	1.481
6: COASH (Coenzyme A)	0.004	0.004	0.004	0.004
7: COQ (Oxidized ubiquinol)	1.16	1.16	1.16	1.17
8: FUM (Fumarate)	0.196	0.196	0.196	0.197
9: GTP (Guanosine triphosphate)	4.667	4.663	4.657	4.651
10: GDP (Guanosine diphosphate)	0.330	0.334	0.340	0.346
11: $H^+$	5.2E-05	5.2E-05	5.21E-05	5.21E-05
12: ICIT (Isocitrate)	0.033	0.033	0.033	0.033
13: $K^+$	137.066	137.159	137.401	137.371
14: PYR (Pyruvate)	0.714	0.714	0.713	0.713
15: MAL (Malate)	0.603	0.602	0.600	0.600
16: $Mg^{2+}$	1.416	1.415	1.409	1.413
17: $NAD^+$ (Nicotinamide adenine dinucleotide)	1.308	1.308	1.308	1.306
18: NADH (Reduced $NAD^+$ )	1.662	1.662	1.662	1.664
19: OAA (Oxaloacetate)	4.37E-07	4.36E-07	4.35E-07	4.34E-07
20: $P_i$ (Inorganic phosphate)	18.980	18.957	18.897	18.906
21: $QH_2$ (Reduced ubiquinol)	0.192	0.190	0.187	0.183
22: SCOA (Succinyl-CoA)	3.21E-04	3.18E-04	3.15E-04	3.12E-04
23: SUC (Succinate)	0.046	0.045	0.045	0.044
<b>Physiochemical and derived parameters</b>				
24: $C_{ox}$ (Oxidized cytochrome-c)	1.793	1.795	1.799	1.802
25: $C_{red}$ (Reduced cytochrome-c)	0.907	0.905	0.901	0.898
26: Mitochondrial membrane potential ( $\Delta\psi$ )	190.7969	190.7028	190.613	190.4295
27: NADH/ $NAD^+$ ratio	1.270	1.271	1.271	1.274



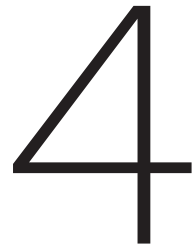
	60% CI	50% CI	40% CI	30% CI	20% CI	10% CI	1% CI
	3.010	3.010	3.010	3.010	3.010	3.010	3.010
	0.734	0.757	0.792	0.848	0.957	1.241	3.303
	0.002	0.002	0.002	0.002	0.002	0.002	0.001
	9.266	9.243	9.208	9.152	9.043	8.759	6.697
	1.473	1.462	1.446	1.424	1.384	1.312	1.152
	0.004	0.004	0.004	0.003	0.003	0.003	0.003
	1.17	1.18	1.19	1.20	1.22	1.25	1.33
	0.198	0.199	0.200	0.202	0.205	0.212	0.212
	4.644	4.633	4.616	4.590	4.538	4.403	3.407
	0.353	0.364	0.381	0.407	0.459	0.594	1.590
	5.21E-05	5.20E-05	5.21E-05	5.20E-05	5.20E-05	5.17E-05	5.10E-05
	0.032	0.032	0.032	0.031	0.030	0.028	0.022
	137.284	137.243	137.353	137.266	137.221	136.452	134.543
	0.714	0.714	0.714	0.715	0.717	0.723	0.749
	0.601	0.601	0.601	0.602	0.603	0.611	0.639
	1.419	1.425	1.433	1.449	1.474	1.548	2.044
	1.303	1.299	1.295	1.287	1.274	1.237	1.059
	1.667	1.671	1.675	1.683	1.696	1.733	1.911
	4.32E-07	4.29E-07	4.25E-07	4.20E-07	4.10E-07	3.88E-07	2.97E-07
	18.931	18.945	18.925	18.956	18.984	19.219	20.072
	0.179	0.173	0.165	0.153	0.133	0.097	0.022
	3.08E-04	3.03E-04	2.95E-04	2.85E-04	2.66E-04	2.29E-04	1.15E-04
	0.043	0.042	0.040	0.037	0.033	0.026	0.008
	1.805	1.811	1.819	1.831	1.853	1.900	2.099
	0.895	0.889	0.881	0.869	0.847	0.800	0.601
	190.1798	189.8552	189.4232	188.6933	187.419	184.3922	171.5277
	1.279	1.286	1.293	1.307	1.332	1.401	1.806



# CHAPTER

## **Isoflurane anesthetic hypersensitivity and progressive respiratory depression in a mouse model with isolated mitochondrial Complex I deficiency**

Published in  
Roelofs, S., **G. R. Manjeri**, P. H. Willems, G. J. Scheffer, J. A. Smeitink  
and J. J. Driessen (2014). "Isoflurane anesthetic hypersensitivity  
and progressive respiratory depression in a mouse model with  
isolated mitochondrial complex I deficiency." **J Anesth.**  
(Shared 1<sup>st</sup> author)

A large, bold, black outline of the number 4, positioned to the right of a vertical line that separates it from the chapter title and publication information.

## Abstract

**Background.** Children with mitochondrial disorders are frequently anesthetized for a wide range of operations. These disorders may interfere with the response to surgery and anesthesia. We examined anesthetic sensitivity to and respiratory effects of isoflurane in the *Ndufs4* knockout (KO) mouse model. These mice exhibit an isolated mitochondrial complex I (CI) deficiency of the respiratory chain, and they also display clinical signs and symptoms resembling those of patients with mitochondrial CI disease.

**Methods.** We investigated seven *Ndufs4*<sup>-/-</sup> knockout (KO), five *Ndufs4*<sup>+/-</sup> heterozygous (HZ) and five *Ndufs4*<sup>+/+</sup> wild type (WT) mice between 22-25 days and again between 31-34 days post-natal. Animals were placed inside an airtight box, breathing spontaneously while isoflurane was administered in increasing concentrations. Minimum alveolar concentration (MAC) was determined with the bracketing study design, using the response to electrical stimulation to the hind paw.

**Results.** MAC for isoflurane was significantly lower in KO mice than in HZ and WT mice:  $0.81\% \pm 0.01$  vs.  $1.55\% \pm 0.05$  and  $1.55\% \pm 0.13$ , respectively, at 22-25 days, and  $0.65\% \pm 0.05$ ,  $1.65\% \pm 0.08$  and  $1.68\% \pm 0.08$  at 31-34 days. The KO mice showed severe respiratory depression at lower isoflurane concentrations than the WT and HZ mice.

**Conclusion.** We observed an increased isoflurane anesthetic sensitivity and severe respiratory depression in the KO mice. Both paradigms were progressive with age. Since the pathophysiological consequences from complex I deficiency are mainly reflected in the central nervous system and our mouse model involves progressive encephalopathy, further investigation of isoflurane effects on brain mitochondrial function is warranted.

## Introduction

Mitochondria produce the energy requirements of cells, adenosine triphosphate (ATP), mainly through the reduction and oxidation reactions of the electron transfer chain (ETC) and oxidative phosphorylation (OXPHOS). The OXPHOS pathway consists of five multi-subunit enzyme complexes (complexes I-V) and two electron carriers (cytochrome C and coenzyme Q).

Mitochondrial disorders are most frequently due to defects in OXPHOS, and are genetically and phenotypically a heterogeneous group of disorders having an incidence of 1 in 10,000 live births (Smeitink, van den Heuvel et al. 2001). The onset of symptoms may vary from birth to late adulthood. Organs that are highly energy-dependent such as the brain, heart and skeletal muscle are most vulnerable to mitochondrial defects. Since a treatment to correct this is not yet available, therapy is purely empirical and is still not very successful (Distelmaier, Koopman et al. 2009).

Children with mitochondrial disease are frequently anaesthetized for diagnostic muscle biopsy, but also for a wide range of other procedures. These children often have several signs and symptoms (encephalomyopathy, respiratory and cardiac compromise, difficulty in swallowing and regurgitation), which may increase the risk associated with anesthesia and surgery (Driessen 2008). Patients with mitochondrial disease resulting from a variety of defects in the respiratory chain and oxidative phosphorylation vary in their response to anesthetics and possibly in their peri-operative risk (Morgan, Hoppel et al. 2002, Driessen 2008).

The most frequently occurring defect in the OXPHOS system in humans is an isolated complex I (NADH:ubiquinone oxidoreductase) deficiency (Loeffen, Smeitink et al. 2000). Most children suffering from complex I deficiency develop symptoms during their first year of life, and show rapid deterioration (Distelmaier, Koopman et al. 2009). The majority of children with complex I deficiency present with Leigh or Leigh-like syndrome, which involves psychomotor retardation, brainstem dysfunction, seizures, failure to thrive, muscular hypotonia, abnormal eye movements and lactic acidosis (Koene, Willems et al. 2011).

The volatile anesthetic isoflurane inhibits complex I enzymatic rates (Kayser, Suthammarak et al. 2011). In the nematode *C. elegans*, animals with a complex I deficiency, are hypersensitive to volatile anesthetics (Kayser, Suthammarak et al. 2011). In a clinical study, Morgan et al. (Morgan, Hoppel et al. 2002) observed profound hypersensitivity to volatile anesthetics in a subset of children with defects in complex I function, requiring very low doses of sevoflurane to reach a bispectral index (BIS) value of 60. However, BIS monitoring, used in that study, is not

a reliable index of anesthetic sensitivity in children who have central nervous system dysfunction (Allen 2003).

The *Ndufs4* subunit plays an important role in the assembly or stability of complex I and mutations in the *Ndufs4* gene, located on chromosome 5, cause a reduced complex I content as detected by blue native gel electrophoresis (BN-PAGE) and enzymatic activity measurements (Kruse, Watt et al. 2008). Patients harboring mutations in this gene show Leigh or Leigh-like syndrome with death occurring at a very young age (Budde, van den Heuvel et al. 2003, Koene, Willems et al. 2011). The clinical signs and symptoms of *Ndufs4* KO mice show extensive similarities to those of patients with mitochondrial complex I disease (Kruse, Watt et al. 2008, Koene and Smeitink 2011). The aim of this study was to investigate the anesthetic sensitivity and respiratory response to exposure of a volatile anesthetic agent, isoflurane, in the *Ndufs4* KO mouse model at two stages, before and after the onset of severe symptoms.

## Methods

All experiments were approved by the Regional Animal Ethics Committee (Nijmegen, The Netherlands) and performed under the guidelines of the Dutch Council for Animal Care. All efforts were made to reduce animal suffering and number of animals used in this study.

### Animals

To determine isoflurane sensitivity in our experimental model, studies were conducted using *Ndufs4*<sup>-/-</sup> knockout (KO) and *Ndufs4*<sup>+/-</sup> heterozygous (HZ) mice, and their wild type (WT) *Ndufs4*<sup>+/+</sup> littermates (mixed 129/Sv: C57BL6 background), n=7, n=5, and n=5 respectively. (Kruse, Watt et al. 2008) Mice were bred locally from heterozygous parent mice. Genotype was confirmed by polymerase chain reaction testing. Both male and female mice were included. Mice had *ad libitum* access to food and water and were fed on a standard animal diet (Ssniff GmbH, Soest, 76. Germany. V1534-300 R/M-H). Animals were group housed at 22°C and were maintained on a day and night rhythm of 12 hours.

### Experimental Design

Measurements took place when the mice were between postnatal (PN) 22-25 days (experiment I) before the pathophysiological symptoms appeared in the KO mice, and again between PN days 31-34 (experiment II) when *Ndufs4* KO mice started to develop pathophysiological symptoms but before major inconvenience, as described by Kruse et al (Kruse, Watt et al. 2008). Weights and symptoms were recorded daily.

Each mouse was individually placed inside an airtight Plexiglas chamber (0.20 l), breathing spontaneously. Isoflurane (TEVA Pharmachemie, Haarlem, The Netherlands) was administered using an IsoTec-5 Isoflurane Anesthesia Vaporizer (Datex-Ohmeda, GE healthcare) with 33 % oxygen in air at a total flow rate of 0.5 l/min. The concentrations of isoflurane and CO<sub>2</sub> were measured continuously at the exhaust port of the chamber using a Capnomac-Ultima monitor (Datex, Helsinki). CO<sub>2</sub> levels in the chamber remained unmeasurably low throughout all experiments proving lack of rebreathing.

Anesthetic endpoints mostly used in mice are the loss of righting reflex (LORR), which is used as a marker of unconsciousness/hypnosis and the withdrawal reflex to tail clamping or electrical pedal stimulation, as a measure of immobilization (Drexler, Antkowiak et al. 2011).

We used the withdrawal reflex to determine the MAC (Eger, Raines et al. 2008). We used the withdrawal reflex to hind paw electrical stimulation, not tail clamping, to determine immobilization, because, in pilot experiments, it gave more reliable and reproducible responses without any local noxious effects. In rats it gave comparable MAC values when compared to tail clamping (Laster, Liu et al. 1993). Concentrations of isoflurane measured in the chamber, after equilibration during 6 minutes, were used as substitute for alveolar concentrations in determining MAC.

The first experiment was performed when the mice were between PN 22-25 days. Based on pilot experiments isoflurane was administered at 1.5% in WT and HZ mice and 1.0% in KO mice. The time to loss of mobility (LOM) and time to loss of righting reflex (LORR) were measured. LOM was reached when a mouse remained immobile for 60 seconds. LORR was defined as the lack of the ability to return to recumbency within 60 seconds after tilting the box 90 degrees. Concentrations of isoflurane in the box at these time points were recorded. When anesthetized a rectal temperature probe, ECG electrodes, and stimulation electrodes to the hind paw were applied. The eyes were lubricated. Animal breathing was clinically assessed by monitoring thoracic movement and by recording respiratory rate. Two experienced anesthesiologists counted the respirations during 15 sec epochs. Temperature was maintained at 36-38 °C, using a heating lamp and warming pad.

Isoflurane was increased stepwise at regular intervals with equilibration time of 6 min. After equilibration the response to electrical stimulation (pulse intensity 4 mA, pulse duration 4 milliseconds, train duration 500 milliseconds, frequency 100 Hertz (interval 10 milliseconds) of the hind paw was recorded. Purposeful movement of the head and/or legs was considered a response. (Irifune, Katayama et al. 2007) When a response was noticed the anesthetic concentration was increased stepwise with 0.2% increments until the response was lost. When this point was reached the anesthetic

concentration was decreased until there was a return of response.(Quasha, Eger et al. 1980, Sonner 2002) The MAC was determined as the average concentration of isoflurane at loss and return of response to pedal electrical stimulation.

After the MAC was determined and after removal of electrodes, isoflurane was reset to 1% in KO, and 1.5 % in WT and HZ mice. After equilibration, isoflurane was discontinued and the time till the return of righting reflex (RORR) and return of ambulation (ROA) were recorded. Total anesthesia duration (TAD) was also recorded.

After the first anesthetic depth determinations were performed between PN 22-25 days, the animals were allowed to fully awaken, and were returned to their housing. A similar experiment was performed when the mice were between PN 31-34 days.

After the end of the second experiment the animals were anesthetized again with a lower isoflurane concentration than the MAC to obtain an arterial blood gas sample, taken directly from the abdominal aorta. In some cases puncture of the abdominal aorta caused a hemorrhage that was aspirated for lactate determination. Arterial blood gas analysis was performed using *i-STAT*<sup>®</sup> System (Abbott Point of Care Inc., Princeton, USA). Subsequently the animals were sacrificed by cervical dislocation.

### Statistical Analysis

Statistical analysis was performed using Prism 5 (GraphPad Software Inc., La Jolla, Ca, USA). Comparisons between the three groups were performed using the non-parametric Kruskal-Wallis test as a Gaussian distribution was not observed. Comparisons between groups were performed using the non-parametric Mann-Whitney test. The Pearson test was used to assess the correlation between the MAC values and the decrease in respiratory rate at the MAC in KO vs WT mice. All data are presented as Mean  $\pm$  Standard Error of the Mean (SEM). Significance was defined as  $P < 0.05$ .

### Results

There were no statistical significant differences in age in both the first and second experiment between all groups. There were no differences in weight between HZ and WT mice. KO mice weighed significantly less ( $12.3 \pm 0.71$  grams), in the second experiment, than WT ( $15.3 \pm 0.60$  grams) and HZ mice ( $17.1 \pm 1.30$  grams),  $P < 0.02$  (table 1). Despite being of the same age the KO mice were clinically clearly distinguishable by their smaller size and hair loss.

During the first experiment the maximum (baseline) respiratory rate of KO mice ( $130 \pm 7.5$  breaths/min), did not differ from WT ( $130 \pm 6.3$  breaths/min) and HZ ( $135 \pm 10.7$  breaths/min) mice. At the more advanced age the KO mice showed a lower maximum (baseline) respiratory rate ( $83 \pm 10.5$  breaths/min) ( $P < 0.001$ ), than WT and



HZ mice ( $139 \pm 2.3$  breaths/min, and  $157 \pm 3.4$  breaths/min) respectively (table 2). During increasing isoflurane concentration there was progressive slowing of the respiratory rate. The maximal decrease in respiratory rate at MAC concentrations was greater in KO mice. Also signs of airway obstruction were more frequent at higher isoflurane concentrations. Both the baseline and the minimal respiratory rates at reaching the MAC were significantly lower at experiment II than I. During the second experiment one KO mouse died of apnea. Respiratory depression caused by isoflurane exposure was quickly reversible by lowering the isoflurane concentration. Although we started at lower isoflurane concentrations in KO mice, they had a significantly shorter onset time of anaesthesia, measured by time until LOM ( $P < 0.02$ ) and LORR ( $P < 0.02$ ), and at lower isoflurane concentrations ( $P < 0.01$ ) when compared to WT and HZ mice in both the first and second experiment (table 3). There were no significant differences between WT and HZ mice. Mean heart rate while being anesthetized with isoflurane

**Table 1. Age and Weight**

		WT	HZ	KO
Age	I	$23.6 \pm 0.51$	$23.2 \pm 0.58$	$23.3 \pm 0.18$
	II	$32.8 \pm 0.58$	$32.6 \pm 0.51$	$32.7 \pm 0.52$
Weight	I	$9.6 \pm 0.77$	$9.5 \pm 0.41$	$7.8 \pm 0.48$
	II	$15.3 \pm 0.60$	$17.1 \pm 1.30$	$12.3 \pm 0.71^*$

WT = Ndufs4 +/+ mice, HZ = Ndufs4 +/- mice, KO = Ndufs4 -/- mice. Age in days, Weight in grams. I = experiment I, II = experiment II. All data in Mean  $\pm$  SEM. \* = Statistical significance

**Table 2. Clinical Features during Isoflurane Anesthesia**

		WT	HZ
Temp	I	$37.2 \pm 0.21$	$36.6 \pm 0.12$
	II	$37.3 \pm 0.17$	$36.5 \pm 0.24$
HR	I	$273 \pm 12.4$	$268 \pm 10.9$
	II	$286 \pm 11.3$	$297 \pm 8.9$
Baseline RR	I	$130 \pm 6.3$	$135 \pm 10.7$
	II	$139 \pm 2.3$	$157 \pm 3.4$
$\Delta$ RR	I	$44 \pm 5.5$	$52 \pm 13.4$
	II	$70 \pm 5.6$	$83 \pm 8.9$

WT = Ndufs4 +/+ mice, HZ = Ndufs4 +/- mice, KO = Ndufs4 -/- mice. Temp = mean temperature in  $^{\circ}\text{C}$ , HR = mean heart rate in beats/minute, Max RR = maximum or baseline respiratory rate in breaths/minute,  $\Delta$  RR = maximal decrease in respiratory rate in breaths/minute. I = experiment I, II = experiment II. All data represent Mean  $\pm$  SEM. \* = Statistical significance

was similar in all groups, in both experiment I and II (table 2). The same was true for mean temperature during the experiment (table 2).

The MAC in KO mice ( $0.81\% \pm 0.01$ ) was significantly lower than in both HZ ( $1.55\% \pm 0.05$ ) and WT ( $1.55\% \pm 0.13$ ) mice, ( $P < 0.003$ ), in the first experiment (table 4). In the second experiment MAC could not be determined in three mice because of severe respiratory depression, before a loss of response to the stimulus was reached at isoflurane concentrations of 0.70%. One of these mice died as a consequence of respiratory depression. The mean MAC in experiment II for KO mice was  $0.65\% \pm 0.05$ , HZ  $1.65\% \pm 0.08$  and WT  $1.68\% \pm 0.08$ , ( $P < 0.02$ ) (table 4). There was no difference in MAC between HZ and WT mice in both experiments (figure 1). The correlation between the MAC and decrease of respiratory rate from baseline is shown in figure 2. There was a significant correlation between MAC of isoflurane and the decrease in respiratory rate in the KO mice, but not in the WT mice.

Only in the first round of experiments KO mice demonstrated a faster return of righting reflex (RORR) than WT and HZ mice,  $P < 0.003$  (table 5). In the second experiment we had to lower isoflurane concentrations rapidly in 6 out of 7 KO mice, because of severe respiratory depression. This could be a factor in the lack of

**Table 3. Loss of Mobility and Righting Reflex**

		LOM		LORR	
		Time (sec)	Isoflurane (%)	Time (sec)	Isoflurane %
Experiment I	WT	85.2 ± 11.5	1.18 ± 0.05	160.2 ± 15.1	1.34 ± 0.03
	HZ	95.8 ± 15.6	1.27 ± 0.07	146.8 ± 17.7	1.38 ± 0.03
	KO	57.3 ± 3.0*	0.74 ± 0.06*	99.0 ± 7.8*	0.84 ± 0.05*
Experiment II	WT	121.6 ± 18.9	1.32 ± 0.003	179.8 ± 23.7	1.37 ± 0.01
	HZ	106.0 ± 14.3	1.22 ± 0.007	165.2 ± 14.4	1.34 ± 0.03
	KO	51.6 ± 5.6*	0.76 ± 0.03*	86.1 ± 8.0*	0.87 ± 0.02*

LOM = Loss of mobility, LORR = Loss of righting reflex. WT = *Ndufs4*<sup>+/+</sup> mice (n=5), HZ = *Ndufs4*<sup>+/-</sup> mice (n=5), KO = *Ndufs4*<sup>-/-</sup> mice (n=5). All data in Mean ± SEM. \* = Statistical significance.

**Table 4. Minimum Alveolar Concentration of Isoflurane**

		WT	HZ	KO
MAC (%)	I	1.55 ± 0.13	1.55 ± 0.05	0.81 ± 0.01*
	II	1.70 ± 0.08	1.68 ± 0.08	0.68 ± 0.05*

WT = *Ndufs4*<sup>+/+</sup> mice (n=5), HZ = *Ndufs4*<sup>+/-</sup> mice (n=5) KO = *Ndufs4*<sup>-/-</sup> mice (n=7), MAC = minimum alveolar concentration of Isoflurane. I = experiment I, II = experiment II. All data are Mean (SEM). \* = statistical significance.

difference in RORR in this experiment. There was no difference in time till return of ambulation (ROA) between groups (*table 5*). In KO mice total anesthesia duration (TAD) was significantly shorter than in WT and HZ mice in both experiments (*table 5*) due to the fact that in KO mice the MAC was achieved at lower concentrations, achieved in a shorter period of time.

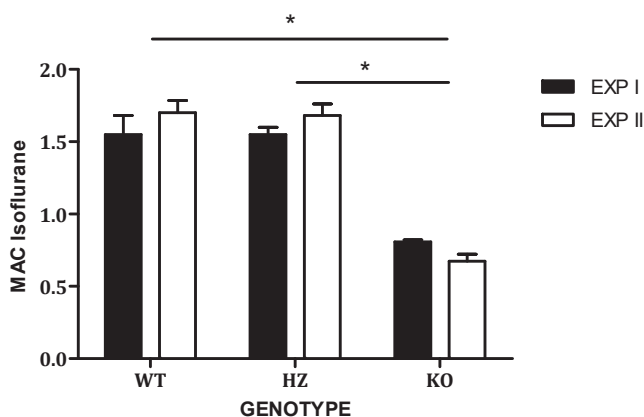


**Figure 1. MAC of Isoflurane: Minimum alveolar concentration (MAC) of Isoflurane for WT=Ndufs4<sup>+/+</sup> (n=5); HZ = Ndufs4<sup>+/-</sup> (n=5); KO = Ndufs4<sup>-/-</sup> (n=7).** EXP I = Experiment I, EXP II = Experiment II. Bars represent mean MAC for WT, HZ, and KO mice. Error bars show the standard error of the mean. The values for the KO mice were significantly different from those for WT and HZ mice, in both experiment I and II. \* $p < 0.005$

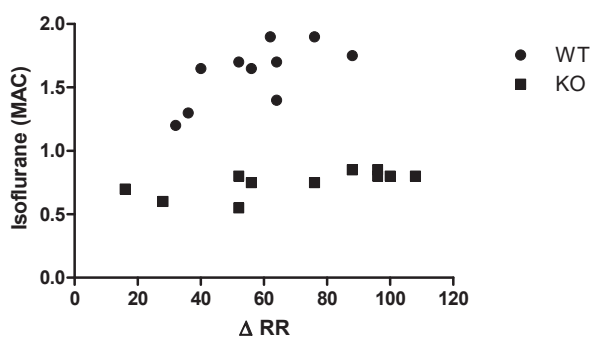


**Figure 2. Decrease in respiratory rate vs MAC.** Cumulative correlation plot between decrease in respiratory rate (DRR) vs minimum alveolar concentration (MAC) in Exp I and Exp II: Correlation was determined for Ndufs4<sup>+/+</sup> (WT) n=5, Ndufs4<sup>-/-</sup> (KO) n=7 mice. Solid black circles indicate the WT mice and solid black squares indicate the KO mice. There was no significant correlation between (DRR) vs MAC in the WT mice (ns)\*, however a significant correlation was observed for the KO mice ( $p = 0.019$ ), (ns = not significant)\*.

There were no statistically significant differences in KO mice between experiment I and II in onset and recovery times.

The results of blood gas analysis are presented in *table 6*. There were no signs of hypoxemia or hypercarbia observed in either group. In two KO mice lactate, determined in the blood aspirated from the hemorrhage that occurred with puncture of the abdominal aorta, was 15.6 and 15.6 mmol/l. These results clearly point to a metabolic acidosis due to lactic acidemia.

**Table 5. Recovery from Anaesthesia**

		WT	HZ	KO
RORR (sec)	I	567 ± 130.2	463 ± 52.5	105 ± 6.8*
	II	238 ± 50.8	239 ± 46.9	202 ± 42.3
ROA (sec)	I	1092 ± 95.2	1233 ± 64.4	681 ± 225.0
	II	712 ± 159.7	702 ± 85.0	420 ± 30.4
TAD (min)	I	120 ± 9.6	110 ± 8.5	69 ± 4.1*
	II	118 ± 10.7	90 ± 5.8	42 ± 3.3*

WT = *Ndufs4*<sup>+/+</sup> mice (n=5), HZ = *Ndufs4*<sup>+/-</sup> mice (n=5), KO = *Ndufs4*<sup>-/-</sup> mice (n=5). RORR = Return of righting reflex, ROA = Return of ambulation, TAD = Total anaesthesia duration. All data in Mean ± SEM. \* = Statistical significance

**Table 6. Arterial Blood Gas analysis at the end of experiments**

	pH	PaO <sub>2</sub>	PaCO <sub>2</sub>	BE	HCO <sub>3</sub> <sup>-</sup>	SaO <sub>2</sub>	Lactate
		(mmHg)	(mmHg)		(mmol/L)	(%)	(mmol/L)
KO	7.02	192	37.4	-21.0	9.6	99	13.30
KO	7.00	x	28.7	-24.0	7.1	x	x
KO	7.09	178	30.2	-21.0	9.2	99	11.29
KO*				-27.0	4.1	98	15.58
KO*				-26.0	2.6	100	15.57
HZ	7.34	206	36.8	-5.0	20.2	100	3.35
HZ	7.38	215	27.8	-9.0	16.5	100	6.01
HZ	7.35	206	34.8	-6.0	19.3	100	4.16
HZ	7.44	302	26.1	-6.0	17.8	100	5.95
WT	7.34	191	37.9	-5.0	20.6	100	3.99
WT	7.42	215	33.2	-2.0	22.0	100	4.49
WT	7.40	213	26.3	-8.0	16.4	100	4.60
WT*					16.4	100	4.19

KO = *Ndufs4*<sup>-/-</sup> mice, WT = *Ndufs4*<sup>+/+</sup> mice, HZ = *Ndufs4*<sup>+/-</sup> mice. \* = analysis after direct aspiration of hemorrhage from abdominal aorta. x = no result.

## Discussion

The main result of our study was increased isoflurane sensitivity in *Ndufs4* knockout mice, compared to their wild type and heterozygous littermates. This involved both the righting reflex, considered as a marker of unconsciousness, and the withdrawal reflex to electrical hind paw stimulation, as a marker of immobilization, used to determine MAC. The MAC was slightly lower at the more advanced age (31-34 days) compared to the younger age (22-25 days). All our KO mice, except one that died from respiratory depression during the experiment, showed a fast and complete recovery from anaesthesia when isoflurane exposure was terminated. *Quintana et al.* (Quintana, Morgan et al. 2012) recently reported almost identical data with a 2.5 - 3-fold higher sensitivity in a tail clamp response to isoflurane and halothane at 23-27 days in *Ndufs4* KO mice compared to WT. The higher sensitivity in their study could be explained by a different stimulation method, but also by shorter equilibration times used in our study. Furthermore a limitation of our study was that it was impossible to administer equal isoflurane concentrations to KO mice since they got severe respiratory depression much faster. Anyway, this effect in complex I deficient mice cannot yet be extrapolated to children with complex I deficiency since a human study did not directly point to a specific hypersensitivity to volatile anesthetics (Driessen, Willems et al. 2007). Furthermore, in our KO mice there is a complete inactivation of the *Ndufs4* gene while in children with *Ndufs4* mutations some residual activity of complex I is still present.

No mention was made about respiratory effects during anesthesia in the report of Quintana et al (Quintana, Morgan et al. 2012) We observed a strong, progressive, near fatal, but completely reversible, respiratory depression during isoflurane exposure in *Ndufs4* KO mice. This already occurred at concentrations well below the MAC for immobilization. *Ndufs4* KO mice are known to develop progressive respiratory dysfunction i.e. bradypnea and apnea, leading to premature death (Quintana, Zanella et al. 2012). Central rather than peripheral mechanisms are involved. Older awake KO mice in that study had lower breathing rates than controls, which was also observed in our study. There were no signs of hypoxemia or hypercarbia in all groups in the arterial blood gas analysis at the end, although this can be partly explained by the fact that all mice were allowed to recover from anesthesia before (briefly) being anesthetized again to obtain the arterial blood sample. However, it is likely that KO mice did develop hypercarbia, and possibly hypoxemia, caused by the severe respiratory depression at reaching MAC concentrations. Future investigations of anesthesia-induced respiratory depression in complex I deficient mice is warranted.

Awaiting such data, it may be presumed that children with complex I deficiency are also at an increased risk of respiratory depression during anesthesia, even before a deep anesthetic phase is reached, and one should monitor ventilation carefully during and after administration of (volatile) anesthesia in case of (suspected) mitochondrial disease.

We did not observe significant differences in heart rate, using electrocardiographic monitoring, during isoflurane anesthesia between all groups. A previous study reported a lower heart rate for KO mice than for control mice, especially in late stages of the disease (Quintana, Zanella et al. 2012). The heart rates in unanaesthetized mice in that study were much higher than heart rates of both KO and control mice in our study during anesthesia.

Despite being used in millions of patients, the mechanism by which volatile anesthetics produce their effects is still scarcely known. The many endpoints associated with the general anesthetic state are probably the result of effects at different sites of action (Humphrey, Sedensky et al. 2002). It was long assumed that they interact non-specifically with neuronal membranes based on their lipophilicity (Eger, Raines et al. 2008). However, at present general anesthetics are believed to exert their effects by binding to specific protein targets, including ligand-gated ion channels, such as GABA<sub>A</sub> receptors, NMDA receptors and a range of two-pore domain potassium channels (Eger, Raines et al. 2008, Franks 2008). Since different classes of general anesthetics act on different spectra of receptors and channels it is unlikely that there is one common mechanism for all general anesthetics.

It has long been known that volatile anesthetics cause depression of mitochondrial function (Cohen 1973). Halothane, isoflurane and sevoflurane inhibit oxidation of substrate at complex I in a dose-dependent fashion (Hanley, Ray et al. 2002). Inhalational anesthetics are also known to uncouple mitochondrial respiration from ATP generation (Rottenberg 1983). They induce mitochondrial flavoprotein oxidation through the opening of adenosine triphosphate-dependent mitochondrial potassium (mitoK-ATP) channel (Kohro, Hogan et al. 2001).

Complex I malfunction causes several mitochondrial effects including reduced ATP-production, changes in membrane depolarization, increased NADH levels, increased production of ROS and lipid peroxidation, alterations in redox state, cellular calcium homeostasis, and changes in mitochondrial morphology (Koene, Willems et al. 2011, Roestenberg, Manjeri et al. 2012). In *C.elegans* with defective function of complex I, there is hypersensitivity to volatile anesthetics causing reversible immobility (Kayser, Suthammarak et al. 2011). Our study confirms these results are also true in a mammalian animal model. Although there is a clear correlation between

complex I-dependent oxidative phosphorylation capacity and anesthetic sensitivity, it is not the absolute rate of complex I enzymatic activity which predicts the threshold for immobilization to volatile anesthetics (Kayser, Suthammarak et al. 2011). At present it remains difficult to explain the exact link between complex I dysfunction and volatile anesthetic hypersensitivity (Quintana, Morgan et al. 2012).

Children with complex I deficiency have early onset neurological deterioration. Optimal complex I function and mitochondrial ROS production are necessary to maintain neuronal activity and synaptic transmission. Cellular ROS production is inversely correlated with CI activity and altered reactive oxygen species levels, as seen in human fibroblasts, and might have a central regulatory role in the pathology of CI deficiency (Distelmaier, Koopman et al. 2009). ROS are routinely generated as by-products of the interaction between free electrons and oxygen and are an unavoidable consequence of aerobic metabolism. Mitochondria are also necessary for the generation of substances that eliminate free radicals formed during aerobic metabolism. If the production of ROS becomes too great to be counterbalanced by its antioxidant system, damage to proteins, lipids and DNA occur. Sensitivity to volatile anesthetics may be related to both complex I mediated impairment of OXPHOS and to oxidative damage to specific molecules (Kayser, Sedensky et al. 2004). It may be that certain specific proteins are damaged due to complex I deficiency and that the accumulation of these damaged molecules is responsible for the increase in anesthetic sensitivity (Kayser, Sedensky et al. 2004, Kayser, Suthammarak et al. 2011).

Volatile anaesthetics also have a well-known protective effect on mitochondria, which is responsible for cardioprotection against ischemia and reperfusion via anesthetic preconditioning (Hirata, Shim et al. 2011). Volatile anesthetics have also been shown to have both neuroprotective and neurotoxic effects in animal models (Zhang, Zhou et al. 2011). Neurotoxic effects of volatile anesthetics occur especially in the developing brain and mitochondrial damage seem to be an important target of anesthesia induced developmental neurodegeneration (Sanchez, Feinstein et al. 2011). Volatile anesthetics may also cause neuroprotection by mild inhibition of respiratory chain complexes I-V and subsequent mitochondrial membrane depolarization (Bains, Moe et al. 2006). It has already been known in 1992 that isoflurane reduces excitatory synaptic transmission in the rat hippocampus (Berg-Johnsen and Langmoen 1992).

In conclusion, there is obviously a broad range of complex biochemical and physiological aspects of complex I dysfunction. Since the pathology from complex I deficiency occurs mainly in the central nervous system (Distelmaier, Koopman et al. 2009), we stress the necessity of specific investigation of the effects of general anesthetics on brain mitochondrial function.

## Acknowledgements

We are grateful for the help of Francien van de Pol, Ing. and Ilona van den Brink, Ing. (Lab technicians, Department of Anesthesiology, Radboud University Nijmegen Medical Centre, Nijmegen, The Netherlands) for their technical assistance in performing the animal experiments.



## References

- Allen, G. C. (2003). "Bispectral index and mitochondrial myopathies." *Anesthesiology* **98**(1): 282; author reply 283.
- Bains, R., M. C. Moe, G. A. Larsen, J. Berg-Johnsen and M. L. Vinje (2006). "Volatile anaesthetics depolarize neural mitochondria by inhibition of the electron transport chain." *Acta Anaesthesiol Scand* **50**(5): 572-579.
- Berg-Johnsen, J. and I. A. Langmoen (1992). "The effect of isoflurane on excitatory synaptic transmission in the rat hippocampus." *Acta Anaesthesiol Scand* **36**(4): 350-355.
- Budde, S. M., L. P. van den Heuvel, R. J. Smeets, D. Skladal, J. A. Mayr, C. Boelen, V. Petruzzella, S. Papa and J. A. Smeitink (2003). "Clinical heterogeneity in patients with mutations in the NDUFS4 gene of mitochondrial complex I." *J Inher Metab Dis* **26**(8): 813-815.
- Cohen, P. J. (1973). "Effect of anesthetics on mitochondrial function." *Anesthesiology* **39**(2): 153-164.
- Distelmaier, F., W. J. Koopman, L. P. van den Heuvel, R. J. Rodenburg, E. Mayatepek, P. H. Willems and J. A. Smeitink (2009). "Mitochondrial complex I deficiency: from organelle dysfunction to clinical disease." *Brain* **132**(Pt 4): 833-842.
- Drexler, B., B. Antkowiak, E. Engin and U. Rudolph (2011). "Identification and characterization of anesthetic targets by mouse molecular genetics approaches." *Can J Anaesth* **58**(2): 178-190.
- Driessen, J., S. Willems, S. Dercksen, J. Giele, F. van der Staak and J. Smeitink (2007). "Anesthesia-related morbidity and mortality after surgery for muscle biopsy in children with mitochondrial defects." *Paediatr Anaesth* **17**(1): 16-21.
- Driessen, J. J. (2008). "Neuromuscular and mitochondrial disorders: what is relevant to the anaesthesiologist?" *Curr Opin Anaesthesiol* **21**(3): 350-355.
- Eger, E. I., 2nd, D. E. Raines, S. L. Shafer, H. C. Hemmings, Jr. and J. M. Sonner (2008). "Is a new paradigm needed to explain how inhaled anesthetics produce immobility?" *Anesth Analg* **107**(3): 832-848.
- Franks, N. P. (2008). "General anaesthesia: from molecular targets to neuronal pathways of sleep and arousal." *Nat Rev Neurosci* **9**(5): 370-386.
- Hanley, P. J., J. Ray, U. Brandt and J. Daut (2002). "Halothane, isoflurane and sevoflurane inhibit NADH:ubiquinone oxidoreductase (complex I) of cardiac mitochondria." *J Physiol* **544**(Pt 3): 687-693.
- Hirata, N., Y. H. Shim, D. Pradic, N. L. Lohr, P. F. Pratt, Jr., D. Weihrauch, J. R. Kersten, D. C. Warltier, Z. J. Bosnjak and M. Bienengraeber (2011). "Isoflurane differentially modulates mitochondrial reactive oxygen species production via forward versus reverse electron transport flow: implications for preconditioning." *Anesthesiology* **115**(3): 531-540.
- Humphrey, J. A., M. M. Sedensky and P. G. Morgan (2002). "Understanding anesthesia: making genetic sense of the absence of senses." *Hum Mol Genet* **11**(10): 1241-1249.
- Irifune, M., S. Katayama, T. Takarada, Y. Shimizu, C. Endo, T. Takata, K. Morita, T. Dohi, T. Sato and M. Kawahara (2007). "MK-801 enhances gabaculine-induced loss of the righting reflex in mice, but not immobility." *Can J Anaesth* **54**(12): 998-1005.
- Kayser, E. B., M. M. Sedensky and P. G. Morgan (2004). "The effects of complex I function and oxidative damage on lifespan and anesthetic sensitivity in *Caenorhabditis elegans*." *Mech Ageing Dev* **125**(6): 455-464.
- Kayser, E. B., W. Suthammarak, P. G. Morgan and M. M. Sedensky (2011). "Isoflurane selectively inhibits distal mitochondrial complex I in *Caenorhabditis elegans*." *Anesth Analg* **112**(6): 1321-1329.

- Koene, S. and J. Smeitink (2011). "Metabolic manipulators: a well founded strategy to combat mitochondrial dysfunction." *J Inherit Metab Dis* **34**(2): 315-325.
- Koene, S., P. H. Willems, P. Roestenberg, W. J. Koopman and J. A. Smeitink (2011). "Mouse models for nuclear DNA-encoded mitochondrial complex I deficiency." *J Inherit Metab Dis* **34**(2): 293-307.
- Kohro, S., Q. H. Hogan, Y. Nakae, M. Yamakage and Z. J. Bosnjak (2001). "Anesthetic effects on mitochondrial ATP-sensitive K channel." *Anesthesiology* **95**(6): 1435-1340.
- Kruse, S. E., W. C. Watt, D. J. Marcinek, R. P. Kapur, K. A. Schenkman and R. D. Palmiter (2008). "Mice with mitochondrial complex I deficiency develop a fatal encephalomyopathy." *Cell Metab* **7**(4): 312-320.
- Laster, M. J., J. Liu, E. I. Eger, 2nd and S. Taheri (1993). "Electrical stimulation as a substitute for the tail clamp in the determination of minimum alveolar concentration." *Anesth Analg* **76**(6): 1310-1312.
- Loeffen, J. L., J. A. Smeitink, J. M. Trijbels, A. J. Janssen, R. H. Triepels, R. C. Sengers and L. P. van den Heuvel (2000). "Isolated complex I deficiency in children: clinical, biochemical and genetic aspects." *Hum Mutat* **15**(2): 123-134.
- Morgan, P. G., C. L. Hoppel and M. M. Sedensky (2002). "Mitochondrial defects and anesthetic sensitivity." *Anesthesiology* **96**(5): 1268-1270.
- Quasha, A. L., E. I. Eger, 2nd and J. H. Tinker (1980). "Determination and applications of MAC." *Anesthesiology* **53**(4): 315-334.
- Quintana, A., P. G. Morgan, S. E. Kruse, R. D. Palmiter and M. M. Sedensky (2012). "Altered anesthetic sensitivity of mice lacking Ndufs4, a subunit of mitochondrial complex I." *PLoS One* **7**(8): e42904.
- Quintana, A., S. Zanella, H. Koch, S. E. Kruse, D. Lee, J. M. Ramirez and R. D. Palmiter (2012). "Fatal breathing dysfunction in a mouse model of Leigh syndrome." *J Clin Invest* **122**(7): 2359-2368.
- Roestenberg, P., G. R. Manjeri, F. Valsecchi, J. A. Smeitink, P. H. Willems and W. J. Koopman (2012). "Pharmacological targeting of mitochondrial complex I deficiency: the cellular level and beyond." *Mitochondrion* **12**(1): 57-65.
- Rottenberg, H. (1983). "Uncoupling of oxidative phosphorylation in rat liver mitochondria by general anesthetics." *Proc Natl Acad Sci U S A* **80**(11): 3313-3317.
- Sanchez, V., S. D. Feinstein, N. Lunardi, P. M. Joksovic, A. Boscolo, S. M. Todorovic and V. Jevtovic-Todorovic (2011). "General Anesthesia Causes Long-term Impairment of Mitochondrial Morphogenesis and Synaptic Transmission in Developing Rat Brain." *Anesthesiology* **115**(5): 992-1002.
- Smeitink, J., L. van den Heuvel and S. DiMauro (2001). "The genetics and pathology of oxidative phosphorylation." *Nat Rev Genet* **2**(5): 342-352.
- Sonner, J. M. (2002). "Issues in the design and interpretation of minimum alveolar anesthetic concentration (MAC) studies." *Anesth Analg* **95**(3): 609-614, table of contents.
- Zhang, J., W. Zhou and H. Qiao (2011). "Bioenergetic homeostasis decides neuroprotection or neurotoxicity induced by volatile anesthetics: a uniform mechanism of dual effects." *Med Hypotheses* **77**(2): 223-229.





# CHAPTER

## Increased mitochondrial ATP production capacity in brain of healthy mice and a mouse model of isolated complex I deficiency after isoflurane anesthesia

# 5

Published in

**Manjeri, G. R.**, R. J. Rodenburg, L. Blanchet, S. Roelofs, L. G. Nijtmans, J. A. Smeitink, J. J. Driessen, W. J. Koopman and P. H. Willems (2016). "Increased mitochondrial ATP production capacity in brain of healthy mice and a mouse model of isolated complex I deficiency after isoflurane anesthesia."

**J Inherit Metab Dis 39(1): 59-65.**

## Abstract

We reported before that the minimal alveolar concentration (MAC) of isoflurane is decreased in complex I-deficient mice lacking the NDUFS4 subunit of the respiratory chain (RC) (1.55 and 0.81% at postnatal (PN) 22-25 days and 1.68 and 0.65% at PN 31-34 days for wildtype (WT) and CI-deficient KO, respectively). 1.0 MAC isoflurane caused a more severe respiratory depression in KO mice (respiratory rate values of 86 and 45 at PN 22-25 days and 69 and 29 at PN 31-34 days for anesthetized WT and KO, respectively). Here, we address the idea that isoflurane anesthesia causes a much larger decrease in brain mitochondrial ATP production in KO mice thus explaining their increased sensitivity to this anesthetic. Brains from WT and KO mice of the above study were removed immediately after MAC determination at PN 31-34 days and a mitochondria-enriched fraction was prepared. Aliquots were used for measurement of maximal ATP production in the presence of pyruvate, malate, ADP and creatine and, after freeze-thawing, the maximal activity of the individual RC complexes in the presence of complex-specific substrates. CI activity was dramatically decreased in KO, whereas ATP production was decreased by only 26% ( $p < 0.05$ ). The activities of CII, CIII and CIV were the same for WT and KO. Isoflurane anesthesia decreased the activity of CI by 30% ( $p < 0.001$ ) in WT. In sharp contrast, it increased the activity of CII by 37% ( $p < 0.001$ ) and 50% ( $p < 0.001$ ) and that of CIII by 37% ( $p < 0.001$ ) and 40% ( $p < 0.001$ ) in WT and KO, respectively, whereas it tended to increase that of CIV in both WT and KO. Isoflurane anesthesia increased ATP production by 52% and 69% in WT ( $p < 0.05$ ) and KO ( $p < 0.01$ ), respectively. Together these findings indicate that isoflurane anesthesia interferes positively rather than negatively with the ability of CI-deficient mice brain mitochondria to convert their main substrate pyruvate into ATP.

## Introduction

Inhaled anesthetics such as isoflurane and sevoflurane are extensively used in clinical practice but much concern remains regarding their possible detrimental effects, particularly on the developing brain (Loepke and Soriano 2008; Hays and Deshpande 2011; Chiao and Zuo 2014). Recent work shows that these anesthetics can induce mitochondrial fission in the developing brain, suggesting a mitochondrial component in the process of anesthesia-induced brain damage (Boscolo, Milanovic et al. 2013).

Further evidence for a putative role of mitochondria in the process of anesthesia-induced brain damage comes from the observation that children with a deficiency of complex I (CI), but not complex III (CIII), of the respiratory chain (RC), are hypersensitive to volatile anesthetics (Morgan, Hoppel et al. 2002; Driessen, Willems et al. 2007). However, it is still debated whether these anesthetics put CI-deficient children at increased risk of neurological complications (Niezgoda and Morgan 2013). Recent studies with mice genetically engineered to lack the NDUFS4 subunit of CI of the RC (referred to herein as “CI-deficient KO mice”) corroborate the finding that the sensitivity to volatile anesthetics is increased in CI deficiency (Quintana, Morgan et al. 2012; Roelofs, Manjeri et al. 2014).

Regarding a putative role of CI in the mechanism of action of volatile anesthetics, studies investigating the effects of direct application of these anesthetics to intact and broken mitochondria conclude that low concentrations reversibly inhibit the oxidation of CI-, but not CII-, linked substrates (Miller and Hunter 1970; Harris, Munroe et al. 1971). Another line of evidence supporting a direct action of volatile anesthetics on CI comes from studies with *C. elegans*. This organism does not possess specialized respiratory systems and complex circulatory organs and relies entirely on the diffusion of gases across the gut lumen and the cuticle (Van Voorhies and Ward 2000). Loss-of-function mutations in CI, but not CII, genes, render these worms hypersensitive to volatile anesthetics in terms of immobility induction (Kayser, Morgan et al. 1999; Falk, Kayser et al. 2006). Analysis of several CI-deficient worm strains with different oxidation rates of CI-linked substrates revealed that the anesthetic sensitivity increased with decreasing oxidation rate (Falk, Kayser et al. 2006). In agreement with these observations, isoflurane was demonstrated to bind to a site distal to the flavoprotein subcomplex of CI (Kayser, Suthammarak et al. 2011). Taken together, these studies indicate that volatile anesthetics bind to CI to reduce its activity and that this inhibitory effect is increased by loss-of-function mutations in CI.

The RC generates the proton motive force used by CV (FOF1-ATP synthase) to produce ATP and with the activity of CI being reduced in CI-deficient KO mice and

CI being a direct target of volatile anesthetics, it is speculated that these anesthetics reduce brain mitochondrial ATP production to a much larger extent in these KO mice than in WT mice. As a consequence, brain ATP levels would be much more decreased in anesthetized KO mice thus explaining their increased sensitivity to volatile anesthetics (Kayser, Sedensky et al. 2004). To test this idea, we determined the maximal rate of ATP production and the maximal activity of the individual RC complexes in a whole brain mitochondria-enriched fraction from the WT and CI-deficient KO mice described in the previous study (Roelofs, Manjeri et al. 2014).

We show that *in vivo* treatment of WT mice with isoflurane decreased the maximal activity of CI, while it increased maximal ATP production. Isoflurane anesthesia also increased maximal ATP production in CI-deficient KO mice. In both WT and KO mice, the effect of isoflurane on brain mitochondrial ATP production was accompanied by an increase in CII and CIII maximal activity and a tendency to increase for CIV. Our data show that isoflurane anesthesia improves rather than worsens the ATP generating ability of brain mitochondria in both WT and CI-deficient KO mice.

## Materials and Methods

All experiments were approved by the Regional Animal Ethics Committee (Nijmegen, The Netherlands) and performed under the guidelines of the Dutch Council for Animal Care. All efforts were made to reduce animal suffering and number of animals used in this study.

### Animals

This study uses the brains from the WT (*ndufs4<sup>+/+</sup>*) and KO (*ndufs4<sup>-/-</sup>*) mice included in our previous study on the anesthetic and respiratory depressant effects of isoflurane (Roelofs, Manjeri et al. 2014). The genotype of the mice was confirmed by polymerase chain reaction and both male and female mice were included. Mice were group-housed at the central animal facility (CDL) of the Radboud University at 22°C on a day and night rhythm of 12 hours. The animals had *ad libitum* access to food and water and were fed on a standard animal diet (Ssniff GmbH, Soest, 76. Germany. V1534-300 R/M-H).

### Isoflurane administration

WT (n=5) and KO (n=7) mice were subjected twice, i.e. at PN 22-25 and PN 31-34 days, to a well-established anesthesia protocol to determine the minimal alveolar concentration (MAC) of isoflurane (Roelofs, Manjeri et al. 2014). Briefly, the isoflurane concentration was increased with steps of 0.2% until the response to electrical stimulation of the



hind paw was lost. When this point was reached the isoflurane concentration was decreased until return of the response. After the first MAC determination at PN 22-25 days, the animals were returned to their housing and determination of the MAC was repeated at PN 31-34 days.

### **Tissue harvesting for biochemical analyses**

Animals were sacrificed at PN 31-34 days by cervical dislocation. Isoflurane-treated mice were sacrificed immediately after determination of the MAC at PN 31-34 days. Whole brains were transferred to ice-cold SEF buffer (0.25 mol/L sucrose, 2mmol/L EDTA, 10 mmol/L Potassium phosphate, pH 7.4), minced with a Sorvall TC2 tissue chopper and homogenized with a glass/Teflon Potter Elvehjem homogenizer within 1 h of harvest. The homogenate was centrifuged at 600g and a portion of the supernatant was used for measurement of the maximal rates of pyruvate oxidation and ATP production. The remainder of the 600g supernatant was frozen in 10 µl aliquots in liquid nitrogen and kept at -80° C for maximal enzymatic activity measurements. The protein concentration was measured according to Rodenburg (Rodenburg 2011).

### **Pyruvate oxidation and ATP production measurements**

To determine the maximal rate of pyruvate oxidation, the freshly prepared 600g supernatant was incubated with radiolabeled substrate ([1-14C] pyruvate). After 20 min the reaction was stopped and the amount of liberated radioactive CO<sub>2</sub> (<sup>14</sup>CO<sub>2</sub>) was quantified (Janssen, Trijbels et al. 2006). The assay medium (pH 7.4) contained K<sup>+</sup>- phosphate buffer (30 mM; source of Pi), KCl (75 mM), Tris (8 mM), K-EDTA (1.6 mM), P<sub>1</sub>,P<sub>5</sub>-Di (adenosine-5') pentaphosphate (Ap5A; 0.2 mM), MgCl<sub>2</sub> (0.5 mM), ADP (2 mM), creatine (20 mM), malate (1 mM) and [1-14C] pyruvate (1 mM). AP5A is a potent adenylate kinase inhibitor required to prevent interference of the adenylate kinase reaction with the levels of produced ATP, as well as with the excess of ADP required for this assay. For measurement of the maximal rate of ATP production, the same assay medium was used but with pyruvate instead of [1-14C] pyruvate. After 20 min, the reaction was stopped by addition of 0.1 M HClO<sub>4</sub>. The reaction mixture was centrifuged at 14000g for 2 min at 2 °C. To the supernatant, 1.2 vol (V/V) of 0.333 M KHCO<sub>3</sub> was added, and this mixture was diluted 2-fold. The amount of ATP and phosphocreatine formed during the reaction were measured in the supernatant using a Konelab 20XT auto-analyzer (Thermo Scientific). Mitochondrial ATP production rate was corrected using a parallel assay in which residual glycolysis was blocked by arsenite (2 mM) (Janssen, Trijbels et al. 2006).

## Respiratory chain enzyme assays

The liquid nitrogen frozen portion of the 600g supernatant was thawed and used for measurement of the maximal activity of the complexes I (CI), II (CII), III (CIII) and IV (CIV) and citrate synthase (CS), as described by Rodenburg (Rodenburg 2011).

## Statistical Analysis

Statistical analysis was performed using Prism 5 (GraphPad Software Inc., La Jolla, Ca). Normal distribution of the datasets was confirmed using Lilliefors test. Results were expressed as mean  $\pm$  SD and comparisons between groups were performed using a two way analysis of variance (ANOVA) and Bonferroni's post-test. Statistical significance was set at ( $p < 0.05$ ).

## Results

In mitochondrial enzyme diagnostics, the activity of CS, which is an indicator of mitochondrial mass, is used for normalization between mitochondria-enriched preparations (Rodenburg 2011). The CS activity per mg protein was the same for WT and KO mice and did not change upon isoflurane anesthesia (**Figure 1**). In the remainder of this paper all values are expressed per mg protein.

The maximal rate of ATP production was significantly decreased by 26% in untreated KO as compared to untreated WT (**Figure 2a**). Unexpectedly, isoflurane anesthesia

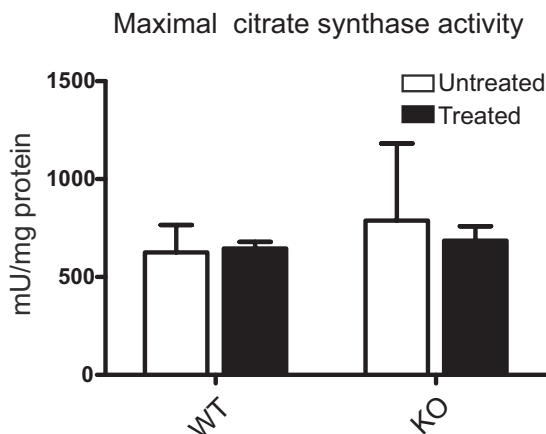


**Figure 1. Effect of isoflurane on citrate synthase activity.** Untreated and isoflurane-treated WT and KO mice were sacrificed at PD 31-34 and a mitochondria-enriched fraction was prepared from total brain. Citrate synthase activity was measured and expressed per mg protein. The data presented show the absence of any difference in between the four experimental conditions. The data presented are the mean  $\pm$  SD of 5 WT and 5 KO untreated and 5 WT and 7 KO isoflurane-treated.

significantly increased this rate in both WT and KO by 52% and 69%, respectively. The maximal rate of pyruvate oxidation revealed a tendency to be lower in untreated KO as compared to untreated WT and isoflurane anesthesia tended to increase this rate in both WT and KO by 26% and 50%, respectively (**Figure 2b**). To evaluate the efficiency by which the oxidation of pyruvate was coupled to the production of ATP, we calculated the ratio of ATP production to pyruvate oxidation. The ratios obtained showed similar values for untreated and treated WT and KO mice (**Figure 2c**).

Analysis of the maximal activity of CI, revealed a significant decrease by 30% in isoflurane-treated WT as compared to untreated WT (**Figure 3a**). As expected, this activity was virtually absent in untreated KO and isoflurane treatment did not lead to any alteration. The maximal activity of CII, was similar between untreated WT and untreated KO (**Figure 3b**). Isoflurane anesthesia significantly increased this activity by 37% and 50% in WT and KO, respectively. The same results were obtained for CIII (**Figure 3c**). Isoflurane anesthesia significantly increased the maximal activity of this complex by 37% and 40% in WT and KO, respectively. For CIV, no difference in maximal activity was observed between untreated WT and untreated KO (**Figure 3d**). Although isoflurane anesthesia tended to increase this activity in both WT (17%) and KO (16%), no statistical significance was reached.

## Discussion

Previous work with the NDUFS4 KO mouse model of human CI deficiency showed a decrease in respiratory rate (Quintana, Morgan et al. 2012; Roelofs, Manjeri et al. 2014) and heart rate (Quintana, Zanella et al. 2012) in the later stages of the disease. The respiratory rate of the KO mice used in this study decreased from 130 at PN 22-25 days to 83 at PN 31-34 days (Roelofs, Manjeri et al. 2014). This decrease in respiratory rate was paralleled by neurological complications that progressed with age (Quintana, Kruse et al. 2010). Although a decrease in respiratory rate suggests ATP shortage, other disease mechanisms remain to be considered, including increased production of reactive oxygen species (Koopman, Distelmaier et al. 2013) and triggering of innate immune responses (Yu, Song et al. 2015).

Here, we show that maximal ATP production from pyruvate and malate is 25% decreased in a mitochondria-enriched fraction from KO mice brain at PN 31-34 days. The same observation was reached in another NDUFS4 KO mouse model (Leong, Komen et al. 2012). At first glance, this relatively moderate decrease seems difficult to reconcile with the virtually complete absence of active CI in a freeze-thawed aliquot of this mitochondria-enriched fraction, see also (Kruse, Watt et al. 2008 and Calvaruso, Willems et al. 2012). However, there is evidence that CIII stabilizes NDUFS4-lacking CI

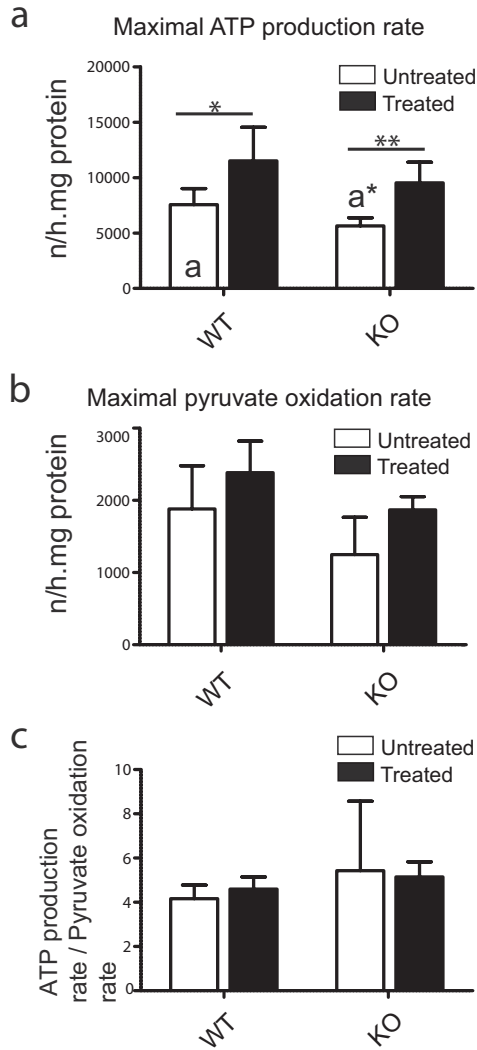


**Figure 2. Effect of isoflurane on ATP production.** Untreated and isoflurane-treated WT and KO mice were sacrificed at PD 31-34 and a mitochondria-enriched fraction was prepared from total brain. The rates of ATP production and pyruvate oxidation were measured at non-rate-limiting concentrations of pyruvate, malate, ADP and creatine and expressed per mg protein. (a) The ATP production rate measured under these conditions was significantly decreased in untreated KO as compared to untreated WT (indicated with a\* as compared with a). Isoflurane anesthesia significantly increased this rate in both WT and KO. (b) The maximal pyruvate oxidation rate tended to be decreased in untreated KO and increased in isoflurane-treated WT and KO. However, none of these differences reached statistical significance. (c) The ratio of the rate of ATP production to that of pyruvate oxidation, reflecting the coupling efficiency, was not significantly different between the different experimental conditions. The data presented are the mean  $\pm$  SD of the number of animals indicated in the caption to figure 1. Statistical significance is displayed as \* ( $p < 0.5$ ) and \*\* ( $p < 0.01$ ).

to provide partial activity (Calvaruso, Willems et al. 2012). This stabilization may be lost upon freeze-thawing of the mitochondria-enriched fraction. Intriguingly, isoflurane anesthesia of KO mice restored brain mitochondrial ATP production to WT levels. This result indicates that the underlying process does not involve irreversible damage, as is thought to occur at increased levels of reactive oxygen species. It is tempting to speculate that isoflurane improves the stabilization of NDUFS4-lacking CI by CIII.

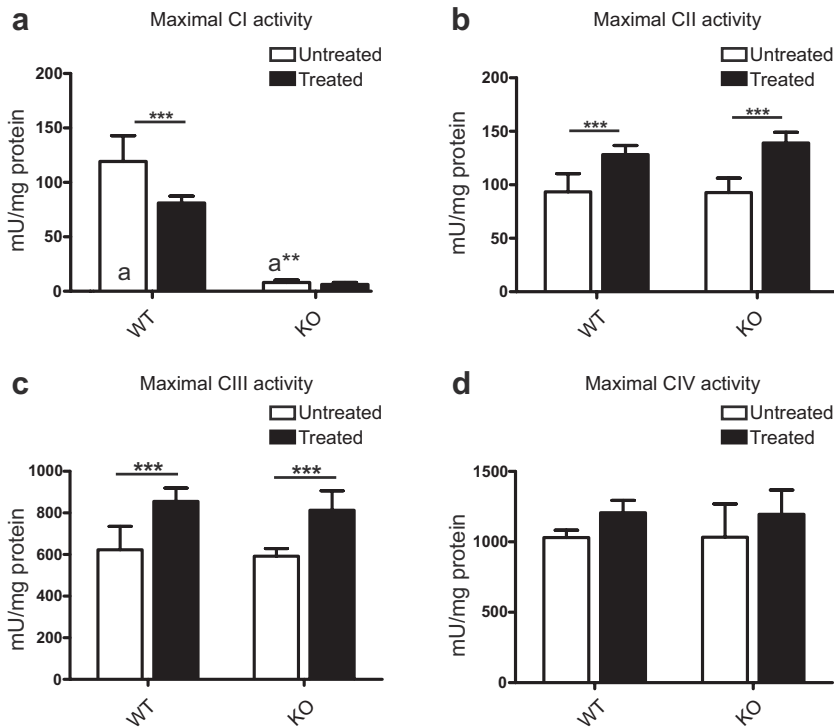


**Figure 3. Effect of isoflurane on the enzymatic activities of the mitochondrial respiratory chain complexes.** Untreated and isoflurane-treated WT and KO mice were sacrificed at PD 31-34 and a mitochondria-enriched fraction was prepared from total brain. The activities of the four respiratory chain complexes were measured under non-rate-limiting substrate conditions and expressed per mg protein. The values obtained reflect the maximum catalytic capacities of the complexes. **(a)** As expected, KO brain was virtually devoid of CI activity (indicated with a\*\* as compared with a). Isoflurane anesthesia significantly decreased this activity in WT. **(b)** The activity of CII did not differ between WT and KO. Isoflurane anesthesia significantly increased this activity to the same extent in both WT and KO. **(c)** The activity of CIII was the same for WT and KO and also in this case isoflurane anesthesia increased this activity to the same extent in both WT and KO. **(d)** Also the activity of CIV was the same for WT and KO. Isoflurane anesthesia tended to increase this activity in both cases but this effect did not reach statistical significance. The data presented are the mean  $\pm$  SD of the number of animals indicated in the caption to figure 1. Statistical significance is displayed as \*\* ( $p < 0.01$ ) and \*\*\* ( $p < 0.001$ ).

The most intriguing observation of the present study is that isoflurane anesthesia increased rather than decreased brain mitochondrial ATP production in both WT and CI-deficient KO mice. To our best knowledge, this is the first report that describes such an effect of a volatile anesthetic, see also (Miro, Barrientos et al. 1999). A recent *in vivo* study showed that isoflurane anesthesia decreased ATP levels in mouse brain (Wang, Xu et al. 2015). Together, these data lead us to postulate that isoflurane acts outside the mitochondrion to reduce the supply of pyruvate, which is the main mitochondrial substrate in brain.

The increase in brain mitochondrial ATP production observed in anesthetized WT and KO mice was paralleled by a tendency to increase for the pyruvate oxidation rate, whereas the CS activity remained unaltered. This may suggest that pyruvate dehydrogenase is not the rate-limiting enzyme in the untreated condition. Isoflurane anesthesia significantly increased the activities of CII and CIII and tended to increase the activity of CIV. This may suggest that the activity of the RC is rate-limiting in the untreated condition and that isoflurane can simultaneously increase their activity by a hitherto unknown mechanism, which may, however, be triggered by ATP shortage (see above). In sharp contrast, the activity of CI was significantly decreased in anesthetized WT mice, indicating that this enzyme is not rate-limiting in the untreated condition.

Analysis of the ratio of ATP production to pyruvate oxidation revealed similar values for WT and CI-deficient KO mice regardless whether they were anesthetized or not. This result indicates, firstly, that the absence of the NDUFS4 subunit does not alter the coupling of pyruvate oxidation to ATP production and, secondly, that *in vivo* exposure to isoflurane does not alter this efficiency. Pyruvate oxidation is measured in the presence of an excess of pyruvate and malate, which is converted into oxaloacetate to trap acetyl-CoA, and an excess of ADP, which is converted into ATP. Under these conditions, a decreased efficiency of the coupling of pyruvate oxidation to ATP production would be indicative of an increased proton leak across the inner mitochondrial membrane. The present finding that *in vivo* exposure to isoflurane does not alter the coupling efficiency is of relevance since *in vitro* studies showed that direct addition of halothane to isolated mitochondria caused a limited uncoupling at concentrations between 0.5 and 2% used clinically to achieve anesthesia (Miller and Hunter 1970).

Thus far, only inhibitory effects of volatile anesthetics on mitochondrial ATP production have been reported (Miller and Hunter 1970; Harris, Munroe et al. 1971). Available evidence indicates that volatile anesthetics act directly on CI (Kayser, Suthammarak et al. 2011) to decrease its activity (Miller and Hunter 1970; Harris, Munroe et al. 1971). Crucially, these studies employ direct application of the anesthetic to isolated mitochondria. For example, halothane, was shown to dose-dependently inhibit the

rate of ADP-stimulated oxygen consumption in the presence of CI-, but not CII-linked substrates (Miller and Hunter 1970). Direct application of halothane to deoxycholate-treated mitochondria confirmed that CI, and not CII, was the primary target of the anesthetic (Harris, Munroe et al. 1971). The present study shows that the *in vitro* activity of CI was also decreased after *in vivo* exposure. The inhibitory effect in direct application studies was reversed in less than 5 min (Miller and Hunter 1970; Harris, Munroe et al. 1971), indicating that the mechanism of inhibition must be different from that in the present study. Our finding of a sustained effect of volatile anesthetics is corroborated by a recent study showing that 4 hours of anesthesia at the larval stage of *C. elegans* caused a marked reduction of the chemotactic response at day 4 of life (Gentry, Steele et al. 2013). Also in this study, it was observed that the degree of reduction was significantly more in worms with a loss-of-function mutation in a CI gene than in wild type worms.

Unfortunately, our anesthesia protocol does not allow drawing conclusions on whether the effects of isoflurane anesthesia at PN 31-34 days are acute or whether, and, if so, to which extent, they are a consequence of processes triggered during the first period of isoflurane anesthesia at PN 22-25 days. Long-term effects of volatile anesthetics have been reported in the literature and can be neuroprotective, as observed in a variety of animal stroke models, reviewed in (Burchell, Dixon et al. 2013) or neurotoxic, as evidenced by animal studies showing that volatile anesthesia can trigger widespread cell death in the neonatal developing brain (Jevtovic-Todorovic, Hartman et al. 2003; Yon, Daniel-Johnson et al. 2005; Istaphanous, Howard et al. 2011; Istaphanous, Ward et al. 2013; Xiong, Zhou et al. 2013)

A limitation of our study is that we used a mitochondria-enriched fraction from whole brain homogenate. Since regional susceptibilities to mitochondrial dysfunction have been reported within the CNS (Leong, Komen et al. 2012; Pinto, Pickrell et al. 2012; Quintana, Zanella et al. 2012), a further detailed investigation should involve specific regions of the brain. Thus, from the results presented in this study, we conclude that isoflurane exposure might preserve the ATP production capacity in brain mitochondria of CI-deficient KO mice and that the isoflurane hypersensitivity in these mice is not a consequence of ATP deficits in the brain.

## Acknowledgements

This research was supported by a grant of the 'Prinses Beatrix Fonds' (No: OP-05-04) and the NWO Centres for Systems Biology Research initiative (CSBR09/013V). We thank Dr. R.D. Palmiter (Howard Hughes Medical Institute and Department of Biochemistry, University of Washington, Seattle, WA, USA) for providing the complex I deficiency mouse model.

## References

- Boscolo A, Milanovic D, Starr JA, et al. (2013) Early exposure to general anesthesia disturbs mitochondrial fission and fusion in the developing rat brain. *Anesthesiology* 118(5): 1086-1097.
- Burchell SR, Dixon BJ, Tang J, Zhang JH (2013) Isoflurane provides neuroprotection in neonatal hypoxic ischemic brain injury. *Journal of investigative medicine : the official publication of the American Federation for Clinical Research* 61(7): 1078-1083.
- Calvaruso MA, Willems P, van den Brand M, et al. (2012) Mitochondrial complex III stabilizes complex I in the absence of NDUFS4 to provide partial activity. *Human molecular genetics* 21(1): 115-120.
- Chiao S, Zuo Z (2014) A double-edged sword: volatile anesthetic effects on the neonatal brain. *Brain sciences* 4(2): 273-294.
- Driessen J, Willems S, Dercksen S, Giele J, van der Staak F, Smeitink J (2007) Anesthesia-related morbidity and mortality after surgery for muscle biopsy in children with mitochondrial defects. *Paediatric anaesthesia* 17(1): 16-21.
- Falk MJ, Kayser EB, Morgan PG, Sedensky MM (2006) Mitochondrial complex I function modulates volatile anesthetic sensitivity in *C. elegans*. *Current biology : CB* 16(16): 1641-1645.
- Gentry KR, Steele LM, Sedensky MM, Morgan PG (2013) Early developmental exposure to volatile anesthetics causes behavioral defects in *Caenorhabditis elegans*. *Anesthesia and analgesia* 116(1): 185-189.
- Harris RA, Munroe J, Farmer B, Kim KC, Jenkins P (1971) Action of halothane upon mitochondrial respiration. *Archives of biochemistry and biophysics* 142(2): 435-444.
- Hays SR, Deshpande JK (2011) Newly postulated neurodevelopmental risks of pediatric anesthesia. *Current neurology and neuroscience reports* 11(2): 205-210.
- Istaphanous GK, Howard J, Nan X, et al. (2011) Comparison of the neuroapoptotic properties of equipotent anesthetic concentrations of desflurane, isoflurane, or sevoflurane in neonatal mice. *Anesthesiology* 114(3): 578-587.
- Istaphanous GK, Ward CG, Nan X, et al. (2013) Characterization and quantification of isoflurane-induced developmental apoptotic cell death in mouse cerebral cortex. *Anesthesia and analgesia* 116(4): 845-854.
- Janssen AJ, Trijbels FJ, Sengers RC, et al. (2006) Measurement of the energy-generating capacity of human muscle mitochondria: diagnostic procedure and application to human pathology. *Clinical chemistry* 52(5): 860-871.
- Jevtovic-Todorovic V, Hartman RE, Izumi Y, et al. (2003) Early exposure to common anesthetic agents causes widespread neurodegeneration in the developing rat brain and persistent learning deficits. *The Journal of neuroscience : the official journal of the Society for Neuroscience* 23(3): 876-882.
- Kayser EB, Morgan PG, Sedensky MM (1999) GAS-1: a mitochondrial protein controls sensitivity to volatile anesthetics in the nematode *Caenorhabditis elegans*. *Anesthesiology* 90(2): 545-554.
- Kayser EB, Sedensky MM, Morgan PG (2004) The effects of complex I function and oxidative damage on lifespan and anesthetic sensitivity in *Caenorhabditis elegans*. *Mechanisms of ageing and development* 125(6): 455-464.



- Kayser EB, Suthammarak W, Morgan PG, Sedensky MM (2011) Isoflurane selectively inhibits distal mitochondrial complex I in *Caenorhabditis elegans*. *Anesthesia and analgesia* 112(6): 1321-1329.
- Koopman WJ, Distelmaier F, Smeitink JA, Willems PH (2013) OXPHOS mutations and neurodegeneration. *The EMBO journal* 32(1): 9-29.
- Kruse SE, Watt WC, Marcinek DJ, Kapur RP, Schenkman KA, Palmiter RD (2008) Mice with mitochondrial complex I deficiency develop a fatal encephalomyopathy. *Cell metabolism* 7(4): 312-320.
- Leong DW, Komen JC, Hewitt CA, et al. (2012) Proteomic and metabolomic analyses of mitochondrial complex I-deficient mouse model generated by spontaneous B2 short interspersed nuclear element (SINE) insertion into NADH dehydrogenase (ubiquinone) Fe-S protein 4 (Ndufs4) gene. *The Journal of biological chemistry* 287(24): 20652-20663.
- Loepke AW, Soriano SG (2008) An assessment of the effects of general anesthetics on developing brain structure and neurocognitive function. *Anesthesia and analgesia* 106(6): 1681-1707.
- Miller RN, Hunter FE, Jr. (1970) The effect of halothane on electron transport, oxidative phosphorylation, and swelling in rat liver mitochondria. *Molecular pharmacology* 6(1): 67-77.
- Miro O, Barrientos A, Alonso JR, et al. (1999) Effects of general anaesthetic procedures on mitochondrial function of human skeletal muscle. *European journal of clinical pharmacology* 55(1): 35-41.
- Morgan PG, Hoppel CL, Sedensky MM (2002) Mitochondrial defects and anesthetic sensitivity. *Anesthesiology* 96(5): 1268-1270.
- Niezgodá J, Morgan PG (2013) Anesthetic considerations in patients with mitochondrial defects. *Paediatric anaesthesia* 23(9): 785-793.
- Pinto M, Pickrell AM, Moraes CT (2012) Regional susceptibilities to mitochondrial dysfunctions in the CNS. *Biological chemistry* 393(4): 275-281.
- Quintana A, Kruse SE, Kapur RP, Sanz E, Palmiter RD (2010) Complex I deficiency due to loss of Ndufs4 in the brain results in progressive encephalopathy resembling Leigh syndrome. *Proceedings of the National Academy of Sciences of the United States of America* 107(24): 10996-11001.
- Quintana A, Morgan PG, Kruse SE, Palmiter RD, Sedensky MM (2012) Altered anesthetic sensitivity of mice lacking Ndufs4, a subunit of mitochondrial complex I. *PloS one* 7(8): e42904.
- Quintana A, Zanella S, Koch H, et al. (2012) Fatal breathing dysfunction in a mouse model of Leigh syndrome. *The Journal of clinical investigation* 122(7): 2359-2368.
- Rodenburg RJ (2011) Biochemical diagnosis of mitochondrial disorders. *Journal of inherited metabolic disease* 34(2): 283-292.
- Roelofs S, Manjeri GR, Willems PH, Scheffer GJ, Smeitink JA, Driessen JJ (2014) Isoflurane anesthetic hypersensitivity and progressive respiratory depression in a mouse model with isolated mitochondrial complex I deficiency. *Journal of anesthesia* 28(6): 807-814.
- Van Voorhies WA, Ward S (2000) Broad oxygen tolerance in the nematode *Caenorhabditis elegans*. *The Journal of experimental biology* 203(Pt 16): 2467-2478.
- Wang H, Xu Z, Wu A, et al. (2015) 2-deoxy-D-glucose enhances anesthetic effects in mice. *Anesthesia and analgesia* 120(2): 312-319.

- Xiong WX, Zhou GX, Wang B, et al. (2013) Impaired spatial learning and memory after sevoflurane-nitrous oxide anesthesia in aged rats is associated with down-regulated cAMP/CREB signaling. *PLoS one* 8(11): e79408.
- Yon JH, Daniel-Johnson J, Carter LB, Jevtovic-Todorovic V (2005) Anesthesia induces neuronal cell death in the developing rat brain via the intrinsic and extrinsic apoptotic pathways. *Neuroscience* 135(3): 815-827.
- Yu AK, Song L, Murray KD, et al. (2015) Mitochondrial complex I deficiency leads to inflammation and retinal ganglion cell death in the *Ndufs4* mouse. *Human molecular genetics*.





# CHAPTER

## How to deal with oxygen radicals stemming from mitochondrial fatty acid oxidation

Published in  
Speijer, D., **G. R. Manjeri** and R. Szklarczyk (2014). "How to deal  
with oxygen radicals stemming from mitochondrial fatty acid  
oxidation." **Philos Trans R Soc Lond B Biol Sci** 369(1646).



## Abstract

Oxygen radical formation in mitochondria is an incompletely understood attribute of eukaryotic cells. Recently, a kinetic model (Speijer 2011) was proposed, in which the ratio between electrons entering the respiratory chain via  $\text{FADH}_2$  or NADH determines radical formation. During glucose breakdown the ratio is low; during fatty acid breakdown, the ratio is high (the ratio increasing –asymptotically– with fatty acid length to 0.5, as compared to 0.2 for glucose) (Speijer 2011). Thus, fatty acid oxidation would generate higher levels of radical formation. As a result, breakdown of fatty acids, performed without generation of extra  $\text{FADH}_2$  in mitochondria, could be beneficial for the cell, especially in the case of long and very long chained ones. This possibly has been a major factor in the evolution of peroxisomes. Increased radical formation, as proposed by the model, can also shed light on the lack of neuronal fatty acid oxidation and tells us about hurdles during early eukaryotic evolution. We will specifically focus on extending and discussing the model in light of recent publications and findings.

## Introduction

Mitochondria, derived from endosymbionts of alpha-proteobacterial origin (Yang, Oyaizu et al. 1985, Thrash, Boyd et al. 2011), underwent complex evolutionary rearrangements influencing the metabolic potential of their archeal host (Yutin, Makarova et al. 2008). During this process, the endosymbiont gene content was severely reduced from at least hundreds of genes (Huynen et al. 2013), to present day mitochondrial genomes encoding only up to 64 proteins in *Reclinomonas americana* (Lang, Burger et al. 1997) and merely 13 in humans. Thus, almost all genes encoding the endosymbiont's original metabolic pathways have been relegated to the nuclear genome, while leaving many, but not all, the endosymbiotic metabolic pathways in the organelle (Gabaldon and Huynen 2005). The proteins originally encoded by the endosymbiotic genome had to be retargeted to mitochondria. Interestingly, this losing of genes from the organelle to the nucleus and accompanying protein rerouting started immediately, in evolutionary terms, after the endosymbiosis event (Huynen, Duarte et al. 2013). Recent analyses show a few endosymbiont systems retained entirely by mitochondria, despite their genes' relocation to the nucleus. These are large protein complexes such as the respiratory chain complexes and the mitochondrial ribosome (Szklarczyk and Huynen 2010). Some of the endosymbiont pathways are now found in other cellular compartments, and many mitochondrial pathways not using large protein complexes bear bacterial -not always proteobacterial- evolutionary footprints. Mitochondria also gained new functions including membrane proteins at the interface with the rest of the cell (Szklarczyk and Huynen 2010) with entirely new roles in for instance cellular apoptosis. The severely reduced genome should thus not be seen to indicate a lack of importance of the organelle.

The mitochondrion is the essential powerhouse of the cell, with more than 90% of all energy (in the form of ATP) generated by the breakdown of glucose coming from oxidative mitochondrial processes in which the electron flow through respiratory chain complexes is coupled to the establishment of a proton motive force used for ATP generation: oxidative phosphorylation, the OXPHOS system (Mitchell 1961, Smeitink, van den Heuvel et al. 2001). Most biochemists would agree that highly complex (multi) cellular organisms seem unlikely to evolve in the absence of the highly efficient ATP generation occurring in mitochondria. However, whether the role of oxygen as the final electron acceptor was crucial and is still debated. In any case, many instances of present-day anaerobic uni- or multicellular eukaryotes are known (Muller, Mentel et al. 2012). For a discussion considering which aspects of

the development of mitochondria from the endosymbiont were crucial in allowing major increases in (genome) complexity see e.g. (Lane and Martin 2010). Regardless, the OXPHOS system is extremely efficient. Oxygen might also have played a more indirect role in enabling further organismal complexity, as it seems indispensable for full-fledged epigenetic signaling (via a.o. the marking of DNA and histone proteins, using methylation of cytosines and lysines, respectively). Getting rid of methylation in these cases seems to depend on oxygenases, and thus on oxygen (Jeltsch 2013).

There is a price to pay however (Harman 1981), the use of molecular oxygen ( $O_2$ ) as the final electron acceptor of the respiratory chain, with the formation of  $H_2O$ , inevitably leads to the formation of very toxic by-products. They are found in the form of reactive oxygen species (Turrens 2003, Murphy 2009, Brand 2010), such as the highly reactive free radicals (superoxide anions,  $\cdot O_2^-$ , and hydroxyl radicals,  $HO\cdot$ ) and peroxides (e.g.  $H_2O_2$ ). It is estimated that of all molecular oxygen consumed 0.1 to 2.0 % ends up in the form  $\cdot O_2^-$ , depending on the respiratory state of the mitochondrion (Murphy 2009). These form large pools of toxic molecules that the cell has to cope with. During the evolution of the two ancestors of the first eukaryotes and later on, several mechanisms evolved to deal with reactive oxygen species (ROS), such as mitochondrial manganese-containing superoxide dismutase (MnSOD), cytoplasmic copper-zinc-containing superoxide dismutase (CuZnSOD), glutathione-based systems and thioredoxins. For an overview of general and mitochondrion-specific anti-oxidant measures, see (Andreyev, Kushnareva et al. 2005).

Most of the present day eukaryotes and animals in particular, use  $O_2$  as the final electron acceptor of the respiratory chain, with exception of organisms using mitosomes, retaining only the role the mitochondrion has in Fe-S cluster assembly, or hydrogenosomes, producing molecular hydrogen instead of water (Lindmark and Muller 1973, Hackstein, Tjaden et al. 2006). Even metazoans have now been found to live under conditions of continuous anoxia (Danovaro, Dell'Anno et al. 2010, Muller, Mentel et al. 2012). Still, most eukaryotes build up the proton motive force for ATP generation using the oxidative OXPHOS system. This means that high amounts of ATP for eukaryotes are intrinsically linked to ROS formation inside the cell: internal radicals are inevitable in complex cellular life. Eukaryotes seem to have responded in two ways: as described above, they have harnessed older mechanisms to cope with the toxic by-products of using oxygen and evolved new mechanisms (Szklarczyk, Nooteboom et al. 2014). Additionally, eukaryotes made a virtue of necessity, by using mitochondria and their oxygen radical generating ability as an important part of the apoptotic process used in (multicellular) eukaryotes (Korsmeyer, Yin et al. 1995, Wang and Youle 2009).



## Challenges during early eukaryotic evolution

During the first stage of metabolic reintegration upon the uptake of the precursor of the mitochondrion the (pre)eukaryote must have been confronted with multiple hurdles during its transition to the full eukaryotic state. We will concentrate on the hurdles presumably involved in catabolic oxidative processes using the alpha-proteobacterial respiratory chain as the final route that the energy rich electrons from different food sources have to take to end up reducing molecular oxygen, allowing optimal ATP generation. Two problems seem logical at the onset of symbiosis. First of all, toxic ROS formed in the respiratory chain becomes a bigger problem for the composite cell, than it was for its constituent alpha-proteobacterium. Radical formation on the outskirts of the bacterium (which could even have played a role in cellular defence) now occurs in the middle of the new cellular entity. Additionally, over time, the new composite organism was likely confronted with other ROS related problems as well, as separate catabolic routes of both endosymbiont and host had to be integrated to form a functioning eukaryotic cell. The host (as reflected by the current location of glycolysis in the cytoplasm) had sugar breakdown pathways, while the proto-mitochondrion was equipped with aerobic catabolic pathways for lipids, amino acids and glycerol, including a complete respiratory chain, beta oxidation and at least part of the citric acid cycle (Gabaldon and Huynen 2003, Gabaldon and Huynen 2004, Hackstein, Tjaden et al. 2006). Though the ability to use alternating sources of energy such as glucose or fatty acids over time is of course an enormous source of versatility, greatly extending possible ecological niches of the eukaryotes [as illustrated by yeast, (Landry, Townsend et al. 2006)], we can think of intrinsic problems here as well.

One of the problems arising has to do with the fact that the relative amounts of  $\text{FADH}_2$  and  $\text{NADH}$  (as reflected in  $\text{FADH}_2/\text{NADH}$  ratios) generated during the breakdown of glucose differ from that of the breakdown of fatty acids. A respiratory chain functioning in glucose breakdown might encounter problems upon switching to fatty acid catabolism due to competition for fully oxidized ubiquinone, as ubiquinone is also used as an acceptor by the electron transfer flavoprotein: ubiquinone oxidoreductase (ETF:QO) oxidizing  $\text{FADH}_2$  (Watmough and Frerman 2010, Speijer 2011). This  $\text{FADH}_2$  is generated from  $\text{FAD}$  by reduction during the first recurring step of beta oxidation for every Acetyl-CoA generated during fatty acid breakdown (a step catalysed by Acyl-CoA Dehydrogenase). This implies that especially during the breakdown of longer fatty acids the competition for ubiquinone becomes more difficult for complex I, which is known to be the

major source of oxygen radicals (Brand 2010). As described before (Speijer 2011), large electron fluxes via both complex I on the one hand and complex II, as well as ETF, on the other, would probably lead to a significant increase in radical formation, see also (Brand, Buckingham et al. 2004, Murphy 2009). We will further focus on the implications of these ‘catabolic’ difficulties with regard to radical formation in (pre) eukaryotic cells for eukaryotic evolution, and for metabolic reprogramming at the cellular and multicellular (tissue) level. A schematic overview of possible solutions to the problem of increased radical formation due to catabolism of substrates associated with high  $FADH_2/NADH$  ratios is given in figure 1.

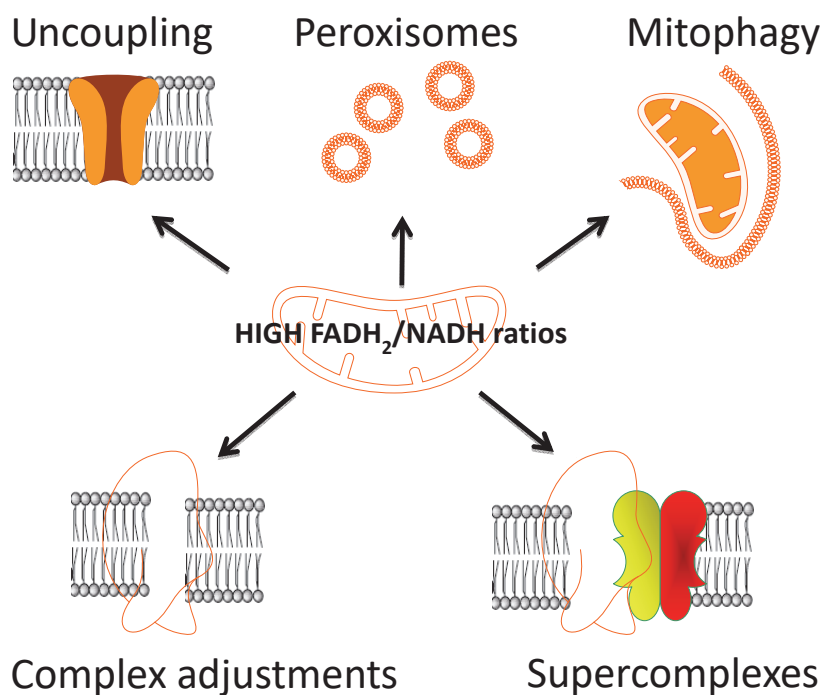


**Figure 1. Schematic representation of possible adaptations to interior radical formation by respiratory chain complexes (especially complex I) upon catabolizing substrates with high  $FADH_2/NADH$  ratios.** Clockwise: 1. Development of mechanisms to induce (regulated) mild uncoupling (e.g. UCPs). 2. Segregation of fatty acid oxidation (completely in neurons, plants and some yeasts, limited to VLCFA's only in most mammalian cells). 3. Evolving specific mitophagy pathways. Apart from mitophagy, a MAD pathway (resembling the ERAD pathway, see text) appeared. 4. Stimulating supercomplex formation, allowing e.g. complex I ‘direct’ access to its ‘own’ ubiquinone pool. 5. Adjusting complexes (especially I) and their synthesis to lessen both radical formation and its impact.

## Did (proto) mitochondria create circumstances favouring the rise of peroxisomes?

A number of predictions can be derived from the hypothesis that high  $\text{FADH}_2/\text{NADH}$  flux ratios lead to increased mitochondrial radical formation, especially in cells with high energy needs. First of all, eukaryotic cells would have an advantage if they evolved mechanisms to lower  $\text{FADH}_2/\text{NADH}$  flux ratios during fatty acid breakdown at a minimal ATP loss. Second, all cells that are difficult to replace or very sensitive to oxidative damage should, as far as possible, forego mitochondrial catabolism in general and beta oxidation specifically. We will consider the possible evolutionary solutions reflecting the first prediction next.

As already stated before (Speijer 2011) the previous considerations give a surprisingly good explanation for the eukaryotic invention of peroxisomes. The hypothesis explaining their origin can be described as follows. Peroxisomes are known to be derived from, or coevolved with, the ER (Gabaldon, Snel et al. 2006, Tabak, Hoepfner et al. 2006, Tabak, van der Zand et al. 2008, Tabak, Braakman et al. 2013). According to the model, the forces giving rise to the evolution of peroxisomes stem from fatty acid catabolism, because of the fact that advantage accrues from mechanisms to lower the  $\text{FADH}_2/\text{NADH}$  ratio during fatty acid breakdown. This is exactly what happened in the emerging peroxisome, the oldest pathway of which is beta oxidation (Gabaldon, Snel et al. 2006), without the generation of  $\text{FADH}_2$  which has to be taken care of by the mitochondrial respiratory chain. Beta oxidation occurs in 4 steps: 1, dehydrogenation (mitochondria) or direct oxidation (peroxisomes), 2, hydration, 3, oxidation by  $\text{NAD}^+$ , and 4, thiolysis, i.e. cleavage by the thiol group of Coenzyme A. The eponymous  $\text{H}_2\text{O}_2$  formed in the first reaction is dealt with by a specific peroxisomal enzyme, catalase. For more specific details see (Reddy and Hashimoto 2001). The ways in which the (partial) redistribution occurred are telling as well. In mammalian peroxisomes, such as our own, the trade-off between minimal ATP loss (the 'ATP content' of  $\text{FADH}_2$  generated in peroxisomes is lost because of direct oxidation, forming  $\text{H}_2\text{O}_2$ ) and overall reduction of the  $\text{FADH}_2/\text{NADH}$  ratio led to the specific breakdown of very long chain fatty acids (VLCFA's) in the peroxisomes only. The VLCFA's have the highest  $\text{FADH}_2/\text{NADH}$  ratios, consistent with our expectations.

In plants and most yeasts, evolution led to the migration of *all* beta oxidation from mitochondria to peroxisomes. This further reduces mitochondrial radical formation by lowering competition between complex I and  $\text{FADH}_2$  containing complexes, but at some energetic cost (see above). So why complete migration in plants and yeasts? Plants are able to be slightly less efficient with energy because

they became autotrophs, synthesizing their own food. Plants gained this ability upon the secondary endosymbiotic event, the uptake of a cyanobacterium, which gave rise to the chloroplast. Many yeasts species seem to use sugars, alcohol or organic acids as major sources of energy and in many cases have retained efficient fermentation pathways. All of this makes a complete relocation of fatty acid oxidation to the peroxisomes possible, while reducing oxygen radical generation. Reduction of radical formation by the respiratory chain can go even further, again at some energetic cost in the form of reduced proton pumping. Interestingly, mitochondria of *Saccharomyces cerevisiae* lack complex I, instead having a rotenone-insensitive NADH dehydrogenase (Ndi1). Ndi1 is formed by a single polypeptide which lacks all proton pumping function (Iwata, Lee et al. 2012). This points to a specific oxygen radical generating vulnerability associated with complex I even in the absence of beta oxidation (see also below). However, it should be mentioned that *Saccharomyces cerevisiae* is not an ideal model in this context, as in its case, respiration seems a condition which it just tries to survive, while thriving during fermentation.

Recently, an evolutionary force associated with fatty acid metabolism playing a role in the evolution of peroxisomes (providing a possible advantage by sequestering toxic by-products of such metabolism), has again been postulated (Gabaldon 2014, Speijer 2014). However, in this case the cellular site at which oxygen radical formation during fatty acid metabolism leads to the selective force favouring peroxisome formation, is thought to be the endoplasmic reticulum, instead of the (proto)mitochondrion (Gabaldon 2014). Also, possible radical formation during fatty acid synthesis, instead of breakdown, is considered a driving force for peroxisomal sequestering of such reactions. There are, however, some issues that need to be resolved (Speijer 2014). As mentioned, the most ancestral peroxisomal pathway is beta oxidation, the 4 steps of which are catalysed by only three enzymes, as step 2 and 3 are catalysed by only one protein: Pox2p (yeast nomenclature), an enzyme stemming from the alpha-proteobacterial heritage. This suggests a crucial contribution of mitochondrial metabolic enzymes to the evolution of peroxisome. Such a mitochondrial 'input' with regard to peroxisomal evolution is further strengthened by the following observations. Mammalian mitochondria and peroxisomes have been shown to communicate and cooperate intensively (Schrader and Yoon 2007). Quite recently, even a direct relationship between both organelles has been found in HeLa cells, taking the form of cargo-selected transport from mitochondria to peroxisomes (Neuspiel, Schauss et al. 2008). We also practically always find peroxisomes and mitochondria together. Amitochondriate, but hydrogenosome containing species such as *Giardia Lamblia* do not contain peroxisomes. Loss of peroxisomes goes together with extremely reduced mitochondrial function, such as lack of beta oxidation, in

apicomplexans. Therefore it appears that a likely candidate for the driving force behind peroxisome evolution is indeed reduction of mitochondrial radical formation inherent in beta oxidation of fatty acids due to the high  $FADH_2/NADH$  ratio involved. We know present-day peroxisomes are derived from the ER (see above). We also know that the peroxisomal protein import machinery is homologous to, and possibly derived from, the ER-associated degradation (ERAD) system (Gabaldon, Snel et al. 2006). Interestingly, a related mitochondrial system (MAD) has been discovered to operate (Margineantu, Emerson et al. 2007, Heo, Livnat-Levanon et al. 2010, Taylor and Rutter 2011). This makes the reconstruction of the strict evolutionary order of events even more difficult. Although purely hypothetical, one could envisage *all* new endomembrane structures, such as peroxisomes, the nucleus, and the ER evolving in reaction to evolutionary pressures resulting from endosymbiont entry. Both ER and Golgi formation took place over a relatively short time span, early on in eukaryotic evolution (Dacks and Field 2007). Indeed, a large number of important evolutionary events occurred rapidly between endosymbiont acquisition and subsequent eukaryotic radiation, which is consistent with early acquisition of, and adjustment to, mitochondria in eukaryotic evolution (Huynen, Duarte et al. 2013). Using an adaptation to the endosymbiont to explain a general characteristic (here the peroxisome) of the eukaryotic lineage is also found in other models. One can think of Martin and Koonin's explanation for the development of a nucleus (and by extension of the ER) *in response to* alphaproteobacterial group II introns migrating to the host genome (Martin and Koonin 2006).

### **Further adaptations to internal radical formation upon competition for ubiquinone**

What other kind of eukaryotic adaptations are possibly related to suppressing radical formation during breakdown of substrates with high  $FADH_2/NADH$  ratios? First of all the widespread tendency of respiratory chain complexes to form quaternary structures called supercomplexes is in line with such a function. For instance, it was observed that all the standard respiratory chain complexes except the  $FADH$  containing complex II can associate in such supercomplexes (Moreno-Lastres, Fontanesi et al. 2012, Barrientos and Ugalde 2013, Lapuente-Brun, Moreno-Loshuertos et al. 2013). Such supercomplex formation could restrict a (dedicated) ubiquinone pool to use by complex I only, reducing the chance of radical formation by reverse electron transfer (RET) from a general pool reduced by complex II. There are many indications that supercomplexes are involved in reducing radical formation (Winge 2012) and that loss of supercomplex formation leads to increased superoxide formation and the mitochondrial aging phenotype, most severely in post-mitotic tissues (Gomez and

Hagen 2012). Supercomplex formation represents a dynamic mechanism allowing cells to organize the respiratory chain optimally in dealing with varying carbon sources (and in specific cell-types (Lapiente-Brun, Moreno-Loshuertos et al. 2013).

Apart from supercomplex formation, the appearance of so-called uncoupling proteins could be linked to the dangers of radical formation by the mitochondrial respiratory chain inside the cell. Extensive radical formation via RET at complex I is found to be more pronounced when electrons are supplied to ubiquinone from succinate, alpha-glycerophosphate or fatty acid oxidation (Murphy 2009). This radical production comes from electrons entering complex I through the ubiquinone-binding site(s), but is only observed if  $D_p$  is high (e.g. during extensive oxidation of *both* NADH and  $FADH_2$ ). All the observations above are consistent with the kinetic model of radical formation due to competition for ubiquinone. The precise molecular mechanisms playing a role are unclear. However, a high  $D_p$  and large electron flows via FADH containing enzymes seem to be essential. In *isolated* mitochondria, RET induced radical formation is abolished upon slight decreases of  $D_p$  (Murphy 2009). This could mean that lowering  $D_p$  by the expression of uncoupling proteins (UCPs) would efficiently reduce radical formation in the cell. The UCPs form a family of proton transporters in the mitochondrial inner membrane which have been implicated in thermo regulation and protection against oxidative damage by their ability to induce uncoupling (Nicholls, Bernson et al. 1978, Azzu and Brand 2010, Jastroch, Divakaruni et al. 2010). UCPs belong to the mitochondrial carriers family, an inner membrane protein family involved in transporting keto acids, amino acids, nucleotides, inorganic ions and co-factors across the mitochondrial inner membrane (Kunji and Robinson 2010). Mitochondrial carriers are part of the organellar interface - and as such arose with the early eukaryote (Szklarczyk and Huynen 2010). More recent evolution of UCPs indicate multiple duplications in vertebrates (Hughes and Criscuolo 2008). Five different UCPs have been identified (Ricquier and Bouillaud 2000). They are found in highly variable amounts in various tissues in all modern mammals (Jastroch, Divakaruni et al. 2010), as well as in plants and unicellular eukaryotes. UCP1-3 have been studied in some detail, but UCP 4 and 5 (interestingly, both mainly expressed in the brain, see below) have only been characterized more recently. UCP1 in mammalian brown adipose tissue has a clear role in heat production, whereas UCP1, UCP2 and UCP3, in other species are implicated in ROS reduction, though their precise roles are still heavily debated. Interestingly, when mammalian UCP1 was expressed in yeast mitochondria, proton transport was increased significantly in the presence of the (saturated C-16) fatty acid palmitate or an oxidized fatty acid (4-hydroxy-2-nonenal) only. Together they

showed a clear synergistic effect (Esteves, Parker et al. 2006). 4-hydroxy-2-nonenal can be formed by the activity of superoxide, a well-known ROS species, which can also activate UCPs on its own. So it seems that, as high ROS formation due to RET in complex I driven by oxidation of fatty acids is acutely sensitive to Dp, it could thus be controlled via slight uncoupling of oxidative phosphorylation. This is accomplished by fatty acids via activation of UCPs. That activation would be even stronger in the simultaneous presence of oxidized fatty acids. See also (Brand, Affourtit et al. 2004) and (Brand, Buckingham et al. 2004). In conclusion, the data regarding most members of the UCP protein family seem to support a role in dealing with specific problems of internal radical formation during fatty acid oxidation.

### The 'special' position of neurons

Above we predicted that all cells which are 'irreplaceable' or extraordinarily sensitive to oxidative damage should have reduced levels of mitochondrial fatty acid oxidation. A prime example of such cells is neurons. Neurons have very high energy demands. It has been calculated that the brain only accounts for ~ 2% of body mass, while it consumes 20% of total oxygen taken up by the entire body. In the brain, neurons have the maximum energy consumption, whereas astrocytes are only responsible for ~5 – 15% of its energy requirements (Attwell and Laughlin 2001). This immense metabolic demand of neurons results from the fact that they are highly differentiated cells needing large amounts of ATP for maintenance of ionic gradients across cell membranes for neurotransmission (Kann and Kovacs 2007). We should also point out that neurons are completely dependent on the OXPHOS system for their ATP needs, as they are not able to switch to glycolysis when OXPHOS becomes limited (Knott, Perkins et al. 2008). In an apparent conflict with these high energy demands, it is beneficial for organisms if neurons are long lived, because they carry essential information for the organism. This poses a dilemma, as oxidative catabolism generates toxic oxygen radicals. Our considerations regarding  $FADH_2/NADH$  ratios explain why neurons do not use beta oxidation (Yang, He et al. 1987, Speijer 2011, Schonfeld and Reiser 2013), instead relying on glucose (and ketone bodies) for their energy supply, even though fatty acids have about twice the energy content of sugars. Despite of the banishment of fatty acids from the menu, neurons of course still need complete oxidative catabolism of glucose, with full mitochondrial involvement. This still results in radical damage, albeit reduced, that neurons accumulate due to their high energy needs.

Mitochondrial diseases have extremely inconsistent clinical presentations, affecting any organ in isolation or combination at any age with variable severity. The genetic basis of these diseases is complex. Mutations in more than a 100 genes

encoded by the nucleus, inherited in a Mendelian manner, or on the mitochondrial genome, inherited maternally, have been found so far (Tucker, Compton et al. 2010, Schapira 2012). Organs with high energy demand are especially afflicted, most prominently the brain (Kirby and Thorburn 2008, Tucker, Compton et al. 2010, Schapira 2012). Neurodegeneration, in which neurons are specifically steadily destroyed, leads to a progressive loss of nervous system structure and function (Przedborski, Vila et al. 2003, Deuschl and Elble 2009). Again, the pathological picture in neurodegenerative disorders is heterogeneous, affecting unique areas of the nervous system. In the brain, Purkinje cells and neurons of the dentate nuclei of the cerebellum as well as neurons of the inferior olivary nuclei of the medulla are considered to be most energy demanding, and thus most susceptible to damage (Breuer, Koopman et al. 2013). Symptoms range from acute and rapid in progression to subtle and chronic (Koopman, Distelmaier et al. 2013). The critical function of the neuronal OXPHOS system in maintaining bioenergetic needs is illustrated by the fact that OXPHOS dysfunction leads to defects in growth and trafficking, as well as to apoptosis and neuronal death (Fukui and Moraes 2008). This in turn can lead to microglial activation, a pathophysiological consequence that can trigger catastrophic events such as further oxidative and nitrosative stress, ultimately leading to further neuronal damage and death (DiFilippo, Chiasserini et al. 2010). OXPHOS dysfunction seems also involved in the occurrence of non-functional synapses and axonal degeneration; see e.g. (Dutta, McDonough et al. 2006).

### **The possible role of mitochondrial ROS production in neurodegenerative disorders**

Despite not using beta oxidation, neuronal radical formation by complex I is still involved in pathogenesis. Increasing evidence shows that disrupted mitochondrial function, especially at complexes I and III, enhances ROS production in neurodegenerative disorders. Here we briefly review the role of ROS in Parkinson's disease (PD), amyotrophic lateral sclerosis (ALS), and Alzheimer's disease (AD) (Lin and Beal 2006, de Moura, dos Santos et al. 2010, Scaglia 2010).

In PD, neurons in the motor centers such as the cerebellum and the striatum are decreased. Substantial decreases in dopaminergic neurons, containing proteinaceous Lewy bodies, of the substantia nigra pars compacta are observed (Tansey and Goldberg 2010). PD patients not only show depletion of dopaminergic neurons, but also decrease in Purkinje cell numbers in the cerebellar cortex, explaining motor skill losses. It is still mostly unknown what causes PD, however genetic mutations in Parkin (Mortiboys, Thomas et al. 2008) and PINK1 (Heeman, Van den Haute et



al. 2011), both implicated in the removal of damaged mitochondria via autophagy have been observed. Defects in mitochondrial respiration, particularly at complex I (Mortiboys, Thomas et al. 2008, Mounsey and Teismann 2010) also result in elevated ROS production which further leads to increased oxidative stress and dopaminergic neuronal degeneration, all strongly correlating with development of PD (de Moura, dos Santos et al. 2010). Interestingly, in the context of our model regarding high  $FADH_2/NADH$  ratios leading to ROS production because of competition for the acceptor ubiquinone, reduced complex I activity can be compensated by increased complex II activity in PD fibroblasts. Indeed, the contribution of complex II to ATP generation is hardly diminished as compared to control fibroblasts (Mortiboys, Thomas et al. 2008). Moreover, 50 % of late onset sporadic PD patient derived fibroblasts even were able to restore complex I activity upon incubation with ubiquinone (Winkler-Stuck et al. 2004). These findings are paralleled in *Drosophila* mitochondria: Parkin and PINK1 mutant phenotypes were found to be enhanced by mutations in the UBIAD1/Heix gene, involved in making the alternative electron acceptor vitamin K2. Overexpressing wt Heix or supplying vitamin K2 'rescued' *Drosophila* from PD-like symptoms (Vos, Esposito et al. 2012).

The motor neuron disease ALS shows loss of motor neurons in cortex, brain stem and spinal cord with aggregated neurofilaments in proximal axons of motor neurons. ALS presents Bunina bodies, eosinophilic aggregates found in anterior horn cells (Goodall & Morrison 2006). Apart from rare predisposing mutations in the mitochondrial superoxide dismutase gene (MnSOD; see above), ALS has no known causes. Surprisingly, in MnSOD mutant rats binding of the misfolded mutant protein to VDAC1 was shown, resulting in reduced VDAC1 activity and loss of motor neurons (Israelson, Arbel et al. 2010). This could imply that loss of MnSOD function in ROS protection is not important in the development of ALS.

AD is characterized by significant decreases in intellectual ability and memory, as well as personality changes (Perry and Hodges 1999). AD gives rise to neurofibrillary tangles, constituting of hyper phosphorylated tau proteins. Extracellular senile plaques of  $\beta$ -amyloid ( $A\beta$ ) are most prominently found on cholinergic neurons supplying the hippocampus (Kar, Slowikowski et al. 2004). Increasing evidence points to a role of OXPHOS dysfunction in the development of AD. In a transgenic mouse model study, decreased mitochondrial membrane potential and decreased ATP levels in neurons could be observed and degree of cognitive impairment correlated with the amount of synaptic mitochondrial dysfunction (Dragicevic, Mamcarz et al. 2010). Interestingly,  $A\beta$  seems to inhibit several key mitochondrial enzymes in the brain, complex IV looking most relevant (Reddy and Beal 2008). This last observation nicely

illustrates one of the key problems in describing a neurodegenerative disease such as AD from a perspective of mitochondrial dysfunction and concomitant radical formation: is it cause or effect (Morais and De Strooper 2010)?

### **Complex I as the most important site of radical formation**

As seen from the description of the clearest example of the involvement of ROS generation and a dysfunctional OXPHOS in the aetiology of neurodegenerative disease, PD, complex I plays a crucial role. It is known to be the major source of oxygen radicals (Brand 2010). Complex I has grown considerably in size during evolution, gathering so-called supernumerary subunits. It grew from its 14 bacterial subunits, to encompass 30 in algae and plants, 37 in fungi and at least 44 in human beings (Balsa, Marco et al. 2012). The process of complexification was most likely already (almost) complete in the very last eukaryotic common ancestor (LECA) (Gabaldon and Huynen 2005, Huynen, de Hollander et al. 2009, Cardol 2011). It is tempting to think, that apart from performing chaperone functions during assembly and membrane insertion, as well as giving stability to this huge protein complex, some supernumerary subunits are specifically involved in minimizing the occurrence of, and combating, radical formation. This however has to await further research into the specific roles of 'extra' subunits.

Interestingly, at the origin of the vertebrate lineage, Acyl-CoA dehydrogenase 9 (ACAD9), closely resembling very long-chain acyl-CoA dehydrogenase (VLCAD), lost its function in mitochondrial oxidation of fatty acids. Instead it became a required factor for complex I assembly (Nouws, Nijtmans et al. 2010). This could be another indication for a functional link between expressing enzymes involved in fatty acid oxidation and stress for complex I (Speijer 2011). Very recently, pluripotent stem cells from patients carrying a common mutation in mitochondrial DNA, m.3243A>G, mutating the tRNA LEU gene, were generated. The most pronounced problems were associated with complex I. Upon differentiation to neurons, complex I seemed to be actively and specifically (!) degraded via mitophagy (involving PINK1 and Parkin-positive autophagosomes). After the concentration of complex I is thus diminished, complex IV becomes slightly impaired, possibly due to extensive radical formation, and complex II is up regulated, presumably to compensate for the loss in ATP generation, as previously observed in patients carrying this mitochondrial DNA mutation (Hamalainen et al. 2013). Although it is known that oxidative stress can induce autophagy (Korsmeyer, Yin et al. 1995, Gurusamy and Das 2009), such specific targeting of malfunctioning complex I points to its crucial position in the balancing act between ATP generation and radical formation.

## Conclusions

Aerobic eukaryotic life has to perform a balancing act between efficient ATP generation and oxygen radical formation. If the cell is easily replaceable in a multicellular organism and it has high energy needs, it will use mitochondrial beta oxidation of fatty acids, with the exception of one class, as explained by the model presented here. Such cells will only relegate VLFCAs to the peroxisomes, giving high ATP yields, while only somewhat reducing radical formation via complex I. Neurons have a different position along the line of mammalian cells as characterized by the trade-off between efficient ATP generation and amount of ROS generated. Neurons will not oxidize any fatty acids, but consume only less energy-rich glucose. However breakdown has to be performed efficiently, with full mitochondrial involvement. Stem cells and some cancer cells (consider the Warburg effect) also only consume glucose, but can rely on permanent glycolysis with resulting lactate being recycled to glucose by other cells in the body (such as the hepatocytes), even further reducing their mitochondrial contribution and amount of ROS generated, especially by complex I. An impressive array of cellular mechanisms evolved partially to cope with the arrival of an internal oxygen radical generator in the form of the (pre)mitochondrion, amongst others: uncoupling mechanisms, partial or total segregation of fatty acid oxidation, mitophagy, the mitochondrion associated decay (MAD) pathway, supercomplex formation, adjustment of the respiratory chain complexes themselves, and even apoptosis when possible. The results described here are fully consistent with the model we focussed on, one in which  $FADH_2/NADH$  ratios, as encountered during breakdown of different metabolites, are crucial to ROS formation. However, in light of all the cellular adaptations just mentioned, proof will not be easy to come by. We have to await future experiments.

## Acknowledgments

This work was supported by Horizon grant (050-71-053) from the Netherlands Organisation for Scientific Research (NWO) and the CSBR (Centres for Systems Biology Research) initiative from NWO (No: CSBR09/013V).

## References

- Andreyev, A. Y., Y. E. Kushnareva and A. A. Starkov (2005). "Mitochondrial metabolism of reactive oxygen species." *Biochemistry (Mosc)* **70**(2): 200-214.
- Attwell, D. and S. B. Laughlin (2001). "An energy budget for signaling in the grey matter of the brain." *J Cereb Blood Flow Metab* **21**(10): 1133-1145.
- Azzu, V. and M. D. Brand (2010). "The on-off switches of the mitochondrial uncoupling proteins." *Trends Biochem Sci* **35**(5): 298-307.
- Balsa, E., R. Marco, E. Perales-Clemente, R. Szklarczyk, E. Calvo, M. O. Landazuri and J. A. Enriquez (2012). "NDUFA4 is a subunit of complex IV of the mammalian electron transport chain." *Cell Metab* **16**(3): 378-386.
- Barrientos, A. and C. Ugalde (2013). "I function, therefore I am: overcoming skepticism about mitochondrial supercomplexes." *Cell Metab* **18**(2): 147-149.
- Brand, M. D. (2010). "The sites and topology of mitochondrial superoxide production." *Exp Gerontol* **45**(7-8): 466-472.
- Brand, M. D., C. Affourtit, T. C. Esteves, K. Green, A. J. Lambert, S. Miwa, J. L. Pakay and N. Parker (2004). "Mitochondrial superoxide: production, biological effects, and activation of uncoupling proteins." *Free Radic Biol Med* **37**(6): 755-767.
- Brand, M. D., J. A. Buckingham, T. C. Esteves, K. Green, A. J. Lambert, S. Miwa, M. P. Murphy, J. L. Pakay, D. A. Talbot and K. S. Echtay (2004). "Mitochondrial superoxide and aging: uncoupling-protein activity and superoxide production." *Biochem Soc Symp*(71): 203-213.
- Breuer, M. E., W. J. Koopman, S. Koene, M. Nooteboom, R. J. Rodenburg, P. H. Willems and J. A. Smeitink (2013). "The role of mitochondrial OXPHOS dysfunction in the development of neurologic diseases." *Neurobiol Dis* **51**: 27-34.
- Cardol, P. (2011). "Mitochondrial NADH:ubiquinone oxidoreductase (complex I) in eukaryotes: a highly conserved subunit composition highlighted by mining of protein databases." *Biochim Biophys Acta* **1807**(11): 1390-1397.
- Dacks, J. B. and M. C. Field (2007). "Evolution of the eukaryotic membrane-trafficking system: origin, tempo and mode." *J Cell Sci* **120**(Pt 17): 2977-2985.
- Danovaro, R., A. Dell'Anno, A. Pusceddu, C. Gambi, I. Heiner and R. M. Kristensen (2010). "The first metazoa living in permanently anoxic conditions." *BMC Biol* **8**: 30.
- de Moura, M. B., L. S. dos Santos and B. Van Houten (2010). "Mitochondrial dysfunction in neurodegenerative diseases and cancer." *Environ Mol Mutagen* **51**(5): 391-405.
- DiFilippo, M., D. Chiasserini, A. Tozzi, B. Picconi and, P. Calabresi (2010). "Mitochondria and the link between neuroinflammation and neurodegeneration." *J Alzheimers Dis* **20 Suppl 2**: S369-S379.
- Deuschl, G. and R. Elble (2009). "Essential tremor--neurodegenerative or nondegenerative disease towards a working definition of ET." *Mov Disord* **24**(14): 2033-2041.
- Dragicevic, N., M. Mamcarz, Y. Zhu, R. Buzzeo, J. Tan, G. W. Arendash and P. C. Bradshaw (2010). "Mitochondrial amyloid-beta levels are associated with the extent of mitochondrial dysfunction in different brain regions and the degree of cognitive impairment in Alzheimer's transgenic mice." *J Alzheimers Dis* **20 Suppl 2**: S535-550.
- Dutta, R., J. McDonough, X. Yin, J. Peterson, A. Chang, T. Torres, T. Guduz, W. B. Macklin, D. A. Lewis, R. J. Fox, R. Rudick, K. Mirnics and B. D. Trapp (2006). "Mitochondrial dysfunction as a cause of axonal degeneration in multiple sclerosis patients." *Ann Neurol* **59**(3): 478-489.

- Esteves, T. C., N. Parker and M. D. Brand (2006). "Synergy of fatty acid and reactive alkenal activation of proton conductance through uncoupling protein1 in mitochondria." *Biochem J* **395**(3): 619-628.
- Fukui, H. and C. T. Moraes (2008). "The mitochondrial impairment, oxidative stress and neurodegeneration connection: reality or just an attractive hypothesis?" *Trends Neurosci* **31**(5): 251-256.
- Gabaldon, T. (2014). "A metabolic scenario for the evolutionary origin of peroxisomes from the endomembranous system." *Cell Mol Life Sci* **71**(13): 2373-2376.
- Gabaldon, T. and M. A. Huynen (2003). "Reconstruction of the proto-mitochondrial metabolism." *Science* **301**(5633): 609.
- Gabaldon, T. and M. A. Huynen (2004). "Shaping the mitochondrial proteome." *Biochim Biophys Acta* **1659**(2-3): 212-220.
- Gabaldon, T. and M. A. Huynen (2005). "Lineage-specific gene loss following mitochondrial endosymbiosis and its potential for function prediction in eukaryotes." *Bioinformatics* **21 Suppl 2**: ii144-150.
- Gabaldon, T., B. Snel, F. van Zimmeren, W. Hemrika, H. Tabak and M. A. Huynen (2006). "Origin and evolution of the peroxisomal proteome." *Biol Direct* **1**: 8.
- Gomez, L. A. and T. M. Hagen (2012). "Age-related decline in mitochondrial bioenergetics: does supercomplex destabilization determine lower oxidative capacity and higher superoxide production?" *Semin Cell Dev Biol* **23**(7): 758-767.
- Gurusamy, N. and D. K. Das (2009). "Autophagy, redox signaling, and ventricular remodeling." *Antioxid Redox Signal* **11**(8): 1975-1988.
- Hackstein, J. H., J. Tjaden and M. Huynen (2006). "Mitochondria, hydrogenosomes and mitosomes: products of evolutionary tinkering!" *Curr Genet* **50**(4): 225-245.
- Harman, D. (1981). "The aging process." *Proc Natl Acad Sci U S A* **78**(11): 7124-7128.
- Heeman, B., C. Van den Haute, S. A. Aelvoet, F. Valsecchi, R. J. Rodenburg, V. Reumers, Z. Debyser, G. Callewaert, W. J. Koopman, P. H. Willems and V. Baekelandt (2011). "Depletion of PINK1 affects mitochondrial metabolism, calcium homeostasis and energy maintenance." *J Cell Sci* **124**(Pt 7): 1115-1125.
- Heo, J. M., N. Livnat-Levanon, E. B. Taylor, K. T. Jones, N. Dephoure, J. Ring, J. Xie, J. L. Brodsky, F. Madeo, S. P. Gygi, K. Ashrafi, M. H. Glickman and J. Rutter (2010). "A stress-responsive system for mitochondrial protein degradation." *Mol Cell* **40**(3): 465-480.
- Hughes, J. and F. Criscuolo (2008). "Evolutionary history of the UCP gene family: gene duplication and selection." *BMC Evol Biol* **8**: 306.
- Huynen, M. A., M. de Hollander and R. Szklarczyk (2009). "Mitochondrial proteome evolution and genetic disease." *Biochim Biophys Acta* **1792**(12): 1122-1129.
- Huynen, M. A., I. Duarte and R. Szklarczyk (2013). "Loss, replacement and gain of proteins at the origin of the mitochondria." *Biochim Biophys Acta* **1827**(2): 224-231.
- Israelson, A., N. Arbel, S. Da Cruz, H. Ilieva, K. Yamanaka, V. Shoshan-Barmatz and D. W. Cleveland (2010). "Misfolded mutant SOD1 directly inhibits VDAC1 conductance in a mouse model of inherited ALS." *Neuron* **67**(4): 575-587.
- Iwata, M., Y. Lee, T. Yamashita, T. Yagi, S. Iwata, A. D. Cameron and M. J. Maher (2012). "The structure of the yeast NADH dehydrogenase (Ndi1) reveals overlapping binding sites for water- and lipid-soluble substrates." *Proc Natl Acad Sci U S A* **109**(38): 15247-15252.
- Jastroch, M., A. S. Divakaruni, S. Mookerjee, J. R. Treberg and M. D. Brand (2010). "Mitochondrial proton and electron leaks." *Essays Biochem* **47**: 53-67.

- Jeltsch, A. (2013). "Oxygen, epigenetic signaling, and the evolution of early life." *Trends Biochem Sci* **38**(4): 172-176.
- Kann, O. and R. Kovacs (2007). "Mitochondria and neuronal activity." *Am J Physiol Cell Physiol* **292**(2): C641-657.
- Kar, S., S. P. Slowikowski, D. Westaway and H. T. Mount (2004). "Interactions between beta-amyloid and central cholinergic neurons: implications for Alzheimer's disease." *J Psychiatry Neurosci* **29**(6): 427-441.
- Kirby, D. M. and D. R. Thorburn (2008). "Approaches to finding the molecular basis of mitochondrial oxidative phosphorylation disorders." *Twin Res Hum Genet* **11**(4): 395-411.
- Knott, A. B., G. Perkins, R. Schwarzenbacher and E. Bossy-Wetzel (2008). "Mitochondrial fragmentation in neurodegeneration." *Nat Rev Neurosci* **9**(7): 505-518.
- Koopman, W. J., F. Distelmaier, J. A. Smeitink and P. H. Willems (2013). "OXPHOS mutations and neurodegeneration." *EMBO J* **32**(1): 9-29.
- Korsmeyer, S. J., X. M. Yin, Z. N. Oltvai, D. J. Veis-Novack and G. P. Linette (1995). "Reactive oxygen species and the regulation of cell death by the Bcl-2 gene family." *Biochim Biophys Acta* **1271**(1): 63-66.
- Kunji, E. R. and A. J. Robinson (2010). "Coupling of proton and substrate translocation in the transport cycle of mitochondrial carriers." *Curr Opin Struct Biol* **20**(4): 440-447.
- Landry, C. R., J. P. Townsend, D. L. Hartl and D. Cavalieri (2006). "Ecological and evolutionary genomics of *Saccharomyces cerevisiae*." *Mol Ecol* **15**(3): 575-591.
- Lane, N. and W. Martin (2010). "The energetics of genome complexity." *Nature* **467**(7318): 929-934.
- Lang, B. F., G. Burger, C. J. O'Kelly, R. Cedergren, G. B. Golding, C. Lemieux, D. Sankoff, M. Turmel and M. W. Gray (1997). "An ancestral mitochondrial DNA resembling a eubacterial genome in miniature." *Nature* **387**(6632): 493-497.
- Lapuente-Brun, E., R. Moreno-Loshuertos, R. Acin-Perez, A. Latorre-Pellicer, C. Colas, E. Balsa, E. Perales-Clemente, P. M. Quiros, E. Calvo, M. A. Rodriguez-Hernandez, P. Navas, R. Cruz, A. Carracedo, C. Lopez-Otin, A. Perez-Martos, P. Fernandez-Silva, E. Fernandez-Vizarra and J. A. Enriquez (2013). "Supercomplex assembly determines electron flux in the mitochondrial electron transport chain." *Science* **340**(6140): 1567-1570.
- Lin, M. T. and M. F. Beal (2006). "Mitochondrial dysfunction and oxidative stress in neurodegenerative diseases." *Nature* **443**(7113): 787-795.
- Lindmark, D. G. and M. Muller (1973). "Hydrogenosome, a cytoplasmic organelle of the anaerobic flagellate *Tritrichomonas foetus*, and its role in pyruvate metabolism." *J Biol Chem* **248**(22): 7724-7728.
- Margineantu, D. H., C. B. Emerson, D. Diaz and D. M. Hockenbery (2007). "Hsp90 inhibition decreases mitochondrial protein turnover." *PLoS One* **2**(10): e1066.
- Martin, W. and E. V. Koonin (2006). "Introns and the origin of nucleus-cytosol compartmentalization." *Nature* **440**(7080): 41-45.
- Mitchell, P. (1961). "Coupling of phosphorylation to electron and hydrogen transfer by a chemi-osmotic type of mechanism." *Nature* **191**: 144-148.
- Morais, V. A. and B. De Strooper (2010). "Mitochondria dysfunction and neurodegenerative disorders: cause or consequence." *J Alzheimers Dis* **20 Suppl 2**: S255-263.
- Moreno-Lastres, D., F. Fontanesi, I. Garcia-Consuegra, M. A. Martin, J. Arenas, A. Barrientos and C. Ugalde (2012). "Mitochondrial complex I plays an essential role in human respirasome assembly." *Cell Metab* **15**(3): 324-335.

- Mortiboys, H., K. J. Thomas, W. J. Koopman, S. Klaffke, P. Abou-Sleiman, S. Olpin, N. W. Wood, P. H. Willems, J. A. Smeitink, M. R. Cookson and O. Bandmann (2008). "Mitochondrial function and morphology are impaired in parkin-mutant fibroblasts." *Ann Neurol* **64**(5): 555-565.
- Mounsey, R. B. and P. Teismann (2010). "Mitochondrial dysfunction in Parkinson's disease: pathogenesis and neuroprotection." *Parkinsons Dis* **2011**: 617472.
- Muller, M., M. Mentel, J. J. van Hellemond, K. Henze, C. Woehle, S. B. Gould, R. Y. Yu, M. van der Giezen, A. G. Tielens and W. F. Martin (2012). "Biochemistry and evolution of anaerobic energy metabolism in eukaryotes." *Microbiol Mol Biol Rev* **76**(2): 444-495.
- Murphy, M. P. (2009). "How mitochondria produce reactive oxygen species." *Biochem J* **417**(1): 1-13.
- Neuspiel, M., A. C. Schauss, E. Braschi, R. Zunino, P. Rippstein, R. A. Rachubinski, M. A. Andrade-Navarro and H. M. McBride (2008). "Cargo-selected transport from the mitochondria to peroxisomes is mediated by vesicular carriers." *Curr Biol* **18**(2): 102-108.
- Nicholls, D. G., V. S. Bernson and G. M. Heaton (1978). "The identification of the component in the inner membrane of brown adipose tissue mitochondria responsible for regulating energy dissipation." *Experientia Suppl* **32**: 89-93.
- Nouws, J., L. Nijtmans, S. M. Houten, M. van den Brand, M. Huynen, H. Venselaar, S. Hoefs, J. Gloerich, J. Kronick, T. Hutchin, P. Willems, R. Rodenburg, R. Wanders, L. van den Heuvel, J. Smeitink and R. O. Vogel (2010). "Acyl-CoA dehydrogenase 9 is required for the biogenesis of oxidative phosphorylation complex I." *Cell Metab* **12**(3): 283-294.
- Perry, R. J. and J. R. Hodges (1999). "Attention and executive deficits in Alzheimer's disease. A critical review." *Brain* **122 ( Pt 3)**: 383-404.
- Przedborski, S., M. Vila and V. Jackson-Lewis (2003). "Neurodegeneration: what is it and where are we?" *J Clin Invest* **111**(1): 3-10.
- Reddy, J. K. and T. Hashimoto (2001). "Peroxisomal beta-oxidation and peroxisome proliferator-activated receptor alpha: an adaptive metabolic system." *Annu Rev Nutr* **21**: 193-230.
- Reddy, P. H. and M. F. Beal (2008). "Amyloid beta, mitochondrial dysfunction and synaptic damage: implications for cognitive decline in aging and Alzheimer's disease." *Trends Mol Med* **14**(2): 45-53.
- Ricquier, D. and F. Bouillaud (2000). "The uncoupling protein homologues: UCP1, UCP2, UCP3, StUCP and AtUCP." *Biochem J* **345 Pt 2**: 161-179.
- Scaglia, F. (2010). "The role of mitochondrial dysfunction in psychiatric disease." *Dev Disabil Res Rev* **16**(2): 136-143.
- Schapira, A. H. (2012). "Mitochondrial diseases." *Lancet* **379**(9828): 1825-1834.
- Schonfeld, P. and G. Reiser (2013). "Why does brain metabolism not favor burning of fatty acids to provide energy? Reflections on disadvantages of the use of free fatty acids as fuel for brain." *J Cereb Blood Flow Metab* **33**(10): 1493-1499.
- Schrader, M. and Y. Yoon (2007). "Mitochondria and peroxisomes: are the 'big brother' and the 'little sister' closer than assumed?" *Bioessays* **29**(11): 1105-1114.
- Smeitink, J., L. van den Heuvel and S. DiMauro (2001). "The genetics and pathology of oxidative phosphorylation." *Nat Rev Genet* **2**(5): 342-352.
- Speijer, D. (2011). "Oxygen radicals shaping evolution: why fatty acid catabolism leads to peroxisomes while neurons do without it: FADH(2)/NADH flux ratios determining mitochondrial radical formation were crucial for the eukaryotic invention of peroxisomes and catabolic tissue differentiation." *Bioessays* **33**(2): 88-94.

- Speijer, D. (2014). "Reconsidering ideas regarding the evolution of peroxisomes: the case for a mitochondrial connection." *Cell Mol Life Sci* **71**(13): 2377-2378.
- Szklarczyk, R. and M. A. Huynen (2010). "Mosaic origin of the mitochondrial proteome." *Proteomics* **10**(22): 4012-4024.
- Szklarczyk, R., M. Nootboom and H. D. Osiewicz (2014). "Control of mitochondrial integrity in ageing and disease." *Philos Trans R Soc Lond B Biol Sci* **369**(1646): 20130439.
- Tabak, H. F., I. Braakman and A. van der Zand (2013). "Peroxisome formation and maintenance are dependent on the endoplasmic reticulum." *Annu Rev Biochem* **82**: 723-744.
- Tabak, H. F., D. Hoepfner, A. Zand, H. J. Geuze, I. Braakman and M. A. Huynen (2006). "Formation of peroxisomes: present and past." *Biochim Biophys Acta* **1763**(12): 1647-1654.
- Tabak, H. F., A. van der Zand and I. Braakman (2008). "Peroxisomes: minted by the ER." *Curr Opin Cell Biol* **20**(4): 393-400.
- Tansey, M. G. and M. S. Goldberg (2010). "Neuroinflammation in Parkinson's disease: its role in neuronal death and implications for therapeutic intervention." *Neurobiol Dis* **37**(3): 510-518.
- Taylor, E. B. and J. Rutter (2011). "Mitochondrial quality control by the ubiquitin-proteasome system." *Biochem Soc Trans* **39**(5): 1509-1513.
- Thrash, J. C., A. Boyd, M. J. Huggett, J. Grote, P. Carini, R. J. Yoder, B. Robbertse, J. W. Spatafora, M. S. Rappe and S. J. Giovannoni (2011). "Phylogenomic evidence for a common ancestor of mitochondria and the SAR11 clade." *Sci Rep* **1**: 13.
- Tucker, E. J., A. G. Compton and D. R. Thorburn (2010). "Recent advances in the genetics of mitochondrial encephalopathies." *Curr Neurol Neurosci Rep* **10**(4): 277-285.
- Turrens, J. F. (2003). "Mitochondrial formation of reactive oxygen species." *J Physiol* **552**(Pt 2): 335-344.
- Vos, M., G. Esposito, J. N. Edirisinghe, S. Vilain, D. M. Haddad, J. R. Slabbaert, S. Van Meensel, O. Schaap, B. De Strooper, R. Meganathan, V. A. Morais and P. Verstreken (2012). "Vitamin K2 is a mitochondrial electron carrier that rescues pink1 deficiency." *Science* **336**(6086): 1306-1310.
- Wang, C. and R. J. Youle (2009). "The role of mitochondria in apoptosis\*." *Annu Rev Genet* **43**: 95-118.
- Watmough, N. J. and F. E. Frerman (2010). "The electron transfer flavoprotein: ubiquinone oxidoreductases." *Biochim Biophys Acta* **1797**(12): 1910-1916.
- Winge, D. R. (2012). "Sealing the mitochondrial respirasome." *Mol Cell Biol* **32**(14): 2647-2652.
- Yang, D., Y. Oyaizu, H. Oyaizu, G. J. Olsen and C. R. Woese (1985). "Mitochondrial origins." *Proc Natl Acad Sci U S A* **82**(13): 4443-4447.
- Yang, S. Y., X. Y. He and H. Schulz (1987). "Fatty acid oxidation in rat brain is limited by the low activity of 3-ketoacyl-coenzyme A thiolase." *J Biol Chem* **262**(27): 13027-13032.
- Yutin, N., K. S. Makarova, S. L. Mekhedov, Y. I. Wolf and E. V. Koonin (2008). "The deep archaeal roots of eukaryotes." *Mol Biol Evol* **25**(8): 1619-1630.







# CHAPTER

## **Evaluation of the therapeutic potential of the antioxidant Trolox in a mouse model with an isolated mitochondrial CI deficiency**

Manjeri G.R., Breuer, M.E., Blanchet L., Verrijp K.,  
Rodenburg R.J., Smeitink J.A., Koopman W.J.H., Willems P.H.

# 7

## Abstract

Complex I (CI) dysfunction leads to a myriad of cell biological aberrations thought to be due to excess ROS levels. Here, we investigate the potential of the water soluble Vitamin E analog, Trolox, as an antioxidant strategy to alleviate the pathophysiological abnormalities observed in an *Ndufs4*<sup>-/-</sup> mouse model of human CI deficiency. *Ndufs4*<sup>-/-</sup> mice showed a progressive decline in rope grip performance, which was delayed ( $p < 0.05$ ) at week 6 of life following twice-daily intraperitoneal injections of 400 mg/kg body weight starting at week 3 of life. Mice were sacrificed at week 6 and biochemical characterization of a mitochondria-enriched preparation from hind limb skeletal muscle revealed no trend toward normalization of the maximal rate of CI-linked ATP production in Trolox-treated *Ndufs4*<sup>-/-</sup> mice. Similarly, measurements of the maximal activities of the individual respiratory chain complexes failed to show any change as compared to vehicle-treated *Ndufs4*<sup>-/-</sup> mice. The area of the granular layer of the cerebral cortex occupied by GFAP positive cells did not differ between vehicle-treated *Ndufs4*<sup>-/-</sup> and wildtype (WT) mice and was not influenced by Trolox-treatment. The same observation was reached for the number of Purkinje cells in the cerebellum. Regarding the retina, layer thickness tended to be decreased for RGC ( $p = 0.06$ ), IPL ( $p = 0.06$ ) and INL ( $p = 0.06$ ) in vehicle-treated *Ndufs4*<sup>-/-</sup> mice. The same layers showed no tendency for decreased thickness between Trolox-treated *Ndufs4*<sup>-/-</sup> and WT mice. Trolox-treated *Ndufs4*<sup>-/-</sup> showed a significant increase in EPL thickness as compared to Trolox-treated WT mice. GFAP staining was increased in RGC+IPL of *Ndufs4*<sup>-/-</sup> mice and remained increased following Trolox treatment. Finally, Trolox-treatment fully restored the decrease in the number of NeuN positive cells observed in the RGC of vehicle-treated *Ndufs4*<sup>-/-</sup> mice. Taking into account the rapidly progressive, lethal phenotype of the *Ndufs4*<sup>-/-</sup> mice, the present finding that Trolox has some beneficial effect on neuro-motor function and retinal integrity might warrant translation to the human situation.

## Introduction

The mitochondrial oxidative phosphorylation (OXPHOS) system is the final biochemical pathway engaged in the generation of ATP and is estimated to generate 90% of cellular ATP (Smeitink, van den Heuvel et al. 2001, Rich 2003). The OXPHOS system is embedded in the lipid bilayer of the mitochondrial inner membrane (MIM) and is made up of five multi-subunit enzyme complexes and two mobile electron carriers *i.e.* ubiquinone (Q) and cytochrome c (cyt c). Electrons liberated from NADH at complex I (CI) or FADH<sub>2</sub> at complex II (CII) flow downhill via coenzyme Q, complex II (CII), cyt c and complex IV (CIV) to oxygen releasing free energy that is used by CI, CIII and CIV to pump protons across the MIM to the intermembrane space. Due to this translocation of protons an electrochemical proton gradient arises, referred to as proton motive force (PMF), that is used by complex V (CV) to drive the condensation of ADP and P<sub>i</sub> into ATP (Smeitink, van den Heuvel et al. 2001).

Inherent to the above process of oxidative phosphorylation (OXPHOS), mitochondria produce significant amounts of incompletely reduced derivatives of molecular oxygen (O<sub>2</sub>) (Brown and Borutaite 2012). These reactive oxygen species (ROS) include superoxide (O<sub>2</sub><sup>•-</sup>), hydrogen peroxide (H<sub>2</sub>O<sub>2</sub>) and the hydroxyl radical (•OH). About, 0.1 to 0.5% of the oxygen consumed by the mitochondria is converted to O<sub>2</sub><sup>•-</sup> (Murphy 2012). This occurs mainly at CI and CIII (Murphy 2009). Under normal conditions, O<sub>2</sub><sup>•-</sup> is detoxified by superoxide dismutases (SODs) resulting in the production of H<sub>2</sub>O<sub>2</sub>. H<sub>2</sub>O<sub>2</sub> is subsequently removed by catalases, glutathione peroxidases and peroxiredoxins (Koopman, Nijtmans et al. 2010). Physiological ROS levels play an important role in various signaling pathways (Finkel 2011, Gough and Cotter 2011). Excess ROS levels as observed in certain OXPHOS diseases lead to cellular dysfunction and, eventually, cell death (Balaban, Nemoto et al. 2005).

Tissues of high energy demand such as skeletal muscle, heart and brain are at increased risk of ROS-induced damage during mitochondrial dysfunction (Quintana, Kruse et al. 2010, Chouchani, Methner et al. 2014, Shi, Ivannikov et al. 2014). Brain is a unique organ; although it represents 2% of total body mass, it consumes 20% of the total oxygen and 25% of the total glucose consumed by the human body (Belanger, Allaman et al. 2011). The brain is especially susceptible to oxidative damage as observed in several neuropathological conditions including Parkinson's disease, Alzheimer's disease, Huntington's disease and amyotrophic lateral sclerosis (ALS) (Wilson 1997, Dringen 2000). There are several factors that contribute to the heightened susceptibility of the brain to oxidative damage. These include a high rate of oxidative energy metabolism, a high content of unsaturated fatty acids that are prone to lipid peroxidation and a low intrinsic antioxidant capacity (Dringen 2000). Any impediment

in electron transfer through the mitochondrial respiratory chain will significantly increase superoxide  $O_2^{\bullet-}$  generation by all single electron donor sites of dysfunctional mitochondria, provided that there is sufficient supply of oxygen (Kudin, Bimpong-Buta et al. 2004, Malinska, Kulawiak et al. 2010, Napankangas, Liimatta et al. 2012).

Analysis of the cell biological consequences of CI dysfunction in primary neuronal cells derived from the *Ndufs4*<sup>fky/fky</sup> mouse, generated by insertion of a transposable element into the *Ndufs4* gene, suggest an impairment in ATP generation without any changes in mitochondrial membrane potential (Bird, Wijeyeratne et al. 2014). Analysis of the maximal rate of CI-linked ATP production in a mitochondrial preparation from several tissues of the *Ndufs4*<sup>-/-</sup> mouse, generated by deletion of exon 2 of the *Ndufs4* gene, showed no difference compared to wildtype for skeletal muscle and heart (Alam, Manjeri et al. 2015) but a significant decrease for brain (Manjeri, Rodenburg et al. 2016) (Chapter 2 of this thesis). Recently, a key consequence of neuronal mitochondrial dysfunction, namely the accumulation of lipid droplets (LD) in glial cells, was uncovered in pre-symptomatic *Ndufs4*<sup>-/-</sup> mouse (Liu, Zhang et al. 2015). This phenomenon was shown to occur prior to the development of neurodegenerative lesions (Quintana, Kruse et al. 2010, Quintana, Zanella et al. 2012). Evidence suggested that increased ROS levels caused activation of c-Jun-N-terminal Kinase (JNK) and Sterol Regulatory Element Binding Protein (SREBP) in CI-deficient neurons, resulting in increased lipid synthesis in neurons and LD accumulation in glial cells and subsequent neurodegeneration by elevated levels of lipid peroxidation. The onset of neurodegeneration could be delayed by N-acetyl cysteine amide (AD4), a blood-brain-barrier penetrating antioxidant, following intraperitoneal injection of 150 mg/kg of body weight prior to the onset of the symptomatic phase between PD21 to PD28 (Liu, Zhang et al. 2015). They proposed that LD accumulation could be potentially used as a biomarker in neurodegeneration. The author's reported a similar mechanism in several drosophila models of CI dysfunction and concluded that ROS-induced formation of LD during neuronal mitochondrial dysfunction is an evolutionarily conserved process. Mitochondrial dysfunction leads to optic dystrophies as observed in children with CI dysfunction. Kruse and co-workers reported that KO mice go blind around PD32 (Kruse, Watt et al. 2008). Yu and co-workers, recently investigated the functional, neuroanatomical and transcriptional consequences of blindness in the *Ndufs4*<sup>-/-</sup> mice (Yu, Song et al. 2015). Recently, it was demonstrated that *Ndufs4*<sup>-/-</sup> mice subjected to chronic hypoxia showed a marked improvement in survival, body weight, body temperature, behavior and neuropathology (Jain, Zazzeron et al. 2016). Here, the authors hypothesized that lowering oxygen demand might limit ROS production during impaired electron

transport. *Ndufs4*<sup>-/-</sup> mice become lethargic around PD30 and severely ataxic around PD35 (de Haas, Russel et al. 2016) when they exhibit splayed legs, are unresponsive to firm nudge, right themselves slowly and occasionally lose balance and fall over. Between PD35 to PD50, they ceased grooming and died (Kruse, Watt et al. 2008). Similar observations have been reported in children with CI deficiency (Fassone and Rahman 2012).

Our previous work has shown that the water-soluble vitamin E analog Trolox can counterbalance many of the aberrations observed in primary fibroblasts from patients with isolated CI deficiency including increased cellular ROS levels, a less negative mitochondrial membrane potential, hampered Ca<sup>2+</sup>-stimulated mitochondrial ATP production (Koopman, Verkaart et al. 2006, Koopman, Verkaart et al. 2008, Distelmaier, Visch et al. 2009, Distelmaier, Valsecchi et al. 2012, Blanchet, Smeitink et al. 2015, Willems, Rossignol et al. 2015). This chapter investigates the effects of chronic Trolox treatment of *Ndufs4*<sup>-/-</sup> mice on behavioral paradigms associated with muscle function and motor coordination. The rationale of this approach is that brain areas associated with neuro-motor function are increasingly affected during mitochondrial dysfunction (Carter, Lione et al. 1999, Karl, Pabst et al. 2003, Kruse, Watt et al. 2008, Quintana, Kruse et al. 2010, Breuer, Willems et al. 2012). In addition, this chapter examines the effect of chronic Trolox treatment of *Ndufs4*<sup>-/-</sup> mice on the biochemical characteristics of the OXPHOS system in a mitochondria-enriched preparation from hind limb skeletal muscle. Finally, this chapter investigates the effect of chronic Trolox treatment on the brain neuro-inflammatory phenotype of *Ndufs4*<sup>-/-</sup> mice.

## Materials and Methods

### Injections and behavioral tests

**Injections** – All experiments were approved by the Regional Animal Ethics Committee (Nijmegen, The Netherlands) and performed under the guidelines of the Dutch Council for Animal Care. All efforts were made to reduce animal suffering and number of animals used in this study. Wild type (WT) and *Ndufs4*<sup>-/-</sup> mice were fed on a standard animal diet (V1534-300 R/M-H, Ssniff GmbH, Soest, Germany) and water available *ad libitum* in standard vivarium conditions with 12 h light dark cycle. Animals were housed in groups at 22° C and only males were used in the experiment. Intraperitoneal injections (2 ml/kg per injection) were performed twice a day the first one between 8:00-9:00 h and the second one between 14:00-15:00 h. Injections began during week 3 of life and continued until sacrifice in week 6. Two behavioral tests, the rope grip (day 1) and the rotarod test (day 2), were carried out at

30 minutes after the morning injection at 3, 5 and 6 weeks of life. After testing, the animals were returned to the colony room. The study included 5 WT and 4 *Ndufs4*<sup>-/-</sup> mice treated with vehicle (1 M NaHCO<sub>3</sub>, S3817 Sigma-Aldrich, The Netherlands, freshly prepared weekly and kept at 4° C) and 6 WT and 5 *Ndufs4*<sup>-/-</sup> mice treated with Trolox (238813-5G Sigma-Aldrich, 400 mg/kg body weight dissolved in 1 M NaHCO<sub>3</sub>). Trolox was dissolved by warming the solution at 37°C and gentle vortexing.

**Rope grip** – Animals were allowed to grasp the middle of a rope (100 cm) suspended above the floor (30 cm) with their fore paws only. Healthy animals will grip the rope with all 4 limbs and successfully crawl to the end. Animals with muscular dysfunction will be unable to do so and fall to the padded apparatus floor. The test was automatically concluded when the animal fell from the rope. The test was repeated three times with a resting interval of 3 min and the average number of successful escapes and the average time on the rope were quantified.

**Rotarod** – The rotarod test consisted of a 3 min training period during which the animals were exposed to the rotating rod set at 10 rotations per minute (RPM). Next, the animals were tested three times on the accelerating rod, with a 3 min resting period in between two consecutive trials. A trial was ended when the animal fell from the rod or when the maximum RPM was reached at 5 min. The average time on the rod was quantified.

### Biochemical analyses

**Tissue harvest** – Immediately after sacrifice by cervical dislocation, entire skeletal muscle from both hind limbs was removed, put in ice-cold SETH buffer (0.25 M sucrose, 2 mM EDTA, 10 mM Tris, 5x10<sup>4</sup> U heparin/L, pH 7.4), minced with a Sorvall TC2 tissue chopper and homogenized with a glass/Teflon Potter Elvehjem homogenizer. The homogenate was centrifuged at 600g and a portion of the supernatant, referred to as mitochondria-enriched fraction, was used for measurement of the maximal rates of pyruvate oxidation and ATP production. The remainder was frozen in 10 µl aliquots in liquid nitrogen and kept at -80° C for measurement of the maximal activity of the individual OXPHOS complexes. Protein concentration was determined by the Lowry method as described before (Janssen, Trijbels et al. 2006).

**Maximal rates of pyruvate oxidation and ATP production** – To determine the maximal pyruvate oxidation rate, a freshly prepared 600g supernatant was incubated with radiolabeled substrate ([1-<sup>14</sup>C] pyruvate). After 20 min, the reaction was stopped and the amount of liberated <sup>14</sup>CO<sub>2</sub> was quantified (Janssen, Trijbels et al. 2006). The



assay medium (pH 7.4) contained  $K^+$ -phosphate buffer (30 mM; source of Pi), KCl (75 mM), Tris (8 mM), K-EDTA (1.6 mM), P<sub>1</sub>P<sub>5</sub>-Di (adenosine-5') pentaphosphate (AP<sub>5</sub>A; 0.2 mM), MgCl<sub>2</sub> (0.5 mM), ADP (2 mM), creatine (20 mM), malate (1 mM) and [1-<sup>14</sup>C] pyruvate (1 mM). AP<sub>5</sub>A is a potent adenylate kinase (AK) inhibitor required to prevent interference of the AK reaction with the ATP produced and excess of ADP required for this assay. The rate of ATP-linked pyruvate oxidation was obtained after subtraction of <sup>14</sup>CO<sub>2</sub> liberated in the absence of ADP. For measurement of the maximal ATP production rate, the same assay medium was used but with pyruvate instead of [1-<sup>14</sup>C] pyruvate. After 20 min, the reaction was stopped by addition of 0.1 M HClO<sub>4</sub>. The reaction mixture was centrifuged at 14000g for 2 min at 2° C. To the supernatant, 1.2 vol (V/V) of 0.333 M KHCO<sub>3</sub> was added and this mixture was diluted 2-fold. The amount of ATP and phosphocreatine formed were measured using a Konelab 20XT auto-analyzer (Thermo Scientific). Mitochondrial ATP production rate was corrected using a parallel assay in which residual glycolysis was blocked by arsenite (2 mM) (Janssen, Trijbels et al. 2006).

**Maximal activity of individual OXPHOS complexes** – The liquid nitrogen frozen portion of the 600g supernatant was thawed and used for measurement of the V<sub>max</sub> of the complexes I (CI), II (CII), III (CIII) and IV (CIV) and citrate synthase (CS), as described previously (Rodenburg 2011).

### (Immuno)histological procedures

**Tissue harvest** – Immediately after sacrifice by cervical dislocation, brains and eyes were removed, fixed in 4% buffered formalin and embedded in paraffin according to standard histological procedures. Tissue sections of 4 μm thickness were made for histological analyses. Brain and retinal sections were stained with Hematoxylin and Eosin (H&E).

**GFAP Staining** – Tissue sections were preincubated for 10 min with 20% FCS (Vector, Burlingame, CA) in PBS. Next, sections were incubated overnight at 4° C with rabbit polyclonal anti-cow Glial Fibrillary Acidic Protein (DAKO), diluted with 1% BSA in PBS. Detection was carried out with the avidin-biotin-peroxidase complex technique using aminoethylcarbazole (AEC) as a substrate (Scytek, Utah, USA).

**NeuN Staining** – Tissue sections were preincubated for 10 min with 20% FCS (Vector labs) in PBS. Next, sections were incubated overnight at 4° C with mouse monoclonal anti-NeuN (clone A60, Millipore), diluted with 1% BSA in PBS. Detection was performed as described above.

## Quantitative analysis

**Brain GFAP staining** – Images (magnification x 40) were acquired on a Zeiss Axioskop II microscope and GFAP intensity was quantified in the granular layer of the cerebellar cortex using KS 400 V3.0 software (Carl Zeiss AG, Germany) with a custom-written macro as described before (Navis, Bourgonje et al. 2013). The values presented are the mean of 10 non-overlapping microscopic fields of view per animal.

**Purkinje cell quantification** – Images (magnification x 40) were acquired as described above and Purkinje cell number was quantified in the Purkinje cell layer bordering the granular layer in the cerebellar cortex using the above software and macro. The values presented are the mean of 10 non-overlapping microscopic fields of view per animal.

**Retinal thickness** – Images (magnification x 40) were acquired as described above and thickness of the indicated retinal layers was quantified using the above software and macro. The values presented are the mean of 3 unique non-overlapping microscopic fields of view per animal.

**Retinal GFAP staining** – GFAP intensity was quantified for the indicated retinal layers as described above. The values presented are the mean of 3 unique non-overlapping microscopic fields of view per animal.

**Retinal NeuN stains** – Images (magnification x 40) were acquired on a Zeiss Axioskop II microscope and NeuN positive cells were quantified in the RGC layer of the retina using AxioVision software (Carl Zeiss AG, Germany) with a custom-written macro. The data presented are the mean of 10 non-overlapping microscopic fields of view per animal.

## Statistical Analyses

Statistical analyses were performed using unpaired Student's t test and results expressed as mean  $\pm$  SD. Statistical significance is indicated by (\* $P$ <0.05, \*\* $P$ <0.01, \*\*\* $P$ <0.001).

## Results

**Effect of Trolox on rope grip and rotarod performance** – The *in vivo* therapeutic potential of Trolox was tested in mice with a systemic knockout of the NDUF54 subunit of complex I (*Ndufs4*<sup>-/-</sup> mice). Vehicle-treated *Ndufs4*<sup>-/-</sup> mice (KO Veh) of

3, 5 and 6 weeks of life showed a progressive decline in rope grip and rotarod performance (Figs. 1a and 1b), suggesting that muscle endurance and motor coordination decrease with age (Breuer, Willems et al. 2012). In both paradigms, vehicle-treated WT mice (WT Veh) behaved similarly at all ages tested. *Ndufs4*<sup>-/-</sup> mice treated with Trolox (KO Trolox) showed improved rope grip and rotarod performance, reaching statistical significance ( $p < 0.05$ ) and close to statistical significance ( $p = 0.07$ ), respectively, at week 6 of life. Trolox did not affect the rope grip and rotarod performance of WT mice (WT Trolox). The decrease in rotarod performance observed with WT Trolox at week 3 of life did not reach statistical significance.

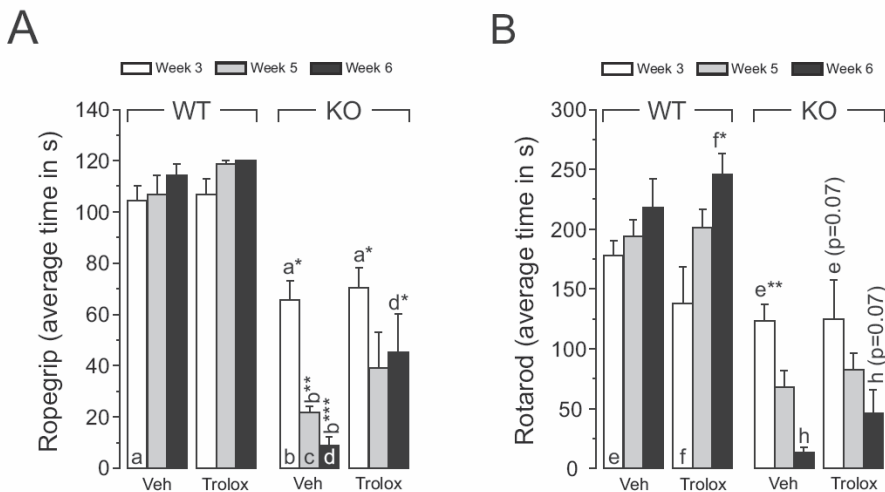


**Fig. 1. Behavioural analysis during chronic Trolox treatment.** Starting at week 3 of life, mice were intraperitoneally injected twice daily (at 8:00-9:00 am and 14:00-15:00 pm) with 400 mg / 2 ml / kg Trolox or 2 ml / kg vehicle (1 M NaHCO<sub>3</sub>). In total, 15 WT (14 in week 5 and 6; WT Veh) and 12 *Ndufs4*<sup>-/-</sup> (9 in week 5 and 6; KO Veh) mice were treated with vehicle and 6 WT (WT Trolox) and 10 *Ndufs4*<sup>-/-</sup> (7 in week 5 and 6; KO Trolox) mice with Trolox. **(A) Rope grip analysis:** KO Veh showed a progressive decrease in rope grip performance when tested at weeks 3, 5 and 6 of life. Trolox did not affect rope grip performance in WT mice as compared to corresponding WT Veh. KO Trolox still showed a progressive decrease in rope grip performance at weeks 3 and 5. However, the value of week 6 was not different from that of week 5 and significantly higher than that of corresponding KO Veh (indicated with d\*). **(b) Rotarod analysis:** KO Veh showed a progressive decrease in rotarod performance. Trolox did not affect rotarod performance in WT mice (WT Trolox) as compared to corresponding WT Veh. KO Trolox still showed a progressive decrease in rotarod performance at weeks 3 and 5. This decrease seemed to be slowed down at week 6. However, the value obtained was not significantly different from that of WT Trolox at week 6 ( $p = 0.07$ ). Statistical analysis was performed with the unpaired independent student's t-test.

**Effect of Trolox on the maximal rate of pyruvate oxidation in intact skeletal muscle mitochondria** – At 6 weeks of life, mice were sacrificed and hind limb muscle was removed, homogenized and centrifuged at 600 g. The mitochondria-enriched 600 g supernatant was used for further analysis. The maximal rate of pyruvate oxidation, measured in the presence of pyruvate, malate, ADP,  $\text{PO}_4^{3-}$  and creatine and corrected for the value obtained in the absence of ADP, was significantly ( $p < 0.05$ ) decreased in vehicle-treated *Ndufs4*<sup>-/-</sup> mice (Fig. 2a, open bars). In neither WT nor *Ndufs4*<sup>-/-</sup> mice, Trolox (closed bars) altered the maximal rate of pyruvate oxidation.

**Effect of Trolox on the maximal rate of ATP production in intact skeletal muscle mitochondria** – The maximal rate of ATP production, measured in the presence of pyruvate, malate, ADP,  $\text{PO}_4^{3-}$  and creatine, was significantly ( $p < 0.05$ ) decreased in vehicle-treated *Ndufs4*<sup>-/-</sup> mice (Fig. 2b, open bars). Trolox treatment (closed bars) did not significantly alter the maximal rate of ATP production in neither WT ( $p = 0.052$ ) nor *Ndufs4*<sup>-/-</sup> mice.

**Effect of Trolox on the maximal activity of CI in broken skeletal muscle mitochondria** – The maximal activity of the individual OXPHOS complexes was measured after freeze-thawing the 600 g supernatant to disrupt the mitochondrial membranes. This procedure allows the use of complex-specific substrates. The data obtained show that CI activity was virtually absent in vehicle-treated *Ndufs4*<sup>-/-</sup> mice (Fig. 2c, open bars) and that Trolox treatment (closed bars) had no effect on CI activity in WT mice. However, Trolox tended ( $p = 0.054$ ) to increase the maximal activity of this complex in *Ndufs4*<sup>-/-</sup> mice.

**Effect of Trolox on the maximal activity of CII, CIII and CIV in broken skeletal muscle mitochondria** – The maximal activity of the complexes II (Fig. 2d, open bars), III (Fig. 2e, open bars) and IV (Fig. 2f, open bars) was not significantly altered in vehicle-treated *Ndufs4*<sup>-/-</sup> mice and none of these activities was changed upon Trolox treatment (closed bars) in neither WT nor *Ndufs4*<sup>-/-</sup> mice.

**Effect of Trolox on maximal citrate synthase activity in skeletal muscle mitochondria** – Citrate synthase (CS) is widely used as an index for mitochondrial mass (Rodenburg 2011). Vehicle-treated *Ndufs4*<sup>-/-</sup> mice did not show any change in CS activity (Fig. 2g, open bars) and neither did Trolox treatment (closed bars).

**Effect of Trolox on brain astrocyte activity** – The decreased performance of *Ndufs4*<sup>-/-</sup> mice in the rope grip and rotarod test point to a loss of motor control. The cerebellum is the section of the brain that is essential for motor coordination and balance. Nerve injury leads to astrocyte activation and the expression of Glial

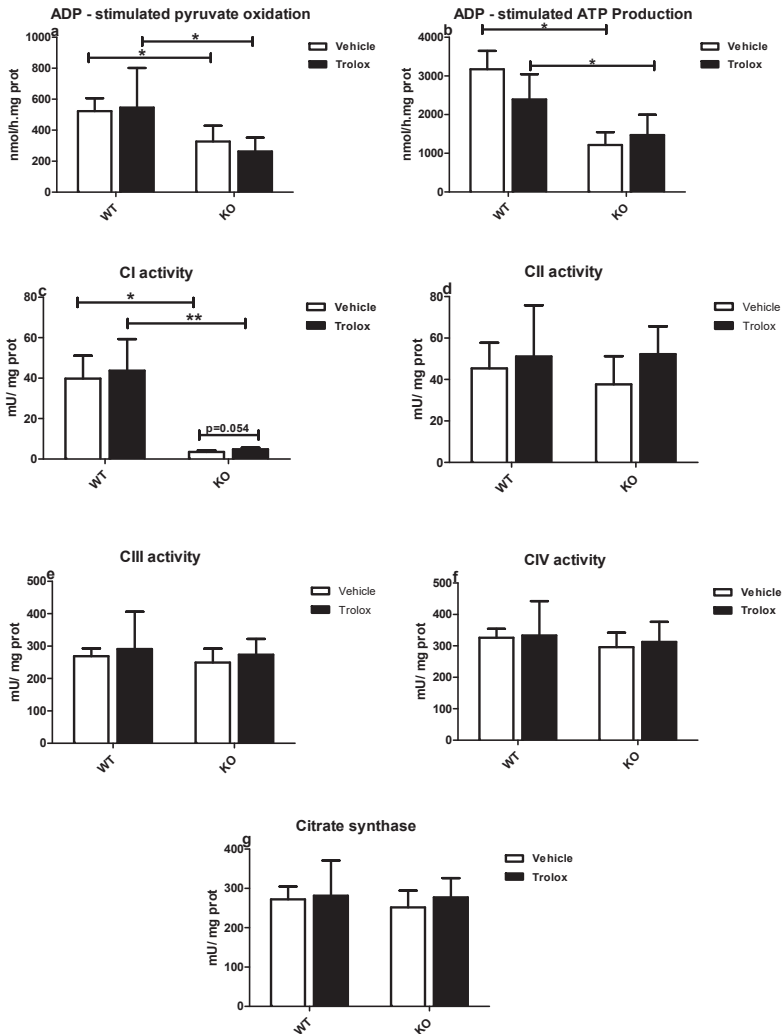


**Fig. 2. Biochemical characterization of the effect of chronic Trolox treatment on the mitochondrial energy generating system of skeletal muscle.** Vehicle-treated WT (n=5) and *Ndufs4*<sup>-/-</sup> (n=4) mice and Trolox-treated WT (n=6) and *Ndufs4*<sup>-/-</sup> (n=5) mice used in the behavioural experiments described in figure 1 were sacrificed between days 42 and 45 of life and a mitochondria-enriched 600g supernatant of a homogenate of hind limb muscle was prepared. Protein concentration was determined by the Lowry method as described before (Janssen, Trijebels et al. 2006). All values presented are expressed per mg of protein. **(a)** Pyruvate oxidation was measured in the presence of excess pyruvate, malate, PO<sub>4</sub><sup>3-</sup> and creatine and in the absence or presence of ADP. **(b)** ATP production was measured in the presence of excess pyruvate, malate, ADP, PO<sub>4</sub><sup>3-</sup> and creatine. **(c-g)** The maximal activity of individual RC complexes and citrate synthase was determined in the presence of an excess of complex-specific substrate after freeze-thawing of the 600 g supernatant. Statistical analysis was performed with the unpaired independent student's t-test. \*P<0.05, \*\*P<0.01.

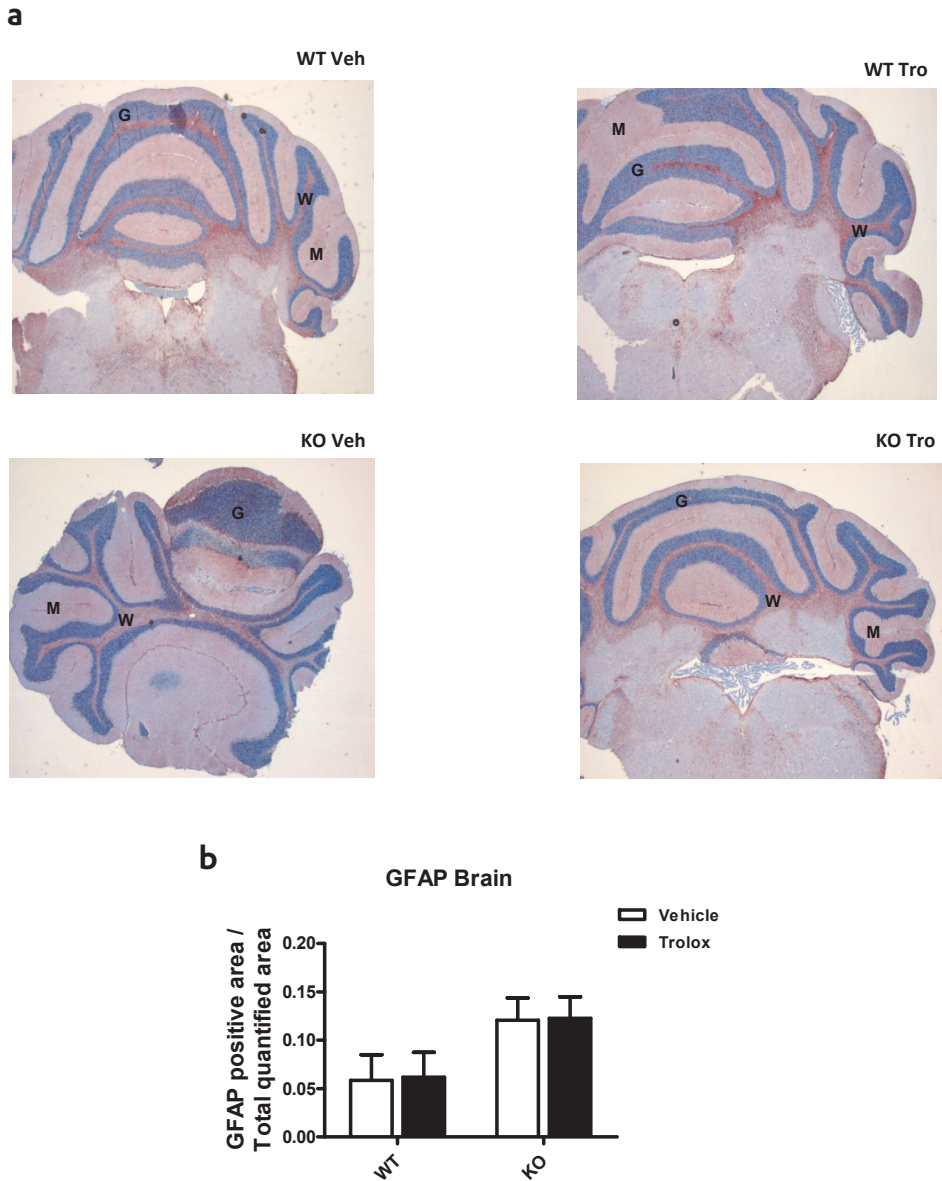


**Fig. 3. Immunohistochemical evaluation of the effect of chronic Trolox treatment on brain astrocyte activity.** Brains of the Trolox- and vehicle-treated mice used in the behavioural experiments described in figure 1 and sacrificed between days 42 and 45 of life as indicated in the legend to figure 2, were used for immunohistochemical evaluation of Glial Fibrillary Acidic Protein (GFAP) expression. **(a)** Sections of vehicle- and Trolox-treated WT and *Ndufs4*<sup>-/-</sup> mice showing GFAP positive cells in the granular layer (G) of the cerebellar cortex. **(b)** Area occupied by GFAP positive cells normalized to the total area of the granular layer analyzed. G, granular layer. W, white matter. M, molecular layer.

Fibrillary Acidic Protein (GFAP) is widely regarded as a sensitive and reliable for marker for reactive astrocytes (Sofroniew and Vinters 2010). Immunostaining showed the presence of GFAP positive cells in the granular layer (G) of the cerebellar cortex (Fig. 3a). However, the area of the granular layer occupied by GFAP positive cells was not significantly altered in vehicle-treated *Ndufs4*<sup>-/-</sup> mice (Fig. 3b, open bars). Trolox treatment did not have any effect on the level of GFAP staining (closed bars).

**Effect of Trolox on Purkinje cell number** – In patients with neurodegenerative diseases, a loss of motor control has been correlated with a decrease in Purkinje cell numbers in the cerebellum (Mounsey and Teismann 2010). This urged us to quantify the number of Purkinje cells in the ganglionic layer of the cerebellar cortex. However, no differences were observed between the four experimental conditions (Fig. 4).

**Effect of Trolox on retinal thickness** – Neonatal *Ndufs4*<sup>-/-</sup> mice were demonstrated to be blind (Kruse, Watt et al. 2008). Mouse eyes injected with rotenone showed a significant thinning of the retinal ganglion cell layer (Zhang, Jones et al. 2002). The retina consists of several layers (depicted in Fig. 5a). Layer thickness tended to be decreased for RGC (Fig. 5b;  $p=0.06$ ), IPL (Fig. 5c;  $p=0.06$ ) and INL (Fig. 5d;  $p=0.06$ ) in vehicle-treated *Ndufs4*<sup>-/-</sup> mice as compared to vehicle-treated WT mice (open bars). On the other hand, no change in layer thickness was observed for EPL (Fig. 5e, open bars) and ENL (Fig. 5f, open bars). The tendency for decreased thickness of RGC, IPL and INL was absent after chronic Trolox treatment

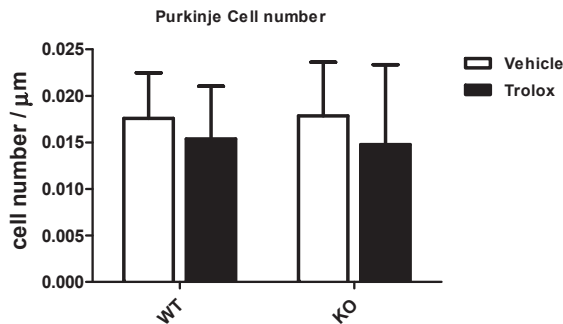


**Fig. 4. Quantification of the effect of chronic Trolox treatment on Purkinje cell density.** Brains of the Trolox- and vehicle-treated mice used in the behavioural experiments described in figure 1 and sacrificed between days 42 and 45 of life as indicated in the legend to figure 2, were used for evaluation of the Purkinje cell density in the Purkinje cell layer bordering the granular layer of the cerebellar cortex (see, Fig. 3a). The number of Purkinje cells is expressed per  $\mu\text{m}$  of Purkinje cell layer.

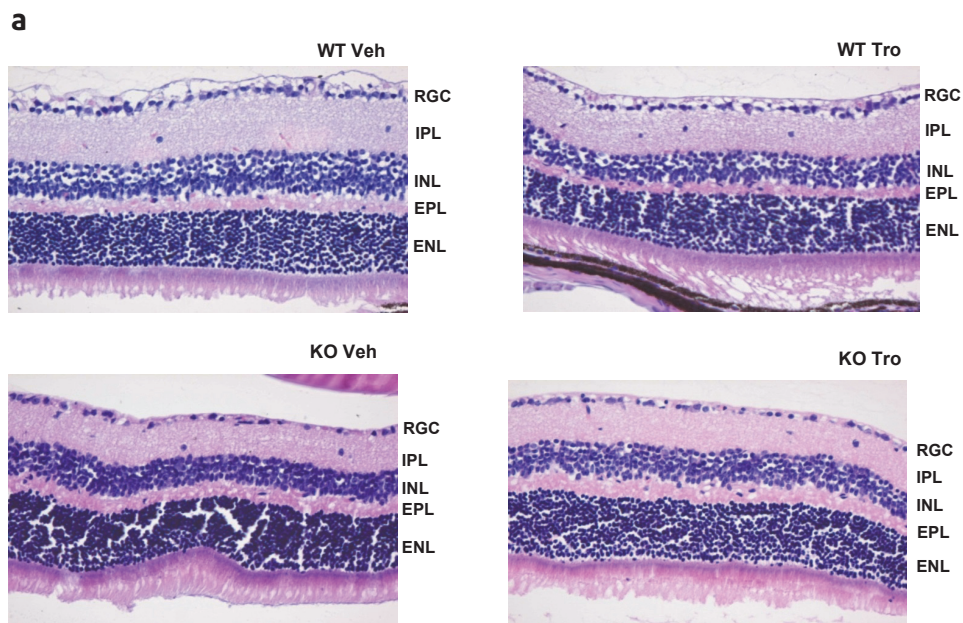
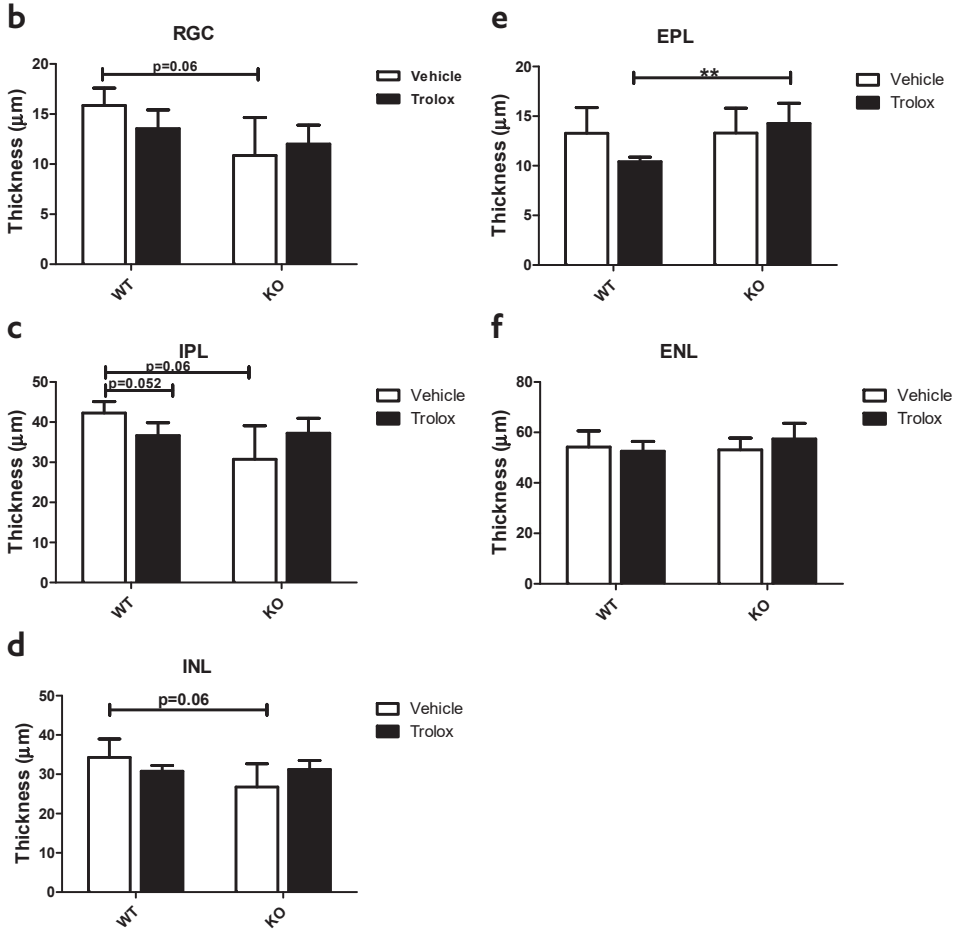


**Fig. 5. Histochemical analysis of the effect of Trolox on the thickness of individual retinal cell layers.** Eyes of the Trolox- and vehicle-treated mice used in the behavioural experiments described in figure 1 and sacrificed between days 42 and 45 of life as indicated in the legend to figure 2, were used for quantification of the thickness of the retinal layers after Hematoxylin and Eosin staining. **(a)** Representative images of the four experimental conditions showing the Retinal Ganglion Cell (RGC) layer, Internal Plexiform Layer (IPL), Internal Nuclear Layer (INL), External Plexiform Layer (EPL) and External Nuclear Layer (ENL). **(b-f)** Thickness of the indicated layer in  $\mu\text{m}$ . Statistical analysis was performed with the unpaired independent student's t-test.  $**P < 0.01$ .

(Figs. 5b-d, closed bars). This effect of Trolox appeared to be due to a decrease in WT mice rather than an increase in *Ndufs4*<sup>-/-</sup> mice (p values of 0.12, 0.052 and 0.082 versus 0.76, 0.17 and 0.35 for its effect on WT and *Ndufs4*<sup>-/-</sup> RGC, IPL and INL, respectively). A significant difference in layer thickness was observed for EPL after chronic Trolox treatment (Fig. 5e, closed bars;  $p = 0.002$ ). Again, this effect of Trolox was mostly contributed by a decrease in WT mice ( $p = 0.12$ ) rather than an increase in *Ndufs4*<sup>-/-</sup> mice ( $p = 0.61$ ). Trolox treatment did not significantly alter the thickness of ENL (Fig. 5f, closed bars).

**Effect of Trolox on retinal astrocyte and Müller glia cell activity** – Immunostaining revealed the presence of Glial Fibrillary Acidic Protein (GFAP)-positive cells and their processes in the retina (Fig. 6a). The area stained for GFAP was significantly increased





in RGC+IPL (Fig. 6b;  $p=0.015$ ) but not in INL (Fig. 6c), EPL (Fig. 6d) and ENL (Fig. 6e) of vehicle-treated *Ndufs4*<sup>-/-</sup> mice as compared to vehicle-treated WT mice (open bars). In neither WT nor *Ndufs4*<sup>-/-</sup> mice Trolox treatment had a significant effect on the area stained for GFAP in any of these layers.

### Effect of Trolox on the number of neuronal nuclei (NeuN) positive cells in the Retinal Ganglion Cell layer

Quantitative analysis of the thickness of the RGC revealed a tendency to decrease in *Ndufs4*<sup>-/-</sup> mice (fig. 5b, open bars;  $p=0.06$ ). Immunostaining for NeuN is widely used to quantify the number of neuronal cells (Mullen, Buck et al. 1992, Xu, Huang et al. 2014). Figure 7a shows the distribution of NeuN positive cells in the retina of vehicle- and Trolox-treated WT and *Ndufs4*<sup>-/-</sup> mice. Quantitative analysis showed that the number of NeuN positive cells was significantly

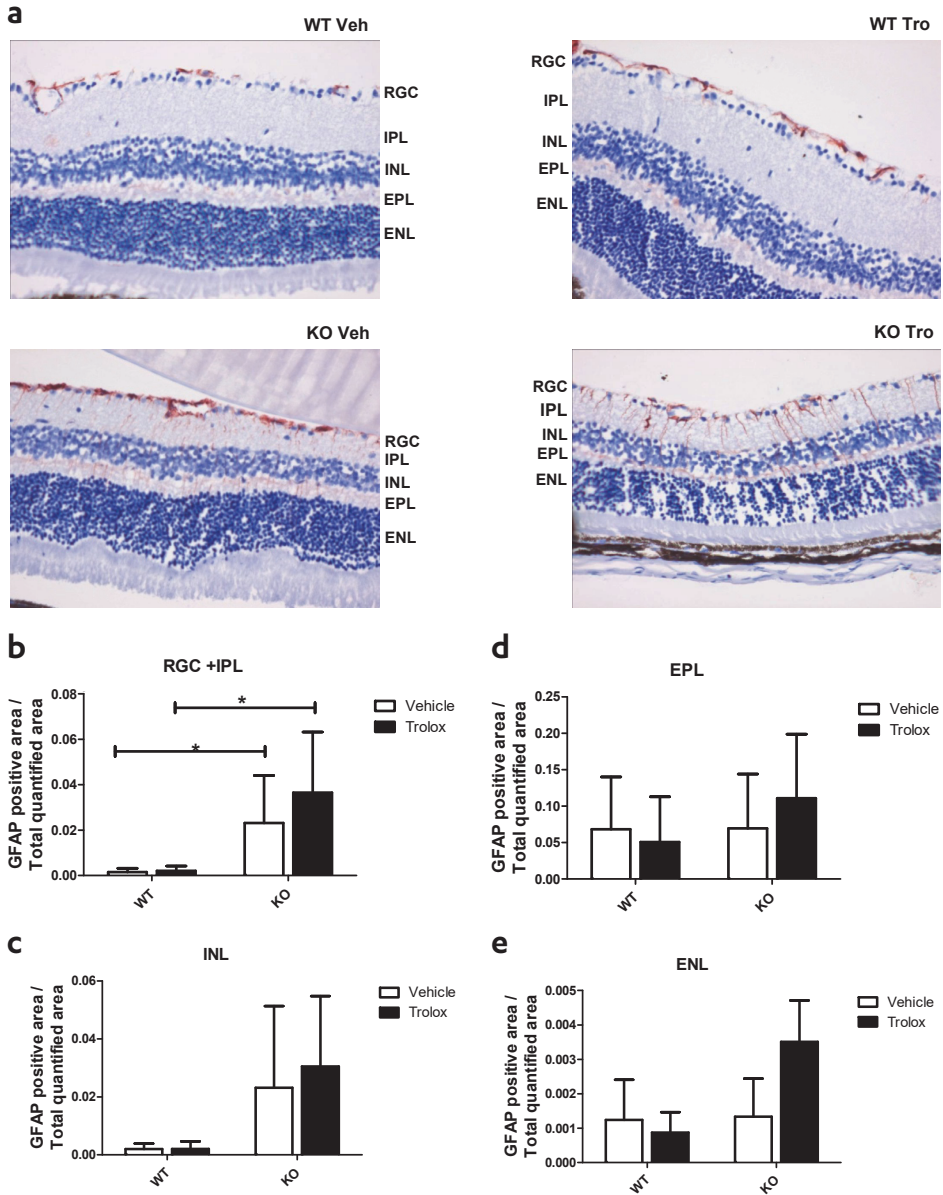


**Fig. 6. Immunohistochemical evaluation of the effect of Trolox on retinal astrocyte and Müller glia cell activity.** Eyes of the Trolox- and vehicle-treated mice used in the behavioural experiments described in figure 1 and sacrificed between days 42 and 45 of life as indicated in the legend to figure 2, were used for immunohistochemical evaluation of Glial Fibrillary Acidic Protein (GFAP) expression. **(a)** Representative images of the four experimental conditions showing GFAP staining in the various retinal layers. **(b-e)** Area stained with GFAP normalized to the total area of the respective layer. Abbreviations are given in the legend to figure 5. Statistical analysis was performed with the unpaired independent student's t-test. \* $P < 0.05$ .

decreased in the RGC of vehicle-treated *Ndufs4*<sup>-/-</sup> mice (Fig. 7b, open bars;  $p=0.049$ ). This decrease was not observed in Trolox-treated in *Ndufs4*<sup>-/-</sup> mice (closed bars). Trolox-treatment did not affect the number of NeuN positive cells in WT mice and significantly increased this number in *Ndufs4*<sup>-/-</sup> mice ( $p=0.036$ ).

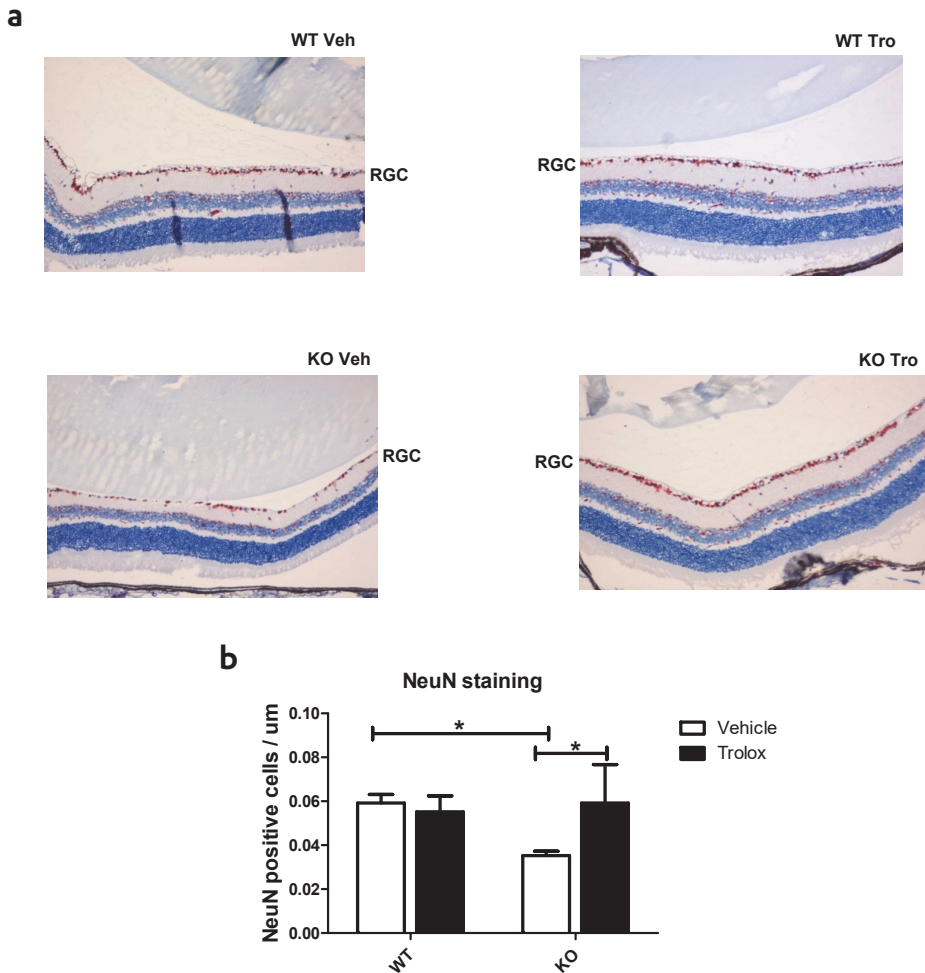


**Fig. 7. Immunohistochemical evaluation of the effect of Trolox on the number of neuronal cells in the Retinal Ganglion Cell layer.** Eyes of the Trolox- and vehicle-treated mice used in the behavioural experiments described in figure 1 and sacrificed between days 42 and 45 of life as indicated in the legend to figure 2, were used for immunohistochemical evaluation of NeuN expression. **(a)** Representative images of the four experimental conditions showing NeuN staining in the various retinal layers. **(b)** Number of NeuN positive cells in the RGC layer. Statistical analysis was performed with the unpaired independent student's t-test. \* $P<0.05$ .

## Discussion

The present study was designed to investigate a potential beneficial effect of Trolox in a mouse model of human isolated complex I deficiency. Trolox is a water-soluble derivative of vitamin E with potent reactive oxygen species (ROS) scavenger activity (Koopman, Nijtmans et al. 2010). Trolox readily permeates the cell membrane and when added to primary skin fibroblasts derived from patients with isolated complex I deficiency, which typically show elevated intracellular ROS levels (Verkaart, Koopman et al. 2007), it was demonstrated to dramatically reduce these levels in an acute fashion (Koopman, Verkaart et al. 2008). Extensive studies have shown that Trolox can (partly) normalize a vast number of aberrant cellular processes in these complex I deficient patient fibroblasts, including the less negative mitochondrial membrane potential, the reduced endoplasmic reticulum  $\text{Ca}^{2+}$  content, and the reduced hormone-stimulated increases in cytosolic and mitochondrial matrix  $\text{Ca}^{2+}$  concentration and mitochondrial ATP production (Willems, Valsecchi et al. 2008, Distelmaier, Visch et al. 2009). Patient-derived skin fibroblasts express a reduced amount of fully assembled, catalytically active complex I and the ability of Trolox to increase this amount was demonstrated (Koopman, Verkaart et al. 2008). Trolox can also reduce the degree of lipid peroxidation, induce a less oxidized mitochondrial thiol redox state and increase glutathione- and mitofusin-dependent mitochondrial filamentation (Distelmaier, Valsecchi et al. 2012). Most importantly, the latter study showed that Trolox evoked an increase in cellular oxygen consumption which indicates an increased performance of the mitochondrial oxidative phosphorylation system.

The systemic *Ndufs4*<sup>-/-</sup> mouse shows many of the characteristics of human isolated complex I deficiency (Kruse, Watt et al. 2008). Analysis of the progression of the clinical phenotype revealed a first lower body weight as compared to the lightest WT littermate at day 8 of life, a first smaller body length as compared to the shortest WT littermate at day 15 of life, a first sign of hair loss (alopecia) at day 19 of life, a first sign of (partially) closed eyes at day 25 of life, a first sign of hypoactivity at day 29 of life, a first sign of ataxia at day 34 of life, a first loss of body weight at day 35 of life and severe ataxia at day 38 of life. Here, it should be noted that mice engineered to lack *Ndufs4* selectively in neurons and glia display the same clinical phenotype, indicating a crucial role of the brain in the pathogenesis of isolated complex I deficiency (Quintana, Kruse et al. 2010).

**Skeletal muscle** - To investigate a potential beneficial effect of Trolox, male WT and *Ndufs4*<sup>-/-</sup> mice were injected intraperitoneally twice per day with Trolox (400 mg/2 ml/kg body weight) or vehicle (1 M  $\text{NaHCO}_3$ ; 2 ml/kg body weight) starting at week 3 of life. Rope grip and rotarod performance were tested at weeks 3, 5 and

6 of life to evaluate the effect of Trolox on muscle endurance and motor coordination (Breuer, Willems et al. 2012). A first important observation in the present study is that chronic Trolox treatment starting at week 3 of life slowed down the progressive decline in rope grip and rotarod performance in *Ndufs4<sup>-/-</sup>* mice. However, Trolox did not improve the decrease in the maximal rate of ATP production, measured in a mitochondria-enriched preparation from hind limb muscle of *Ndufs4<sup>-/-</sup>* mice at week 6 (between days 42 and 45) of life, shown to parallel the decline in rope grip and rotarod performance. In a previous study, we demonstrated that the maximal rate of mitochondrial ATP production was not yet decreased in *Ndufs4<sup>-/-</sup>* mice sacrificed between 31 and 34 days of life (Chapter 2). This effect was found to be accompanied by an increase in maximal activity of components of the mitochondrial ATP generating system, including the enzyme citrate synthase and the OXPHOS complexes II, III and IV. Although caution must be exerted when interpreting changes in OXPHOS protein expression (Tronstad, Nooteboom et al. 2014), the idea that OXPHOS dysfunction triggers an adaptive increase in mitochondrial mass is supported by the observation that at 30 days of life, *Ndufs4<sup>-/-</sup>* mice displayed increased mitochondrial numbers in the sub sarcolemma of the soleus, normal rates of phosphocreatine recovery in the ischemic hind limb reperfusion paradigm and unaltered total muscle ATP and phosphocreatine levels (Kruse, Watt et al. 2008). The present study shows that the maximal activity of the above-mentioned enzymes is no longer increased at days 42-45 of life. Together, these results suggest that initially a compensatory mechanism is able to maintain the maximal rate of mitochondrial ATP production but that after 31-34 days of life this mechanism starts to fail. Importantly, our previous work indicates that this putative compensatory mechanism is absent in brain.

The present finding that *in vivo* application of Trolox does not improve the maximal rate of mitochondrial ATP production in a mitochondria-enriched preparation from hind limb muscle of WT and *Ndufs4<sup>-/-</sup>* mice is at variance with previous results obtained with primary skin fibroblasts derived from healthy volunteers (Distelmaier, Valsecchi et al. 2012) and patients with isolated complex I deficiency (Koopman, Verkaart et al. 2008, Distelmaier, Visch et al. 2009). The latter studies show a wide range of beneficial effects of Trolox, including the upregulation of components of the OXPHOS system and a consequent increase in the rate of cellular oxygen consumption. Given the significant effect of Trolox on rope grip performance, we conclude that the protocol of *in vivo* application of Trolox was adequate but that the translation of experimental results from single cells to living animals is far from trivial.

**Cerebellum** - Impairment of motor coordination points to the cerebellum. Although GFAP positive cells were present in the granular layer (G) of the cerebellar cortex, their number was not significantly altered in *Ndufs4*<sup>-/-</sup> mice. Measurements in skin fibroblasts from complex I deficient patients invariably show increased rates of ROS production (Verkaart, Koopman et al. 2007, Koopman, Verkaart et al. 2008). Depending on the type of ROS, the levels reached and the cellular compartment in which these levels are reached, a wide range of cellular processes can be influenced either by favorable or unfavorable redox modifications (Koopman, Nijtmans et al. 2010). A first indication of the existence of redox modifications in the brain of *Ndufs4*<sup>-/-</sup> mice came from a study showing increased protein carbonylation in the olfactory bulb (OB) (Quintana, Kruse et al. 2010). It was suggested that the increase in carbonyl groups, which is a consequence of protein oxidation, was due to glial activation. Recent experiments, performed with *Drosophila* mitochondrial mutants, provide evidence that neurodegeneration is caused by a sequence of events starting with increased neuronal ROS levels and ROS-induced inhibition of c-Jun-N-terminal Kinase (JNK) phosphatase increasing the activity of the JNK/Sterol Regulatory Element Binding Protein (SREBP) to stimulate the acetyl-CoA carboxylase (ACC)-catalyzed synthesis of neuronal lipids synthesis and followed by glial lipid accumulation and, finally, enhanced glial lipid peroxidation (Liu, Zhang et al. 2015). The process of glial lipid droplet accumulation was inhibited by overexpression of human copper-zinc superoxide dismutase and administration of the antioxidant N-acetyl cysteine amide (AD4), stressing the prerequisite role of ROS. Lipid droplet accumulation was also reported in astroglia and microglia of *Ndufs4*<sup>-/-</sup> mice (Liu, Zhang et al. 2015). Maximal accumulation occurred at day 23 of life, when spongiform lesions (Quintana, Kruse et al. 2010, Quintana, Zanella et al. 2012) were not yet observed. Lipid droplet abundance was high in the OB and vestibular nuclei (VN) and mild in other brain sections, including the cerebellum. At day 35 of life, lipid droplet accumulation was dramatically decreased in VN, but not OB, whereas spongiform lesions were clearly visible in both brain sections. An increase in reactive astrocytes in the granular layer (G) of the cerebellum is widely regarded as an evident pathological sign in neurodegeneration. Indeed, evidence was provided that reactive glia causes initial activation of apoptotic pathways followed by a switch to necrosis (Quintana, Kruse et al. 2010). This switch is compatible with our finding that the maximal rate of mitochondrial ATP production is significantly decreased in a mitochondria-enriched fraction from whole brain of *Ndufs4*<sup>-/-</sup> mice sacrificed at days 31-34 of life (Manjeri, Rodenburg et al. 2016). This, in turn, is compatible with the observed aberrant morphology of neuronal mitochondria in these brain regions (Quintana, Kruse et al. 2010). Here we show, however, that

chronic Trolox treatment did not influence the number of reactive astrocytes in the granular layer (G) of the cerebellum. In agreement with the lack of effect of Trolox on glial activation, visual inspection revealed that Trolox treatment did not prevent the formation of spongiform lesions in *Ndufs4*<sup>-/-</sup> mice (data not shown). Similar to Trolox, N-acetyl cysteine amide, a blood-brain-barrier penetrating antioxidant, improved rotarod performance when injected intraperitoneally (Liu, Zhang et al. 2015). In this case, however, the antioxidant (150 mg/kg) was applied daily starting from day 21 of life until day 28 of life and a significant increase in rotarod performance was observed at day 30 of life followed by a progressive decline. The application of Trolox (400 mg/kg) also started in week 3 of life but was performed twice per day. The first rotarod test was performed at day 35 of life and only a slight tendency for improvement was observed. However, a stronger tendency for improvement was observed at week 6 of life ( $p=0.07$ ), whereas a significant effect was observed in the rope grip test. Together, these data indicate that antioxidant treatment can improve muscle endurance and motor coordination in a mouse model of human isolated complex I deficiency. Although the present study shows the presence of reactive astrocytes in the granular layer (G) of the cerebellum of WT mice, their number was neither increased in *Ndufs4*<sup>-/-</sup> mice nor reduced by Trolox treatment.

**Retina** - A second important observation in this study is that the density of NeuN positive cells was significantly decreased in the Retinal Ganglion Cell (RGC) layer of *Ndufs4*<sup>-/-</sup> mice and that chronic Trolox treatment fully normalized this density. The loss of NeuN positive cells was paralleled by an increase in GFAP staining in the RGC + Internal Plexiform Layer (IPL). Retinal ganglion cells relay information from the photoreceptor cells to the brain and their dysfunction has been implicated in Leber hereditary optic neuropathy (LHON), a maternally inherited mitochondrial disease characterized by severe visual loss (Guy, Feuer et al. 2014). Recent experiments with *Ndufs4*<sup>-/-</sup> mice revealed a significant decrease in retinal ganglion cell function at day 32 of life and a substantial loss of these cells at day 42 of life (Yu, Song et al. 2015). The same study reported a marked increase in retinal transcript levels of genes of the innate immune system and inflammatory response pathway between days 22 and 33 of life. The underlying mechanism was proposed to be a 'non-self' response to misfolded complex I. Alternatively, recent work provides evidence that the liver of systemic *Ndufs4*<sup>-/-</sup> mice oxidizes glucose rather than fatty acids resulting in increased circulatory levels of fatty acids and lactate and that these metabolites interact with toll-like receptors 2 and 4 on macrophages to further increase intracellular ROS levels finally resulting in a state of systemic inflammation (Jin, Wei et al. 2014). Another study

showed that inhibition of the mechanistic target of rapamycin (mTOR) pathway by rapamycin reduced neuroinflammation and prevented spongiform brain lesions, suggesting that this pathway is activated in systemic *Ndufs4*<sup>-/-</sup> mice (Johnson, Yanos et al. 2013). In this case, it was proposed that rapamycin induced a shift from glucose to amino acid oxidation thus reducing the accumulation of glycolytic intermediates. Finally, rapamycin was demonstrated to prevent the increase in retinal transcripts of innate immune system and inflammatory response pathway genes (Yu, Song et al. 2015). These findings are compatible with the observed increase in GFAP staining in RGC + IPL (this study) and other brain sections of late-stage *Ndufs4*<sup>-/-</sup> mice (Quintana, Kruse et al. 2010), indicating astroglial activation as a next step in the process of neurodegeneration. The present finding that chronic Trolox treatment prevents the loss of retinal ganglion cells without reducing the increased level of GFAP staining is surprising but leaves the intriguing question of whether this treatment can prevent the development of blindness in these complex I deficient mice. Electroretinography measurements (Kruse, Watt et al. 2008, Yu, Song et al. 2015) are likely to provide an answer to this question.

Using the *Ndufs4*<sup>-/-</sup> mouse, we here show that the water-soluble vitamin E analog, Trolox, may have therapeutic potential in human CI deficiency. Only recently, this conclusion was corroborated by a study showing that daily intraperitoneal injection of the blood-brain-barrier penetrating antioxidant, N-acetyl cysteine amide (AD4), between PD21 and PD28, significantly improved the rotarod performance of *Ndufs4*<sup>-/-</sup> mice (Kruse, Watt et al. 2008). Based on the data presented in the present paper, a number of Trolox variants was developed and tested in primary fibroblasts from patients with isolated CI deficiency (Blanchet, Smeitink et al. 2015). The most promising of these variants was selected for further therapy development.



## References

- Alam, M. T., G. R. Manjeri, R. J. Rodenburg, J. A. Smeitink, R. A. Notebaart, M. Huynen, P. H. Willems and W. J. Koopman (2015). "Skeletal muscle mitochondria of NDUF54 mice display normal maximal pyruvate oxidation and ATP production." *Biochim Biophys Acta*.
- Balaban, R. S., S. Nemoto and T. Finkel (2005). "Mitochondria, oxidants, and aging." *Cell* **120**(4): 483-495.
- Belanger, M., I. Allaman and P. J. Magistretti (2011). "Brain energy metabolism: focus on astrocyte-neuron metabolic cooperation." *Cell Metab* **14**(6): 724-738.
- Bird, M. J., X. W. Wijeyeratne, J. C. Komen, A. Laskowski, M. T. Ryan, D. R. Thorburn and A. E. Frazier (2014). "Neuronal and astrocyte dysfunction diverges from embryonic fibroblasts in the *Ndufs4<sup>fky/fky</sup>* mouse." *Biosci Rep* **34**(6): e00151.
- Blanchet, L., J. A. Smeitink, S. E. van Emst-de Vries, C. Vogels, M. Pellegrini, A. I. Jonckheere, R. J. Rodenburg, L. M. Buydens, J. Beyrath, P. H. Willems and W. J. Koopman (2015). "Quantifying small molecule phenotypic effects using mitochondrial morpho-functional fingerprinting and machine learning." *Sci Rep* **5**: 8035.
- Breuer, M. E., P. H. Willems, F. G. Russel, W. J. Koopman and J. A. Smeitink (2012). "Modeling mitochondrial dysfunctions in the brain: from mice to men." *J Inherit Metab Dis* **35**(2): 193-210.
- Brown, G. C. and V. Borutaite (2012). "There is no evidence that mitochondria are the main source of reactive oxygen species in mammalian cells." *Mitochondrion* **12**(1): 1-4.
- Carter, R. J., L. A. Lione, T. Humby, L. Mangiarini, A. Mahal, G. P. Bates, S. B. Dunnett and A. J. Morton (1999). "Characterization of progressive motor deficits in mice transgenic for the human Huntington's disease mutation." *J Neurosci* **19**(8): 3248-3257.
- Chouchani, E. T., C. Methner, G. Buonincontri, C. H. Hu, A. Logan, S. J. Sawiak, M. P. Murphy and T. Krieg (2014). "Complex I deficiency due to selective loss of *Ndufs4* in the mouse heart results in severe hypertrophic cardiomyopathy." *PLoS One* **9**(4): e94157.
- de Haas, R., F. G. Russel and J. A. Smeitink (2016). "Gait analysis in a mouse model resembling Leigh disease." *Behav Brain Res* **296**: 191-198.
- Distelmaier, F., F. Valsecchi, M. Forkink, S. van Emst-de Vries, H. G. Swarts, R. J. Rodenburg, E. T. Verwiel, J. A. Smeitink, P. H. Willems and W. J. Koopman (2012). "Trolox-sensitive reactive oxygen species regulate mitochondrial morphology, oxidative phosphorylation and cytosolic calcium handling in healthy cells." *Antioxid Redox Signal* **17**(12): 1657-1669.
- Distelmaier, F., H. J. Visch, J. A. Smeitink, E. Mayatepek, W. J. Koopman and P. H. Willems (2009). "The antioxidant Trolox restores mitochondrial membrane potential and Ca<sup>2+</sup>-stimulated ATP production in human complex I deficiency." *J Mol Med (Berl)* **87**(5): 515-522.
- Dringen, R. (2000). "Metabolism and functions of glutathione in brain." *Prog Neurobiol* **62**(6): 649-671.
- Fassone, E. and S. Rahman (2012). "Complex I deficiency: clinical features, biochemistry and molecular genetics." *J Med Genet* **49**(9): 578-590.
- Finkel, T. (2011). "Signal transduction by reactive oxygen species." *J Cell Biol* **194**(1): 7-15.
- Gough, D. R. and T. G. Cotter (2011). "Hydrogen peroxide: a Jekyll and Hyde signalling molecule." *Cell Death Dis* **2**: e213.
- Guy, J., W. J. Feuer, V. Porciatti, J. Schiffman, F. Abukhalil, R. Vandenbroucke, P. R. Rosa and B. L. Lam (2014). "Retinal ganglion cell dysfunction in asymptomatic *G11778A*: Leber hereditary optic neuropathy." *Invest Ophthalmol Vis Sci* **55**(2): 841-848.

- Jain, I. H., L. Zazzeron, R. Goli, K. Alexa, S. Schatzman-Bone, H. Dhillon, O. Goldberger, J. Peng, O. Shalem, N. E. Sanjana, F. Zhang, W. Goessling, W. M. Zapol and V. K. Mootha (2016). "Hypoxia as a therapy for mitochondrial disease." *Science* **352**(6281): 54-61.
- Janssen, A. J., F. J. Trijbels, R. C. Sengers, L. T. Wintjes, W. Ruitenbeek, J. A. Smeitink, E. Morava, B. G. van Engelen, L. P. van den Heuvel and R. J. Rodenburg (2006). "Measurement of the energy-generating capacity of human muscle mitochondria: diagnostic procedure and application to human pathology." *Clin Chem* **52**(5): 860-871.
- Jin, Z., W. Wei, M. Yang, Y. Du and Y. Wan (2014). "Mitochondrial complex I activity suppresses inflammation and enhances bone resorption by shifting macrophage-osteoclast polarization." *Cell Metab* **20**(3): 483-498.
- Johnson, S. C., M. E. Yanos, E. B. Kayser, A. Quintana, M. Sangesland, A. Castanza, L. Uhde, J. Hui, V. Z. Wall, A. Gagnidze, K. Oh, B. M. Wasko, F. J. Ramos, R. D. Palmiter, P. S. Rabinovitch, P. G. Morgan, M. M. Sedensky and M. Kaeberlein (2013). "mTOR inhibition alleviates mitochondrial disease in a mouse model of Leigh syndrome." *Science* **342**(6165): 1524-1528.
- Karl, T., R. Pabst and S. von Horsten (2003). "Behavioral phenotyping of mice in pharmacological and toxicological research." *Exp Toxicol Pathol* **55**(1): 69-83.
- Koopman, W. J., L. G. Nijtmans, C. E. Dieteren, P. Roestenberg, F. Valsecchi, J. A. Smeitink and P. H. Willems (2010). "Mammalian mitochondrial complex I: biogenesis, regulation, and reactive oxygen species generation." *Antioxid Redox Signal* **12**(12): 1431-1470.
- Koopman, W. J., S. Verkaart, S. E. van Emst-de Vries, S. Grefte, J. A. Smeitink, L. G. Nijtmans and P. H. Willems (2008). "Mitigation of NADH: ubiquinone oxidoreductase deficiency by chronic Trolox treatment." *Biochim Biophys Acta* **1777**(7-8): 853-859.
- Koopman, W. J., S. Verkaart, S. E. van Emst-de Vries, S. Grefte, J. A. Smeitink and P. H. Willems (2006). "Simultaneous quantification of oxidative stress and cell spreading using 5-(and-6)-chloromethyl-2',7'-dichlorofluorescein." *Cytometry A* **69**(12): 1184-1192.
- Kruse, S. E., W. C. Watt, D. J. Marcinek, R. P. Kapur, K. A. Schenkman and R. D. Palmiter (2008). "Mice with mitochondrial complex I deficiency develop a fatal encephalomyopathy." *Cell Metab* **7**(4): 312-320.
- Kudin, A. P., N. Y. Bimpong-Buta, S. Vielhaber, C. E. Elger and W. S. Kunz (2004). "Characterization of superoxide-producing sites in isolated brain mitochondria." *J Biol Chem* **279**(6): 4127-4135.
- Liu, L., K. Zhang, H. Sandoval, S. Yamamoto, M. Jaiswal, E. Sanz, Z. Li, J. Hui, B. H. Graham, A. Quintana and H. J. Bellen (2015). "Glial lipid droplets and ROS induced by mitochondrial defects promote neurodegeneration." *Cell* **160**(1-2): 177-190.
- Malinska, D., B. Kulawiak, A. P. Kudin, R. Kovacs, C. Huchzermeyer, O. Kann, A. Szewczyk and W. S. Kunz (2010). "Complex III-dependent superoxide production of brain mitochondria contributes to seizure-related ROS formation." *Biochim Biophys Acta* **1797**(6-7): 1163-1170.
- Manjeri, G. R., R. J. Rodenburg, L. Blanchet, S. Roelofs, L. G. Nijtmans, J. A. Smeitink, J. J. Driessen, W. J. Koopman and P. H. Willems (2016). "Increased mitochondrial ATP production capacity in brain of healthy mice and a mouse model of isolated complex I deficiency after isoflurane anesthesia." *J Inherit Metab Dis* **39**(1): 59-65.
- Mounsey, R. B. and P. Teismann (2010). "Mitochondrial dysfunction in Parkinson's disease: pathogenesis and neuroprotection." *Parkinsons Dis* **2011**: 617472.
- Mullen, R. J., C. R. Buck and A. M. Smith (1992). "NeuN, a neuronal specific nuclear protein in vertebrates." *Development* **116**(1): 201-211.
- Murphy, M. P. (2009). "How mitochondria produce reactive oxygen species." *Biochem J* **417**(1): 1-13.

- Murphy, M. P. (2012). "Modulating mitochondrial intracellular location as a redox signal." *Sci Signal* **5**(242): pe39.
- Napankangas, J. P., E. V. Liimatta, P. Joensuu, U. Bergmann, K. Ylitalo and I. E. Hassinen (2012). "Superoxide production during ischemia-reperfusion in the perfused rat heart: a comparison of two methods of measurement." *J Mol Cell Cardiol* **53**(6): 906-915.
- Navis, A. C., A. Bourgonje, P. Wesseling, A. Wright, W. Hendriks, K. Verrijp, J. A. van der Laak, A. Heerschap and W. P. Leenders (2013). "Effects of dual targeting of tumor cells and stroma in human glioblastoma xenografts with a tyrosine kinase inhibitor against c-MET and VEGFR2." *PLoS One* **8**(3): e58262.
- Quintana, A., S. E. Kruse, R. P. Kapur, E. Sanz and R. D. Palmiter (2010). "Complex I deficiency due to loss of Ndufs4 in the brain results in progressive encephalopathy resembling Leigh syndrome." *Proc Natl Acad Sci U S A* **107**(24): 10996-11001.
- Quintana, A., S. Zanella, H. Koch, S. E. Kruse, D. Lee, J. M. Ramirez and R. D. Palmiter (2012). "Fatal breathing dysfunction in a mouse model of Leigh syndrome." *J Clin Invest* **122**(7): 2359-2368.
- Rich, P. (2003). "Chemiosmotic coupling: The cost of living." *Nature* **421**(6923): 583.
- Rodenburg, R. J. (2011). "Biochemical diagnosis of mitochondrial disorders." *J Inherit Metab Dis* **34**(2): 283-292.
- Shi, Y., M. V. Ivannikov, M. E. Walsh, Y. Liu, Y. Zhang, C. A. Jaramillo, G. T. Macleod and H. Van Remmen (2014). "The lack of CuZnSOD leads to impaired neurotransmitter release, neuromuscular junction destabilization and reduced muscle strength in mice." *PLoS One* **9**(6): e100834.
- Smeitink, J., L. van den Heuvel and S. DiMauro (2001). "The genetics and pathology of oxidative phosphorylation." *Nat Rev Genet* **2**(5): 342-352.
- Sofroniew, M. V. and H. V. Vinters (2010). "Astrocytes: biology and pathology." *Acta Neuropathol* **119**(1): 7-35.
- Tronstad, K. J., M. Nooteboom, L. I. Nilsson, J. Nikolaisen, M. Sokolewicz, S. Grefte, I. K. Pettersen, S. Dyrstad, F. Hoel, P. H. Willems and W. J. Koopman (2014). "Regulation and quantification of cellular mitochondrial morphology and content." *Curr Pharm Des* **20**(35): 5634-5652.
- Verkaart, S., W. J. Koopman, S. E. van Erst-de Vries, L. G. Nijtmans, L. W. van den Heuvel, J. A. Smeitink and P. H. Willems (2007). "Superoxide production is inversely related to complex I activity in inherited complex I deficiency." *Biochim Biophys Acta* **1772**(3): 373-381.
- Willems, P. H., R. Rossignol, C. E. Dieteren, M. P. Murphy and W. J. Koopman (2015). "Redox Homeostasis and Mitochondrial Dynamics." *Cell Metab* **22**(2): 207-218.
- Willems, P. H., F. Valsecchi, F. Distelmaier, S. Verkaart, H. J. Visch, J. A. Smeitink and W. J. Koopman (2008). "Mitochondrial Ca<sup>2+</sup> homeostasis in human NADH:ubiquinone oxidoreductase deficiency." *Cell Calcium* **44**(1): 123-133.
- Wilson, J. X. (1997). "Antioxidant defense of the brain: a role for astrocytes." *Can J Physiol Pharmacol* **75**(10-11): 1149-1163.
- Xu, F., H. Huang, Y. Wu, L. Lu, L. Jiang, L. Chen, S. Zeng, L. Li and M. Li (2014). "Upregulation of Gem relates to retinal ganglion cells apoptosis after optic nerve crush in adult rats." *J Mol Histol* **45**(5): 565-571.
- Yu, A. K., L. Song, K. D. Murray, D. van der List, C. Sun, Y. Shen, Z. Xia and G. A. Cortopassi (2015). "Mitochondrial complex I deficiency leads to inflammation and retinal ganglion cell death in the Ndufs4 mouse." *Hum Mol Genet*.
- Zhang, X., D. Jones and F. Gonzalez-Lima (2002). "Mouse model of optic neuropathy caused by mitochondrial complex I dysfunction." *Neurosci Lett* **326**(2): 97-100.



# CHAPTER

**General summary  
and Future perspectives**

8



Patients with dysfunction of the OXPHOS system may present at any age with a wide variety of signs and symptoms affecting any organ of the body (Chinnery 1993). The genetic basis of these diseases is complex. Assembly and maintenance of a fully functional OXPHOS system is under dual genetic control of the nDNA and the mtDNA and any mutation in any gene that affects the functionality of the OXPHOS system might lead to OXPHOS dysfunction-related clinical symptoms (Koopman, Willems et al. 2012, Koopman, Distelmaier et al. 2013). Mutations in nuclear genes are inherited in a Mendelian manner, whereas mutations in mitochondrial genes are inherited maternally. Organs with high energy demand are especially afflicted, predominantly the brain (Kirby and Thorburn 2008, Tucker, Compton et al. 2010, Schapira 2012). Neurons are gradually destroyed, resulting in a progressive loss of nervous system structure and function (Przedborski, Vila et al. 2003, Deuschl and Elble 2009). The pathological picture in neurodegenerative disorders is heterogeneous, affecting unique areas of the nervous system. In the brain, Purkinje cells and neurons of the dentate nuclei of the cerebellum as well as neurons of the inferior olivary nuclei of the medulla are considered to be most energy demanding, and thus most susceptible to damage (Breuer, Koopman et al. 2013). Symptoms range from acute and rapid in progression to subtle and chronic (Koopman, Distelmaier et al. 2013). The critical function of the neuronal OXPHOS system in maintaining bioenergetic needs is illustrated by the fact that OXPHOS dysfunction leads to defects in growth and trafficking, as well as to apoptosis and neuronal death (Fukui and Moraes 2008). This, in turn, can lead to microglial activation, a pathophysiological consequence that can trigger catastrophic events such as further oxidative and nitrosative stress, ultimately leading to further neuronal damage and death (Di Filippo, Chiasserini et al. 2010). Supplementary Table 1 in Koopman, Distelmaier et al. lists the many genes in the nDNA and mtDNA that have been demonstrated to carry mutations resulting in dysfunction of the OXPHOS system associated with neurodegeneration (Koopman, Distelmaier et al. 2013). The products of these genes include (i) structural OXPHOS subunits, (ii) OXPHOS assembly factors, (iii) Fe-S biogenesis enzymes, (iv) enzymes involved in the synthesis of CoQ10 and cyt-c, (v) mt-rRNAs, (vi) mt-tRNAs, (vii) mtDNA repair enzymes, (viii) mtDNA replication, transcription and translation factors, (ix) enzymes involved in the maintenance of the mitochondrial dNTP pool, (x) mitochondrial ribosomal proteins, (xi) mt-tRNA synthetases and (xii) nucleoid-associated proteins. However, this list is far from complete because proper function of the OXPHOS system will also be hampered by mutations in nuclear genes encoding the mitochondrial phosphate carrier, the adenine nucleotide translocator, the mitochondrial protein

import system, the mitochondrial quality control system, the integrity of the inner mitochondrial membrane, etc.

\* \* \*

The aim of this thesis was to obtain a better understanding of the pathophysiological consequences of isolated mitochondrial CI deficiency using the WB *Ndufs4*<sup>-/-</sup> mouse model (Kruse, Watt et al. 2008) and to contribute to a relevant therapeutic strategy to alleviate and/or ameliorate this disease. To this end, we characterized the phenotypic manifestations of the *Ndufs4* deletion by monitoring signs and symptoms from postnatal day 0 until their predefined humane endpoint (**Chapter 1**). In agreement with other studies, we found that *Ndufs4*<sup>-/-</sup> mice replicated several clinical milestones observed in children with isolated CI deficiency including hypotonia, progressive muscle weakness, epileptic episodes (seizures) and ataxia (de Haas, Russel et al. 2016). Based on these findings it was concluded that the WB *Ndufs4*<sup>-/-</sup> mouse could be a relevant model to evaluate therapeutic strategies intended for translation to man.

\* \* \*

Given the dramatic phenotypic of the WB *Ndufs4*<sup>-/-</sup> mouse, we were intrigued by the observation that these mice displayed no deficit in maximal rate of ATP production when assessed in the ischemic hind limb paradigm *in vivo* (Kruse, Watt et al. 2008). Similarly, *in vitro* analysis of the maximal rate of mitochondrial ATP production in a mitochondria-enriched fraction from heart tissue of a conditional heart-specific *Ndufs4*<sup>-/-</sup> mouse showed only a tendency to decrease when determined in the presence of either glutamate and malate or pyruvate and malate and when expressed per unit of mitochondrial mass after normalization to the maximal activity of citrate synthase (Sterky, Hoffman et al. 2012). This result shows that, despite the virtual absence of CI activity, there is only a small, if any, decrease in maximal mitochondrial ATP production capacity per unit of mitochondrial mass. These observations urged us to measure the maximal rate of mitochondrial ATP production in a mitochondria-enriched fraction from three tissues of high energy demand, namely skeletal muscle, heart and brain and compare the values obtained between WB *Ndufs4*<sup>-/-</sup> mice and their wild type littermates (**Chapter 2**). We show that the maximal rate of mitochondrial ATP production was significantly decreased in skeletal muscle and brain and close to significantly in heart by 51%, 25% and 32%, respectively, in WB *Ndufs4*<sup>-/-</sup> mice when expressed per unit of mitochondrial mass after normalization to the maximal activity



of citrate synthase. The maximal activity of CI, expressed per unit of mitochondrial mass, was much more dramatically reduced in all three tissues. These results are in agreement with those of Sterky and Hoffman et al. (Sterky, Hoffman et al. 2012) in that all three tissues, despite the virtual absence of CI activity, show a decreased though still substantial mitochondrial ATP production capacity when expressed per unit of mitochondrial mass. Most importantly, in contrast to brain, skeletal muscle and heart showed no differences in maximal rate of mitochondrial ATP production when expressed per mg of protein. This indicates that the total mitochondrial ATP production capacity per unit of tissue mass was decreased in brain but not in the latter two organs. Skeletal muscle and heart, but not brain, showed a significant increase in maximal citrate synthase activity (values of 72%;  $p=0.017$  and 49%;  $p=0.002$ ), respectively, indicating that these two tissues, in sharp contrast to brain, had been able to perform an adaptive increase in mitochondrial mass to compensate for the decrease in mitochondrial ATP production capacity per unit of mitochondrial mass. In agreement with this idea, we observed that, when expressed per unit of tissue mass, the maximal activity of CII was significantly increased by 56% ( $p=0.033$ ) in skeletal muscle with a tendency to increase in heart, that of CIII showed a tendency to increase by 45% ( $p=0.069$ ) in skeletal muscle and by 11% ( $p=0.071$ ) in heart and that of CIV was significantly increased in both skeletal muscle by 70% ( $p=0.024$ ) and in heart by 51% ( $p=0.005$ ), whereas, in sharp contrast, for none of the complexes the maximal activity was altered in brain. From these results it was concluded that the brain, which lacks the adaptive response, is most probably the most vulnerable tissue in WB complex I deficiency involving a disease causing mutation in the *Ndufs4* gene. This conclusion is substantiated by the increased degeneration observed in olfactory bulb, brainstem and cerebellum of WB *Ndufs4*<sup>-/-</sup> mice and conditional brain-specific *Ndufs4*<sup>-/-</sup> mice display the same clinical phenotype (Quintana, Kruse et al. 2010, Kayser, Sedensky et al. 2016) Together, these results strongly favor the brain as primary target for therapeutic intervention (Koopman, Beyrath et al. 2016).

\* \* \*

In **Chapter 3** we employed an *in silico* strategy to try and understand the mechanism by which *Ndufs4*<sup>-/-</sup> skeletal muscle mitochondria, despite an ~80% decrease in maximal CI activity when expressed per unit of tissue mass, are still able to produce ATP from CI-specific substrates (pyruvate and malate) at a maximal rate that is similar to that obtained with wild type skeletal muscle mitochondria when expressed per unit of tissue mass (see, Chapter 2). To this end, we adapted a mathematical model

of mitochondrial metabolism that was validated for skeletal muscle mitochondria by Beard and co-workers (Wu, Yang et al. 2007) to match our experimental conditions. Thus, mitochondria were considered as an input–output system, converting pyruvate (input) into ATP (output) via the integrated action of transporters, pyruvate dehydrogenase, citric acid cycle enzymes and the OXPHOS system. By including the percent change in maximal activity of the complexes I, II, III and IV expressed per unit of tissue mass, the wild type skeletal muscle-specific model was transformed into an *Ndufs4*<sup>-/-</sup> skeletal muscle-specific model, which allowed calculating the maximal rates of pyruvate oxidation and ATP production per unit of tissue mass. Our calculations predicted that the experimentally measured changes in maximal activity of the complexes I, II, III and IV expressed per unit of tissue mass resulted in control maximal rates of mitochondrial pyruvate oxidation and ATP production in *Ndufs4*<sup>-/-</sup> skeletal muscle when expressed per unit of tissue mass. This prediction was in complete agreement with our experimental results. *In silico* analysis furthermore predicted that CI deficiency alters the concentration of intermediate metabolites, modestly increases the mitochondrial NADH/NAD<sup>+</sup> ratio and stimulates the lower half of the citric acid cycle, including CII. Several of these predicted changes were previously reported in experimental models of CI deficiency. Interestingly, our model predictions suggested that CI deficiency only has major metabolic consequences when, in adapted skeletal muscle tissue, the maximal activity of CI decreases below 90% of normal levels. This result is compatible with the idea of a biochemical threshold effect.

\* \* \*

Children with mitochondrial disorders involving the energy generating system are frequently anaesthetized for a wide range of operations. However, these disorders may alter the response to anaesthesia. It has been shown that the volatile anaesthetic isoflurane inhibits the activity of CI (Kayser, Suthammarak et al. 2011). Moreover, CI deficient *C. Elegans* have been shown to be hypersensitive to volatile anaesthetics (Kayser, Suthammarak et al. 2011). Together with reports that WB *Ndufs4*<sup>-/-</sup> mice develop progressive respiratory dysfunction i.e. bradypnea and apnea, leading to premature death (Quintana, Zanella et al. 2012), these findings urged us to examine the sensitivity of these mice to isoflurane. **Chapter 4** shows that WB *Ndufs4*<sup>-/-</sup> mice displayed a progressive increase with age of both isoflurane sensitivity and respiratory depression. In a recent study, Zimin and co-workers knocked out the *Ndufs4* gene in GABAergic neurons (GABA-specific knock-out mice), VGLUT2-positive glutamatergic

neurons (VGLUT2-specific knock-out mice) and cholinergic neurons (CHAT-specific knock-out mice) and observed that VGLUT2-specific knock-out mice and WB *Ndufs4*<sup>-/-</sup> mice were equally sensitive to isoflurane and halothane, whereas GABA-specific knock-out mice and CHAT-specific knock-out mice were no longer hypersensitive to these anaesthetics, indicating that excitatory glutamatergic transmission is a major contributor to volatile anaesthetic hypersensitivity in *Ndufs4*<sup>-/-</sup> mice (Zimin, Woods et al. 2016).

\* \* \*

Since the pathology of CI deficiency appears to occur mainly in the central nervous system (Distelmaier, Koopman et al. 2009), we conducted a specific investigation towards the effects of isoflurane anaesthesia on brain mitochondrial function. In Chapter 2 we reported that the mitochondrial ATP production capacity per unit of tissue mass is significantly decreased by 26% ( $p=0.028$ ) in WB *Ndufs4*<sup>-/-</sup> brain. Based on this finding, it was hypothesized that a decrease in mitochondrial ATP production capacity might underly the observed hypersensitivity of WB *Ndufs4*<sup>-/-</sup> mice to volatile anaesthetics such as isoflurane and halothane. Surprisingly, the data presented in **Chapter 5** demonstrate that isoflurane anaesthesia significantly increased the maximal rate of mitochondrial ATP production by 52% ( $p<0.05$ ) and 69% ( $p<0.01$ ) when expressed per unit of tissue mass in a mitochondria-enriched preparation of wild type and WB *Ndufs4*<sup>-/-</sup> brain, respectively. Remarkably, in agreement with literature findings, isoflurane anaesthesia decreased the maximal activity of CI by 30% ( $p<0.001$ ) in wild type brain. This result is in agreement with our conclusion in Chapter 3 that CI activity can be lowered to a tissue-specific threshold before this lowering starts to affect the mitochondrial ATP production capacity. In sharp contrast, isoflurane anaesthetics increased the activity of CII by 37% ( $p<0.001$ ) and 50% ( $p<0.001$ ) and that of CIII by 37% ( $p<0.001$ ) and 40% ( $p<0.001$ ) in wild type and WB *Ndufs4*<sup>-/-</sup> brain, respectively, whereas it tended to increase that of CIV in both wild type and WB *Ndufs4*<sup>-/-</sup> brain. Together, these findings indicate that isoflurane anaesthesia interferes positively rather than negatively with the ability of CI deficient mice brain mitochondria to convert their main substrate pyruvate into ATP. It remains to be established whether this isoflurane anaesthesia-induced increase in mitochondrial ATP production capacity might exert unwanted effects in brain cells relevant for the observed respiratory depression. A major limitation of our study is that we used a mitochondria-enriched fraction from whole brain, whereas many studies report regional differences in susceptibility to mitochondrial dysfunction

within the central nervous system (Leong, Komen et al. 2012, Pinto, Pickrell et al. 2012, Quintana, Zanella et al. 2012). Kayser and co-workers recently observed that the respiratory capacity of synaptosomes from degeneration prone regions of the brain, namely olfactory bulb, brainstem and cerebellum was significantly reduced in *Ndufs4*<sup>-/-</sup> mice (Kayser, Sedensky et al. 2016). Crucially, this decrease was already observed before the onset of the neurological symptoms. Importantly, these authors failed to show any reduction in respiratory capacity of synaptosomes from degeneration resistant parts of the brain. These results corroborate previous findings of region specific brain damage in *Ndufs4*<sup>-/-</sup> mice (Quintana, Kruse et al. 2010) and indicate that local insufficiencies in ATP production capacity of nerve terminals may underlie the occurrence of specific brain areas where neurodegeneration takes place. It remains to be established whether volatile anaesthetics act on these CI deficiency susceptible brain regions and/or on other regions in the *Ndufs4*<sup>-/-</sup> brain.

\* \* \*

In the same study, Kayser and co-workers addressed the presence of 4-hydroxy-2-nonenal (HNE)-modified proteins as evidence for increased formation of reactive oxygen species (ROS) (Kayser, Sedensky et al. 2016). The authors observed an increased expression of HNE-modified proteins in CI deficiency susceptible brain areas and not in CI deficiency resistant brain areas. However, this observation was reached in both wild type and *Ndufs4*<sup>-/-</sup> mice, suggesting that ROS-induced HNE-modification does not play a role in region specific neurodegeneration. In sharp contrast, Quintana and co-workers reported a significant increase in protein carbonylation in the olfactory bulb of the conditional brain specific *Ndufs4*<sup>-/-</sup> mouse, suggesting a role for ROS-induced protein carbonylation in region specific neurodegeneration (Quintana, Kruse et al. 2010). In **Chapter 6**, we discuss those neurons which because of their presumed susceptibility to oxidative damage contribute most to the neurological phenotype in the *Ndufs4*<sup>-/-</sup> mouse models. Neurons have very high energy demands and it is calculated that the brain, which only accounts for ~ 2% of the total body mass, is responsible for 20% of the total oxygen consumption by the body. In the brain, the vast majority of energy consumption takes place in the neurons, whereas astrocytes are responsible for only 5-15% of the total energy requirement of the brain (Attwell and Laughlin 2001). This immense energy demand of neurons results from the fact that they are highly differentiated cells that require large amounts of ATP to maintain the ionic gradients across the cell membrane that are necessary for proper neurotransmission (Kann and Kovacs

2007). Neurons completely depend on the OXPHOS system for their ATP needs and, importantly, a switch to glycolysis, when OXPHOS becomes limited, will not generate sufficient ATP (Knott, Perkins et al. 2008). Neurons are long lived, which is important because their synaptic contacts carry essential information for the organism. These two properties of neurons may pose a serious problem, as mitochondrial oxidative ATP production is inevitably associated with the production of toxic oxygen radicals at CI and CIII (Brand 2010, Forkink, Smeitink et al. 2010, Koopman, Nijtmans et al. 2010, Distelmaier, Valsecchi et al. 2012). It is for this reason that neurons are thought to not oxidize fatty acids because for every Acetyl-CoA that is generated during fatty acid breakdown, a step catalysed by Acyl-CoA dehydrogenase, one FADH<sub>2</sub> and one NADH is produced. This results in a by far larger increase in the amount of FADH<sub>2</sub> than during the oxidation of glucose and it is this FADH<sub>2</sub> that is oxidized by the electron transfer flavoprotein: ubiquinone oxidoreductase (ETF:QO) thus competing with CI for the reduction of ubiquinone to ubiquinol (Watmough and Frerman 2010, Speijer 2011). As a consequence, NADH will build up increasing the probability of increased ROS production by CI itself and/or mitochondrial NADH hydrogenases such as  $\alpha$ -glycerophosphate dehydrogenase located on the outer surface of the mitochondrial inner membrane and  $\alpha$ -ketoglutarate dehydrogenase (Adam-Vizi and Tretter 2013). Thus neurons do not use beta oxidation (Yang, He et al. 1987, Speijer 2011, Schonfeld and Reiser 2013) but, instead, rely on glucose and ketone bodies for their energy supply, even though fatty acids have about twice the energy content of glucose. Despite the banishment of fatty acids from the menu, neurons still produce ROS during mitochondrial ATP production from glucose and ketone bodies. It is speculated that this lifelong ROS production, despite the presence of numerous antioxidant systems, gradually damages neurons resulting in a progressive loss of neuron function. If this process is somehow accelerated it may contribute to brain diseases in the elderly such as Alzheimer's disease, Amyotrophic Lateral Sclerosis (ALS) and Parkinson's disease.

\* \* \*

Having characterized the phenotypic consequences of the WB *Ndufs4* deletion in Chapter 1 and biochemical consequences in organs of high energy demand in Chapter 2, we investigated the *in vivo* therapeutic potential of the water soluble Vitamin E analogue Trolox in the WB *Ndufs4*<sup>-/-</sup> mouse. Trolox was chosen because thorough *in vitro* testing had shown that many of the cell biological aberrations observed in primary skin fibroblasts from patients with isolated CI deficiency could

be reversed or partially reversed with this antioxidant (see Chapter 1). In **Chapter 7** we show that twice daily intraperitoneal injection of Trolox starting from week 3 of life retarded the progressive decline in muscle endurance and motor coordination in WB *Ndufs4*<sup>-/-</sup> mice as demonstrated by improved rope grip and rotarod performance, reaching statistical significance ( $p < 0.05$ ) and close to statistical significance ( $p = 0.07$ ), respectively, at week 6 of life. Animals were sacrificed at week 6 of life and analysis of the maximal rate of mitochondrial ATP production per unit of tissue mass in a mitochondria-enriched fraction of hind limb muscle revealed a significant decrease in vehicle-treated WB *Ndufs4*<sup>-/-</sup> mice. In sharp contrast, the work presented in Chapter 2 showed the absence of any difference in maximal rate of mitochondrial ATP production per unit of tissue mass between WB *Ndufs4*<sup>-/-</sup> mice at days 31-34 of life and their wild type littermates. Analysis of the maximal citrate synthase activity revealed a significant increase in WB *Ndufs4*<sup>-/-</sup> mice at days 31-34 of life but not in WB *Ndufs4*<sup>-/-</sup> mice at week 6 of life, suggesting that the proposed adaptive increase in mitochondrial mass at days 31-34 of life is no longer present in end stage WB *Ndufs4*<sup>-/-</sup> mice. Analysis of a mitochondria-enriched fraction of hind limb muscle from Trolox-treated WB *Ndufs4*<sup>-/-</sup> mice revealed a close to significant ( $p = 0.054$ ) increase in maximal CI activity. However, this tentative increase in CI activity was not accompanied by an increase in maximal rate of mitochondrial ATP production. These findings suggested that Trolox might not exert its effect at the level of the skeletal muscle but rather at the level of the brain. The area of the granular layer of the cerebral cortex occupied by GFAP positive cells did not differ between vehicle-treated wild type and *Ndufs4*<sup>-/-</sup> mice and was not influenced by Trolox-treatment. The same observation was reached for the number of Purkinje cells in the cerebellum. Regarding the retina, layer thickness tended to be decreased for RGC ( $p = 0.06$ ), IPL ( $p = 0.06$ ) and INL ( $p = 0.06$ ) in vehicle-treated *Ndufs4*<sup>-/-</sup> mice. The same layers showed no tendency for decreased thickness between Trolox-treated *Ndufs4*<sup>-/-</sup> and wild type mice. Trolox-treated *Ndufs4*<sup>-/-</sup> mice showed a significant increase in EPL thickness as compared to Trolox-treated wild type mice. GFAP staining was increased in RGC+IPL of *Ndufs4*<sup>-/-</sup> mice and remained increased following Trolox treatment. Finally, Trolox-treatment fully restored the decrease in the number of NeuN positive cells observed in the RGC of vehicle-treated *Ndufs4*<sup>-/-</sup> mice. Taking into account the rapidly progressive, lethal phenotype of the *Ndufs4*<sup>-/-</sup> mice, the present finding that Trolox has some beneficial effect on neuro-motor function and retinal integrity might warrant translation to the human situation.

\* \* \*

Using the *Ndufs4*<sup>-/-</sup> mouse, we here show that the water-soluble vitamin E analog, Trolox, may have therapeutic potential in human CI deficiency. Only recently, this conclusion was corroborated by a study showing that daily intraperitoneal injection of the blood-brain-barrier penetrating antioxidant, N-acetyl cysteine amide (AD4), between PD21 and PD28, significantly improved the rotarod performance of *Ndufs4*<sup>-/-</sup> mice (Kruse, Watt et al. 2008). Based on the data obtained in our cell biological studies, a number of Trolox variants was developed and tested in primary fibroblasts from patients with isolated CI deficiency (Blanchet, Smeitink et al. 2015). The most promising of these variants was selected for further therapy development. Together with the data presented in the literature, the findings presented in Chapter 7 of this thesis warrant a multipronged therapeutic intervention strategy consisting of 1) a blood-brain barrier permeant antioxidant activity to dampen the induction of ROS, especially in regions such as the olfactory bulb, vestibular nuclei, inferior olive, cerebellum and brain stem, 2) an immunosuppressant activity to prevent the innate immune response against self-antigens and 3) a mitochondrial biogenesis activity to increase the ATP production capacity in the afflicted regions of the brain.

## References

- Adam-Vizi, V. and L. Tretter (2013). "The role of mitochondrial dehydrogenases in the generation of oxidative stress." *Neurochem Int* **62**(5): 757-763.
- Attwell, D. and S. B. Laughlin (2001). "An energy budget for signaling in the grey matter of the brain." *J Cereb Blood Flow Metab* **21**(10): 1133-1145.
- Blanchet, L., J. A. Smeitink, S. E. van Emst-de Vries, C. Vogels, M. Pellegrini, A. I. Jonckheere, R. J. Rodenburg, L. M. Buydens, J. Beyrath, P. H. Willems and W. J. Koopman (2015). "Quantifying small molecule phenotypic effects using mitochondrial morpho-functional fingerprinting and machine learning." *Sci Rep* **5**: 8035.
- Brand, M. D. (2010). "The sites and topology of mitochondrial superoxide production." *Exp Gerontol* **45**(7-8): 466-472.
- Breuer, M. E., W. J. Koopman, S. Koene, M. Nooteboom, R. J. Rodenburg, P. H. Willems and J. A. Smeitink (2013). "The role of mitochondrial OXPHOS dysfunction in the development of neurologic diseases." *Neurobiol Dis* **51**: 27-34.
- Chinnery, P. F. (1993). *Mitochondrial Disorders Overview*. GeneReviews(R). R. A. Pagon, M. P. Adam, H. H. Ardinger et al. Seattle (WA).
- de Haas, R., F. G. Russel and J. A. Smeitink (2016). "Gait analysis in a mouse model resembling Leigh disease." *Behav Brain Res* **296**: 191-198.
- Deuschl, G. and R. Elble (2009). "Essential tremor--neurodegenerative or nondegenerative disease towards a working definition of ET." *Mov Disord* **24**(14): 2033-2041.
- Di Filippo, M., D. Chiasserini, A. Tozzi, B. Picconi and P. Calabresi (2010). "Mitochondria and the link between neuroinflammation and neurodegeneration." *J Alzheimers Dis* **20 Suppl 2**: S369-379.
- Distelmaier, F., W. J. Koopman, L. P. van den Heuvel, R. J. Rodenburg, E. Mayatepek, P. H. Willems and J. A. Smeitink (2009). "Mitochondrial complex I deficiency: from organelle dysfunction to clinical disease." *Brain* **132**(Pt 4): 833-842.
- Distelmaier, F., F. Valsecchi, M. Forkink, S. van Emst-de Vries, H. G. Swarts, R. J. Rodenburg, E. T. Verwiel, J. A. Smeitink, P. H. Willems and W. J. Koopman (2012). "Trolox-sensitive reactive oxygen species regulate mitochondrial morphology, oxidative phosphorylation and cytosolic calcium handling in healthy cells." *Antioxid Redox Signal* **17**(12): 1657-1669.
- Forkink, M., J. A. Smeitink, R. Brock, P. H. Willems and W. J. Koopman (2010). "Detection and manipulation of mitochondrial reactive oxygen species in mammalian cells." *Biochim Biophys Acta* **1797**(6-7): 1034-1044.
- Fukui, H. and C. T. Moraes (2008). "The mitochondrial impairment, oxidative stress and neurodegeneration connection: reality or just an attractive hypothesis?" *Trends Neurosci* **31**(5): 251-256.
- Kann, O. and R. Kovacs (2007). "Mitochondria and neuronal activity." *Am J Physiol Cell Physiol* **292**(2): C641-657.
- Kayser, E. B., M. M. Sedensky and P. G. Morgan (2016). "Region-Specific Defects of Respiratory Capacities in the *Ndufs4*(KO) Mouse Brain." *PLoS One* **11**(1): e0148219.
- Kayser, E. B., W. Suthammarak, P. G. Morgan and M. M. Sedensky (2011). "Isoflurane selectively inhibits distal mitochondrial complex I in *Caenorhabditis elegans*." *Anesth Analg* **112**(6): 1321-1329.
- Kirby, D. M. and D. R. Thorburn (2008). "Approaches to finding the molecular basis of mitochondrial oxidative phosphorylation disorders." *Twin Res Hum Genet* **11**(4): 395-411.



- Knott, A. B., G. Perkins, R. Schwarzenbacher and E. Bossy-Wetzel (2008). "Mitochondrial fragmentation in neurodegeneration." *Nat Rev Neurosci* **9**(7): 505-518.
- Koopman, W. J., J. Beyrath, C. W. Fung, S. Koene, R. J. Rodenburg, P. H. Willems and J. A. Smeitink (2016). "Mitochondrial disorders in children: toward development of small-molecule treatment strategies." *EMBO Mol Med* **8**(4): 311-327.
- Koopman, W. J., F. Distelmaier, J. A. Smeitink and P. H. Willems (2013). "OXPHOS mutations and neurodegeneration." *EMBO J* **32**(1): 9-29.
- Koopman, W. J., L. G. Nijtmans, C. E. Dieteren, P. Roestenberg, F. Valsecchi, J. A. Smeitink and P. H. Willems (2010). "Mammalian mitochondrial complex I: biogenesis, regulation, and reactive oxygen species generation." *Antioxid Redox Signal* **12**(12): 1431-1470.
- Koopman, W. J., P. H. Willems and J. A. Smeitink (2012). "Monogenic mitochondrial disorders." *N Engl J Med* **366**(12): 1132-1141.
- Kruse, S. E., W. C. Watt, D. J. Marcinek, R. P. Kapur, K. A. Schenkman and R. D. Palmiter (2008). "Mice with mitochondrial complex I deficiency develop a fatal encephalomyopathy." *Cell Metab* **7**(4): 312-320.
- Leong, D. W., J. C. Komen, C. A. Hewitt, E. Arnaud, M. McKenzie, B. Phipson, M. Bahlo, A. Laskowski, S. A. Kinkel, G. M. Davey, W. R. Heath, A. K. Voss, R. P. Zahedi, J. J. Pitt, R. Chrast, A. Sickmann, M. T. Ryan, G. K. Smyth, D. R. Thorburn and H. S. Scott (2012). "Proteomic and metabolomic analyses of mitochondrial complex I-deficient mouse model generated by spontaneous B2 short interspersed nuclear element (SINE) insertion into NADH dehydrogenase (ubiquinone) Fe-S protein 4 (Ndufs4) gene." *J Biol Chem* **287**(24): 20652-20663.
- Pinto, M., A. M. Pickrell and C. T. Moraes (2012). "Regional susceptibilities to mitochondrial dysfunctions in the CNS." *Biol Chem* **393**(4): 275-281.
- Przedborski, S., M. Vila and V. Jackson-Lewis (2003). "Neurodegeneration: what is it and where are we?" *J Clin Invest* **111**(1): 3-10.
- Quintana, A., S. E. Kruse, R. P. Kapur, E. Sanz and R. D. Palmiter (2010). "Complex I deficiency due to loss of Ndufs4 in the brain results in progressive encephalopathy resembling Leigh syndrome." *Proc Natl Acad Sci U S A* **107**(24): 10996-11001.
- Quintana, A., S. Zanella, H. Koch, S. E. Kruse, D. Lee, J. M. Ramirez and R. D. Palmiter (2012). "Fatal breathing dysfunction in a mouse model of Leigh syndrome." *J Clin Invest* **122**(7): 2359-2368.
- Schapira, A. H. (2012). "Mitochondrial diseases." *Lancet* **379**(9828): 1825-1834.
- Schonfeld, P. and G. Reiser (2013). "Why does brain metabolism not favor burning of fatty acids to provide energy? Reflections on disadvantages of the use of free fatty acids as fuel for brain." *J Cereb Blood Flow Metab* **33**(10): 1493-1499.
- Speijer, D. (2011). "Oxygen radicals shaping evolution: why fatty acid catabolism leads to peroxisomes while neurons do without it: FADH(2)/NADH flux ratios determining mitochondrial radical formation were crucial for the eukaryotic invention of peroxisomes and catabolic tissue differentiation." *Bioessays* **33**(2): 88-94.
- Sterky, F. H., A. F. Hoffman, D. Milenkovic, B. Bao, A. Paganelli, D. Edgar, R. Wibom, C. R. Lupica, L. Olson and N. G. Larsson (2012). "Altered dopamine metabolism and increased vulnerability to MPTP in mice with partial deficiency of mitochondrial complex I in dopamine neurons." *Hum Mol Genet* **21**(5): 1078-1089.
- Tucker, E. J., A. G. Compton and D. R. Thorburn (2010). "Recent advances in the genetics of mitochondrial encephalopathies." *Curr Neurol Neurosci Rep* **10**(4): 277-285.

- Watmough, N. J. and F. E. Frerman (2010). "The electron transfer flavoprotein: ubiquinone oxidoreductases." *Biochim Biophys Acta* **1797**(12): 1910-1916.
- Wu, F., F. Yang, K. C. Vinnakota and D. A. Beard (2007). "Computer modeling of mitochondrial tricarboxylic acid cycle, oxidative phosphorylation, metabolite transport, and electrophysiology." *J Biol Chem* **282**(34): 24525-24537.
- Yang, S. Y., X. Y. He and H. Schulz (1987). "Fatty acid oxidation in rat brain is limited by the low activity of 3-ketoacyl-coenzyme A thiolase." *J Biol Chem* **262**(27): 13027-13032.
- Zimin, P. I., C. B. Woods, A. Quintana, J. M. Ramirez, P. G. Morgan and M. M. Sedensky (2016). "Glutamatergic Neurotransmission Links Sensitivity to Volatile Anesthetics with Mitochondrial Function." *Curr Biol*.







# CHAPTER

**Samenvatting**

9



De oxidatieve fosforylering (OXFOS) staat (samen met de citroenzuurcyclus) centraal in de stofwisseling van alle organismen die zuurstof gebruiken. Dit metabole proces vindt plaats in de mitochondriën, waar speciale enzymen (o.a. complexen I-IV) voedingsstoffen oxideren en de hierbij vrijgekomen energie opslaan in de vorm van adenosinetrifosfaat (ATP). Patiënten met een disfunctioneel OXFOS systeem, wat leidt tot een verstoorde cellulaire energiehuishouding, kunnen ongeacht hun leeftijd diverse tekenen en symptomen van orgaanschade vertonen. De genetische basis van deze ziekten is complex. Het nucleair en mitochondrieel DNA zijn samen verantwoordelijk voor de genetische controle van de assemblage en het onderhoud van een volledig functioneel OXFOS systeem. Iedere mutatie in een gen dat de functionaliteit van het OXFOS systeem beïnvloedt, kan leiden tot OXFOS disfunctie gerelateerde klinische symptomen. Mutaties in nucleaire genen worden op een Mendeliaanse wijze overgeërfd, terwijl mutaties in de mitochondriale genen maternaal worden overgeërfd. Organen met een hoog energieverbruik worden het hardst getroffen, in het bijzonder de hersenen. De neuronen gaan geleidelijk ten onder, wat tot een progressief verlies van de structuur en functie van het zenuwstelsel leidt. De progressie van de symptomen varieert van acuut en snel tot subtiel en chronisch. De essentiële functie van het neuronale OXFOS systeem in het handhaven van bioenergetische behoeften wordt geïllustreerd door het feit dat OXFOS disfunctie leidt tot defecten in neuronale groei en transport, alsook apoptose en neuronale dood. Dit kan op zijn beurt microgliale activering veroorzaken, wat desastreuze gevolgen kan hebben zoals verdere oxidatieve en nitrosatieve stress, met additionele neuronale beschadiging en de dood tot gevolg.

\* \* \*

Het doel van dit proefschrift was om, met behulp van het *Ndufs4*<sup>-/-</sup> muismodel, een beter inzicht in de pathofysiologische gevolgen van geïsoleerde mitochondriële complex I (CI) deficiëntie te krijgen en om bij te dragen aan een relevante therapeutische strategie voor het verlichten en/of afzwakken van deze ziekte. Daartoe hebben we de fenotypische uitingen van de *Ndufs4* deletie gekarakteriseerd, door de tekenen en symptomen vanaf postnataal dag 0 tot het humane eindpunt bij te houden (**Hoofdstuk 1**). In overeenstemming met andere studies vonden we dat *Ndufs4*<sup>-/-</sup> muizen verschillende klinische kenmerken vertoonden zoals waargenomen bij kinderen met geïsoleerde CI deficiëntie waaronder hypotonie, progressieve spierzwakte, epileptische aanvallen en ataxie. Op basis van deze bevindingen

werd geconcludeerd dat de *Ndufs4*<sup>-/-</sup> muis een relevant model zou kunnen zijn om therapeutische strategieën die bestemd zijn voor vertaling naar de mens te evalueren.

\* \* \*

Gezien het ernstige fenotype van de *Ndufs4*<sup>-/-</sup> muis, waren we geïntrigeerd door onze *in vivo* waarneming dat de maximale snelheid van de ATP productie niet aangedaan was in deze muizen, ondanks het vrijwel geheel ontbreken van CI-activiteit. Dit motiveerde ons om mitochondria verrijkte fracties van specifieke weefsels in deze muizen te bestuderen (**Hoofdstuk 2**). De maximale snelheid van de mitochondriële ATP productie bleek aanzienlijk afgenomen te zijn in skeletspierweefsel, de hersenen en het hart per eenheid mitochondriale massa na normalisatie ten opzichte van de maximale citraat synthase activiteit. De maximale activiteit van CI bleek nog veel sterker verminderd te zijn in deze weefsels. Echter, wanneer de maximale mitochondriale ATP productie snelheid uitgedrukt werd per mg eiwit, bleek deze niet afgenomen te zijn in het skeletspierweefsel en het hart, in tegenstelling tot de hersenen. Dit betekent dat de totale mitochondriale ATP productiecapaciteit per eenheid weefselmassa enkel verlaagd is in dit laatste orgaan. Verder onderzoek demonstreerde een toename in de maximale citraat synthase, CII, III en IV activiteit in skeletspierweefsel en het hart, indicatief voor een adaptieve verhoging van de mitochondriale massa in deze weefsels. Het ontbreken van dezelfde adaptieve verhoging in de hersenen, toont aan dat dit waarschijnlijk het meest kwetsbare weefsel is in CI deficiëntie veroorzaakt door een mutatie in het *Ndufs4* gen.

\* \* \*

In **Hoofdstuk 3** hebben we een *in silico* strategie gebruikt om te trachten het mechanisme te achterhalen waarmee *Ndufs4*<sup>-/-</sup> skeletspierweefsel mitochondriën, ondanks een ~80% daling van de maximale CI activiteit, nog steeds in staat zijn om ATP te produceren uit CI-specifieke substraten met een maximale snelheid die vergelijkbaar is met die verkregen met wildtype skeletspierweefsel mitochondriën per eenheid weefselmassa (zie Hoofdstuk 2). Hiervoor hebben we een eerder gevalideerd wiskundig model voor mitochondriale stofwisseling in skeletspierweefsel aangepast aan onze experimentele omstandigheden. De hieruit voortgevloede berekeningen voorspelden dat de experimenteel gemeten veranderingen in maximale activiteit van CI, II, III en IV per eenheid weefselmassa resulteerden in



maximale snelheden van mitochondriale pyruvaat oxidatie en ATP productie in *Ndufs4*<sup>-/-</sup> skeletspierweefsel per eenheid weefsel massa die nagenoeg identiek waren aan die van de controle. Deze voorspelling was in volledige overeenstemming met onze experimentele resultaten.

\* \* \*

Kinderen met mitochondriale aandoeningen van het energie genererende systeem worden vaak geanestheseerd voor een breed scala aan operaties. Echter kunnen deze aandoeningen de reactie van de patiënt op de anesthesie veranderen. Aangetoond is dat het vluchtige anesthetische isofluraan de activiteit van CI remt. Bovendien is gebleken dat CI deficiënt *C. elegans* overgevoelig is voor vluchtige anesthetica. Samen met eerder bewijs dat *Ndufs4*<sup>-/-</sup> muizen progressieve ademhalingsstoornissen ontwikkelen, met een vroege dood tot gevolg, hebben deze bevindingen ons aangespoord om de gevoeligheid van deze muizen voor isofluraan te onderzoeken. **Hoofdstuk 4** laat zien dat *Ndufs4*<sup>-/-</sup> muizen een geleidelijke toename met de leeftijd lieten zien van zowel isofluraan gevoeligheid als ademhalingsdepressie. Onlangs werd aangetoond dat glutamaat gemedieerde transmissie een belangrijke rol speelt in de overgevoeligheid voor vluchtige anesthetica in *Ndufs4*<sup>-/-</sup> muizen.

\* \* \*

De resultaten in **Hoofdstuk 5** laten zien dat isofluraananesthesie tot een aanzienlijke toename van de maximale mitochondriale ATP productiesnelheid leidt per eenheid weefselmassa in een mitochondria verrijkte fractie van wildtype en *Ndufs4*<sup>-/-</sup> hersenen. Opvallend is dat, in overeenstemming met de literatuur, isofluraananesthesie de maximale activiteit van CI met 30% verlaagde in wildtype hersenen. Dit resultaat is in overeenstemming met de conclusie uit Hoofdstuk 3 dat CI activiteit kan worden verlaagd tot een weefselspecifieke drempel, zonder dat dit de mitochondriale ATP productiecapaciteit negatief beïnvloed. Tegenovergesteld, verhoogde isofluraananesthesie de activiteit van zowel CII, CIII als CIV in wildtype en *Ndufs4*<sup>-/-</sup> hersenen. Samen tonen deze bevindingen aan dat isofluraananesthesie een positief effect heeft op de capaciteit van hersenmitochondriën van CI deficiënte muizen om hun belangrijkste substraat pyruvaat om te zetten in ATP.

\* \* \*

In **Hoofdstuk 6** bespreken we neuronen die vanwege hun vermoedelijke gevoeligheid voor oxidatieve schade het meest bijdragen aan het neurologische fenotype in  $Ndufs4^{-/-}$  muismodellen. De zeer hoge energiebehoefte van neuronen verklaart waarom de hersenen, die slechts ~2% van het totale lichaamsgewicht uitmaken, verantwoordelijk zijn voor 20% van het totale zuurstofverbruik door het lichaam. Neuronen zijn sterk gedifferentieerde cellen die grote hoeveelheden ATP verbruiken om de ionische gradiënten van hun celmembraan in stand te houden, welke vereist zijn voor effectieve neurotransmissie. Neuronen zijn afhankelijk van het OXFOS systeem voor hun ATP behoefte, aangezien een overstap naar glycolyse, wanneer OXFOS beperkt is, onvoldoende ATP genereert. Neuronen zijn langlevende cellen, wat belangrijk is omdat hun synaptische verbindingen essentieel zijn voor het goed blijven functioneren van het brein. Deze twee eigenschappen kunnen een ernstig probleem vormen, aangezien mitochondriale oxidatieve ATP productie gepaard gaat met de productie van toxische zuurstofradicalen. Er wordt verondersteld dat dit de voornaamste reden is waarom neuronen geen vetzuren oxideren, aangezien voor elk acetyl-CoA dat ontstaat tijdens vetzuur afbraak, een  $FADH_2$  en een NADH molecuul worden geproduceerd. Dit resulteert in een veel grotere toename van de hoeveelheid  $FADH_2$  in de cel, dan het geval is bij de oxidatie van glucose. Dit  $FADH_2$  wordt geoxideerd door het enzym “electron transfer flavoproteïn: ubiquinone oxidoreductase”, dat daardoor met CI concurreert voor de reductie van ubiquinon naar ubiquinol. Dit leidt tot een opstapeling van NADH en daarmee een hogere kans op een toename in de productie van reactieve zuurstofverbindingen (ROS) door CI zelf en/of door mitochondriale NADH hydrogenases. Neuronen prefereren daarom glucose (en ketonlichamen) voor hun energievoorziening, ondanks dat vetzuren ongeveer tweemaal zoveel energie genereren. Desondanks vormen neuronen nog steeds ROS tijdens de mitochondriale ATP productie. Er wordt gespeculeerd dat deze levenslange ROS productie, ondanks de aanwezigheid van talrijke antioxidantsystemen, een ophoping van beschadigingen en daarmee een progressief verlies van neuronfunctie veroorzaakt. Een mogelijke versnelling van dit proces zou kunnen bijdragen aan hersenziekten bij ouderen zoals de ziekte van Alzheimer, amyotrofische laterale sclerose (ALS) en de ziekte van Parkinson.

\* \* \*

Trolox is een wateroplosbare analoog van vitamine E met vergelijkbare antioxidanteigenschappen. In **Hoofdstuk 7** tonen we aan dat tweemaal daagse intraperitoneale injectie van Trolox vanaf week 3 na de geboorte, de geleidelijke

afname van het spieruithoudingsvermogen en de motorische coördinatie van *Ndufs4*<sup>-/-</sup> muizen vertraagde. Analyse van de maximale snelheid van de mitochondriale ATP productie per eenheid weefselmassa in een mitochondria verrijkte fractie van de achterpootspieren van 6 weken oude dieren liet een afname zien in vehikel-behandelde *Ndufs4*<sup>-/-</sup> muizen ten opzichte van controle dieren. Dit in tegenstelling tot onze bevindingen in Hoofdstuk 2, waar geen verschil in de maximale snelheid van mitochondriële ATP productie tussen 31-34 dagen oude WB *Ndufs4*<sup>-/-</sup> en hun wildtype nestgenoten gevonden werd. De eerder aangetoonde toename in de maximale citraat synthase activiteit in 31-34 dagen oude *Ndufs4*<sup>-/-</sup> muizen, bleek afwezig te zijn in 6 weken oude *Ndufs4*<sup>-/-</sup> muizen. Dit suggereert dat de eerder voorgestelde adaptieve verhoging van mitochondriale massa niet meer aanwezig is in eindstadium *Ndufs4*<sup>-/-</sup> muizen. Analyse van de mitochondria verrijkte fracties van achterpoot spierweefsel van Trolox-behandelde *Ndufs4*<sup>-/-</sup> muizen liet tevens een ogenschijnlijke toename van de maximale CI activiteit zien. Deze toename bleek niet gepaard te gaan met een verhoging van de maximale mitochondriale ATP productiesnelheid. Deze bevindingen suggereren dat Trolox geen effect heeft op de skeletspieren, maar juist op de hersenen. Het door GFAP positieve cellen gepopuleerde deel van de granulaire laag van de cerebrale cortex, alsmede het aantal Purkinje cellen in het cerebellum van *Ndufs4*<sup>-/-</sup> muizen werd niet beïnvloed door Trolox-behandeling. In het netvlies zagen we een afname in de apoptose van neuronale nuclei wanneer *Ndufs4*<sup>-/-</sup> muizen behandeld werden met Trolox, tot een niveau gelijk aan dat van wildtype muizen. Desalniettemin zal de analyse van een of meerdere functionele parameters uit moeten wijzen of deze inhibitie van neuronale celdood door Trolox resulteert in een toename van het gezichtsvermogen.

\* \* \*

Naar aanleiding van onze celbiologische studies zijn er een aantal Trolox varianten ontwikkeld en getest op primaire fibroblasten van patiënten met geïsoleerde CI deficiëntie. De meest veelbelovende varianten zijn reeds geselecteerd voor de ontwikkeling van nieuwe behandelingen voor deze ziekte. Samen met reeds gepubliceerde data, rechtvaardigen onze bevindingen in Hoofdstuk 7 een therapeutische strategie bestaande uit 1) antioxidanten die de bloed-hersenbarrière kunnen passeren en zo de inductie van ROS kunnen temperen; 2) immunosuppressiva om de humorale immuunrespons tegen lichaamseigen antigenen te voorkomen; en 3) stimulatie van de mitochondriale biogenese om de ATP productiecapaciteit in de getroffen gebieden van de hersenen te verhogen.



## List of Publications

1. Cheng, S. C., B. P. Scicluna, R. J. Arts, M. S. Gresnigt, E. Lachmandas, E. J. Giamarellos-Bourboulis, M. Kox, **G. R. Manjeri**, J. A. Wagenaars, O. L. Cremer, J. Leentjens, A. J. van der Meer, F. L. van de Veerdonk, M. J. Bonten, M. J. Schultz, P. H. Willems, P. Pickkers, L. A. Joosten, T. van der Poll and M. G. Netea (2016). "Broad defects in the energy metabolism of leukocytes underlie immunoparalysis in sepsis." **Nat Immunol 17(4): 406-413.**
2. **Manjeri, G. R.**, R. J. Rodenburg, L. Blanchet, S. Roelofs, L. G. Nijtmans, J. A. Smeitink, J. J. Driessen, W. J. Koopman and P. H. Willems (2016). "Increased mitochondrial ATP production capacity in brain of healthy mice and a mouse model of isolated complex I deficiency after isoflurane anesthesia." **J Inherit Metab Dis 39(1): 59-65.**
3. Venter, G., M. Wijers, F. T. J. J. Oerlemans, **G. Manjeri**, J. A. M. Fransen, B. Weiringa (2015) Glycolytic Metabolism is Differentially Coupled to Proliferative Potential and Morphodynamic Capacity in RAW 264.7 And Mafb/C-Maf Deficient Macrophage Lineages. **J Clin Cell Immunol 6:292. doi: 10.4172/2155-9899.1000292.**
4. Alam, M. T., **G. R. Manjeri**, R. J. Rodenburg, J. A. Smeitink, R. A. Notebaart, M. Huynen, P. H. Willems and W. J. Koopman (2015). "Skeletal muscle mitochondria of NDUF54-/- mice display normal maximal pyruvate oxidation and ATP production." **Biochim Biophys Acta 1847(6-7): 526-533. (Shared 1<sup>st</sup> author)**
5. Roelofs, S., **G. R. Manjeri**, P. H. Willems, G. J. Scheffer, J. A. Smeitink and J. J. Driessen (2014). "Isoflurane anesthetic hypersensitivity and progressive respiratory depression in a mouse model with isolated mitochondrial complex I deficiency." **J Anesth. (Shared 1<sup>st</sup> author)**
6. Cheng, S. C., J. Quintin, R. A. Cramer, K. M. Shepardson, S. Saeed, V. Kumar, E. J. Giamarellos-Bourboulis, J. H. Martens, N. A. Rao, A. Aghajani-farah, **G. R. Manjeri**, Y. Li, D. C. Ifrim, R. J. Arts, B. M. van der Veer, P. M. Deen, C. Logie, L. A. O'Neill, P. Willems, F. L. van de Veerdonk, J. W. van der Meer, A. Ng, L. A. Joosten, C. Wijmenga, H. G. Stunnenberg, R. J. Xavier and M. G. Netea (2014). "mTOR- and HIF-1 $\alpha$ -mediated aerobic glycolysis as metabolic basis for trained immunity." **Science 345(6204): 1250684.**

7. Forkink, M., **G. R. Manjeri**, D. C. Liemburg-Apers, E. Nibbeling, M. Blanchard, A. Wojtala, J. A. Smeitink, M. R. Wieckowski, P. H. Willems and W. J. Koopman **(2014)**. "Mitochondrial hyperpolarization during chronic complex I inhibition is sustained by low activity of complex II, III, IV and V." **Biochim Biophys Acta 1837(8): 1247-1256**.
8. Speijer, D., **G. R. Manjeri** and R. Szklarczyk **(2014)**. "How to deal with oxygen radicals stemming from mitochondrial fatty acid oxidation." **Philos Trans R Soc Lond B Biol Sci 369(1646)**.
9. Roestenberg, P., **G. R. Manjeri**, F. Valsecchi, J. A. Smeitink, P. H. Willems and W. J. Koopman **(2012)**. "Pharmacological targeting of mitochondrial complex I deficiency: the cellular level and beyond." **Mitochondrion 12(1): 57-65. (Shared 1<sup>st</sup> author)**
10. Valsecchi, F., W. J. Koopman, **G. R. Manjeri**, R. J. Rodenburg, J. A. Smeitink and P. H. Willems **(2010)**. "Complex I disorders: causes, mechanisms, and development of treatment strategies at the cellular level." **Dev Disabil Res Rev 16(2): 175-182**.
11. Sun, X. M., A. Canda-Sanchez, **G. R. Manjeri**, G. M. Cohen and M. J. Pinkoski **(2009)**. "Phenylarsine oxide interferes with the death inducing signaling complex and inhibits tumor necrosis factor-related apoptosis-inducing ligand (TRAIL) induced apoptosis." **Exp Cell Res 315(14): 2453-2462**.

## Curriculum Vitae

Ganesh R. Manjeri was born in the city of Mysore, Karnataka, India on the 14<sup>th</sup> of January 1984. He completed his Senior Secondary School Certificate from Sri Ma Bal Niketan, Thane, Maharashtra, India in 1999. Following which, he completed his Higher Secondary School Certificate from B.N.Bandodkar College of Science, Thane, Maharashtra, India in 2001. In 2002, he started his University degree at St. Xavier's College Mumbai, India. He graduated in 2005 as a Bachelor of Science (B.Sc.) in Zoology and Biochemistry, 1<sup>st</sup> class. In 2006, he started his postgraduate study at the University of Leicester, UK. He completed his Master of Science (M.Sc.) degree in Cancer Cell and Molecular Biology, 1<sup>st</sup> class, in 2007. During this period, he undertook his research internship in the lab of Dr. Michael J. Pinkoski at the Medical Research Council (MRC) Toxicology Unit, Leicester, where he investigated the role of **"TRAIL induced apoptosis in lymphoid tumours"**. After his M.Sc., he worked as a Research Assistant at Kings College London, UK in the lab of Professor J. Paul Banga, here he was responsible for quantifying Thyroid stimulating hormone receptor (TSHR) expression in thyroid cancer cell lines with an aim of creating xenograft tumour mouse models to image thyroid malignancies via previously described radiolabelled high-affinity monoclonal antibodies towards the TSHR. In 2009, Ganesh moved to RWTH University, Aachen, Germany where he worked as a pre-doctoral fellow in the lab of Professor Hermann E. Wasmuth by investigating the role of a chemokine, Macrophage inhibitory migration factor (MIF) in liver fibrosis. In August 2009, he started his doctoral studies at Radboudumc with Professor Jan A.M. Smeitink and Dr. Peter H.G. Willems in the Departments of Biochemistry and Paediatrics. The aim of his doctoral thesis was **"Characterization of the *Ndufs4*<sup>-/-</sup> model to evaluate a novel therapeutic strategy towards mitochondrial dysfunction"**. In 2015, Ganesh moved back to the UK, where he started working as a Research Fellow in the Institute of Metabolism and Systems Research at the University of Birmingham with Professor Gareth G. Lavery to investigate changes in the NAD<sup>+</sup> metabolome during health and aging in transgenic mouse models.





## Acknowledgements

This thesis is an effort of many minds, in a quest to come closer to cure mitochondrial disease. I would like to thank everyone who has been a part of this journey.

To **Prof. Smeitink, Dr. Willems** and **Dr. Koopman** - Thank you for giving me the opportunity to pursue my PhD in your lab and supervising my PhD work. **Peter and Werner**, thank you for all your suggestions during the course of my PhD and for the endless hours you spent in helping me come up with all the articles which are a part of this thesis.

To all the past and present members of Membrane Biochemistry **Peggy, Fede, Suzaan, Marleen, Mina, Julien, Megan, Marco, Dania, Tauqeer, Sander, Jori, Hoa, Farhan, Lisanne and Sjenet**, thank you for all your support during my PhD.

**Herman**, thank you for your care and concern during my PhD and all the interesting suggestions you came up with during our group meetings.

**Fede**, thank you for being you! You gave me the best welcome to the lab and Nijmegen in general, thank you for that. Even though, geographical distances have separated us, you will always be a friend and a colleague wherever we are or will be!

**Cindy**, thank you for sharing your strength with me at all times, you have seen me through my worst, best and everything in between. Your company through this journey has been extremely reassuring, especially since, you helped me keep my sanity through this chaos. You also introduced me to several beautiful people in Nijmegen. You are a strong individual and I wish you success in whatever you do and wherever you go!

**Lionel**, my go to guy for statistics, thank you for spending all those hours, helping me make sense of raw numbers. I admire your patience even when I was going bonkers and the wonderful schematic of the respiratory chain that you designed for my EBEC talk of 2012!

Life outside the lab was equally important to me and I would like to thank my social circle for their invaluable care and backing, especially, when experiments and long hours in the lab didn't seem to produce tangible results. A special mention, to the

**3 A's** of my life a.k.a. the three musketeers – **Anchel, Angela and Antoine**, thank you to you and your families for showing me that love and goodness of the heart trumps everything in life!

My housemates from over the years **Anchel, Angela, Antoine, Sip, Till, Pedro, Nuria, Rocio** and **Cindy Ronnau**, thank you for your time during everyday life, the breakfasts, lunches, dinners and bike-rides we shared together.

To my extended family spanning the **7<sup>th</sup>, 6<sup>th</sup> and 5<sup>th</sup> floor of the RIMLS** – **Joanna and Tomasz, Sergio and Elisa, Lauriane, Pedro and Caro, Anil and Asha, Jenny, Ganesh P, Sabina, Olga and Pavel, Julia, Jan-Hendrik, Cornelia, Ingeborg, Stefania** and **Simone** thank you for all the Fridays, Birthdays, weekends, Veirdaagse we celebrated together.

To my friends who always shared their lunch hour with me **Benny, Vicky, Pedro, Marco F, Davide** and **Markus** thank you, eating alone was always monotonous - thanks for never letting that happen!

My association with **Cindy** brought another special person into my life, thank you **Martin** for all the talks over dinners and Deut! Also, thank you for introducing me to **Marco B.** Cindy thank you also for acquainting me to **Cesar** – Our association has just enriched my life in so many ways!

My journey only started with the conviction of the 2 pillars in my life, **Appa and Mummy** – **I dedicate this PhD to you!**

**Karthik**, we have shared everything in life from our mother's womb – thank you bro for everything, I wish you and **Sowmya** success in the journey you are going to embark on!

My better half **Ramya**, you are the best thing to have happened to me. My biggest strength and inspiration, thank you for being a part of my life and seeing me through the last leg of this journey!

Finally, last but not the least – **My beautiful city and people of Nijmegen** – You embraced me with open arms and never ever made me feel like an outsider – my heartfelt gratitude for your acceptance.